Process simulation as a decision support tool for biopharmaceutical process development in a South African context

Wesley Collair

In fulfilment of the requirements for the degree of Master of Science

Supervisor: **Dr. Siew L. Tai**

Department of Chemical Engineering
Faculty of Engineering and the Built Environment
University of Cape Town

September 2019

Plagiarism Declaration

1. This dissertation has been submitted to the Turnitin module and I confirm that my supervisor has seen my report and any concerns revealed by such have been resolved with my supervisor.
2. I know that plagiarism is wrong. Plagiarism is to use another's work and to pretend that it is one's own.
3. I have used the Harvard (University of Cape Town variant) system for citation and referencing. Each significant contribution to, and quotation in, this report from the work, or works, of other people has been attributed, and has been cited and referenced.
4. This is my own unaided work, except for assistance received from the teaching staff.
5. I have not allowed, and will not allow, anyone to copy my work with the intention of passing it off as his or her own work.

Signed: Signed by candidate

Wesley Collair

Date:

04/10/2019

Signed at Kenilworth

Abstract

In 2010 the incidence of neo-natal Group B *Streptococcus* (GBS) disease in South Africa was 3 per 1000 live births, more than twice the global average of 1.21 per 1000 live births. A recent life cycle impact assessment showed that a new vaccine against GBS disease in South Africa could have a potential value of $ 2 million - $ 4 million /kg (R 25 million – R 50 million /kg), as an attractive investment opportunity if a novel process can be successfully synthesised and licensed commercially.

In the current global market new biopharmaceutical products require innovative and expedited development pathways. To achieve this, low-cost analytical tools with short turnaround times are needed to assist with process development decision making. Process simulation is one such tool which has been shown to be useful for evaluating process development decisions without the typically expensive investment required for experimental development of a new process.

Three technology platforms (stainless steel, single-use, and a hybrid of both) were identified for use in a novel process to manufacture a GBS serotype III polysaccharide-protein conjugate antigen, for formulation into a vaccine against GBS disease. The three technology choices were compared and evaluated for the novel process at two fermentation scales of 20 L and 200 L, with cost of goods (COG) used as a comparison of economic performance for the six different scenarios. It was hypothesised that single use technology would yield the lower COG at both scales compared to stainless steel. Based on a literature survey, single use technology should require lower capital costs for pilot scale processes and should also have lower operating costs due to single use equipment not requiring sterilisation in place (SIP) and cleaning in place (CIP). It was further hypothesised that hybrid technology would yield the lowest COG by combining the best properties of stainless steel and single use technologies.

A 3 x 2 factorial experiment design was used to structure the simulation exercise with three technologies at each of the two scales. A GBS serotype III process model was synthesised from literature sources, with fermentation stoichiometry based on an empirical material balance and fermentation kinetics fitted to a two-parameter Monod kinetic model. Equipment, consumables, and raw materials specifications were made using literature and empirical models. A base case simulation model, built for 20 L scale using stainless steel technology, was developed into the five additional scenarios. The best performing scenario in terms COG was then selected for sensitivity analysis using three parameters: fermentation titer, solid-liquid separation efficiency, and electricity dependence on diesel generation.

At 20 L scale there was little difference in COG between the three technology options, with COG range across the three platforms of $ 9.7 million – $ 9.8 million /kg. At 200 L scale the best performing technology was stainless steel with a COG of $ 3.7 million /kg, which was $ 600 000 /kg less than the COG for single use of $ 4.3 million/kg. The difference was due to a higher cost of consumables for single use technology, and negligible differences in capital costs for single use over stainless steel. The effect of SIP and CIP costs on operating cost for stainless steel technology was found to be small compared to the greater consumables cost for single use. The 200 L stainless steel process was found to be sensitive to fermentation titer, with an increase in titer to 600 mg/L resulting in the lowest COG of $ 2.2 million /kg. The process was found to be least sensitive to electricity dependence on diesel, with only a $ 60 000 /kg increase in COG when 75% of electricity was derived by diesel generator.

The hypothesis was disproved, with single use technology having the higher COG at both 20 L and 200 L scales compared to stainless steel technology. Hybrid technology did not yield the lowest COG either, instead resulting in a COG somewhere between stainless steel and single use. Stainless steel technology outperformed single use and hybrid technologies in COG at both scales, contrary to both parts of the hypothesis. A process to make a GBS vaccine could be profitable at scales of 200 L and above using stainless steel technology. Process simulation modelling was effective for evaluating process technology options without performing costly physical experiments. The simulation exercise provided valuable information on the economic impact of process development decisions as well as context specific information for the South African context. This methodology is therefore recommended for commercial biopharmaceutical process development, particularly for evaluating techno-economic scenarios in different decision pathways during the development process.

Acknowledgements

This research was funded by:

The Biologicals and Vaccines Institute of South Africa

The Wilhelm Frank Trust

This research was supported academically by:

The University of Cape Town Centre for Bioprocess Engineering Research

Dr. Siew L. Tai

Nadia Collair

Ivan & Lynette Collair, Kyle Collair & Kate Schrire

thank you for all your support

Table of Contents

List of Figures

List of Tables

Glossary of Terms

Acetoin	3-hydroxybutanone
Activation	Addition of reactive functional groups to facilitate conjugation
Adiabatic	No energy crossing the system boundary ($\Delta Q=0$)
Aerobic	In the presence of biologically available oxygen
Aliphatic	Relating to a covalent bond with a carbon atom
Anaerobic	Without the presence of biologically available oxygen
Antigen	Compound which induces an immunologic response
Aseptic	Sterile, no viable microorganisms present
Base case	Simulation model scenario used as a starting point for developing further scenarios
Batch process	Process with a defined start time, finite running time, and defined end time
Biomass	Large quantity of biological cells, typically gram or kilogram scale
Biopharmaceutical	Pharmaceutical products produced using biological expression systems
Bioreactor	Vessel used for the culture of biological organisms (typically mammalian cells)
Capsid	Protective outer wall of a bacterium
Capsular polysaccharide	Polysaccharide attached to the outer wall bacterial capsid
Carrier protein	Detoxified bacterial toxin protein, “carries” covalently attached antigens
Cascade control	Fast responding inner control loop with slower responding outer loop
Clean in place	To clean a piece of equipment in the same location where it is installed
Conjugate	Polysaccharide covalently linked to a carrier protein
Consumable	Material that is used to facilitate a process and then discarded after use
Continuous process	Process without a finite running time, nor a defined end time
Cross-contamination	Contamination of material of high purity by another material used in the same equipment or area
Cyanylation	Chemical reaction where free hydroxyl groups are converted to cyanoester groups: R-OH → R-OCN
Debottlenecking	Identifying the part of a process which is limiting to productivity and suggesting ways to reduce or eliminate the limitation
Decontaminate	To kill microorganisms to less than 1 surviving from 1 million viable
De-N-acetylate	Removal of acetyl functional group from an N-acetyl functional group, the result is a primary amine group: R-NHCOCH3 → R-NH2
Derivatized	Chemical reaction which produces a derivative product which has a structure similar to the starting material
Diafiltration	Size exclusion separation by passing through a filter medium with continuous discharge of carrier and replacement with fresh carrier solution

Discount rate	Rate of return on an investment. Discount rate accounts for cost of finance, real return, and risk return.
Doubling time	Time taken for total number of cells in a culture to double
Doubling time	Time taken for the number of organisms in a culture to double
Extra-cellular	Outside the cell wall
Extractables	Compounds that can move from material into a carrier fluid under normal conditions
Extraction	Release of a compound from a solid into a liquid extractant solution
Fermentation	Conversion of ADP to ATP by substrate level phosphorylation
Fermentor	Vessel used for the culture of microbial organisms
Glycosidic linkages	Covalent bond joining a carbohydrate to another carbohydrate or group
Hetero-lactic	Fermentation reaction products include at least one other type of organic acid in addition to lactic acid. For example, acetic acid and lactic acid.
Hexavalent	Vaccine formulation containing six antigens
Homo-lactic	Fermentation reaction products include only lactic acid
Hurdle rate	The discount rate at which NPV=0.
Hybrid technology	Combination of stainless-steel and single-use technologies
Inactivation	To kill all viable microorganisms at the end of fermentation culture
Inoculum	Small volume of live organisms added to a larger volume of growth medium
Internal Rate of Return	A discount rate which can be used to evaluate the present value of future cash flows (IRR > hurdle rate at NPV=0)
Intra-cellular	Within the cell wall
Kinetic	Time dependent property or properties of a chemical reaction
Laminar flow	Fluid flow pattern in which fluid “streams” do not overlap or cross paths
Leachables	Compounds that can move from a material into a carrier fluid under normal conditions
Lymphocyte	Type of immune cells (white blood cells) found in vertebrates
Medium	Solution containing more than one substrate, used for culturing
Microbial	Relating to bacterial microorganisms
Monoclonal antibody	Antibody with monovalent antigen binding affinity
Monoseptic	One unique species of microorganism
Neo-natal	Babies less than 6 months of age
Neutral	pH of 7.00
Neutralize	pH adjustment of a solution until the solution pH is neutral
Net Present Value	Interest adjusted present value of future cash flows
Organic	Compounds based on covalently bonded carbon atoms
Orthogonal carbon	Three-dimensional woven carbon medium with strands in x and y co-ordinates perpendicular to each other, and strands in z co-ordinate supporting x and y strands
Pathogen	Bacterium or virus that causes disease

Pellet	Solid product from centrifugation separation process
Permeate	Solution containing compounds which pass through a tangential flow filtration membrane
Phagocytosis	Process by which a host organism's immune cells destroy foreign particles
Polycarbonate	Durable plastic compounds derived from petroleum hydrocarbon starting materials
Polysaccharide	Carbohydrate compound of repeating monosaccharides joined by glycosidic linkages
Precipitation	Phase change of a solute from liquid in solution to solid
Process simulation	Execution of computer model simulation of a process
Recombinant	Organism with an artificially modified genome
Re-N-acetylate	Re-addition of acetyl functional group to a primary amine group, the result is an N-acetyl functional group: R-NH2 → R-NHCOCH3
Respiration	Conversion of ADP to ATP by oxidative phosphorylation
Retentate	Solution containing compounds which are retained by a tangential flow filtration membrane
Sensitivity	Response of a simulation model outputs to changes in information inputs
Simulation model	Mathematical model of a real process, taking information as inputs and producing information outputs which simulate real material and energy inputs and outputs
Single use technology	Process technology (vessels, separation, fluid management) where equipment/consumables are disposed of as waste after one use
Specific growth rate	Unit time dependence factor of microbiological growth
Stainless steel technology	Process technology (vessels, separation, fluid management) based on re-useable equipment/consumables
Sterilize	To kill microorganisms to less than 1 surviving from 1 million viable
Sterilize in place	Sterilize a piece of equipment in the same location where it is installed
Substrate	Starting material which is consumed in a biochemical reaction to produce products
Supernatant	Liquid product from centrifugation separation process
Technology platform	Classification of equipment and consumables which have common technological properties
Technology tree	Diagram describing possibilities for different technologies as branches from
Titer	Concentration of product in a culture at the end of the fermentation process
Unit operation	Simulated event or process which takes place in a simulated piece of equipment
Unit procedure	Series of unit operations taking place in one piece of equipment
Validation	Proving a process, material, or piece of equipment performs as designed and intended to
Wild type	Naturally occurring organism (no genome modification)

Acronyms and Abbreviations

ADH	Adipic acid Di-Hydrazide
ADP	Adenosine Diphosphate
ATP	Adenosine Triphosphate
CAPEX	Capital Expenses
CDAP	1-Cyano-DimethylAminoPyridinium
COG	Cost of Goods
CPS	Capsular Polysaccharide
CRM-197	Cross Reactive Material 197
DCW	Dry Cell Weight
DES	Discrete Event Simulation
DFC	Direct Fixed Capital
DO	Dissolved Oxygen
DTP	Diphtheria, Tetanus & Pertussis
EDC	1-Ethyl-3-(3-Dimethylaminopropyl) Carbodiimide
EPI	Expanded Program on Immunisation
EPI-SA	Expanded Program on Immunisation in South Africa
FORTRAN	Formula Translation
GAVI	Global Alliance for Vaccines and Immunisation
GBS	Group B Streptococcus
GE	General Electric
GSK	GlaxoSmithKline
HIV	Human Immunodeficiency Virus
HY	Hybrid technology platform
IAP	Intrapartum Antibiotic Prophylaxis
IP	Intellectual Property
IRR	Internal Rate of Return
LAF	Laminar Air Flow
LCA	Life Cycle Assessment
LCIA	Life Cycle Impact Assessment
MES	4-MorpholinoEthaneSulfonic acid
NPV	Net Present Value
OD	Optical Density
OPEX	Operating Expenses
PBS	Phosphate Buffered Saline
PFD	Process Flow Diagram
Polio	Poliomyelitis
R&D	Research & Development
RMPRU	Respiratory and Meningeal Pathogens Research Unit

SA	South Africa
SS	Stainless Steel technology platform
STR	Stirred Tank Reactor
SU	Single Use technology platform
SUT	Single Use Technology
TB	Tuberculosis
TEA	Triethylamine
TRIS	Tris (Hydroxymethyl) Aminomethane
TT	Tetanus Toxoid
UNICEF	United Nations Children's Fund
UPC	Unit Production Cost, equivalent to COG
US	United States of America
VBA	Visual Basic for Applications
VLP	Virus Like Particles
WFI	Water for Injection
WHO	World Health Organisation

Chemical Formulae

$(C_{35}H_{52}O_{31}N_2)_n$	GBS serotype III Capsular polysaccharide
C_2H_5OH	Ethyl alcohol (Ethanol)
$C_6H_{12}O_6$	D-(+)-Glucose
$CaCl_2$	Calcium chloride
$CH_3CHOHCOCH_3$	3-hydroxybutanone
$CH_3CHOHCOOH$	Lactic acid
CH_3COOH	Acetic acid
CO_2	Carbon dioxide
HCl	Hydrochloric acid
HCOOH	Formic acid
KH_2PO_4	Potassium di-phosphate
Na_2CO_3	Sodium carbonate
$Na_2HPO_4.2H_2O$	Disodium phosphate (dihydrate)
NaCl	Sodium chloride
$NaH_2PO_4.H_2O$	Monosodium phosphate (monohydrate)
NaOH	Sodium hydroxide
TRIS	Tris (hydroxymethyl) aminomethane

Units

$	US Dollars (2017 exchange rates)
% DO	Percentage dissolved oxygen concentration relative to saturation concentration (100% DO)
% vv	Percentage by volume per volume
°C	Degrees Celsius
µg	Microgram (1 x 10^{-9} kg)
µm	Micrometer (1 x 10^{-6} m)
atm	Atmosphere (101325 Pa)
bar	1000 kPa
barg	Bar pressure in addition to 1 atm
Da	Dalton
g	Gram (1 x 10^{-3} kg)
gDCW	Grams of dry cell weight
h	hour
kDa	Kilodalton (1 x 10^{3} Da)
kg	kilogram
kVA	Kilovolt-Ampere (1 x 10^{3} VA)
L	Liter (1 x 10^{-3} m^3)
M	Moles per liter (mol/L)
m	meter
mg	Milligram (1 x 10^{-6} kg)
min	Minute
mL	Milliliter (1 x 10^{-6} m^3)
mm	Millimeter (1 x 10^{-3} m)
mol	Mole (Approximately 6.022141x10^{23})
MT	Million tons
N	mol/L at 25 °C, 1 atm
NL/min	L/min at 0 °C, 1 atm
nm	Nanometer (1 x 10^{-9} m)
OD_{590}	Optical Density at a wavelength 590 nanometers
Pa	Pascal (1 $kg.m^{-1}s^{-2}$)
pH	Negative logarithm (base 10) of hydrogen ion activity in solution
R	South African Rands (2017 exchange rates)
rpm	Revolutions per minute
s	Second
t	Metric tons
vvm	Volume per total Volume, per Minute
y	Year

1 Introduction

1.1 Manufacturing Human Vaccines

Vaccines are one of the most effective modern healthcare interventions due to their low cost and efficacy in preventing the spread of infectious diseases. Vaccines protect vulnerable patients by conferring to the recipient long term immunity against disease (Kremer, 2002; Pagliusi, Leite, et al., 2013; Rader & Langer, 2014). The eradication of many of the most deadly infectious diseases is a result of decades of scientific research and development, although in recent times post-modernist populism has given rise to science deniers who believe vaccines cause diseases rather than cure them (Kata, 2012).

Before vaccines, contracting a highly infectious disease like measles or smallpox meant death for the infected patient (Hotez, 2017). There have been many ground-breaking advances in medical science in the field of vaccines, as shown below in **Figure 1**. One of the first documented cases of use of a vaccine to provide immunity against an infectious disease was in 1796, when Edward Jenner used cowpox pus to immunise patients against the human disease smallpox. A major breakthrough in the field of vaccines and immunology was Jonas Salk's 1955 discovery of an effective vaccine against Poliomyelitis (Josefsberg & Buckland, 2012). Polio is a virus that attacks the nerves and spinal cord, causing deformation and debilitation which is especially cruel when the victims are young children (WHO, 2017a). As shown in **Figure 1**, since the discovery of the Polio vaccine a number of technologies have been developed for vaccine manufacture including recombinant virus like particles (VLPs) and conjugated polysaccharide vaccines, the latter of which first appeared in 1987 (Josefsberg & Buckland, 2012). The modern era of high-quality vaccines regulated by current Good Manufacturing Practice (cGMP) began in 1998 with GlaxoSmithKline's *Havrix*® Hepatitis A vaccine.

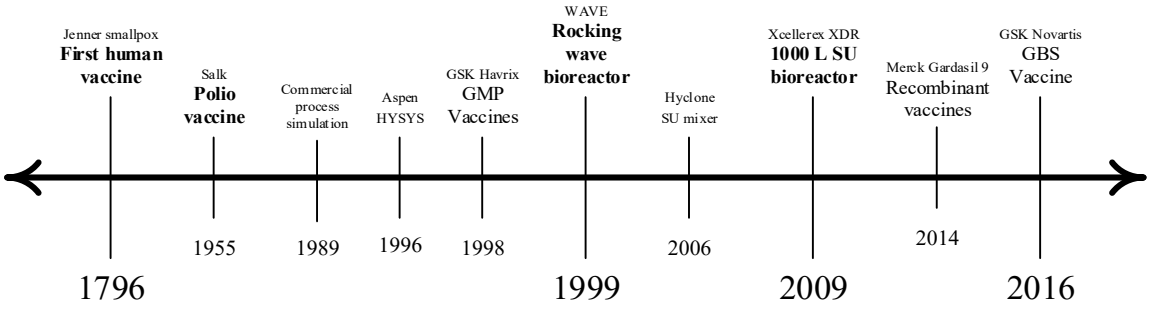

Figure 1: A brief history of vaccines, bioprocessing simulation, and single use technology

The global demand for medicinal pharmaceutical products is dynamic, with new markets continuously emerging in developing countries, as well as growing demand in established markets such as Europe, Asia and the US (Kremer, 2002; Papavasileiou et al., 2007; Pagliusi, Makhoana, et al., 2013; Ampofo, 2016). To meet this demand manufacturers invest heavily in research and development of new products, with an estimated average investment of $ 2.8 billion (2013 USD) per approved compound (DiMasi, Grabowski & Hansen, 2016). With such large investments and limited patent protection for intellectual property it is essential that manufacturers minimize the time to market for new products, and recover their investments into research and development (Papavasileiou et al., 2007; Papavasileiou, Siletti & Petrides, 2008; Toumi et al., 2010).

1.1.1 The South African Context for Manufacturing Human Vaccines

In the 1980s and 90s South Africa's state vaccine manufacturing programme produced human vaccines for tuberculosis (TB), polio, rabies, diphtheria tetanus & pertussis (DTP), typhoid, smallpox, and yellow fever. This programme was abandoned in the early 2000s due to an inability to keep up with the global renaissance in vaccine processing technology, and stricter regulations which required large capital investments in order to keep up with the rapidly transforming industry (Makhoana, 2011). In an attempt

to restore domestic vaccine manufacturing capacity to South Africa, a public-private partnership (PPP) between the South African Government and the Biovac Consortium was launched in 2003 (Stanford, 2003). The African market for vaccines has always been a lucrative prospect due to governments and non-governmental organisations like UNICEF each spending billions every year to procure vaccines from manufacturers in other countries and distribute them to African countries.

While local vaccine manufacturing capacity was being lost, South Africa had implemented the WHO's Expanded Programme on Immunisation (EPI) in 1995 (Baker, 2010). On the modern EPI-SA infants and children are vaccinated against a range of diseases as a basic public health service. The EPI-SA has been successful in reducing the mortality rate of children under 5 (Madhi, 2015) in a country where many types of disease burdens are higher than global averages. As a result many vaccines including those intended for children on the EPI are trialled in South Africa (Madhi et al., in press, 2000, 2010; Klugman et al., 2003; Day et al., 2013; Geldenhuys et al., 2015; Madhi, 2015); however, no human vaccines were manufactured in South Africa as of 2019.

Streptococcus agalactiae, also identified as Group B *Streptococcus* (GBS) by Lancefield's classification (Lancefield, 1932), is the most prevalent cause of severe early onset bacterial infection in infants. In some cases GBS infection leads to infant mortality or permanent disability, with a mortality rate of between 10% and 50% of invasive cases (WHO, 2017b). The bacteria are believed to be transmitted from mother to child during childbirth, with an estimated 20% of all women being carriers (Burns & Plumb, 2013).

The disease burden of GBS around the world is relatively low compared to heart-disease, diabetes, auto-immune diseases, cancer, and HIV. Incidence of neo-natal and infant GBS disease in 2010 was as low as 0.3 cases per 1000 live births in the USA, up to ten times lower than South Africa with 3 cases per 1000 live births (Schrag & Verani, 2013; Kim et al., 2014). The discrepancy between the market power of the South African region, and the high GBS disease burden in South Africa is a potential reason why no commercial vaccine exists, despite the morbidity of the victims being infants and children.

The inertia of the market for a GBS vaccine has somewhat been overcome by the WHO and various research groups through awareness initiatives, and based on the need to develop a GBS vaccine on humanitarian grounds rather than commercial viability (WHO, 2017b). The existing use of alternative therapies such as Intrapartum Antibiotic Prophylaxis (IAP) has slowed the progress of vaccine development research; however, IAP is ineffective in preventing late onset GBS infection and is logistically impractical in rural areas of developing countries like South Africa. Despite the availability of IAP and the relatively small market for a GBS vaccine, development is currently underway by multiple research groups and commercial vaccine manufacturers (Burns & Plumb, 2013; Kim et al., 2014; WHO, 2017b).

1.1.2 Process Simulation for Biopharmaceutical Processes

The goal of pharmaceutical manufacturing processes is to maximise productivity, which is complimented by prioritising speed to market during process development (Sinclair & Monge, 2002; Buckland, 2005; Ransohoff, 2005; Sinclair & Monge, 2005). The role of process simulators in this approach is to assist with process development decision making within expedited time frames, without the cost of investing in physical experiments. *Aspen Batch Plus and Intelligen SuperPro Designer* are described as the best available commercial simulation products which offer an integrated process modelling package (Gosling, 2005; Farid, Washbrook & Titchener-Hooker, 2007; Toumi et al., 2010), with all the required features for an effective process simulator.

Process simulators have been used in the chemical processing industry since the 1960s as a tool for evaluation of the performance of operations planning and techno-economic efficiency (Shanklin et al., 2001; Papavasileiou et al., 2007; Toumi et al., 2010). Early process simulation tools were developed in-house by chemical companies for specific continuous processes using coding languages like FORTRAN (Lang, Biegler & Grossmann, 1988). These early models developed quickly into commercial

packages, successful in part due to the availability of fundamental first principles models such as thermodynamic equilibrium for the modelling of various unit operations (Shanklin et al., 2001).

The application of process simulation to biopharmaceutical manufacturing is primarily at the pre-feasibility design stage of large-scale process development. This type of exercise is performed by relevant trained engineering personnel either as consulting service, or in-house by commercial biopharmaceutical manufacturers. These tools are used to evaluate process development decisions before investing in new products or expanding existing capacity.

1.1.3 Vaccine Manufacturing Technology

There are many processes used around the world for making vaccines. A vaccine product may contain a variation of chemical structures of the same antigenic compound, which makes vaccines more easily defined by the process of manufacture than laboratory measurements of the product characteristics (Josefsberg & Buckland, 2012).

Vaccine antigens can be produced either by culture of a naturally occurring organism (wild type) that expresses a specific antigen, or by engineering the genome of an organism (recombinant) to induce expression of the antigen. Antigens may be expressed either intra-cellularly or extra-cellularly, depending in the organism and the nature of the antigen itself. Biological cultures are grown in large quantities in fermentors or bioreactors, followed by purification to recover the antigen only, and then formulation into a vaccine product (Smith, Lipsitch & Almond, 2011; Cox, 2012; Josefsberg & Buckland, 2012). After formulation, the vaccine is packaged in an aseptic environment and distributed through a supply chain network designed and operated to preserve the potency and efficacy of the vaccine product (Lydon & Raubenheimer, 2011).

Due to the varying range of diseases that vaccines are used against, the process of making a vaccine is often unique, making the entire industry widely varied. A technology tree of different types of vaccines is shown in **Figure 2** below, and based on a review of Vaccine technologies by Josefsberg & Buckland (2012). Each colour below represents a different process approach.

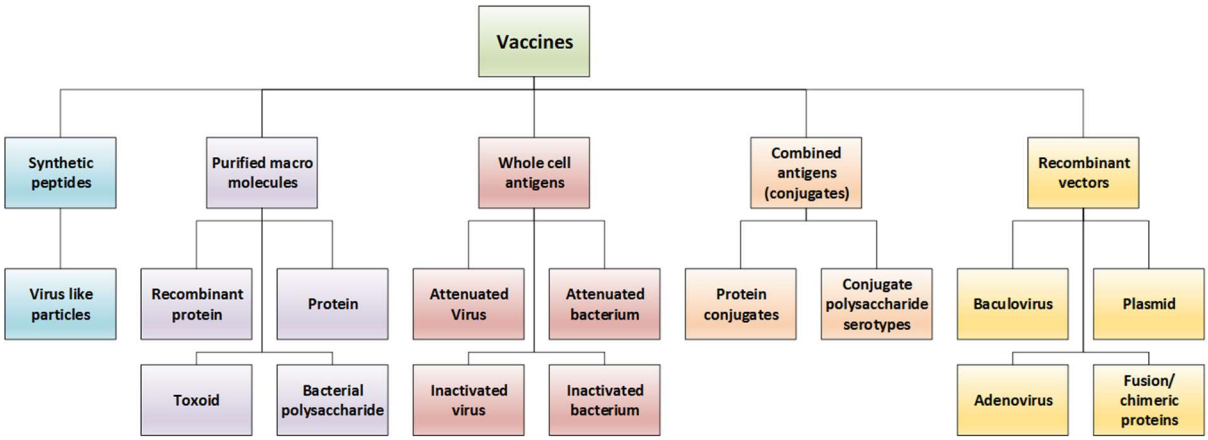

Figure 2: Different vaccine products
Based on (Josefsberg & Buckland, 2012)

The “gold-standard” for bioreactor technology in vaccine production is the stainless-steel stirred tank reactor (STR). The widespread use of STR technology in a range of modern bioprocessing industries from mining to pharmaceuticals is attributed primarily to their enhanced flexibility for a wide range of applications whilst achieving high mixing performance (Nienow, 2014). The nature of industrial bioprocessing is generally one which requires control of mass transfer, which translates into control of the growth characteristics of the culture inside the processing vessel. These physical phenomena have been the driving force for technological development of many industrial bioprocesses (Godoy-Silva, Berdugo & Chalmers, 2010; Nienow, 2014, 2015).

Stainless steel stirred tanks feature robust mechanical or magnetic agitation systems, allowing for either high or low power to volume ratio around the impeller zone, depending on the requirements of the process. This feature remains a critical one for microbial culture where fast cell growth and high cell density require equivalent mass transfer and heat dissipation (Löffelholz et al., 2013; Shukla & Gottschalk, 2013). Stainless steel fermentors, a type of STR with a high vessel aspect ratio, have been successfully used to produce vaccines against pneumococcal disease, diphtheria, tetanus, and pertussis (whooping cough). The manufacturing preference for stainless steel has been largely unchallenged until the turn of the 21st century, when single use technology became a viable alternative for many applications, particularly for shear sensitive processes like monoclonal antibodies or microalgae production (Chisti, 2007; New Brunswick Scientific et al., 2009; Pörtner, 2015).

The first successful demonstration of a single use bioreactor was Vijay Singh's rocking bag reactor for small to medium scale (0-100L) cell culture (Singh, 1999, 2001). A more robust bioreactor design, shown in **Figure 3** (below), was patented in 2009 by Xcellerex (now GE Healthcare) (Hodge, Galliher & Fisher, 2009). The design featured a plastic bag set inside an open tank body with temperature control jacket. The bag contained an agitator coupled magnetically to an external drive unit. In contemporary bioreactor engineering this type of STR design may be used for mammalian cell culture up to volumes of 2000 L, but has only limited application for microbial cultures (Shukla & Gottschalk, 2013). The same design concept has been applied to micro-scale reactors as small as 10 mL (Sartorius Stedim - Tap, 2018), allowing for end to end use of a single reactor design from cell bank development to industrial manufacture.

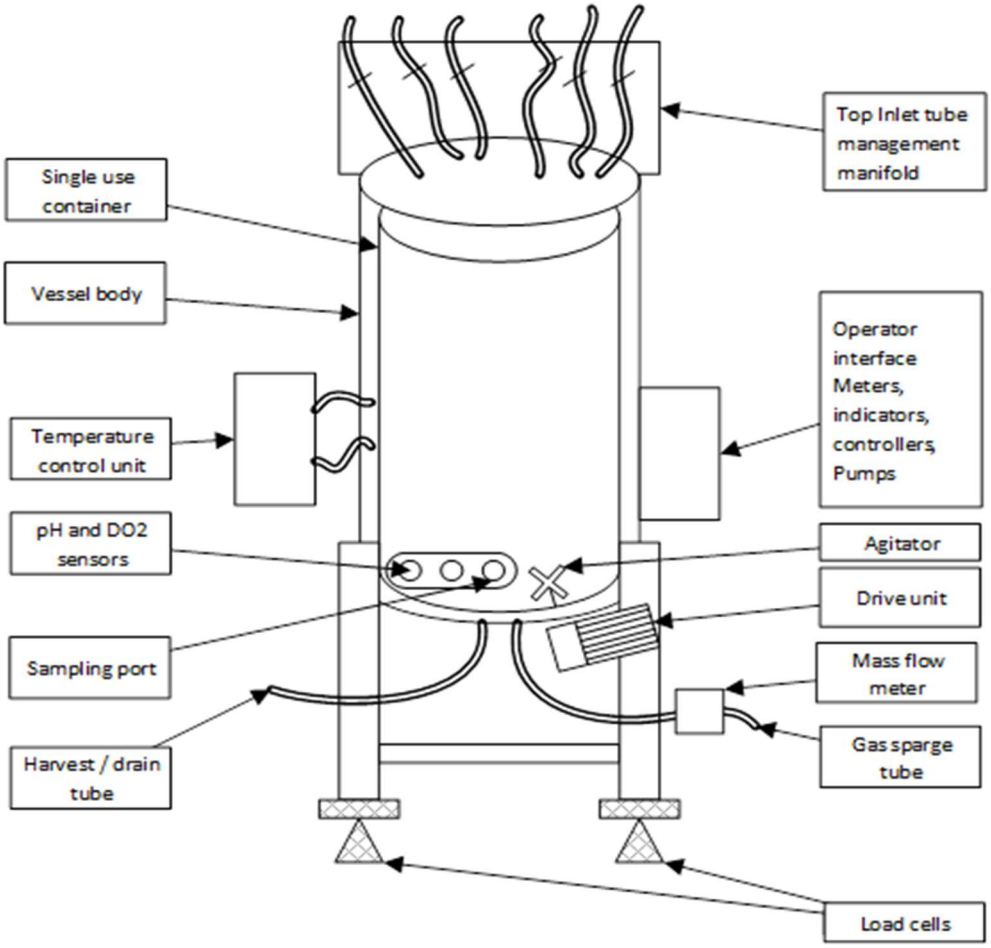

Figure 3: Single use bioreactor design
Redrawn from Hodge, Galliher & Fisher, (2009)

1.2 Scope and constraints

This investigation included the development and production of at least six simulation models of a process for the production of a polysaccharide-protein conjugate vaccine antigen against Group B *Streptococcus* (GBS) serotype III. The process was limited to antigen production and did not include formulation and filling of the final vaccine product. The simulation models included various scenarios involving the use of three different technology platforms: stainless steel, single-use, and hybrid technologies. The project was extended to predicting the effect of scale up from 20 L to 200 L fermentation capacity. A sensitivity analysis was done to expand one of the six models into multiple scenarios to test the sensitivity of the selected model to input parameters.

Real experimental data (unpublished raw data) was used to develop a structured kinetic model for batch fermentation of *Streptococcus agalactiae* (GBS). Purification and conjugation models were based on literature only and were not based on experimental data. A simplified representation of the scope and limitations of this project as described above is shown in **Figure 4** below. Content included in this investigation is shown in green, with content not included shown in red.

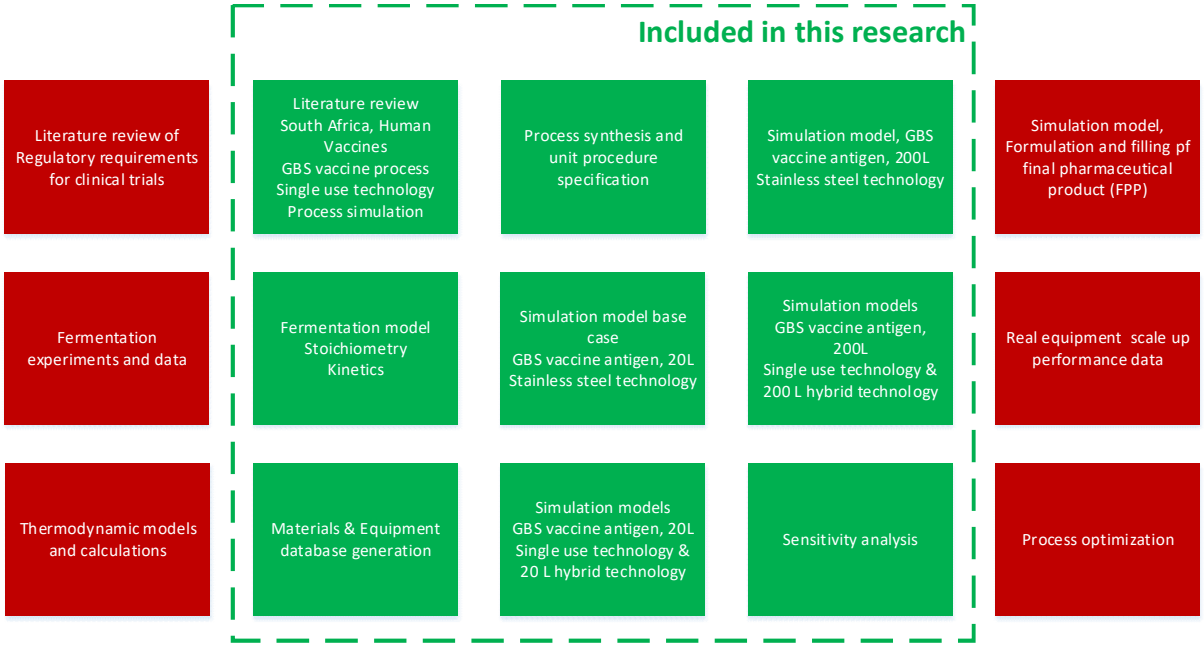

Figure 4: Process simulators project scope and limitations.

1.3 Defining and Investigating the Problem

Developing a new vaccine manufacturing process in South Africa is complex and requires multiple processing options to be considered for achieving required product quality, regulatory compliance, and lowest cost. Process engineering science may be most effective at evaluating the latter, with the assumption that a real process development approach would normally account for all other relevant considerations. Tools for performing this evaluation should in turn be evaluated for their effectiveness in assisting the most cost-effective choices between different processing options.

Computerised process simulation is used extensively in process engineering, but its use for biopharmaceutical process development in South Africa is not extensively documented in literature. The South African context for manufacturing a GBS vaccine had to be defined for this project, as a justification for choosing this process as a case study to demonstrate the use of process simulation in the identified context. A process for making GBS vaccine antigen had to be defined, as well as investigation of some of the different technology platforms available for executing the process. To evaluate these technology choices, the capabilities of process simulation tool had to be defined as a

framework for the outputs for the simulation models to be demonstrated. These aspects, brought together, inform a hypothesis (or hypotheses) around the cost effectiveness of the GBS vaccine process. The results of testing this hypothesis were then used to evaluate the effectiveness of process simulation as a decision support tool for biopharmaceutical process development in South Africa.

1.4 Structure of this dissertation

1. **Introduction**
   - Summary of project context for vaccine manufacturing in South Africa, process simulation tools for biopharmaceutical process development, and vaccine manufacturing technology options.
   - Scope and constraints of the project.
2. **Literature survey**
   - As per the approach defined in the introduction, a detailed survey of:
     - State of human vaccine manufacturing in South Africa as of 2017.
     - Selected examples of existing GBS vaccine process technology.
     - Selected examples of computerised process simulations for biopharmaceutical process development.
     - Introduction to commercial drivers for single use technology and the benefits and limitations thereof.
   - Definition of a problem statement as informed by the preceding literature survey
   - Hypothesis/hypotheses formulated in response to the problem statement
3. **Methodology and experimental approach**
   - Statement of research methodology to be used
   - Description of the experimental structure and approach to be followed for execution.
   - Detailed documentation of the execution of the experimental approach:
     - Process definition by synthesis of multiple existing technologies for GBS vaccine.
     - Specification of a base case simulation model, including the use of specific data input relative to a South African context.
     - Description of the approach used for the evolution of new scenarios from base case model.
     - Structure and specifications for sensitivity analyses on the best performing case scenario, including specific input relative to a South African context.
4. **Results**
   Reporting the findings from the execution of the experimental approach:
   - Fermentation kinetic model parameters found, which will then be used in the simulation models.
   - Reporting the simulation models produced as a result of the simulation exercise.
   - Compiled economic performance results of computer simulations, including graphic comparisons between the three different technology platforms.
   - Results of sensitivity analyses on best case scenario.
5. **Discussion**
   - Describing relationships and trends observed in the economic performance results at the two different scales, and between the three different technology platforms.
   - Comment on the feasibility of the process, in terms of Internal Rate of Return (IRR) relative to a specified discount rate (the hurdle rate).
   - Discussion of the influence of the methods and experimental approach on results.
   - Discussion of the influence of the South African context on results.
   - Comment of the use of process simulators for biopharmaceutical process development.
6. **Conclusion & recommendations**
   - Assessment of the hypothesis/hypotheses.
   - Conclusions on the following:
     - Best performing technology platform and scale for the process modelled
     - Feasibility of the process, in terms of IRR relative to the hurdle rate used.
     - The use of process simulation for process development in a South African context.
   - Recommendations on the use of simulation modelling as a decision support tool for biopharmaceutical process development in a South African context
   - Recommendation on potential future applications of this research.

2 Literature Review

2.1 South African Human Vaccine Manufacturing

South Africa in the Global Vaccine Market

In 1998 Africa represented just 1% of the global market for pharmaceuticals (by monetary value) with government spending on healthcare in sub-Saharan Africa averaging just $ 18 per capita, compared to $ 4000 per capita in the USA (Kremer, 2002). In the 2017 biopharmaceutical world market shown in **Figure 5**, South African manufacturing made up less than 0.2% (BioPlan Associates, 2017).

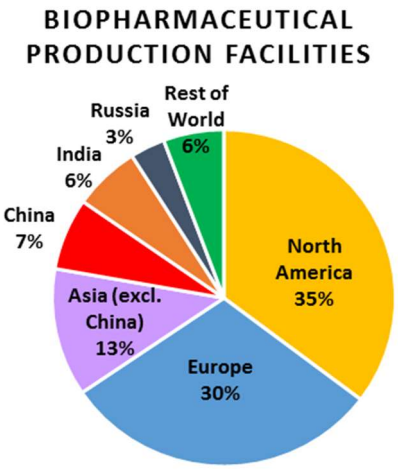

Figure 5: World Biopharmaceutical Markets
Drawn based on (BioPlan Associates, 2017).

Despite not producing human vacccines, the humanitarian market for vaccines in the sub-Saharan Africa region is lucrative. Over 60% of vaccines procured by UNICEF in 2011 were used in this region (Ampofo, 2016), which was valued as a potential market over $ 560 million in 2013 (Pagliusi, Makhoana, et al., 2013). This same market nearly doubled in value by 2014 to $ 900 million (Ampofo, 2016). At present, UNICEF procures vaccines for many Global Alliance for Vaccines and Immunization (GAVI) eligible African countries (shown in **Figure 6**). Sub-Saharan Africa and North Africa are the general exceptions to this trend, yet only five African countries have vaccine manufacturing facilities: Egypt, Senegal, Tunisia, South Africa, and Ethiopia (Makhoana, 2011; Ampofo, 2016).

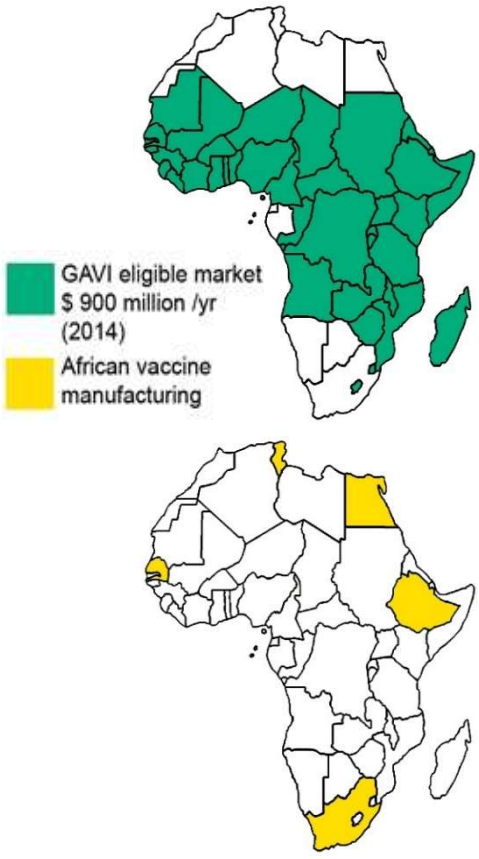

Figure 6: African vaccine market demand (top) and supply (bottom) capacity.
Drawn based on (Ampofo, 2016)

The scarcity of producers on the African continent is due to high barriers to market entry. Vaccines are a technically challenging product to design and produce, as illustrated by the broad range, and specificity of claims made in modern vaccine patents (Khandke et al., 2016). Regulatory requirements for licensing and possible royalty payments to third party developers can also be barriers. There are long time-scales involved in creating a vaccine manufacturing enterprise capable of patenting new technologies (Buckland, 2005; Smith, Lipsitch & Almond, 2011).

Immunisation in South Africa

The South African Department of Health introduced the WHO Expanded Program on Immunisation (EPI) to South Africa in 1995 (Baker, 2010). The EPI-SA is a public health policy for infant and early childhood immunisation against diseases including polio, tuberculosis, pneumococcal disease, and rotavirus. The EPI-SA has been criticised by ex-officials in the program, with challenges described relating to human-resource constraints and cold-chain management (Bateman, 2016).

Despite the supposed challenges, the EPI SA has also experienced a number of successes (Dlamini & Maja, 2016):

- First in Africa to publicly roll-out both the Pneumococcal and Rotavirus vaccines - both in 2009.
- Implementation of a patient friendly single liquid dose hexavalent (6-in-1) vaccine in 2015.

The EPI-SA is credited by Madhi, (2015) for reducing child deaths under 5 in the period between 2000 and 2013. This statistic increased from 75 753 deaths in 2000 to 89 418 in 2005, but the impact of the EPI saw the number decrease to 47 409 by 2013. Madhi's research is (as of 2019) conducted at the Respiratory and Meningeal Pathogens Research Unit (RMPRU) at Chris Hani Baragwanath hospital in Johannesburg (RMPRU, 2019). This unit is responsible for a large body of research outputs which provide insight into disease burdens in Southern Africa and also into efforts to curb infectious diseases in South African children including pneumococcal disease, HIV, tuberculosis, and rotavirus (Madhi et al., in press, 2000, 2010; Klugman et al., 2003; Madhi, 2015).

Madhi and the RMPRU have also been involved in research into a maternal vaccine against GBS disease (RMPRU, 2019), publishing investigations which describe the need for- and potential effectiveness of a maternal GBS vaccine in South Africa (Madhi et al., 2003; Cutland et al., 2009; Kim et al., 2014; Kobayashi et al., 2016). This body of work adds to the international publications on GBS disease and the need for a GBS vaccine (Burns & Plumb, 2013; Schrag & Verani, 2013; Heath, 2016).

Group B *Streptococcus* (GBS) Disease

Group B *Streptococcus* is the most prevalent cause of severe early onset bacterial infection in infants, and in some cases leads to infant mortality or permanent disability. The bacteria are believed to be transmitted from mother to child during childbirth or during late pregnancy (Edmond et al., 2012). It is estimated that between 20 and 25% of all women are carriers of GBS (Burns & Plumb, 2013).

In 2010 the incidence of neo-natal GBS infection in South Africa was 3 per 1000 live births, while the same number for Africa was 1.21 per 1000 live births. In Africa the mortality rate for GBS disease was 22% (Kim et al., 2014). In developed countries like the United States of America (USA) the infection rate in 2010 was only 0.26 per 1000 live births. In the USA and United Kingdom (UK), mothers are screened for GBS colonization and treated with intrapartum antibiotic prophylaxis (IAP) if required. In countries like South Africa without screening infrastructure, IAP is administered in SA based on an assessment of risk factors (Bomela, Ballott & Cooper, 2001). Although IAP is reported to have 80-90% efficacy in preventing early-onset GBS disease (0-7 days), it has no effect in preventing late-onset disease (7-90 days). A vaccine could increase prevention of GBS disease in South Africa by almost four times the efficacy of current best-practices (Schrag & Verani, 2013; Kim et al., 2014; Heath, 2016). When compared to existing available GBS treatments, a Life Cycle Impact Assessment (LCIA) by Kim et al., (2014) found that a GBS Vaccine would be cost-effective as a public healthcare intervention even at a selling price of $20 - $30 (US) per dose, equivalent to about R 250 – R 400.

2.2 Manufacturing Conjugate Polysaccharide Vaccines

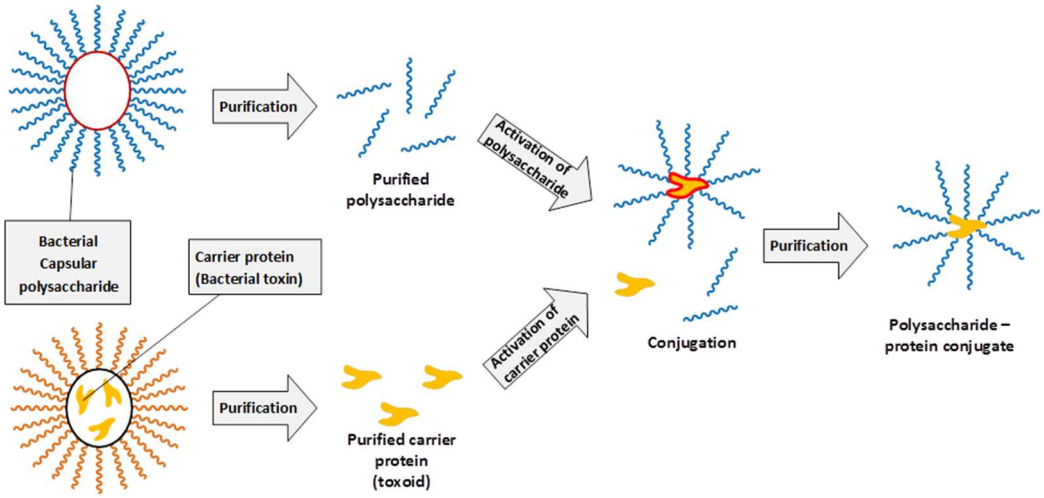

Figure 7: Simplified process for a protein-polysaccharide conjugate vaccine.
Redrawn from (Gambillara, 2012)

Figure 7 above shows a representation of how conjugate vaccines are synthesised by covalently bonding one or more antigens, such as a bacterial polysaccharide, to a carrier protein. Antigens may be produced by either classical fermentation (bacterial, mammalian) or by recombinant protein expression. Some pathogenic gram-negative bacteria produce a capsular polysaccharide which interferes with the immune response of the host organisms and allows the bacterium to evade phagocytosis (Bae et al., 2009; Paoletti, 2016). The same polysaccharide may be used as an antigen to produce an immunologic response in a patient receiving the antigen in a vaccine.

Polysaccharide vaccines produce a satisfactory specific immune response, conferring relatively short-term protection. The linking of the polysaccharide to a carrier protein as shown in **Figure 7** previously, stimulates a stronger immune response than that elicited by the native polysaccharide alone (Jennings & Lugowski, 1982; Michon & Blake, 2001; Lees, Sen & Lopezacosta, 2006; Frasch, 2009; Lee et al., 2009; Josefsberg & Buckland, 2012; Hamidi et al., 2016). The recipient's immune system generates the required immunologic response to the native polysaccharide with antigen specific B lymphocytes (B cells), but linking the polysaccharide to a carrier protein induces the response of T lymphocytes (T cells) which can program long term immunity (Frasch, 2009). A block diagram describing the process for conjugate vaccines is shown in **Figure 8**.

Bacterial polysaccharides and proteins can both be produced by culturing bacteria. In the case of polysaccharide production, the extracellular polysaccharide is released into the culture liquid by chemical treatment which simultaneously decontaminates the product (killing the pathogen). The polysaccharide is then recovered by gravitational separation, size exclusion filtration, affinity filtration, and/or precipitation, depending on its chemical nature (Jennings & Lugowski, 1982; Michon & Blake, 2001; Frasch, 2009; Josefsberg & Buckland, 2012). The carrier protein is fermented separately, and purified by homogenization, gravitational separation, size exclusion filtration, and affinity filtration.

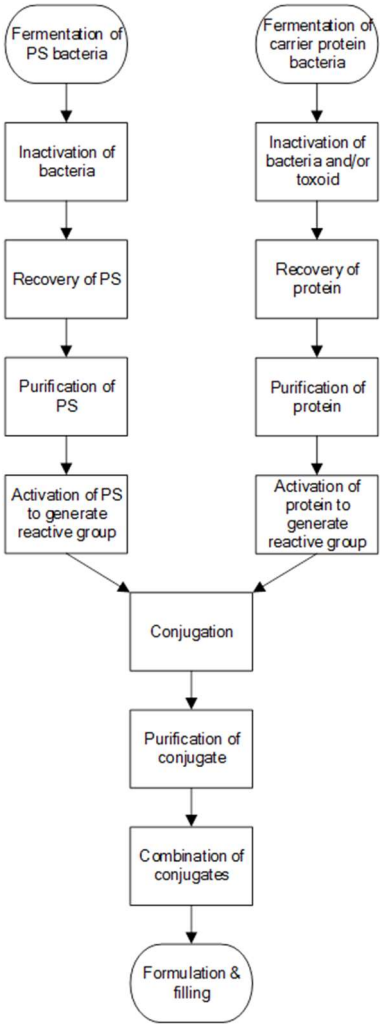

Figure 8: Block flow of conjugate vaccine production process.
Redrawn from (Josefsberg & Buckland, 2012)

Processes to Manufacture a GBS Vaccine Antigen

A number of patents have been awarded to various inventors for a method of producing and purifying capsular polysaccharides of *Streptococcus agalactiae* also known as Group B *Streptococcus* (GBS). GSK (formerly Novartis A.G.) has patented a fermentation, purification, and conjugation process for three different serotypes of GBS capsular polysaccharide (CPS) to a carrier protein. The GSK trivalent conjugate vaccine patent describes a state-of-the-art process to manufacture a GBS conjugate vaccine; however, there have been a number of other patents which describe the process of obtaining the CPS and conjugating it to a protein which are also worthy of consideration for a novel process. Fermentation of GBS at 20 L – 200 L scales is classified as Biosafety Level 2.

2.2.1.1 GBS Fermentation Stoichiometry

Mickelson (1972) studied the aerobic metabolism of *Streptococcus agalactiae* (GBS) by analysis of products after a monoseptic culture of GBS. The primary carbon source studied was glucose, with cultures grown in chemically defined medium with a composition as shown in **Table 2-1** below:

Table 2-1 Chemically defined culture medium used by Mickelson (1972)

Component	Concentration	Units
Glucose	7	mmol/L
Casitone	0.5	% w/w
Yeast extract	1.0	% w/w
Phosphate	0.05	mol/L
Thiamine	0.5	µg/mL
Riboflavin	0.5	µg/mL
Niacin	1.0	µg/mL
Pantothenate	0.5	µg/mL
Pyridoxal	1.0	µg/mL
Biotin	0.0025	µg/mL
Magnesium Sulfate heptahydrate	0.2	mg/mL
Sodium Chloride	0.01	mg/mL
Manganese Sulfate tetrahydrate	0.01	mg/mL
Iron (II) Sulfate heptahydrate	0.01	mg/mL

Six cultures were used to generate data for two experiments in triplicate. The cultures were grown in a 30 mL working volume inside respirometer vessels with 160 mL total volume. Conditions were maintained at pH 6.8 and 37 °C, and agitation was at 90 oscillations per minute.

Mickelson calculated that under anaerobic conditions the GBS cultures metabolised 75% of glucose to lactic acid, and the balance to acetic acid, formic acid, and ethanol. Mickelson reported that under anaerobic conditions the GBS cultures generated an average of 2 moles ATP per mole of glucose consumed from substrate level phosphorylation. Under aerobic conditions, Mickelson reported one mole of oxygen was utilised per mole of glucose consumed, and that about a third of glucose consumed was converted to lactic acid, with the remainder to acetic acid, formic acid, acetoin, and carbon dioxide. Under aerobic conditions 5 moles of ATP were generated per mole of glucose consumed. Mickelson estimated 50% of the ATP was generated from substrate level phosphorylation and 50% from oxidative phosphorylation.

The following stoichiometric equations were reported by Mickelson (1972):

Aerobic conditions

$$C_6H_{12}O_6 \rightarrow 2CH_3CHOHCOOH$$
$$Glucose \rightarrow 2\ Lactic\ acid$$

Equation 2-1

$$C_6H_{12}O_6 \rightarrow 2CH_3COOH + CO_2 + HCOOH + CH_3CHOHCOCH_3$$
$$Glucose \rightarrow 2\ Acetic\ acid + Carbon\ dioxide + Formic\ acid + Acetoin$$

Equation 2-2

$$\boldsymbol{C_6H_{12}O_6 \rightarrow 0.78\ CH_3CHOHCOOH + 0.85\ CH_3COOH + 1.13\ CO_2 + 0.12\ HCOOH + 0.09\ CH_3CHOHCOCH_3}$$
$$\boldsymbol{Glucose \rightarrow 0.78\ Lactic\ acid + 0.85\ Acetic\ acid + 1.13\ Carbon\ dioxide + 0.12\ Formic\ acid + 0.09\ Acetoin}$$

Equation 2-3

Anaerobic conditions

$$C_6H_{12}O_6 \rightarrow CH_3CHOHCOOH + CH_3COOH + C_2H_5OH + HCOOH$$
$$Glucose \rightarrow Lactic\ acid + Acetic\ acid + Ethyl\ alcohol + Formic\ acid$$

Equation 2-4

$$C_6H_{12}O_6 \rightarrow 1.48\ CH_3CHOHCOOH + 0.26\ CH_3COOH + 0.15\ C_2H_5OH + 0.28\ HCOOH + 2ATP$$
$$Glucose \rightarrow 1.48\ Lactic\ acid + 0.26\ Acetic\ acid + 0.15\ Ethyl\ alcohol + 0.28\ Formic\ acid + 2ATP$$

Equation 2-5

While Mickelson's analysis is thorough and includes the major metabolic systems of *Streptococcus agalactiae*, his findings and the analytical methods used were over 35 years old as of 2019.

2.2.1.2 GBS Growth Media

(Wessels et al., 1989, 1990) describe the successful culture of Group B Streptococcus serotype III strain M781 grown on purified Columbia Broth medium. A commercially available composition of Columbia Broth is shown in **Table 2-2** below. In the experiment of Wessels et al. (1990) the medium is also supplemented with a glucose solution of 80 g/L.

Table 2-2 Becton Dickinson Columbia Broth Composition

Component	Conc.[g/L]
Pancreatic digest of Casein	10.0
Yeast Extract	5.0
Proteose Peptone No. 3	5.0
Tryptic Digest of Beef Heart	3.0
L-Cysteine HCl	0.1
Dextrose	2.5
Sodium Chloride	5.0
Magnesium Sulfate (anhydrous)	0.1
Ferrous Sulfate	0.02
Sodium Carbonate	0.6
Tris (Hydroxymethyl) Aminomethane	0.83
Tris (Hydroxymethyl) Aminomethane.HCl	2.86

Source: (Zimbro, 2009)

2.2.1.3 US 8 445 239 B2 - Fermentation processes for cultivating streptococci and purification processes for obtaining CPS therefrom (Costantino et al., 2013)

A process for a GBS conjugate vaccine patented GSK (formerly Novartis A.G.) begins with an inoculum prepared in four 5 L Fernbach shake flasks, each with 1 L of complex growth medium with a composition shown in **Table 2-3** below:

Table 2-3 Complex seed medium for inoculum preparation

Component	Conc.[g/L]
D-Glucose monohydrate	28.7
Yeast Extract	14.8
$Na_2HPO_4.2H_2O$	7.0
$NaH_2PO_4.H_2O$	1.7
	Conc.[mg/L]
Thiamine	0.4
Riboflavin	0.4
Pyridoxine HCl	0.4
Niacinamide	0.4
Biotin	0.9

The flasks are inoculated with 2.75 mL each of working cells. The flask contents are then cultured at 35 °C, with agitation of 200 rpm until an OD_{590} of 0.6 – 1.2 (approximately 4 hours), after which the contents are harvested and pooled in a 5 L glass bottle, to serve as the inoculum for a 300 L fermentor. The fermentor is filled with 150 L of growth medium with a composition shown in **Table 2-4** below:

Table 2-4 Growth medium for pilot scale fermentation

Component	Conc.[g/L]
D-Glucose monohydrate	33.7
Yeast Extract	17.3
$Na_2HPO_4.2H_2O$	1.6
	Conc.[mg/L]
Biotin	1.4

After sterilizing the medium by 0.2 µm filtration into the vessel, the fermentor is inoculated with 4 L of inoculum with an average OD_{590} of 0.6 – 1.2. The batch phase of the fermentation is controlled at 36°C, 0.2 barg head pressure, and pH 7.3. The initial agitation is set to 50 rpm and aeration at 20 NL/min. Dissolved oxygen level is maintained at 30% DO, and regulated by a PID control cascade with stirring speeds of 50 – 350 rpm, followed by aeration of 20 – 100 NL/min, and finally by oxygen partial pressure using an addition of 0 – 100 NL/min pure oxygen. At an OD_{590} of 2.5 - 3.0, an addition of 3.6 L of 150 g/L yeast extract solution is made at 550 mL/min to maintain the culture doubling time at approximately 5 h. At an OD_{590} of 4.5 - 5.0, a second addition of 13.4 L of 150 g/L yeast extract solution is made at 550 mL/min to maintain the culture doubling time at approximately 50 min. At an OD_{590} of 10 - 12, a third feed of 17 L of 550 g/L D-Glucose monohydrate is made at a linear feed rate of 95 mL/min. The final productivity of capsular polysaccharide is between 0.35 g/L and 1.00 g/L.

The vessel is harvested directly via transfer line into a continuous flow disc stack bowl centrifuge, where the biomass is separated from the spent medium at a rate of 100 L/h for 7 minutes. The biomass is then

washed with water at 100 L/h for 3 minutes. The pellet is collected in a 100 L disposable mixing system while the supernatant is discarded to waste treatment. The pellet is inactivated by the addition of 4 M NaOH to a final concentration of 0.8 M based on a pellet density of 1 kg/L. During this step, the capsular polysaccharide is released into solution. The inactivation & extraction proceeds for 36 h at 37 °C and 180 rpm agitation.

A buffer of 1 M TRIS base is added to the inactivated product to a final concentration of 0.1 M, based on the mass of inactivated material. The product is then neutralized in the disposable mixing bag by addition of 6 M HCl until the final pH is in the range 7.5 – 8.5. Proteins and nucleic acids are then precipitated by addition of solutions of 2 M $CaCl_2$ and 96% ethanol, to final concentrations of 0.05 M, and 30%, respectively.

The product of the previous step is then concentrated 10 times by 0.22 µm tangential flow filtration (TFF), followed by dialysis against 3 volumes of buffer solution with a composition shown in **Table 2-5**:

Table 2-5 Precipitation dialysis buffer

Component	Conc.[g/L]
NaCl	34.8
TRIS	4.5
$CaCl_2$	11.0
Ethanol	25 wt%

The permeate containing the waste biomass and precipitate is collected in a 200 L disposable bag via 0.22 µm filtration and sent to waste disposal. The retentate (of about 10 kg) containing the polysaccharide is then diafiltered through a 30 kDa TFF membrane, against 20 volumes of 50 mM TRIS + 0.5 M NaCl buffer at pH 8.8, followed by 10 volumes of 0.3 M Na_2CO_3 + 0.3 M NaCl buffer at pH 8.8. The retentate is collected through a 0.2 µm filter and stored at 2 – 8 °C for up to 15 days. The retentate is then depth filtered through activated carbon supported on cellulose to remove all residual protein contaminants. The filtrate is collected through a 0.2 µm filter and stored at 2 – 8 °C for up to 15 days.

The filtrate from the depth filtration step is diluted to 2 mg/mL polysaccharide using 0.3 M Na_2CO_3 + 0.3 M NaCl buffer at pH 8.8. The diluted product is then re-N-acetylated using 8.3% (vv) acetic anhydride in water and approximately 8% Ethanol. The acetic anhydride solution is added to the polysaccharide solution ibn a ratio 0.5 L per litre and reacted at room temperature for 2 h. The re-N-acetylated product is then filtered through a 30 kDa TFF membrane against 13 volumes of 10 mM KH_2PO_4. The retentate is collected through a 0.2 µm filter and stored at – 20 °C until needed.

The purified polysaccharide is then typically subjected to a conjugation process; however, the details of this are not included in the invention described by Costantino et al. (2013).

A process flow diagram of this process is shown in **Figures 9 and 10** on the proceeding pages.

Costantino et al. (2013), Polysaccharide production for GBS conjugate vaccine - Process Flow Diagram sheet 1 of 2

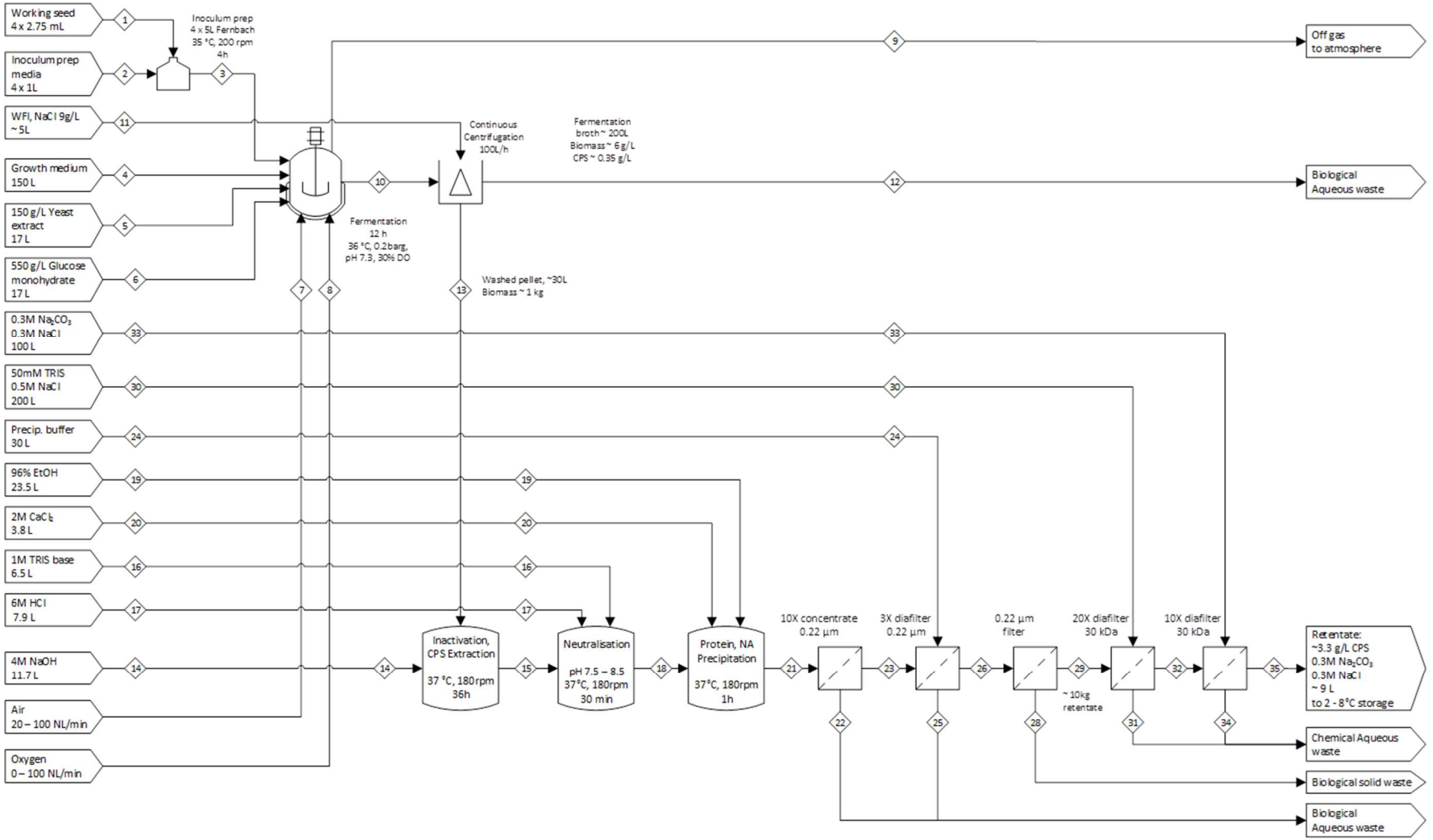

Figure 9: Process for fermentation and purification of GBS polysaccharide - Page 1 of 2

Costantino et al. (2013), Polysaccharide production for GBS conjugate vaccine - Process Flow Diagram sheet 2 of 2

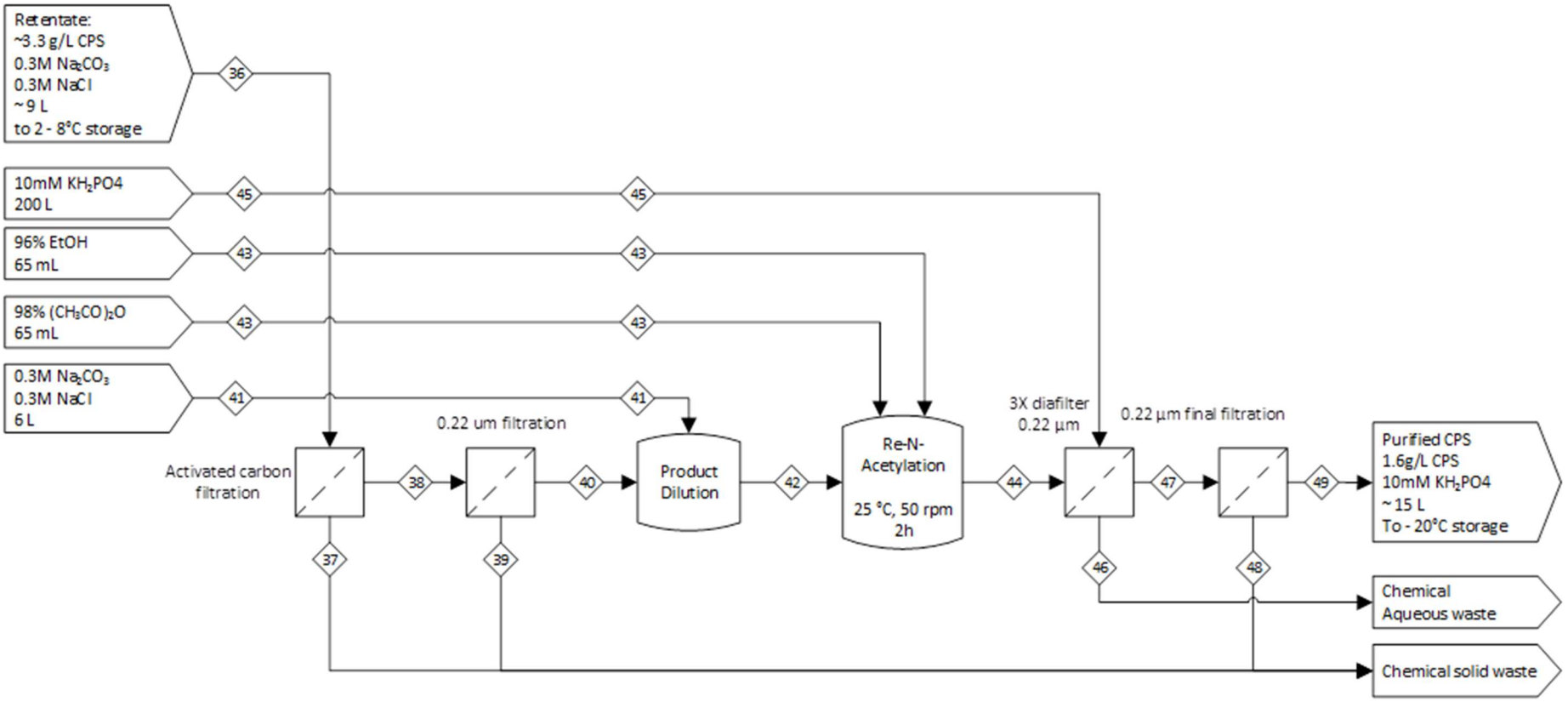

Figure 10: Process for fermentation and purification of GBS polysaccharide - Page 2 of 2

2.2.1.4 Activation of carrier protein by ADH derivatization, and recovery of proteins by ammonium sulfate precipitation

Rana et al., (2016) describe the preparation of polysaccharide – protein conjugate vaccines against *Neisseria meningitides* to an activated carrier protein. The invention is described for use with either Tetanus Toxoid (TT) or CRM-197 as a carrier protein, which is derivatized by reaction with Adipic acid Di-Hydrazide (ADH) in the presence of 1-Ethyl-3-(3-dimethylaminopropyl) carbodiimide (EDC). In the process described by Rana et al. (2016) the carrier protein is reacted with ADH hydrochloride in the presence of EDC in a buffer of 4-Morpholinoethanesulfonic acid (MES). The product is a protein with carboxyl functional groups substituted with aliphatic amino functional groups. The aliphatic amino groups are suitably reactive with available functional groups on an activated polysaccharide.

This method of activation has also been described by Bartoloni et al. (1995) for activation of group B *Neisseria meningitides* capsular polysaccharide for conjugation to either Tetanus toxoid or CRM-197 carrier proteins. In this case the method is used to derivatize the polysaccharide rather than the carrier protein as in the example of Rana et al., (2016).

Recovery of large molecular weight products from solution is described by precipitation with saturated Ammonium Sulfate, in the case of Bartoloni et al. (1995) the method is used for recovery of a carrier protein CRM-197.

2.2.1.5 Activation of polysaccharide by cyanylation

The invention of Capiau et al. (2000) describes protein – polysaccharide conjugate vaccines of several bacterial species: *Haemophilus Influenza b*, *Neisseria meningitidis*, *Streptococcus Pneumoniae*, and *Moraxella catarrhalis*. The patent claims application of this method to *Streptococcus agalactiae* but this embodiment is not explicitly described. The invention utilises a specific conjugation chemistry of activation of the polysaccharide by cyanylation with 1-cyano-dimethylaminopyridinium (CDAP) tetrafluoroborate. The reaction with CDAP forms reactive cyanoester (O-CN) groups on the polysaccharide. This is achieved by the swap of a cyano group from the CDAP with a proton from a hydroxyl group on the CPS. The cyanoester is very reactive and forms stable linkages with amino groups on the activated protein.

This method has been described by (Frasch, 2009) as an alternative to a more established polysaccharide activation by periodate oxidation.

2.2.1.6 Conjugation of polysaccharides to proteins by reductive amination

Roy, Katzenellenbogen & Jennings (1984) describe the method of covalent bonding of polysaccharides to amino functional groups of a protein by reductive amination with sodium cyanoborohydride. This method of conjugating proteins to polysaccharides is a direct reaction mechanism in which the cyanoborohydride ion acts as a nucleophile to reduce free functional groups on the polysaccharide, generating a stable covalently bonded alkylamine. The reaction is reported to be extremely slow when conducted on native polysaccharide reactants but can be accelerated by the addition of more reactive functional groups such as aldehydes or carbonyl groups. The latter can be conveniently added by oxidation of the polysaccharide with sodium periodate, as described by Lees, Sen & Lopezacosta, (2006). Periodate attacks vicinal diols selectively, opening the ring of a cyclic polysaccharide and creating two terminal carbonyl groups. These carbonyl groups are the sites for conjugation to a carrier protein by reductive amination. Reductive amination appears to be a popular method for conjugating proteins to polysaccharides and has been used by multiple authors (Jennings & Lugowski, 1982; Wessels et al., 1990; Mistrette, Danve & Moreau, 2010; Buurman et al., 2019).

However, it is important to note that periodate oxidation opens the polysaccharide ring structure, which could negatively affect the immunogenicity of the polysaccharide as a vaccine antigen (Roy, Katzenellenbogen & Jennings, 1984).

2.3 Process simulation for Biopharmaceuticals

Commercial batch process simulation software

The requirements of an effective batch process simulator are described by multiple authors (Petrides et al., 1989; Shanklin et al., 2001; Papavasileiou et al., 2007; Toumi et al., 2010):

- Ability to generate a single visual representation of the entire process.
- Solve material and energy balances for each process stream.
- Estimate the size of process equipment.
- Estimate equipment occupancies.
- Estimate resource and utility usage and supply capacity.
- Evaluate the economic feasibility of the process.
- Calculate batch time and scheduling.

There are many simulation tools available commercially, but *Aspen Batch Plus*, and *Intelligen SuperPro Designer* are the two most popular commercial software packages. There are also other discrete event simulation (DES) software products such as *Rockwell Arena* and *Witness*, or *ImagineThat Extend* which can be used for process simulation (Gosling, 2005; Papavasileiou, Siletti & Petrides, 2008). A more versatile tool is *Microsoft Excel* which can be used to model chemical- and bio-processes, but may require additional coding with Visual Basic for Applications (VBA) scripts (Papavasileiou, Siletti & Petrides, 2008; Toumi et al., 2010). VBA has also been useful for interfacing data between different software tools, for example using an *Excel* add-in such as *Oracle Crystal Ball* to perform a Monte Carlo simulation sensitivity analysis (Biwer, Griffith & Cooney, 2005; Papavasileiou et al., 2007; Toumi et al., 2010; Chuan et al., 2014).

Aspen Plus and *Intelligen SuperPro* were both introduced to the market around the same time in the 1990s, although initially *Aspen Plus* was found to contain a number of software bugs compared to *Intelligen SuperPro*. Gosling, (2005) reported that *Aspen Plus* had an advantage for simulating dynamic processes with transient behaviour, or processes requiring more flexibility in some operations. *SuperPro Designer* appears to be a popular choice amongst researchers and commercial pharmaceutical manufacturers, possibly due to the less expensive software license fees and the availability of comprehensive models of a variety of commercial bio-processes (Papavasileiou et al., 2007; Papavasileiou, Siletti & Petrides, 2008; Toumi et al., 2010; Chuan et al., 2014; Kulkarni, 2015).

The capabilities of both packages are generally similar, and both also have limitations. Neither software is able to account for all of the dynamic aspects inherent in batch processes, such as flexible scheduling of resources and equipment, or modelling of auxiliary shared services like clean in place (CIP) and sterilize in place (SIP) operations (Shanklin et al., 2001; Gosling, 2005; Farid, 2007; Toumi et al., 2010). *SuperPro Designer* can fulfil the need for flexible scheduling when used together with *SchedulePro* scheduling and debottlenecking software (Toumi et al., 2010).

Building a simulation model

Building a batch process simulation model begins by compiling a comprehensive and reliable database of materials, labour, and processing equipment. For more accurate results it may also be necessary to include data on process performance in the model database. Collecting reliable information on costs and usage parameters of materials and equipment increases model accuracy, but information is not always available for every aspect of every component. Missing data requires assumptions to be made either by consulting subject matter experts, or by using literature and making assumptions based on scientifically accepted empirical knowledge (Papavasileiou et al., 2007; Toumi et al., 2010; Hamidi et al., 2016).

The process model is developed from the Process Flow Diagram (PFD), by building up unit procedures sequentially. Each unit procedure is built from multiple unit operations, and the process model is built from unit procedures which model real process equipment operations, or steps in a process. The model is also tested after each added step to confirm that it produces sensible results before connecting material flows to the next processing step (Petrides et al., 1989; Toumi et al., 2010). When the sequential building up of unit procedures is complete, the resulting process model is a "base case" of the process. The base case is the starting point for all subsequent process development and optimization investigations (Petrides et al., 1989; Tan et al., 2006; Farid, Washbrook & Titchener-Hooker, 2007; Papavasileiou, Siletti & Petrides, 2008; Hamidi et al., 2016).

After establishing a base-case process model; process development decisions are made by making a specific change to the base case and comparing the resulting model to evaluate the change (Papavasileiou et al., 2007; Toumi et al., 2010; Chuan et al., 2014). This "technology tree" approach to model development is shown in **Figure 11** (right). After each progression, the various outcomes can be compared to the base case or to each other.

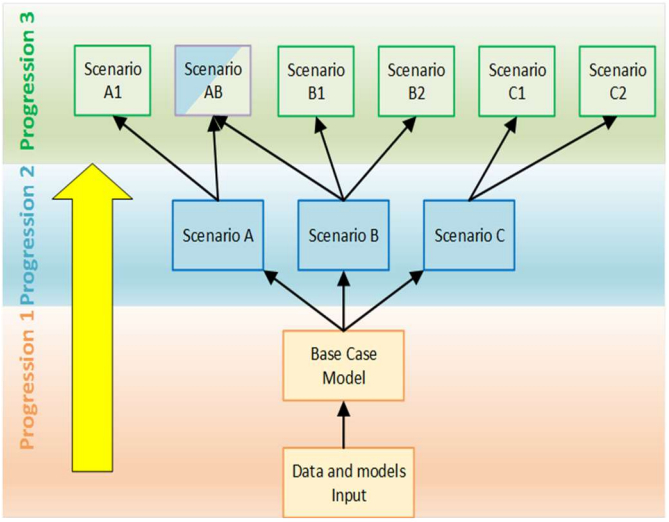

Figure 11: Technology tree approach used for process simulation

Typically, process inputs are evaluated by sensitivity analysis. A method similar to that used by Toumi et al., (2010) was used by Chuan et al., (2014) for selecting the most economical processing route for a recombinant viral protein vaccine. Both authors utilised Monte Carlo sensitivity analysis to quantitatively evaluate the uncertainty in the result of a simulation. This type of analysis is characterized by testing the sensitivity of model outputs to randomized input data. The resulting outputs are typically plotted in a histogram that resembles a distribution curve. This provides a much larger data set which can be used to determine more accurate estimations for the mean and standard deviation of the mean. The data set can then be used to determine the probability that a given result, say, a base case or optimization model, is achievable. This type of sensitivity analysis is one of the only practical ways to quantitatively determine the uncertainty of a simulation result or series of results.

It should be noted that publications such as Toumi et al. (2010) and Chuan et al. (2014) used *Intelligen SuperPro Designer* and followed a similar methodology for evaluating techno-economic process development decisions. Their method for sensitivity required VBA scripting software to process the amount of data needed to generate sensitivity distributions. An example of this type of software is *Oracle Crystal ball* (Oracle, 2008) plugin for *Microsoft Excel*.

The methodology for creating a simulation model of a biopharmaceutical process using *Intelligen SuperPro Designer* has been demonstrated for many different types of processes (Petrides et al., 1989; Petrides, Koulouris & Siletti, 2003; Papavasileiou et al., 2007; Toumi et al., 2010; Chuan et al., 2014), making *SuperPro Designer* a useful database of bio-pharmaceutical process equipment, labour, and materials. The steps for building a process model can thus be summarised as follows:

1. Create database of materials and equipment performance data
2. Build unit procedures from unit operations.
3. Complete base-case model.
4. Evaluate process decisions by comparing results after varying model inputs / structure.
5. Complete one or more model scenarios, compare to base case and to other scenarios.
6. Perform sensitivity analysis of the models to changes in information inputs.

Benefits and Limitations of Process Simulation Exercises

The basic outputs from a batch process simulation for biopharmaceutical processes are published for a variety of processes (Petrides et al., 1989; Papavasileiou et al., 2007; Papavasileiou, Siletti & Petrides, 2008; Toumi et al., 2010) which have been summarised in **Table 2-6** on the proceeding page. It can be observed from the outputs listed below, that the required outputs of an effective simulation model follow directly from the requirements of an effective simulator tool discussed previously in 2.4.1:

- A comprehensive visual process flow diagram
- Mathematical solutions to all Material and energy balances
- Equipment size estimates & occupancy Gantt charts
- Utility usage and supply capability
- Economic analysis of capital and operating costs
- Throughput analysis
- Sensitivity analysis

Table 2-6 Selected simulation outputs from various publications

Research paper	Product / capacity	Capital investment (CAPEX)	Unit production cost (UPC)	Equipment / process	Utilities	Sensitivity analysis	Unique outputs / findings
Petrides et al., (1989)	Porcine growth hormone, 6000 kg/y	$ 29.5 million (1988 USD)	$ 1267 /kg	25% product recovery	$6 million /y spent on detergents for downstream purification	Recovery and solubilisation of inclusion bodies greatest contributors to operating costs	Bioprocess simulator does not answer problems, but rather provides information on which problems to solve
Papavasileiou, Siletti & Petrides, (2008)	Monoclonal antibody, 202.5 kg/y, 2g/L titre	Not reported	$ 415 / kg stainless steel. $ 317 / kg single use	Single use mixing for buffer preparation results in similar facility-dependant costs	Single use technology implementation results in 65% reduction in WFI requirements due to reduced size and number of CIP skids	Monte Carlo, no result reported	Turning point scale for single use technology at 8000 L fermentation capacity beyond which stainless steel is competitive
(Farid, 2007)	Monoclonal antibody, 250 kg/y	$125 - $145 million	$ 260 000 /kg	20 000 L bioreactor,	High cleaning costs for membrane separations	Monte Carlo, downstream processing costs a major factor	Transgenic corn determined as cheapest process technology
Toumi et al., (2010)	Monoclonal antibody or fusion protein, 100 L/batch	Not reported	Not reported	$ 2.6 million reduction in auxiliary equipment requirements	WFI surge tank 130 000 L, still capacity 11 000 L/h	Monte Carlo, no result reported	Simulation as an Interdisciplinary process development platform was most beneficial output
Chuan et al., (2014)	H1N1 influenza capsomere vaccine, 115 kg/year	$ 17.3 million (2013 USD assumed)	$ 81 600 /kg	Fermentor optimum size of 500 L	$ 88 500 /year	Monte Carlo, final biomass concentration 50% of observed variance in UPC	10 000 L fermentation (320 million doses) in minimum 2.3 days for pandemic response

Benefits of Process Simulation Exercises

Economic analysis is one of the most reliable outputs of process simulation due to the availability and accessibility of relatively accurate input data (prices, labour cost, taxation, etc.). Simulation exercises can evaluate the advantages and disadvantages of two competing systems based on the outcomes of different process models. Some of the key findings from economic evaluations for five selected studies are summarised in **Table 2-6** on the preceding page. **Table 2-6** shows that techno-economic studies using process simulation are able to generate quantitative data for a number of different scenarios. Of key importance to the value of these studies is the low initial investment required. Simulations require very little in terms of man hours and materials as compared to setting up and executing the same number of experiments to physically generate data on different process options.

The primary output of a simulation model is to provide information on the key areas of focus for process development including but not limited to: equipment types and sizes, types and quantities of raw materials, utilities, shared services, and operations scheduling (Papavasileiou et al., 2007; Papavasileiou, Siletti & Petrides, 2008; Toumi et al., 2010; Chuan et al., 2014). Toumi et al. (2010) identified valuable indirect benefits of a rigourous simulation exercise for the development of a large-scale process to produce monoclonal antibodies. The simulation exercise provided a universal platform for communication between process development scientists, engineers, and their operations team. The facilitation of communication between teams with different specialisations on a large-scale project with complex interdependencies was emphasised as a key outcome of the simulation exercise, and one that was not part of the initial aims of the exercise.

Simulation exercises are useful at the pre-feasibility stage of project development, for making decisions early on and focusing on key areas. As such, simulation models may also be applied in a cyclic process development and design spaces. Simulation modelling is a versatile tool, in that it may be used at any stage of a design process for generating information and evaluating decisions.

Limitations of Process Simulation Exercises

A popular phrase for simulation modelling is that a model is only as good as the data that goes into it. This is often represented by a difference between real process outputs and simulation model results. The output of a process model is also affected by the accuracy of the mathematical models and algorithms used within the unit procedures (Petrides et al., 1989). More rigorous models can improve prediction of real outputs; however, this is only possible where such models exist (Shanklin et al., 2001). This is the greatest limitation of simulation modelling, in that real processes are too complex to be modelled precisely by mathematical equations. It should; however, be noted that the required precision of simulation models is not to be exact but rather to direct process development, making them no less effective despite this limitation.

The published literature on process simulation exercises is more aligned with the European and US markets for biopharmaceutical products, with many studies published on monoclonal antibody production processes, with fewer studies focusing on vaccine production processes (Petrides et al., 1989; Farid, 2007; Papavasileiou, Siletti & Petrides, 2008; Toumi et al., 2010; Chuan et al., 2014). Application of simulation modelling as an analytical tool for other types of processes and in other contexts will require more rigorous database construction, as the existing databases in commercial software packages are generic for the US & European context.

2.4 Single use process technology

The first successful demonstration of single use bioreactor was Vijay Singh's rocking bag reactor for small to medium scale (0 - 100 L) cell culture (Singh, 1999, 2001), shown in **Figure 12**. The technology for single use mixing vessels that could compete with industrial stainless-steel technology was developed over time though. Some of the first patents were different to the universally accepted STR type design. One such design by Hyclone Laboratories employed a hydraulic mixing block (Stewart, 1999) which was used in a patent for a single use bag mixer by Merck (Ekambaram et al., 2000).

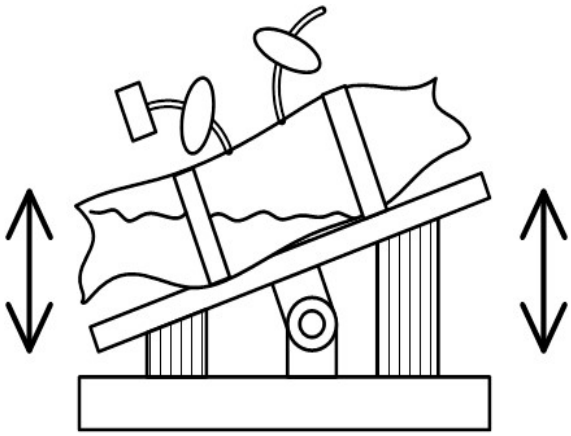

Figure 12: Rocking platform bioreactor.
Redrawn from (Singh, 1999, 2001)

A magnetic drive mixer was patented in the 1980s for use in stainless steel tanks by Rains & Rathbun (1980), but this was not realised in single use mixers for another 20 years. The advent of single use mixers in the early 2000s required a novel solution to physically separate the agitator bearing and drive unit to enable the use of integral plastic film technology. Hyclone laboratories was one of the first to employ this design in a single use STR in 2006 (Goodwin, Elgan & Larsen, 2006). A more sophisticated design (shown in **Figure 3** on page 4) using a magnetic bearing similar to that of Rains & Rathbun (1980) with a turbine mixer set inside a plastic film bag was patented in 2009 by Xcellerex (Hodge, Galliher & Fisher, 2009).

This type of design has been used by bioreactor manufacturers such as Sartorius Stedim, GE Healthcare (GE acquired Hyclone and Xcellerex), and Pall. The general design of modern developments of single use bioreactors uses a magnetically coupled impeller inside an integral plastic bag. Contemporary single use reactor systems feature steel or polycarbonate tanks with the product contact portion of the vessel made from plastic polymers. The benefit is that the inner plastic bag can be sterilized by gamma irradiation before use and disposed of immediately after use, eliminating the need for in-house validation of cleaning and sterilization processes.

Commercial driving force for single use technology

In two decades spanning 1999 to 2019, one of the most important decisions for new and existing bio-pharmaceutical manufacturing has been whether (and if so to what extent) to deploy Single Use Technology (SUT). Initially, SUT was initially introduced as a strategy for mitigating cross-contamination between different products in multi-product facilities (Shukla & Gottschalk, 2013), but has been demonstrated to also have the capability to enable additional economic, regulatory, and technological advantages (Ransohoff, 2005; Shukla & Gottschalk, 2013; Lopes, 2015).

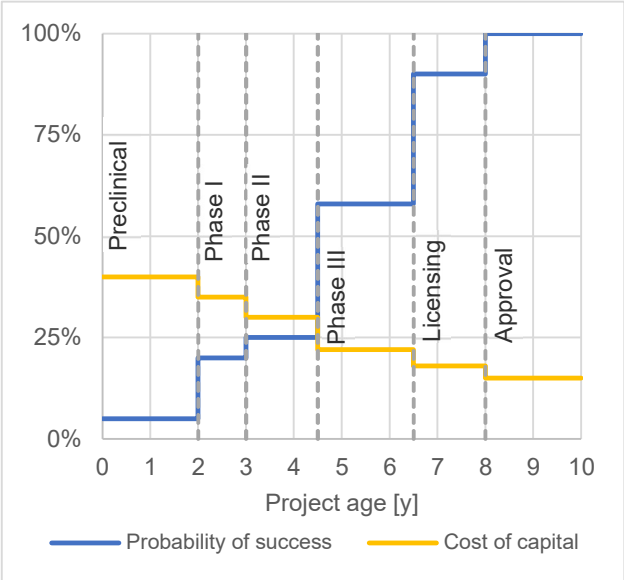

Figure 13: Project risk for novel biologics.
Redrawn from (Ransohoff, 2005)

SUT can be attractive for high risk projects such as new drug development, due to the decreased capital cost, reduced operating costs, and increased speed to market (Gottschalk, 2008; Allison & Richards, 2014; Lopes, 2015). As much as 90% of investigational drug projects do not make it

through full clinical trials to commercialisation, and those that are successful can cost investors up to $2.8 billion in total investment and opportunity costs (DiMasi, Grabowski & Hansen, 2016). It can be seen in **Figure 13** (previous page bottom right) that project risk is extremely high in the initial stages of a project, where the prospect of success is low, and the cost of capital is high. Introducing SUT can reduce financial risk for new projects by reducing the capital costs, particularly in pre-clinical and early clinical development stages of the project life cycle.

Advantages and Disadvantages of Single Use technology

Single use technology has both advantages and disadvantages. Each unit operation in a bioprocess needs to be evaluated on a case-by-case basis for the appropriateness of SUT (Gottschalk, 2008). Some of the commonly listed advantages and disadvantages in published literature are shown in **Table 2-7** on the proceeding page.

Table 2-7 Advantages and disadvantages of Single Use Technology

Advantages	Examples of advantages	Disadvantages	Examples of disadvantages
Reduced capital cost	Monoclonal antibody multi-product facility COG model capital cost savings of 40 €/g (Sinclair & Monge, 2005) Capital costs an order of magnitude lower than for single use facilities compared to stainless steel based facilities (Zheng, 2010) Viral vaccine process potential 50% reduction in capital costs by implementing single use technology (Lopes, 2015)	**High cost of consumable material**	Monoclonal antibody multi-product facility COG model consumable cost increase of 25 €/g (Sinclair & Monge, 2005)
Process and product flexibility	Single use technology more cost-effective for multi-product facilities (Sinclair & Monge, 2005) Process performance is not compromised by SUT (Whitford, 2010) Single use technology for an aseptic filling operation reduced campaign fill time from 36 h to 12 h per 100 000 vials (Merck Millipore, 2013).	**Loses competitiveness with stainless steel at large scales (above 2000 L)**	High consumables costs limit the scalability of single use processes (Eibl et al., 2010) Single use bag requirements increase with scale, a monoclonal antibody process at 2000 L scale using 60 x 200 L reactor bags per batch would require 220 bags per batch when scaled up to 8000 L (Papavasileiou, Siletti & Petrides, 2008).
Reduced risk of cross contamination	Disposable product contact layer reduces risk of cross contamination (Eibl et al., 2010; Zheng, 2010; Flaherty & Perrone, 2012; Shukla & Gottschalk, 2013; Lopes, 2015)	**Validation of Leachables and Extractables**	Extensive validation requirements for single use components (Lopes, 2015)
Reduced utility costs for CIP & SIP	Monoclonal antibody 2x2000 L fermentation, cost savings: 28 800 kWh, $ 250 000 WFI generation, $ 7 300 CIP chemicals (Flaherty & Perrone, 2012) Monoclonal antibody 200 kg/y single use 65% less WFI and CIP chemicals, 50% less steam (Papavasileiou, Siletti & Petrides, 2008).	**Increased emissions footprint of single use materials (petroleum plastics)**	Monoclonal antibody, 1000 L scale: Total energy demand for manufacture stainless steel technology of 1000 MJ, while the equivalent plastic single use bags, total energy demand is 4000 MJ (Rawlings & Pora, 2009)
Reduced Labour costs	Monoclonal antibody multi-product facility COG model Labour savings of 30 €/g (Sinclair & Monge, 2005) Monoclonal antibody 2x2000 L fermentation, labour savings: $ 60 000 in direct labour costs for cleaning tanks (Flaherty & Perrone, 2012)	**Technology gap to stainless steel**	Lack of reliable single use sensors (Aranha, 2004; Eibl et al., 2010; Löffelholz et al., 2013) Maximum scale of equipment available for single use is 2000 L, for stainless steel 20 000 L (Shukla & Gottschalk, 2013; Pörtner, 2015)
Reduced overall cost of goods	Monoclonal antibody 200 kg/y, cost of goods for single use $ 317 /kg, vs. $ 415 /kg for stainless steel (Papavasileiou, Siletti & Petrides, 2008)		

Leachables and Extractables

Many types of single use equipment and consumables (e.g. bags, filter membranes, transfer and connection assemblies) are constructed with plastic product contact parts, These plastic parts carry a risk of transfer of organic compounds (polycarbonates) from the product contact surface into product solutions or solvents (organic acids, ethanol). An illustration of these effects is shown in **Figure 14**.

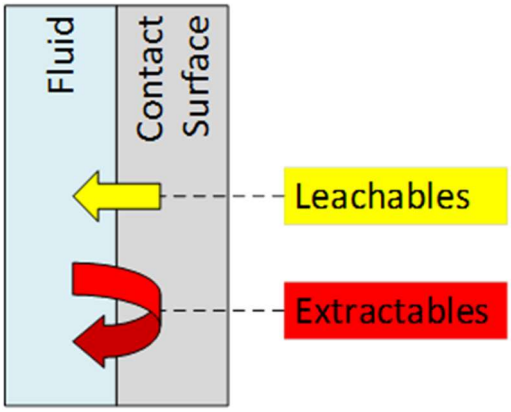

Figure 14: Leachables and extractables
Redrawn from (Merck Millipore, 2013)

Some compounds (e.g. 2-Ethylhexanoic acid or Lauric acid (Martin & Ding, 2009)) found in the product contact layer of single use components (liquid filters, reactor bags) can leach into a typical pharmaceutical solvent (e.g. 1 N sodium hydroxide or 30% ethanol) under normal conditions such as those found in a typical production environment. These types of compounds are called ***Leachables*** – *compounds that can move from the material into a drug substance under normal conditions* (Martin & Ding, 2009).

A much larger range of different compounds (e.g. Palmitic acid) found in the product contact layer of single use materials can be extracted into a carrier solvent (e.g. 10 N acetic acid or 10 N sodium hydroxide) by continuous liquid extraction under extreme conditions (concentrated organic solvent or low pH). These types of compounds are called ***Extractables*** – *compounds that can move from the material into a model solvent under extreme conditions.* (Martin & Ding, 2009).

The concentrations of these two types of compounds (Leachables and Extractables) allowable in a drug substance are specified by regulatory authorieis such as the FDA, WHO, and SAHPRA, as potential contaminants. The costs associated with testing single use components for compatiblity with a process is a technologoical risk described by mupltiple literature sources on the implementation of single use technology (Sinclair & Monge, 2002; Aranha, 2004; Martin & Ding, 2009; Eibl et al., 2010; Martin, 2010; Zheng, 2010; Löffelholz et al., 2013; Shukla & Gottschalk, 2013).

Manufacturers of SUT disclose their materials of construction, but the burden of process validation for regulatory product licensing purposes still lies with the manufacturer. Validation for stainless steel equiment is well-known in the biopharmacuetical industry, and includes welding, passivation, pickling, and electropolishing certification, as well as valves, sensors and fittings with quality certification. Validation for SUT is less well-known compared to requirements for stainless-steel, but typically requires extractables and leachables testing with all process fluids (normal conditions) as well as validation of the bag manufacturing process itself.

2.5 Defining the Research Project

Problem Statement

GBS disease affects a small percentage of the global population; however, the incidence is large enough to warrant a humanitarian intervention to prevent further loss of life and suffering (Edmond et al., 2012; Kim et al., 2014; Kobayashi et al., 2016). Vaccines are scientifically proven beyond doubt to be one of the safest and most effective healthcare interventions, yet as of 2019 there is no vaccine for GBS disease. A Life Cycle Assessment (LCA) study by Kim et al., (2014) reported that a maternal vaccine against GBS disease could be sold for up to $30 per dose (R 400), giving the finished vaccine a *potential value of between $2 million and $4 million/kg* depending on the final dosage.

Time to market for new vaccine products is critical since IP protection is limited and R&D investment needs to be recovered quickly (Ransohoff, 2005; DiMasi, Grabowski & Hansen, 2016). Patents offer international protection for countries (including South Africa) which are party to the World Intellectual Property Organisation (WIPO) IP protection treaties, but these protections typically cover specific claims and can be challenged in court. New vaccine development must follow an integrated approach which includes process and analytical method development within relatively short time frames, and without compromising quality (Chu & Robinson, 2001; Buckland, 2005; Chuan et al., 2014; Hamidi et al., 2016). Low-cost analytical tools are needed to assist with process development in the expedited project development pathway, particularly with decision making when multiple processing routes and technology choices are available. This type of decision support tool must identify the most critical areas of a process to be considered in further detail before proceeding with pilot scale operations (Shanklin et al., 2001; Gosling, 2005; Papavasileiou et al., 2007; Toumi et al., 2010).

Developing and operating biopharmaceutical processes in South Africa is a unique scenario subject to limited industrial manufacturing capacity. The South African market for biopharmaceuticals is small compared to global competitors, making it challenging for manufacturers to procure starting materials and to find buyers for products at competitive prices. Projects are exposed to the financial risks of an economy based on volatile commodities markets, and investors face unique context specific risks in addition to an already high-risk investment environment associated with novel biopharmaceutical products. Identifying these and evaluating the quantitative impact on a prospective process under development could help to mitigate some of the risks involved.

Simulation model objectives

- Build a relevant database of materials, equipment, and process parameters from literature (Dean, 1999; Perry & Green, 2008; Haynes, 2014), and appropriate software tools (Aspen Technology Inc., 2017; Intelligen Inc., 2017).
- Determine a simple kinetic model (Monod, 1949) for GBS serotype III cultivation at 20 L scale.
- Build a process simulation model of a trial GBS vaccine process at 20 L and 200 L production scales using three different technology approaches (Stainless Steel, Single Use, and Hybrid) at each of the two scales.

Analysis objectives

- Quantitative: Economic evaluation of three technology choices - stainless steel, single use, and hybrid technology, at two scales – 20 L and 200 L, using a trial GBS vaccine as an example.
- Qualitative: Evaluate the use of simulation model results for technology selection and scale-up performance forecasting.
- Quantify the uncertainty associated with the models used to generate results by conducting a sensitivity analysis of the model outputs to the model inputs.
- Evaluate the use of process simulation tools for a novel GBS vaccine process in a South African context.

Research hypotheses

Cost of goods influences a new vaccine's commercial viability in an industry where lower product price is competitive with market power. A Techno-economic evaluation of three technology options for the production of a GBS trial vaccine antigen will provide information to reduce financial risk and support more commercially viable decisions during process development.

In the case study of a trial vaccine; it is hypothesised that single use vessels will yield a lower cost of goods at 20 L and 200 L process scale, as compared to stainless steel vessels. This is hypothesised due to an expected reduction in operating costs for clean- and sterilize-in-place requirements for stainless steel technology. A hybrid of the two technology options would yield an even lower cost of goods by combining the best economic properties of both single use and stainless-steel technologies.

Purpose & Function of this Research

The purpose of this research is to test the application of an existing process design and analysis tool to a context which is not well understood. The method of computer simulation modelling for evaluating process development decisions is an established tool in commercial bioprocessing, yet its application to biopharmaceutical processes in a South African context is not well documented compared to the established biopharma markets of Europe, the US and Asia. The South African industry is in its infancy compared to the latter global market powerhouses, a comparison that lends credence to the idea that the same rules of thumb for process development may or may not apply in the South African context.

The evaluation of single use vs. stainless steel technology is a well-known process development decision. Single use technology is often promoted as a time and money saving option, particularly for early process development. Part of the purpose of this research is to test this popular opinion in a South African context, where the deployment of new technology may be affected by economic and other forces.

The function of this research is therefore to generate information on a novel vaccine process, and then to analyse the information to determine its relevance in terms of the problem statement. Firstly, the function is to determine the most cost-effective technology for a novel vaccine process, and secondly to determine the suitability of process simulation tools for biopharmaceutical process development in a South African context. The hypothesis being tested is deliberately formulated based on a literature survey which is overwhelmingly based in the more established biopharma markets. The result of the thesis should therefore give insight into the economic climate faced by South African biopharmaceutical processing industry as compared to traditional knowledge of this field in Europe and the US.

This research is not intended to function as the sole consideration for the suitability of process simulation tools for biopharmaceuticals process development in South Africa but is intended to provide quantitative data on the subject from a process engineering perspective. In performing its function successfully, this research will make an evaluation of the feasibility of a novel GBS vaccine process, and also evaluate the suitability of process simulation tools for biopharmaceutical process development in a South African context. Subsequently this research may be used to support a decision to either use or not to use these tools for the development of future processes in this specific context.

Key Research Questions

- Which technology platform between single use and stainless-steel technology performs better in terms of cost of goods for production of a trial GBS vaccine antigen?
- What kind of information can process simulation generate about scale-up implications of technology choices for the GBS vaccine antigen manufacturing process?
- Which areas of the GBS vaccine antigen production process are most sensitive to input information and initial modelling assumptions?
- What is the influence of a South African context on the development and operation of a process to make a GBS vaccine antigen?

3 Approach to Project and Methodology

3.1 Research methodology

A modified version of the scientific method described by Harrison (2017) (**Figure 15**) was used for this thesis. The modified approach was to define the problem after the literature survey rather than beforehand. This was done to create a better context specific understanding of the problem by literature survey before attempting to define it. Each step of the methodology was as follows:

1. Characterise the problem by a literature survey (**Refer to 2.1 – 2.4**)
2. Define a problem (**Refer to 2.5**)
3. Define a hypothesis (**Refer to 2.5**)
4. Design and execute experiments
5. Analyse results
6. Draw conclusions and make recommendations.

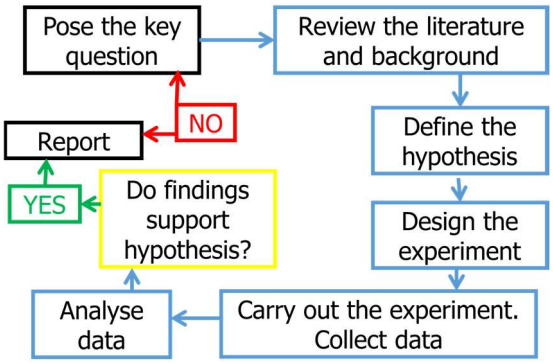

Figure 15: The Scientific method with iterative approach (Harrison, 2017)

3.2 Experimental approach

The experimental design was factorial in that the different process options were compared based on simulation exercises with the experiment having a 2x3 factorial structure, shown in **Table 3-1** below. The experiment was designed to evaluate the effect of scaling up three different approaches to process technology for the development of a process to manufacture a protein-polysaccharide conjugate vaccine against GBS disease. The process scale up was evaluated at 20 L and 200 L:

Table 3-1 Experimental matrix for factorial experiment design

	Stainless steel technology	**Single use technology**	**Hybrid technology**
GBS III conjugate 20 L	Stainless steel fermentor and media tanks, glassware	Single use fermentor, disposable containers and mixing bags	Stainless steel fermentor disposable containers and mixing bags
GBS III conjugate 200 L	Stainless steel fermentor and tanks, glassware	Single use fermentor, disposable containers and mixing bags	Stainless steel fermentor, disposable containers and mixing bags

Three process models were built, starting with the industry standard practice of using stainless steel process equipment and glass laboratory equipment. The stainless-steel model forms the base case, from which scenarios were developed with either single use or hybrid technology platforms. The method for execution of the experimental programme was as follows:

1. Fermentation experiments conducted in triplicate at 2 L scale.
2. A reaction equation for aerobic stoichiometry of *S.agalactiae* on glucose was derived from literature (Mickelson, 1972).
3. A simple fermentation kinetics model was derived using Microsoft Excel, using experimental data for cultivation of *S.agalactiae* serotype III on glucose (The Biovac Institute, 2018).
4. A process model of a trial GBS vaccine process was built using Intelligen SuperPro Designer 9.5. The process was synthesised from literature on similar existing processes (Bartoloni et al., 1995; Swennen, 2012; Costantino et al., 2013; Rana et al., 2016).

5. The scenarios as shown in **Table 3-1** were developed from the base case.
6. A sensitivity analysis was performed on the scenario with the lowest cost of goods, using selected parameters and assumptions from the base case scenario.
7. Different scenarios were compared to each other, with an evaluation of technology options based on the cost of goods. The analysis was extended to include project feasibility, based on an estimated product value in the current market.
8. Conclusions were drawn on the best technology and scale for the chosen process, as well as on the potential feasibility of the process. Further conclusions were drawn on the relevance of process simulation tools for process development in the context of the developing South African vaccine manufacturing sector.

3.3 Materials & methods

The process models which form part of the research output of this thesis were built following a structured approach as described in the following section. The models were built in four steps:

Step 1: Define a real process by written process description and process flow diagram

Step 2: Build a base case simulation model of the real process defined in Step 1

Step 3: Develop alternative scenarios from the base case, either by new technology platforms, or by scaling up the process

Step 4: Develop alternative scenarios from the best performing model in the previous step, to test the model sensitivity to inputs and assumptions.

Defining a Real Process to make a GBS polysaccharide-protein conjugate

The starting point of the process was considered to be media preparation and inoculum preparation for fermentation. The base case at 20L scale was specified using stainless steel as a technology platform (Stainless steel fermentor and buffer tanks and pharmaceutical glassware for smaller volumes). The fermentation process was based on a patent of Novartis (acquired by GSK) (Swennen, 2012), with extraction of the Capsular Polysaccharide (CPS) from the cells by treatment with sodium hydroxide (Schifferle et al., 1985; Wessels et al., 1989; Michon & Blake, 2001). The purification process was based on another patent of GSK for adherent carbon filtration (Costantino et al., 2013), followed by a conjugation process adapted from multiple sources: Activation of the polysaccharide by cyanylation with CDAP (Capiau et al., 2000; Shafer et al., 2000) or by periodate oxidation (Roy, Katzenellenbogen & Jennings, 1984), while activation of the carrier protein would be done either by reaction with ADH and EDC (Bartoloni et al., 1995; Rana et al., 2016) or by reductive amination (Jennings & Lugowski, 1982; Wessels et al., 1990; Mistrette, Danve & Moreau, 2010; Buurman et al., 2019).

It was decided to proceed with cyanylation and ADH derivatization as a conjugation method as it is reported in literature (Roy, Katzenellenbogen & Jennings, 1984; Frasch, 2009) that periodate oxidation carries a risk of compromising immunogenicity of polysaccharides due to the opening of the cyclic ring.

The major product of this process was a purified protein-polysaccharide conjugate. The product value was estimated as $ 4 million /kg as described in the Problem Statement on page 26.

Fermentation process description

The cell banks were aliquoted in 1mL of wild-type GBS serotype III bacteria suspended in glycerol and stored at -80°C. The raw material for fermentation was Columbia growth medium (Swennen, 2012; Costantino et al., 2013) and cell bank vials of GBS III bacteria. The medium composition has been defined by Zimbro (2009) but contains animal derived nutrients (beef heart) which were substituted for non-animal derived components, such as yeast extract or soytone (Vrang et al., 2002; Swennen, 2012). This is recommended for human vaccines as per current Good Manufacturing Practices (Pharmaceutical Inspection Co-operation Scheme, 2014).

The modified medium composition is shown in **Table 3-2** below.

Table 3-2 Fermentation medium Composition

Component	Conc.[g/L]
D-(+)-Glucose	20.0
Tryptic digest of casein (Soytone)	27.0
Yeast Extract	5.0
Sodium Chloride	5.0
L-Cysteine HCl	0.1
Sodium Carbonate	0.6
Magnesium Sulfate (anhydrous)	0.14
Ferrous Sulfate	0.02

A 300 mL inoculum was prepared in the above medium by cultivation at 37°C and 150 rpm for 3h in baffled shake flasks inside a temperature-controlled incubator. Inoculum medium was supplemented with a buffer of 0.83 g/L Tris (Hydroxymethyl) Aminomethane (TRIS) and 2.86 g/L TRIS.HCl. The feed to the fermentation process was composed of 30 g/L Yeast Extract and 400 g/L Dextrose in WFI.

The fermentation was carried out for 8 h at 37 °C with aeration of 0.5 vvm with production of Biomass and Capsular Polysaccharide (CPS). For modelling, SuperPro 9.5 academic software built in fed-batch mass/time model was used (Intelligen Inc., 2017). The fermentor was assumed to have a maximum stirred volume of 26 L for addition of the inactivation agent. Optical density at 590 nm (X), and glucose concentration (S) were recorded every hour for 8 hours. The resulting data was used to derive parameters for a Monod kinetic model of the fermentation.

The process described below was not performed experimentally in this thesis but was used to define the structure of simulation models.

The culture is inactivated with 5N NaOH to a final concentration of 0.8 N for 16 hours at 55 °C. This performs a dual operation by inactivation of the microorganism and releasing the CPS into solution (Schifferle et al., 1985; Wessels et al., 1989; Michon & Blake, 2001). Inactivation was followed by harvesting to a receiving tank with stirrer for neutralization with 6N HCl. Nucleic acids and proteins were precipitated in the same vessel by addition of 2 N $CaCl_2$ and 96% ethanol (Costantino et al., 2013), to a final concentrations of 0.13 N and 30%, respectively. The precipitation reaction proceeded adiabatically for 1 h before harvesting to centrifugation.

Purification process description

A disk stack bowl centrifuge was used to recover the supernatant containing the CPS, which was concentrated 40 X by Tangential Flow Filtration (TFF) through a 30 kDa membrane, followed by 20 X diafiltration into 50mM TRIS + 8.5 mM NaCl buffer. The retentate is further 10 X diafiltered into 0.3N Na_2CO_3 (Costantino et al., 2013). The retentate was then filtered through an orthogonal carbon filter to remove residual proteins by adsorption. The filtrate was collected in a reaction vessel, to which saturated acetic anhydride was added to a concentration of 0.8N, to re-N-acetylate the CPS (Schifferle et al., 1985; Wessels et al., 1989; Michon & Blake, 2001). The reaction proceeds adiabatically for 1 h before filtration through a 0.22 µm filter into a sterile holding bag for storage at 2 – 8 °C.

Conjugation process description

The carrier protein was activated with 0.5N ADH in the presence of 0.1N EDC (Bartoloni et al., 1995; Rana et al., 2016). The reaction proceeded for 2 h at 4°C. The activated protein was then 20 X diafiltered into a buffer of 10mM MES and 0.2M NaCl.

The purified CPS was activated with 100 mg/mL CDAP in acetonitrile (Shafer et al., 2000; Frasch, 2009; Rana et al., 2016) to a final mass ratio of 3:4 CDAP:CPS. The reaction proceeds for 2 minutes and 30 seconds at 4°C and pH 9.2, before addition of 0.2M Triethylamine (TEA) in 2:1 volumetric ratio with the CDAP solution. The activated protein was then added to the mixture and the reaction proceeds for 24 h at 4°C with agitation of 50 rpm.

After the conjugation reaction was completed, the conjugate was precipitated by addition of saturated ammonium sulfate (Bartoloni et al., 1995). The precipitation proceeded adiabatically for 12h with agitation of 50 rpm, before recovery of the precipitate by centrifugation in a tubular centrifuge. After centrifugation the pellet was re-suspended in MES/NaCl buffer before 20 X diafiltration through a 30 kDa membrane into Phosphate Buffered Saline (PBS). The solution was filtered through a 0.22 µm membrane under LAF into a sterile holding bag. The final product was stored -20 °C until formulation (not included in this process).

A Process Flow Diagram (PFD) of this process at 20L fermentation scale using stainless steel technology platform was drawn. The diagrams are shown in **Figures 16 and 17** on the proceeding pages.

Process Flow Diagram of GBS 20L stainless steel technology platform

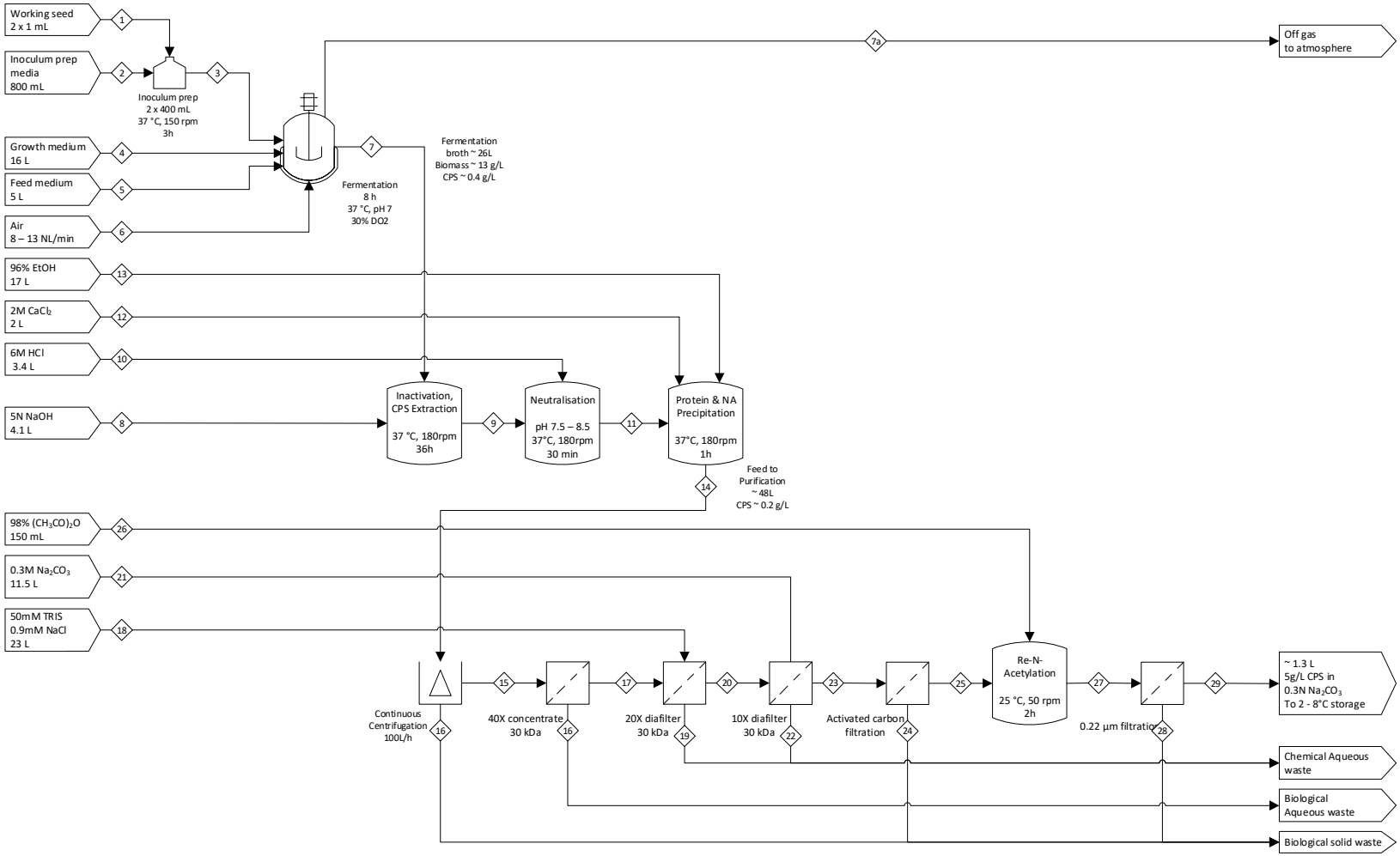

Figure 16: Process Flow Diagram of GBS 3 20L stainless steel process page 1 of 2

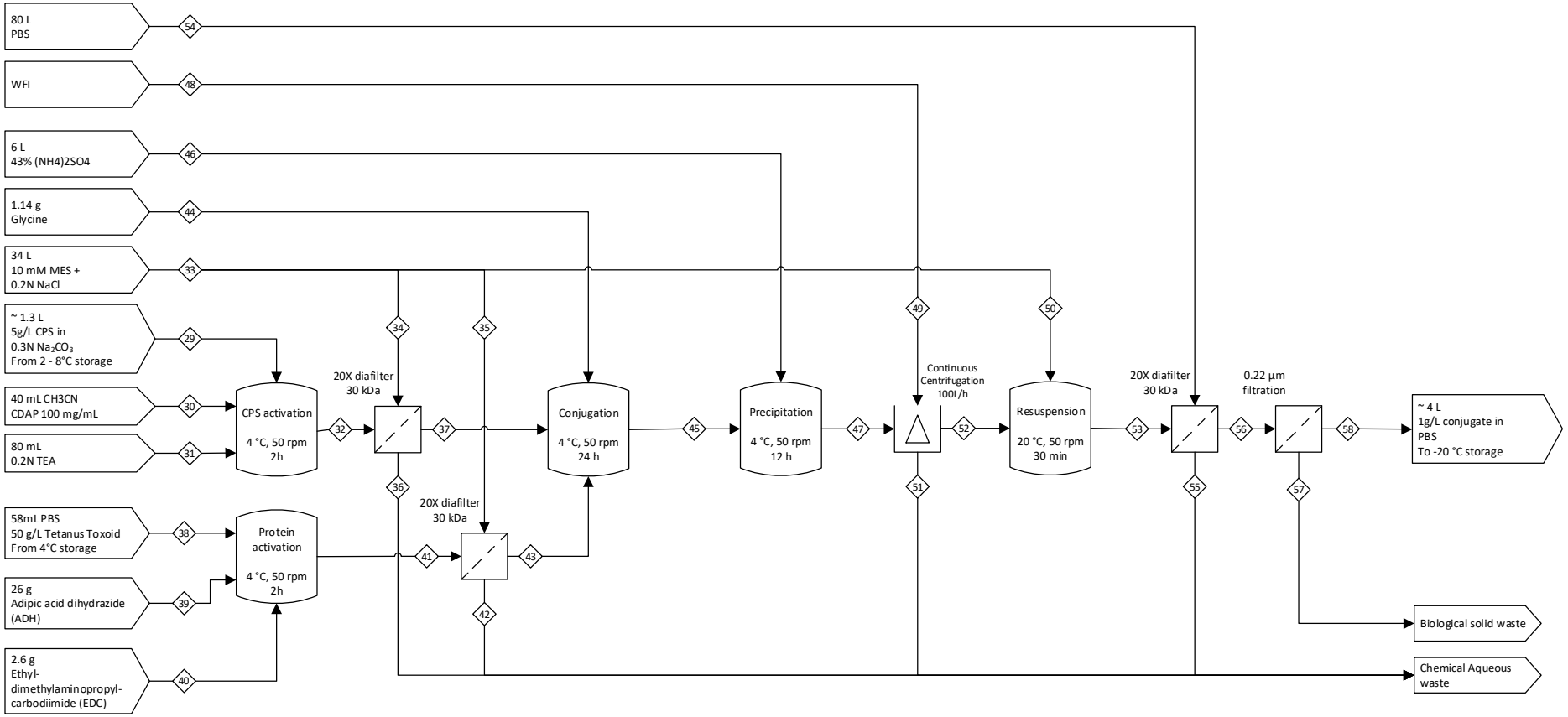

Figure 17: Process Flow Diagram of GBS 3 20L stainless steel process page 2 of 2

Building a Simulation model of 20L GBS III conjugate process (Base Case Model)

The base case simulation model was built in *SuperPro* starting with unit procedures Inoculum preparation and fermentation media preparation. The next unit procedure was fermentation, followed by each successive procedure until final filtration of the purified conjugate drug substance. This method is more conveniently presented in **Table 3-3** below. A detailed version of model construction is documented in **Table A-4** in Appendix A. Screen capture images of the resulting models are shown in Appendix A. Equipment specifications and costs (**Table A-5**), consumables specifications and costs (**Table A-8**), and raw materials specifications and costs (**Table A-11**) are listed in detail in Appendix A.

Table 3-3 Building a Simulation Model of a 20 L Process to make a GBS conjugate antigen

Model Tag	Real process step(s)	SuperPro unit procedure(s)
SS-01f	Inoculum medium filtration 0.22 µm using peristaltic pump	→ Filtration → Dead End Filtration  SS-01f / P-101 0.22um Filtration
SS-01	Inoculum preparation 2 x Fernbach flasks each with 400 mL (800 mL total) Inoculum medium (**Table A-15**). Each flask inoculated with 1mL of wild type GBS type III in glycerol. Inoculum cultured for 3 hours at 37 °C, surface aerated.	→ Inoculum preparation → in a Shake flask 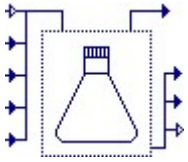 SS-01 / I-101 Inoculum
S-02	Media preparation 16L of batch media in a 50L, stainless steel media preparation tank	→ Storage/Blending → Bulk → Batch → in a Blending Tank 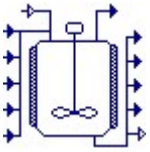 SS-02 / T-101 50L Media tank

Model Tag	Real process step(s)	SuperPro unit procedure(s)
S-02f	Inoculum medium filtration 0.22 µm using peristaltic pump	→ Filtration → Dead End Filtration  SS-02f / P-101 0.22um Filtration
S-03	20 L fed-batch fermentation, 320 mL inoculum into 16 L batch medium (**Table A-16**), 5 L feed (**Table A-17**). Culture at 36 °C for 12h, pH 7.3, 0.2 barg, 0.5 vvm sterile air Inactivation for 16 h at 55 °C in 0.8M NaOH	→ Batch vessel procedure → In a Seed Fermentor 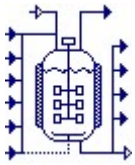 SS-03 / R-101 Fermentation
S-04	Neutralisation to pH 7.0 with 6N HCl, followed by 60min precipitation of nucleic acids for 60min in 0.05N $CaCl_2$ and 30% Ethanol. Assumptions: 100% precipitation of proteins and nucleic acids	→ Storage/Blending → Bulk → Batch → in a Blending Tank 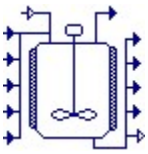 SS-04 / T-102 Neut./Precip.
S-05	Centrifuge in disk stack centrifuge with 88% solid liquid separation efficiency for supernatant recovery	→ Centrifugation → Disk stack 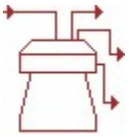 SS-05 / C-201 Centrifugation

Model Tag	Real process step(s)	SuperPro unit procedure(s)
S-06	Tangential flow filtration, concentrate to approximately 1 L, followed by 20X diafiltration against TRIS 50mM + NaCl 0.5M. Assumptions: 5% product loss.	→ Filtration → Diafiltration 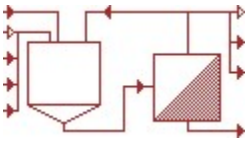 SS-06 / TF-201 TFF TRIS
S-07	Tangential flow filtration, 10X diafiltration against 0.3N Na_2CO_3. Assumptions: 5% product loss.	→ Filtration → Diafiltration 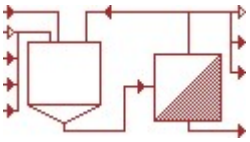 SS-07 / TF-201 TFF Na2CO3
S-08	Hold TFF product capture vessel	→ Storage/Blending → in a Disposable → Generic container 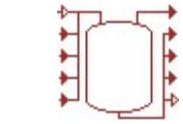 SS-08 / ST-201 TFF hold
S-09	Protein removal by adherent filtration though orthogonal carbon filter Assumptions: 15% product loss	→ Filtration → Dead End Filtration 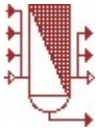 SS-09 / F-201 Protein removal

Model Tag	Real process step(s)	SuperPro unit procedure(s)
S-10	Re-N-acetylation of polysaccharide with Acetic anhydride (final conc. 8.3%vv). Reaction at room temperature for 2 h.	→ Storage/Blending → in a Disposable → Generic container 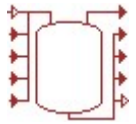 SS-10 / ST-201 Re-N-Acetylation
S-11	Bioburden reduction filtration 0.22 µm using peristaltic pump	→ Filtration → Dead End Filtration 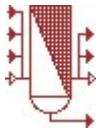 SS-11 / P-201 0.22um filtration
S-12	Cold storage temporary hold for 16h at 2–8 °C	→ Storage blending → Bulk → Batch → in a Tote 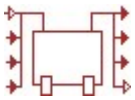 SS-12 / Cold Room 2 - 8 °C hold
S-13	Polysaccharide activation with CDAP (3:4 mass ratio CDAP:PS) at 4°C for 2 h, 90% conversion of PS	→ Batch vessel procedure → in a Seed Bioreactor  SS-13 / R-301 PS activation

Model Tag	Real process step(s)	SuperPro unit procedure(s)
S-14	Diafilter activated polysaccharide against 20x volumes of 10 mM MES + 0.2N NaCl. 5% product loss.	→ Filtration → Diafiltration 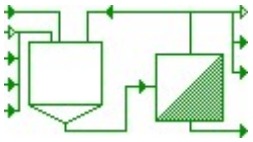 SS-14 / TF-201 TFF Mod-PS
S-15	Carrier protein activation with Adipic Acid Dihydrazide (ADH) 25°C for 1 h, 90% conversion of carrier protein	→ Batch vessel procedure → in a Seed Bioreactor  SS-15 / R-302 TT activation
S-16	Diafilter activated TT protein against 20x volumes of 10 mM MES + 0.2N NaCl	→ Filtration → Diafiltration 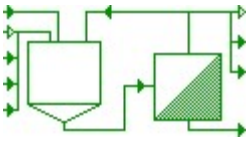 SS-16 / TF-301 TT diafilter
S-17	Conjugation of derivatized TT protein to activated polysaccharide, 52% conversion of Modified Polysaccharide	→ Batch vessel procedure → in a Seed Bioreactor  SS-17 / R-303 Conjugation

Model Tag	Real process step(s)	SuperPro unit procedure(s)
S-18	Ammonium Sulfate precipitation of conjugate, 5% product loss.	→ Batch vessel procedure → in a Seed Bioreactor  SS-18 / R-304 Conj. Precipitation
S-19	Centrifuge in tubular bowl centrifuge with 95% solid-liquid separation efficiency for solids recovery. Blot excess liquid with sterile paper.	→ Centrifugation → Bowl 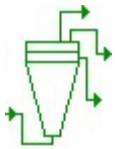 SS-19 / C-301 Centrifugation
S-20	Resuspension in 10 mM MES + 0.2N NaCl, 2% product loss	→ Storage/Blending → in a Disposable → Generic container 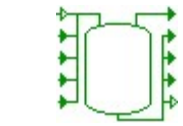 SS-20 / ST-201 Resuspension
S-21	Diafilter (polishing) Conjugate against 20x volumes of Phosphate buffered saline (PBS). 5% product loss	→ Filtration → Diafiltration 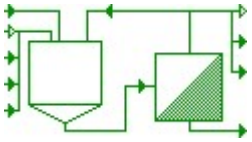 SS-21 / TF-302 TFF polish

Model Tag	Real process step(s)	SuperPro unit procedure(s)
S-22	Bioburden reduction final filtration before transfer to formulation. 1% product loss.	→ Filtration → Dead End Filtration  SS-22 / P-201 Final filtration

3.4 Base Case Model Specifications and Assumptions

Process assumptions

Several simplifications and assumptions were made to complete the base case process model. Areas which required most simplification were chemical reactions and solid-liquid separations. In doing so it was assumed that the function of the models was not to predict thermodynamic behaviour, but rather techno-economic behaviour.

Where reliable thermodynamic models were not available, or where literature sources were limited or non-specific, model parameters were adjusted according to the assumptions listed in **Table 3-4** below. A recurrent assumption for chemical reactions where no reaction data was found, was that products were simulated as water (with conservation of mass). This was made based on another assumption that the real products of these reactions were dilute (Concentration < 5% by mass) and could thus be simulated as water. In many cases, specific model inputs were chosen to achieve an assumed output yield.

Table 3-4 Model Assumptions and Simplifications

Model Tag(s)	Real process	Model assumptions and simplifications
SS-01f, SS-02f, SS-11, SS-22	0.22 µm filtration	Assumed 100% Biomass removal (no other components removed in model) Assumed Flux rate 4000 L/m^{2}h (EMD Millipore, 2013)
SS-01, SS-03	Fermentation of GBS bacteria on Columbia growth medium	Specified Nitrogen source as Soytone (8.7% Nitrogen) and Yeast extract (11% Nitrogen) (BD Biosciences, 2006).
SS-02	Medium preparation	Assumed 30 min mixing time for 95% homogeneity
SS-03, SS-01	Fermentation	Simulated fermentation stoichiometry as **Equation 3-1** Assumed 400 mg/L fermentation titer Assumed 8 h fermentation time Simulated inactivation as **CH3COHCOOH → WFI** Assumed 16 h inactivation reaction time
SS-04	Neutralization of sodium hydroxide with hydrochloric acid **NaOH (aq) + HCl (aq) → NaCl (aq) + H_2O**	Assumed Extent of reaction 100% (wrt. NaOH) Assumed 60 min reaction time
SS-04	Precipitation of nucleic acids with calcium chloride and ethanol.	Assumed 5% product loss Reactions simplified to: **$CaCl_2$ → WFI** Assumed extents of reaction 100% **PS-III → WFI (X=5%)** Assumed extents of reaction 5% Assumed 60 min reaction time

Model Tag(s)	Real process	Model assumptions and simplifications
SS-05	Centrifugation	Assumed 100% Biomass to solids Assumed 12% product (CPS) to waste Assumed 30% sedimentation efficiency Assumed 30 min centrifugation time
SS-06	Diafiltration	Assumed 90% < recovery of CPS to retentate Simplified to CPS rejection coefficient of 0.9975 (94% recovery)
SS-07	Diafiltration	Assumed 90% < recovery of CPS to retentate Simplified to CPS rejection coefficient of 0.9975 (92% recovery)
SS-09	Protein removal	Assumed 15% product loss Assumed filter flux rate 250 L/m^2
SS-10	Re-N-Acetylation **$R\text{-}NH_2 + (CH_3CO)_2O \rightarrow R\text{-}NHCOCH_3$**	Reaction simplified to: **$(CH_3CO)_2O$ -> WFI** Assumed Extents of reaction 100% Assumed no product loss Assumed 60 min reaction time
SS-12	Cold storage for 16 h at 2-8 C	Simulated cold room equipment as a temperature-controlled tote with electrical cooling to simulate gas compressor running cost. Excluded refrigerant from utilities costing.
SS-13	Polysaccharide activation by cyanylation with CDAP **R-OH + R'-CN^+ → R-OCN + R'-N**	Simulated reactions as: **PS-III → Mod-PS-III** **TEA → WFI** Assumed extents of reaction 90% by mass for both reactions above Assumed 2 h reaction time
SS-14	Diafiltration of activated CPS	Assumed 90% < recovery of Mod-CPS to retentate Simplified to Mod-CPS rejection coefficient of 0.9975 (95% recovery)
SS-15	Carrier protein activation by ADH / EDC	Simulated reactions as: **TT + ADH → TT-ADH** Assumed extents of reaction 90% by mass of TT **EDC → WFI (X=90%)** Assumed extents of reaction 90% by mass Assumed 60 min reaction time

Model Tag(s)	Real process	Model assumptions and simplifications
SS-16	Diafiltration of activated carrier protein	Assumed 90% < recovery of TT-ADH to retentate Simplified to TT-ADH rejection coefficient of 0.9975 (95% recovery)
SS-17	Conjugation **R-OCN + R'-ADH → R-R'**	Simulated reactions as **Mod-PS-III + TT-ADH → TT-PS-III** Assumed extents of reaction 100% relative to TT Assumed 24 h reaction time
SS-17	Quenching of reaction by solid Glycine	Simulated reactions as **Glycine → WFI** Assumed extents of reaction 100% Assumed 30 min reaction time
SS-18	Conjugate precipitation by Salting out	Assumed 95% recovery of conjugate Simulated reactions as: **$(NH_4)_2SO_4$ → WFI** Assumed extents of reaction 95% **TT-PS-III → WFI** Assumed extents of reaction 5% Assumed 60 min reaction time
SS-19	Centrifugation in tubular bowl centrifuge	Assumed 95% recovery of conjugate to solids Assumed 30 min centrifugation time
SS-20	Conjugate resuspension in MES buffer	Assumed 2% product loss Simulated product loss as: **TT-PS-III → WFI** Assumed extents of reaction 2% Assumed 60 min reaction time
SS-21	Diafiltration of conjugate into PBS	Assumed 90% < recovery of conjugate to retentate Simplified to TT-PS-III rejection coefficient of 0.9975 (95% recovery)

Fermentation Stoichiometry

Fermentation stoichiometry was developed by combining three literature sources (Mickelson, 1967, 1972; Swennen, 2012) and using material balances to simplify complex fermentation bio-reactions into a single stoichiometric equation.

Mickelson (1972) conducted two experiments, each in triplicate, and quantified the reaction products through various chemical assays available at the time. Mickelson (1972) presented the following model for the aerobic degradation of glucose by *Streptococcus agalactiae*:

Aerobic conditions

$$C_6H_{12}O_6 \rightarrow 2CH_3CHOHCOOH$$
$$Glucose \rightarrow 2\ Lactic\ acid$$

Equation 2-1

$$C_6H_{12}O_6 \rightarrow 2CH_3COOH + CO_2 + HCOOH + CH_3CHOHCOCH_3$$
$$Glucose \rightarrow 2\ Acetic\ acid + Carbon\ dioxide + Formic\ acid + Acetoin$$

Equation 2-2

$$\boldsymbol{C_6H_{12}O_6 \rightarrow 0.78\ CH_3CHOHCOOH + 0.85\ CH_3COOH + 1.13\ CO_2 + 0.12\ HCOOH + 0.09\ CH_3CHOHCOCH_3}$$
$$\boldsymbol{Glucose \rightarrow 0.78\ Lactic\ acid + 0.85\ Acetic\ acid + 1.13\ Carbon\ dioxide + 0.12\ Formic\ acid + 0.09\ Acetoin}$$

Equation 2-3

Mickelson (1972) excluded capsular polysaccharide (CPS) from his analysis, most likely due to the small quantities produced during fermentation relative to organic acids and carbon dioxide. Swennen (2012) reported the yield of CPS from a controlled fed-batch fermentation of GBS serotype III should be at least 30 mg/g dry cell weight (DCW) and preferably 60 mg/gDCW.

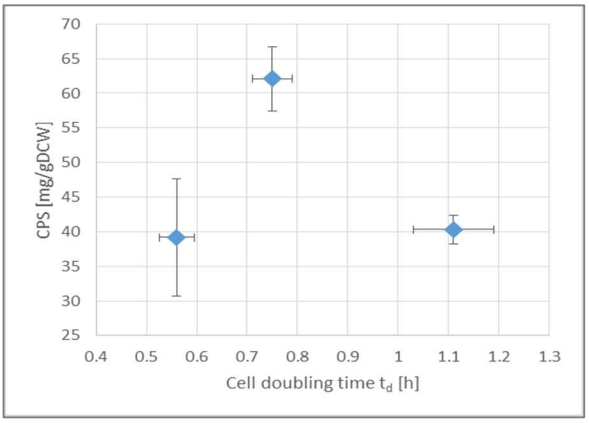

Figure 18: CPS productivity for GBS serotype 3
Based on Costantino et al. (2013)

Swennen (2012) showed that CPS yield was proportional to final biomass concentration. For GBS strain M781 – 3 (a strain of GBS serotype III) the typical fermentation titers achieved by Costantino et al. (2013) are shown in **Figure 18**.

Equation 3-1 below was derived by adding to Mickelson's (1972) equation: By adding oxygen and biologically available nitrogen (NH_3) to the reactants, and adding biomass ($CH_{1.8}O_{0.5}N_{0.2}$), water, and CPS ($(C_{35}H_{52}O_{31}N_2)_n$ to the products, and by using available degrees of freedom in the form of an empirical material balance for the coefficients (refer to Appendix A for material balance calculations).

$$\boldsymbol{C_6H_{12}O_6 + a\ O_2 + b\ NH_3 \rightarrow c\ CH_{1.8}O_{0.5}N_{0.2} + d\ CO_2 + e\ H_2O + f\ CH_3CHOHCOOH + g\ CH_3COOH + h\ CH_3CHOHCOCH_3 + i\ HCOOH + j\ CPS}$$

Equation 3-1

Fermentation Kinetics

Three fermentations were carried out at 2 L scale, as described previously in **3.3.1**. The optical density at a wavelength of 590 nm, and glucose concentration were recorded at specific intervals. The experimental data was fitted to the Monod growth model, defined by **Equation 3-2**:

$$\boldsymbol{\mu = \mu_{max} \frac{S}{K_S + S}}$$ Equation 3-2

(Monod, 1949)

μ	Specific growth rate [h^{-1}]	S	Limiting substrate concentration
μ_{max}	Maximum specific growth rate [h^{-1}]	K_S	Half rate constant $S_{\left\vert \frac{\mu}{\mu_{max}}=0.5 \right.}$

To determine the parameter K_S, the differential equation for the growth of cells **Equation 3-3** below had to be solved:

$$\boldsymbol{\frac{dX}{dt} = \mu X}$$ Equation 3-3

Integration between the starting biomass concentration X_o, at time t_o, and any biomass concentration X at time t:

$$\int_{X_o}^{X} \frac{dX}{X} = \mu \int_{t_o}^{t} dt$$

$$\mu(t - t_o) = \ln \frac{X}{X_o}$$

$$\mu(t) = \frac{\ln \frac{X}{X_o}}{t - t_o}$$

One approach to determine the maximum specific growth rate $\boldsymbol{\mu_{max}}$ was to plot optical density as a proxy for biomass ($\boldsymbol{X}$) over time, and then fit an exponential trend line to the data. The maximum specific growth rate $\boldsymbol{\mu_{max}}$ could be estimated from the exponent of the trend-line (**Equation 3-4** on the proceeding page), as shown in **Figure 19** on the proceeding page.

Method 1 exponential trend line

$$\frac{dX}{dt} = \mu X$$

$$\int \frac{1}{X} dX = \mu \int dt$$

$$\ln X + B = \mu t + A$$

$$\ln X = \mu t + C$$

$$X = e^{(\mu t + \ )} = e^{\mu t} e^{C}$$

$$X = Ke^{\mu t}$$ Equation 3-4

By plotting log(X) vs. t including the exponential growth phase, the value of μ_{max} was estimated by the exponent of **Equation 3-4** for the data in the exponential growth phase. This assumed that the maximum specific growth rate occurs during this phase of the culture.

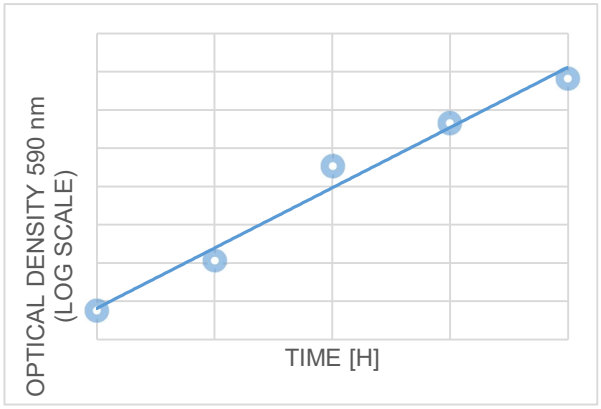

Figure 19: Typical plot of optical density over time with exponential trend line

The half rate constant K_s was estimated by plotting specific growth rate vs. substrate concentration and fitting a logarithmic trend line (**Equation 3-6** below) to the data, as shown in **Figure 20** (below right). This yielded an analytical expression (**Equation 3-7** below) for K_s (Refer to Appendix A for derivation).

$$S\Big|_{\frac{\mu}{\mu_{max}}=0.5}$$ Equation 3-5

$$\mu = \alpha \ln S + \beta$$ Equation 3-6

$$K_s = e^{\left(\frac{0.5\mu_{max}-\beta}{\alpha}\right)}$$ Equation 3-7

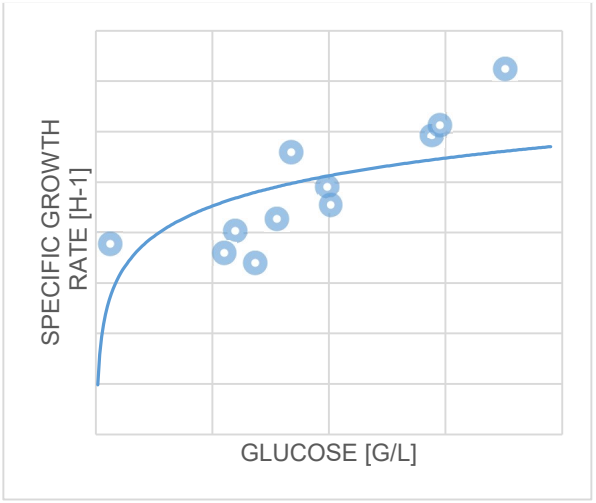

Figure 20: Typical plot of specific growth rate vs. glucose concentration, with logarithmic trend line

Method 2 linear trend line

An alternative approach for finding K_S and μ_{max} was by rearranging **Equation 3-2** into terms $\frac{S}{\mu}$ vs. S, which results in **Equation 3-8** (bottom), and plotting the straight line to derive the parameters:

$$\mu = \mu_{max}\frac{S}{K_S + S}$$ Equation 3-2

$$\mu\left(\frac{K_S + S}{S}\right) = \mu_{max}\frac{S}{K_S + S}\left(\frac{K_S + S}{S}\right)$$

$$\mu_{max} = \mu(t)\frac{K_S + S}{S}$$

$$\frac{\mu}{S} = \frac{\mu_{max}}{K_S + S}$$

$$\frac{S}{\mu} = \frac{1}{\mu_{max}}S + \frac{K_S}{\mu_{max}}$$ Equation 3-8

The typical plot of **Equation 3-8**, with slope of $\frac{1}{\mu_{max}}$, and a y-axis intercept of $\frac{K_S}{\mu_{max}}$, is shown in **Figure 21** below.

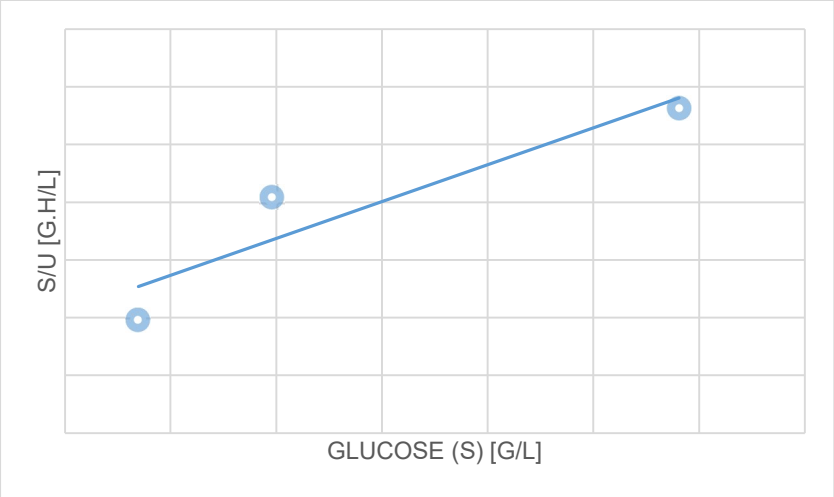

Figure 21: Typical plot of S/μ vs. S with straight trend line

This plot yielded the following solutions for K_S and μ_{max}:

$$\mu_{max} = \frac{1}{m} \qquad K_S = \frac{c}{m}$$

Both of the abovementioned Methods 1 and 2, were used to determine Monod kinetic parameters for use in the simulation models. The averages of parameters for each of the three fermentation experiments from each of the two methods were calculated (refer to **Appendix A** for derivations). The method for selecting the preferred method was by comparing literature values for the culture doubling time with the doubling times calculated by each of the two Method, using **Equation 3-9**. The criteria for selecting the preferred method was that the kinetic parameters that produced the closest doubling time to a literature source (Swennen, 2012; Costantino et al., 2013) was selected as the preferred method.

$$t_d = \frac{\ln 2}{\mu_{max}} \qquad \text{Equation 3-9}$$

3.5 Model development into New Scenarios

The approach to model development was similar to that shown in **Figure 11** in section **2.3.** Three progressions from the base case model generated 6 different models, shown in **Figure 22** below. The base case model (Model 1 in **Figure 22**) was chosen as a 20L fermentation scale, with an established stainless-steel technology platform. The first progression produced two variations on the base case, a single use technology platform (Model 2.1 in **Figure 22**) and a hybrid of single use and stainless-steel technology (Model 2.2 in **Figure 22**). The third development was to scale-up the base case model to 200 L fermentation scale (Model 3.1 in **Figure 22**), followed by development of the 200L scale model into two variations employing the alternative technology platforms of single use (Model 3.2 in **Figure 22**), and hybrid (Model 3.3 in **Figure 22**).

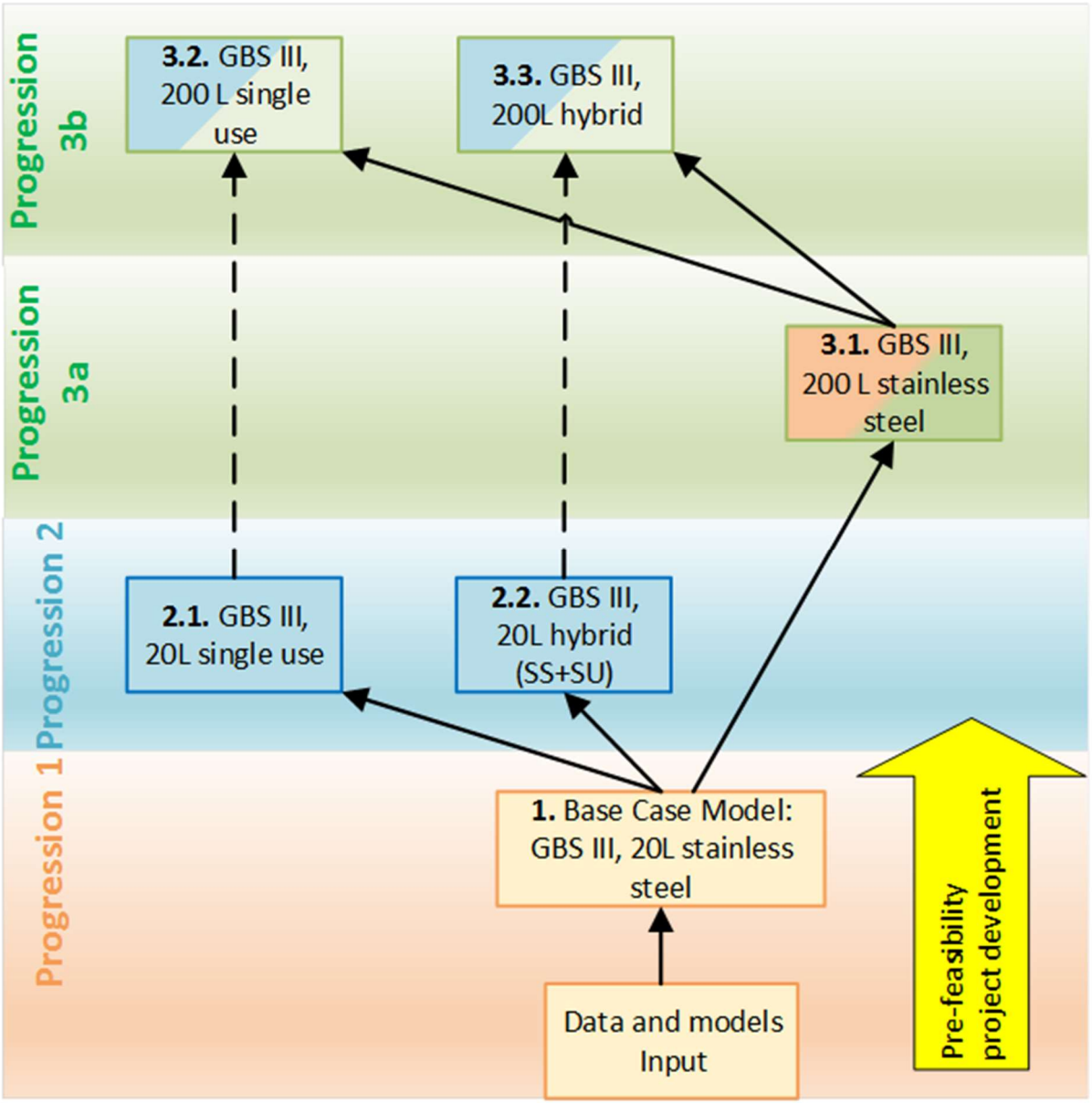

Figure 22: Model development approach

*The resulting models are submitted as electronic files with this thesis. Detailed model specifications and screen capture images appear in **Appendix A**. All electronic files submitted are listed in **Chapter 4: Results**.*

It was assumed that the following properties and specifications of the models did not change with new scenarios:

- Available equipment & consumables types
- Reaction stoichiometry and extents of reactions
- Process scheduling limited to one week per batch
- Raw materials specifications*
- Utilities specifications
- Labour unit costs
- Economic assumptions (hurdle rate etc.)
- Fermentation stoichiometry and kinetic parameters*

*For 200L fermentation the fermentation procedure time was reduced from 8 h to 7 h. This was required as the simulations would not converge to a solution when keeping the fermentation time at 8 h and the raw materials input to the fermentation constant. The error was found to be due to nutrient limitation and a specific minimum fermentation product concentration at the endpoint, which could be overcome either by increasing the nutrient input to the unit procedure, or by reducing the fermentation time. The latter was chosen (time reduction) as it did not have an effect on the recipe scheduling and maintained a consistent raw material input for all the 200 L scale scenarios.

3.6 Sensitivity Analysis

A sensitivity analysis was conducted for this thesis instead of a comprehensive type of Monte Carlo sensitivity analysis as described in the literature review of **Chapter 2**. The 200 L scale stainless steel technology simulation model was investigated for sensitivity of cost of goods (COG) and Internal Rate of Return (IRR) to four specific input or assumption parameters: fermentation titer, solid-liquid separation efficiency, TFF cartridge replacement frequency, and electricity dependency on diesel.

Fermentation titer was defined as the concentration of CPS in stream exiting the final fermentation unit procedure SS200-04. Solid-liquid separation efficiency was defined as the percentage of protein-polysaccharide conjugate recovered as solids in the final centrifugation unit procedure SS200-20. Fermentation titer was adjusted for the various scenarios by adjusting the volume of feed nutrients to the fermentation procedure, while solid-liquid separation efficiency was adjusted directly by specification of the material balances for the final centrifugation unit-operation. TFF cartridge replacement frequency was defined as the number of batches completed before replacing the filtration membranes used in TFF unit procedures (SS200-07, SS200-08, SS200-15, SS200-17, and SS200-22).

The first two parameters, titer and separation efficiency, were chosen to give an indication of profitability gains which could be made during the optimization stage of process development. The third parameter, TFF cartridge replacement, was chosen to give an indication of the effect of operational decisions for the execution of the process. An extended use cycle for TFF cartridges would be subject to increased validation costs; however, a process developer may need to consider balancing this with a potential reduction in COG with less frequent replacement.

These sensitivity scenarios are shown in **Table 3-5** below:

Table 3-5 Sensitivity Scenarios

Sensitivity scenario (fermentation titer)	Fermentation titer (mg/L)	Separation efficiency	TFF cartridge replacement cycles
Very low	200	33%	3
Low	300	50%	5
Base case	400	67%	10
High	500	75%	12
Very high	600	90%	15

The fourth parameter, electricity dependency on diesel, was chosen to test for sensitivity to reflect an operational risk to manufacturing process industries in South Africa due to mismanagement at the South African state-owned power utility Eskom. This has resulted in extended periods of planned rolling black-outs (Eskom Holdings SOC Limited, 2019). During these periods, manufacturing sites dependent on Eskom for their electricity are forced into unplanned downtime, where no manufacturing activity can take place as a result.

Electricity costs were estimated by replacing a percentage of conventional electricity requirements by an increased cost to generate electricity on-site by diesel generator. The result was a composite cost of electricity per kWh (refer to **Appendix A** for sample calculation). The cost of electricity was adjusted in the SuperPro models for each of the sensitivity scenarios. The cost of additional equipment for electricity generation, shown below in **Table 3-6**, was adjusted in the models by increasing the factorial of unlisted equipment in the capital cost adjustment tab of the SuperPro models.

Table 3-6 Sensitivity to Electricity Dependence on Diesel

Electricity from diesel	Composite Electricity Cost [$ /kWh]	Additional equipment	Unlisted equipment cost factorial	Additional equipment cost
0%	0.10	N/A	0.20	N/A
10%	0.15	1 generator	0.21	$ 50 000
30%	0.20	1 generator + UPS	0.22	$ 100 000
50%	0.30	2 generators + UPS	0.23	$ 150 000
75%	0.35	4 generators + UPS	0.25	$ 250 000

Each of the scenarios in the different sensitivity scenarios were reported in terms of cost of goods (COG), and Internal Rate of Return (IRR), where possible (IRR was non-real for some scenarios). Both metrics were generated for each model by the Economic Evaluation Report from *SuperPro* software. IRR was included for the sensitivity analyses as a parameter which included the cost of capital as well as operating costs. The combined effects of these process characteristics determined which process embodiments would be feasible for a commercial project.

4 Results

4.1 GBS III Fermentation Kinetic Model Parameters Results

Method 1 Exponential trend line

A plot in **Figure 23** below shows the average optical density at 590 nm over time intervals of 1 hour, for three fermentations. The range includes the exponential growth phase, with an exponential trend line that appears linear with a logarithmic y-axis. The exponent of the trend line is 1.092 corresponding to the maximum specific growth rate per hour.

$$X = Ke^{\mu t} \qquad \text{Equation 3-4}$$

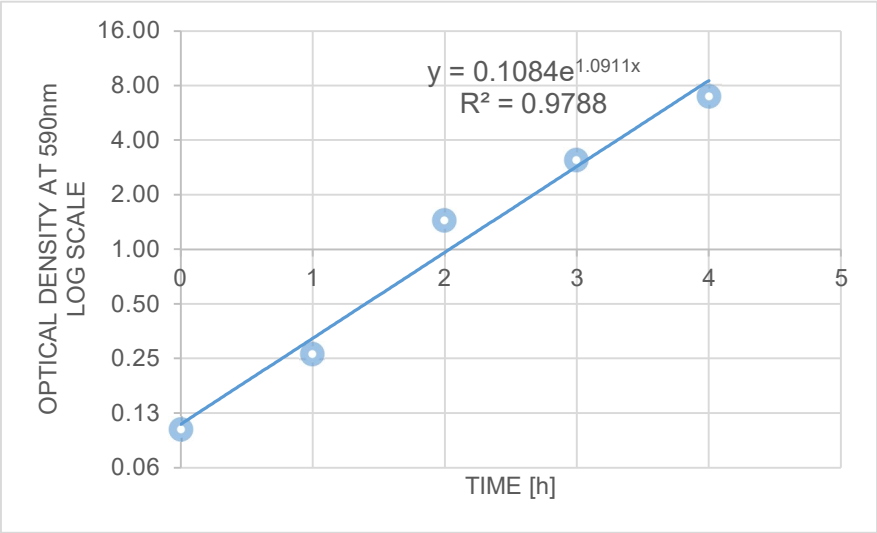

Figure 23: Optical Density vs. time for Fermentation experiment 1

$$X = 1.084e^{1.0911t}$$

To find the half rate constant, the substrate concentration was plotted against specific growth rate, yielding a logarithmic trend line shown in **Figure 24** (right), with **Equation 3-5** and **Equation 3-6**.

$$S\Big|_{\frac{\mu}{\mu_{max}}=0.5} \qquad \text{Equation 3-5}$$

$$\mu = \alpha \ln S + \beta \qquad \text{Equation 3-6}$$

The value of K_s was determined by solving **Equation 3-6** for the value of S for $\frac{\mu}{\mu_{max}} = 0.5$, where $\mu_{max} = 1.092\ h^{-1}$ as per **Figure 24**. Doubling time was determined where $t_d = \frac{\ln 2}{\mu_{max}}$. (Refer to **Appendix A** for derivations).

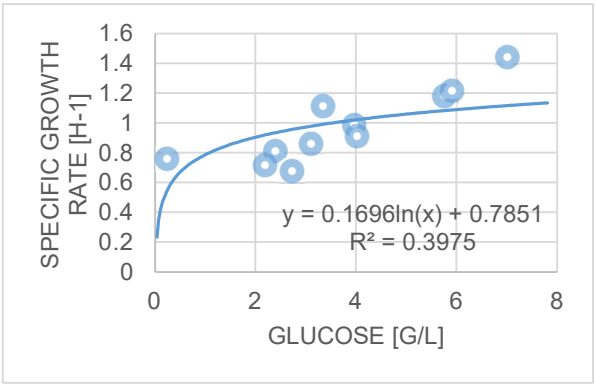

Figure 24: Specific growth rate vs. Glucose concentration for Fermentation experiment 1

$\mu_{max} = 1.091\ h^{-1}$	$K_s = 0.243\ g/L$	$t_d = 0.635\ h$

Fermentation experiment 1: Parameters derived by Method 1

The same approach was followed for two additional fermentation experiments, yielding the plots for Method 1 for experiments 2 and 3, respectively:

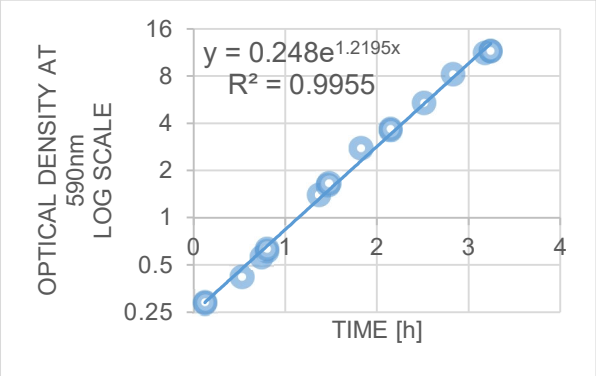

Figure 27: Optical Density vs. time for Fermentation experiment 2

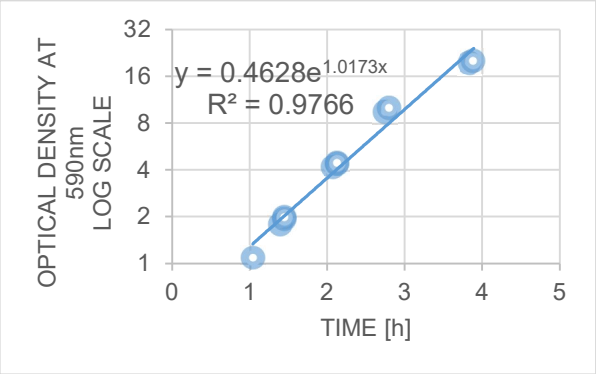

Figure 28: Optical Density vs. time for Fermentation experiment 3

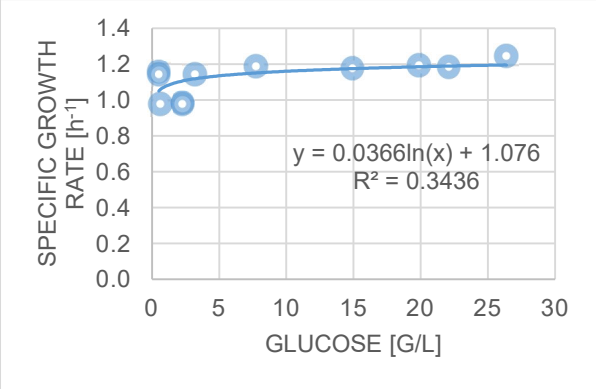

Figure 26: Specific growth rate vs. Glucose concentration for Fermentation experiment 2

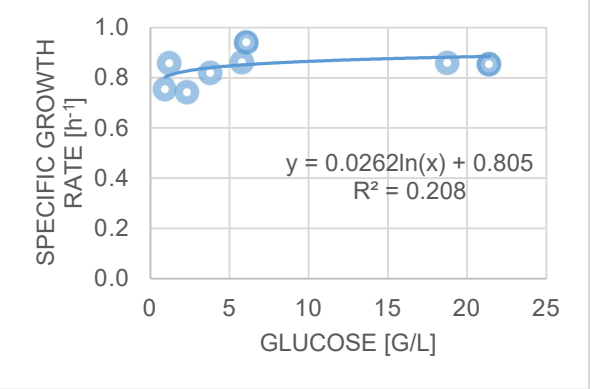

Figure 25: Specific growth rate vs. Glucose concentration for Fermentation experiment 3

The kinetic parameters found by Method 1 for the three experiments are shown in **Table 4-1** below.

Table 4-1 Fermentation kinetic parameters summary – Method 1

Method 1	Experiment 1	Experiment 2	Experiment 3	AVERAGE	STDEV
μ max [h^{-1}]	1.091	1.220	1.017	1.109	0.084
K_s [g/L]	0.243	0.000	0.000	0.081	0.115
t_d [h]	0.635	0.568	0.681	0.628	0.046

Method 2 Linear trend line

A plot of $\frac{S}{\mu}$ vs. S during the exponential growth phase yielded a linear trend line with **Equation 3-8**.

$$\frac{S}{\mu} = \frac{1}{\mu_{max}} S + \frac{K_S}{\mu_{max}}$$ Equation 3-8

This is shown in **Figure 29** below:

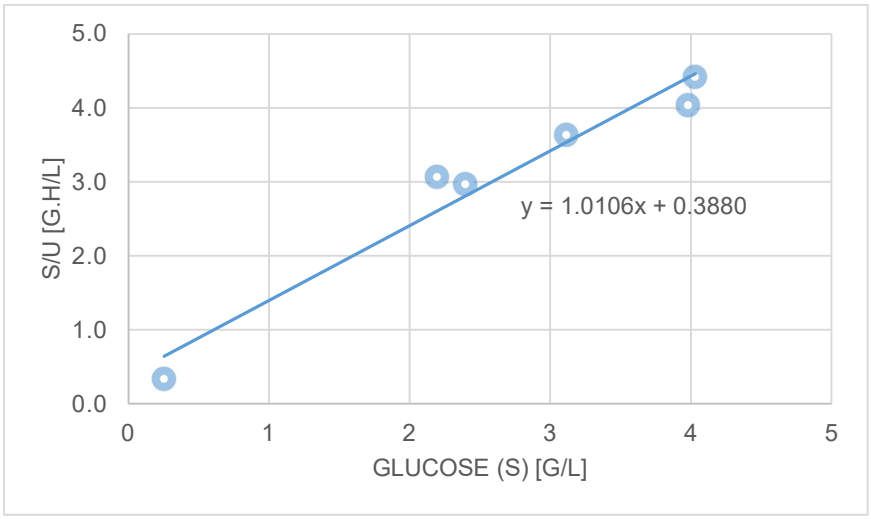

Figure 29: Composite plot of rearranged Monod equation – Fermentation experiment 1

$$\frac{S}{\mu} = 1.0106S + 0.3880$$

The plot above yielded the value of the two parameters required for the Monod kinetic model. The doubling time was also found using the formula $t_d = \frac{\ln 2}{\mu_{max}}$.

$\mu_{max} = 0.990\ h^{-1}$	$K_S = 0.384\ g/L$	$t_d = 0.700\ h$
Fermentation experiment 1: Parameters derived by Method 2		

The same approach was followed for two additional fermentation experiments, yielding the plots for Method 2 for experiments 2 and 3, respectively:

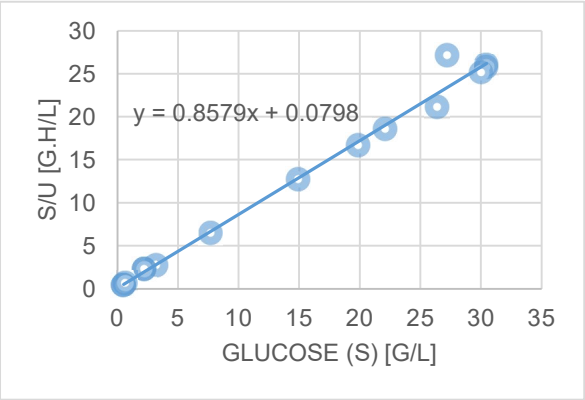

Figure 31: Composite plot of rearranged Monod equation – Fermentation experiment 2

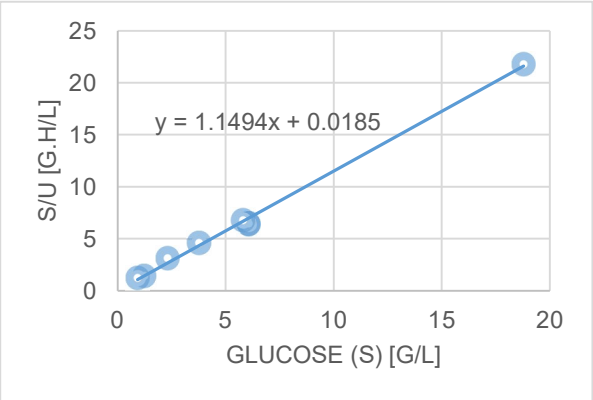

Figure 30: Composite plot of rearranged Monod equation – Fermentation experiment 3

The kinetic parameters found by Method 2 for the three experiments are shown in **Table 4-2** below.

Table 4-2 Fermentation kinetic parameters summary – Method 2

Method 2	Experiment 1	Experiment 2	Experiment 3	AVERAGE	STDEV
μ max [h^{-1}]	0.990	1.166	0.870	1.008	0.121
K_s [g/L]	0.384	0.093	0.016	0.164	0.158
t_d [h]	0.700	0.595	0.797	0.697	0.083

Methods 1 and 2 produced similar results for the Monod kinetic model parameters μ_{max} and K_S shown in **Tables 4-1 and 4-2**. The Average maximum specific growth rate (μ_{max}) was found to be 1.109 ± 0.084 h^{-1} for Method 1, and 1.008 ± 0.121 h^{-1} for Method 2.

The doubling times (t_d) were also similar, with Method 1 average doubling time of 0.628 ± 0.046 h, and Method 2 average doubling time of 0.697 ± 0.083 h. Reported doubling times for GBS serotypes Ia, III, and V by Costantino et al. (2013) and Swennen (2012) were between 0.56 h and 1.11 h for GBS serotype III (strain M-781). This confirms that both methods produced parameters within the range of those published in literature.

It was noted that the average value for the substrate half-rate constant, K_S, was very low when using Method 1, and that the average value was lower than the standard deviation. This was found to be due to the use of the logarithmic plot, with very low R^2 values of between 0.208 and 0.398 for all three experiments.

Due to the greater uncertainty associated with Method 1 ***it was decided to use the parameters derived by Method 2.***

$$\mu_{max} = 1.008 \pm 0.121\ h^{-1} \qquad K_S = 0.164 \pm 0.158\ g/L \qquad t_d = 0.697 \pm 0.083\ h$$

Parameters derived by Method 2

4.2 Simulation models Results

Simulation Models Economic Results

The simulation methods described in **Chapter 3** produced six models. A summary of the computer files submitted as part of the Results of this thesis is shown in **Tables 4-3 and 4-4** below. These files can also be found online using the DOI: **10.25375/uct.9920081**.

Table 4-3 Simulation models produced

Model	Product	Fermentation scale	Technology platform	File name
1	GBS serotype III conjugate	20 L	Stainless steel (SS)	01_GBS3-20L-SS-kinetic2.spf
2			Single Use (SU)	02_GBS3-20L-SU-kinetic2.spf
3			Hybrid (HY)	03_GBS3-20L-HY-kinetic2.spf
4		200 L	SS	04_GBS3-200L-SS-kinetic2.spf
5			SU	05_GBS3-200L-SU-kinetic2.spf
6			HY	06_GBS3-200L-HY-kinetic2.spf

Table 4-4 Reports Generated by *SuperPro* Designer

Model	Materials & Streams Report	Economic Evaluation Report
1	01_GBS3-20L-SS-kinetic2_SR.xls	01_GBS3-20L-SS-kinetic2_EER.xls
2	02_GBS3-20L-SU-kinetic2_SR.xls	02_GBS3-20L-SU-kinetic2_EER.xls
3	03_GBS3-20L-HY-kinetic2_SR.xls	03_GBS3-20L-HY-kinetic2_EER.xls
4	04_GBS3-200L-SS-kinetic2_SR.xls	04_GBS3-200L-SS-kinetic2_EER.xls
5	05_GBS3-200L-SU-kinetic2_SR.xls	05_GBS3-200L-SU-kinetic2_EER.xls
6	06_GBS3-200L-HY-kinetic2_SR.xls	06_GBS3-200L-HY-kinetic2_EER.xls

Table 4-5 below summarises the economic performance results of each simulation model in terms of Capital expense (CAPEX) per kg over 10 years, annual operating expense (OPEX), and the cost of goods per kg (COG). An additional column reports the break-even price for a 5 µg dose of the product, GBS serotype III conjugate antigen. The suggested selling price for the product is $ 30 /dose.

Table 4-5 Economic Performance Summary

Model	Scale	Technology	Total Capital cost (2017 $/ kg)	Operating cost (2017 $/y)	Cost Of Goods ($/kg)	Break-even Price ($/dose)
1	20 L	SS	$ 5 851 000	$ 1 677 000	$ 9 661 000	$ 48.31
2		SU	$ 4 384 000	$ 1 693 000	$ 9 756 000	$ 48.78
3		HY	$ 5 248 000	$ 1 701 000	$ 9 799 000	$ 49.00
4	200 L	SS	$ 1 206 000	$ 6 086 000	$ 3 747 000	$ 18.74
5		SU	$ 1 325 000	$ 6 964 000	$ 4 289 000	$ 21.45
6		HY	$ 1 234 000	$ 6 225 000	$ 3 833 000	$ 19.17

Table 4-5 shows that increasing the process scale ten-fold (20 L to 200 L) has an effect of approximately doubling (x2) capital costs, tripling (x3) operating costs, and halving cost of goods (x½).

Figure 32 (top right) presents the costs summary at 20 L scale, as described in **Table 4-3**. Single use technology offers the lowest total capital expense (CAPEX) at $ 4.4 million / kg product (over 10-year project life), while CAPEXs for stainless steel technology and hybrid technology were more expensive at $ 5.9 million /kg, and $ 5.2 million /kg, respectively. The operating expenses (OPEXs) for the different technology platforms were relatively similar at about $ 1.7 million each, while the Cost of Goods (COGs) for each were also relatively similar at about $ 9.8 million/kg. As shown in **Figure 32**, CAPEX for stainless steel technology was $ 1.5 million /kg greater than for single use technology.

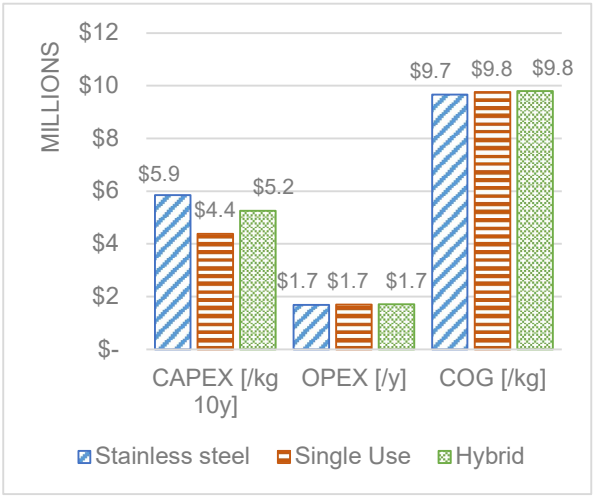

Figure 32: Costs Summary at 20 L Scale

Figure 33 (middle right) presents the costs summary at 200 L scale as described in **Table 4-3**. Stainless-steel was the cheapest technology with a CAPEX of $ 1.2 million /kg, while single use and CAPEX was $ 1.3 million /kg. At the larger 200 L scale, OPEX for stainless steel was $ 6.1 million/y, with Single Use technology at $7.0 million/y, and Hybrid technology at and $ 6.2 million/y. Stainless steel also had the lowest COG of $ 3.7 million/kg, while hybrid was slightly greater at $ 3.8 million/kg. Single use was most expensive at $ 4.3 million/kg.

Figure 33 also shows that OPEX for single use technology was $ 1.0 million greater than that of stainless steel, while OPEX for hybrid technology was only $ 0.2 million greater than stainless steel.

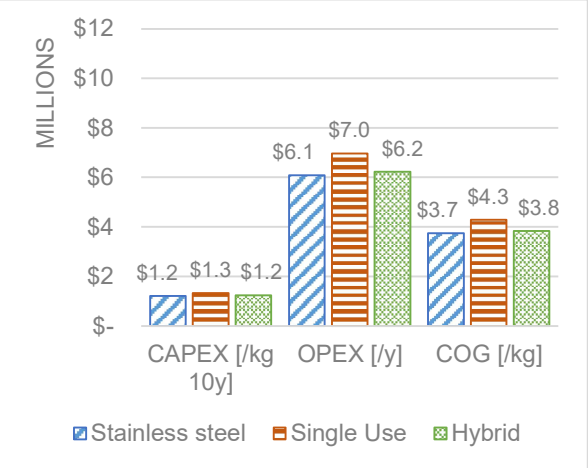

Figure 33: Costs Summary at 200 L Scale

Table 4-6 below summarises the economic performance of the six simulation models in terms of relevant variable costs. The costs in 2017 US dollars per annum per kg of product for raw materials, consumables, and waste disposal are shown, while utility consumption for WFI and steam are shown as tons per kg product per year (t/kg.y), and million tons per kg product per year (MT/kg.y), respectively.

Table 4-6 Major Variable Costs results

Model	Scale	Technology	Raw materials (2017 $/kg.y)	Consumables (2017 $/kg.y)	WFI (t/kg.y)	Steam (MT/kg.y)	Waste disposal (2017 $/kg.y)
1	20 L	SS	$ 1 600 000	$ 1 518 000	281.8	84.1	$ 88 235
2		SU	$ 1 559 000	$ 3 094 000	167.1	81.2	$ 94 118
3		HY	$ 1 576 000	$ 2 288 000	197.1	82.4	$ 94 118
4	200 L	SS	$ 1 771 000	$ 630 000	70.7	11.2	$ 86 420
5		SU	$ 1 821 000	$ 1 037 000	47.9	9.1	$ 91 358
6		HY	$ 1 764 000	$ 698 000	56.4	10.1	$ 87 037

Table 4-6 illustrates that increasing the process ten-fold (20 L to 200 L) resulted in an approximate ten-fold (x10) increase in raw material costs, while consumables costs increased by about three-fold (x3).

Figure 34 (top right) presents materials costs at 20 L scale, as described in **Table 4-6**. Raw materials costs across the technology platforms were similar at about $ 1.6 million /kg.y, while consumables costs were more varied. Stainless steel technology yielded the lowest consumables cost of $ 1.5 million /kg.y, while single use technology yielded the highest of $ 3.1 million /kg.y about double that of stainless steel. Hybrid technology was in-between at $ 2.3 million /kg.y. The trend in consumables costs may be attributed to the additional single use mixing bags, reactor bags, and shake flasks required to operate a process with single use fluid handling capability.

Figure 34: Annual Materials Costs at 20L Scale

Figure 35 (middle right) presents materials costs at 200 L scale, as described in **Table 4-6**. At 200 L scale raw materials cost for the different technology platforms were similar at about $ 1.8 million /kg.y. Consumables cost was highest for single use technology at $ 1.0 million /kg.y, with stainless steel lowest at $ 0.6 million /kg.y, and consumables for hybrid technology costing $ 0.7 million /kg.y. In **Figure 35**, the observed trend in consumables costs at 200 L scale is similar to the trend at 20 L scale shown in **Figure 34**. This suggests that consumables costs trends may be characteristic of each specific technology-platform. It was also noted that the economy of scale at 200 L resulted in a reduction in both raw material and consumable costs per kg product.

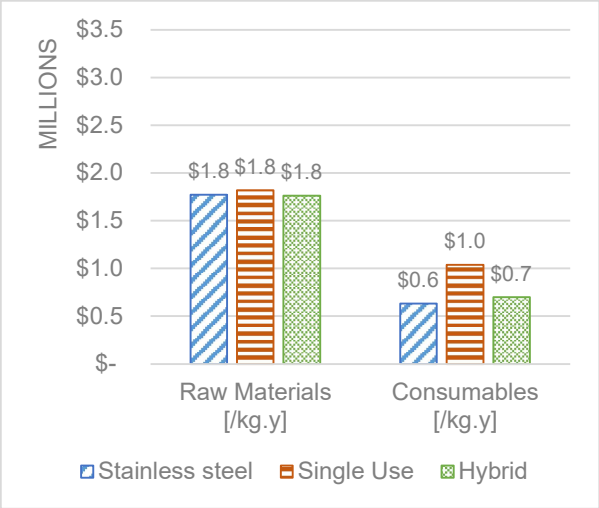

Figure 35: Annual materials costs at 200 L scale

The break-down of resource utilisation and waste disposal costs per kg of product, at 20 L scale, is shown below in **Figure 36**, as described in **Table 4-6**:

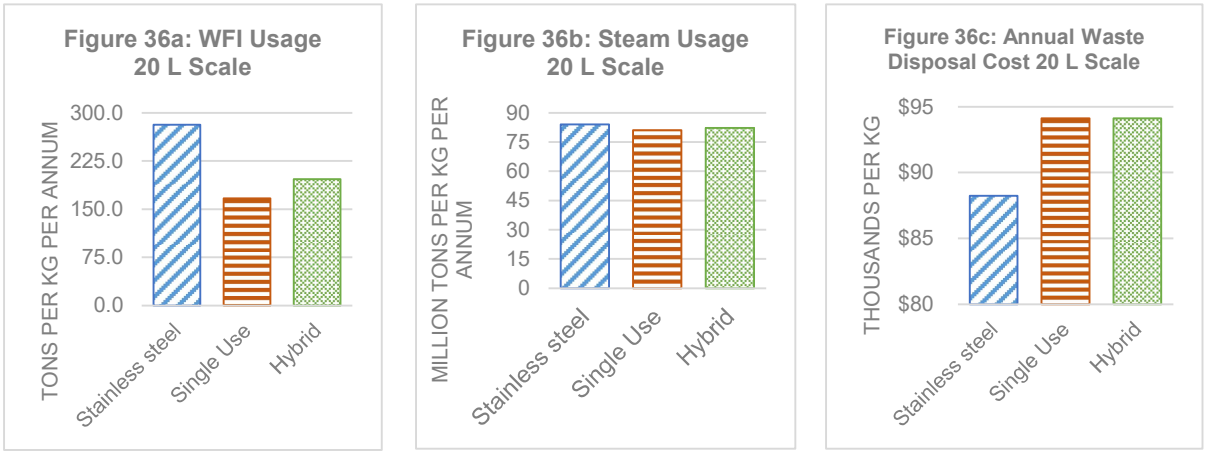

Figure 36: Annual usage of WFI and Steam per kg product, and annual cost of waste disposal per kg product, all at 20 L scale

As shown in **Figure 36**, WFI and steam consumption at 20 L scale were greatest for stainless steel technology at 281.8 t/kg.y WFI and 84.1 MT/kg.y steam, while single use technology required only 167.1 t/kg.y of WFI and 81.2 MT/kg.y steam. Hybrid technology featured intermediate consumption with WFI usage of 197.1 t/kg.y and steam usage of 82.4 MT/kg.y. The difference in WFI and steam usage between stainless steel (281.8 t/kg.y WFI, 84.1 MT/kg.y steam) and single use (167.1 t/kg.y WFI, 81.2 MT/kg.y steam) technology is attributed to the CIP and SIP requirements of stainless-steel technology. Waste disposal costs were similar for all three technology platforms at $ 88 000 /kg.y for stainless steel and $ 94 000 /kg.y for each of single use and hybrid technology. This is some indication that despite a perceived increase in solid waste from implementing single use technology, at the 20 L scale there is only a $ 6 000 /kg.y cost increase.

The break-down of resource utilisation and waste disposal costs at 200 L process scale is shown in **Figure 37** below, as described in **Table 4-6**. At 200 L scale utility consumption for stainless steel was 70.7 t/kg.y of WFI and 11.2 MT/kg.y of steam. Single use technology featured the lowest utility usage of 47.9 t/kg.y of WFI and 9.1 MT/kg.y of steam. Hybrid technology was found to have a WFI usage of 56.4 t/kg.y and a steam usage of 10.1 MT/kg.y at 200 L scale.

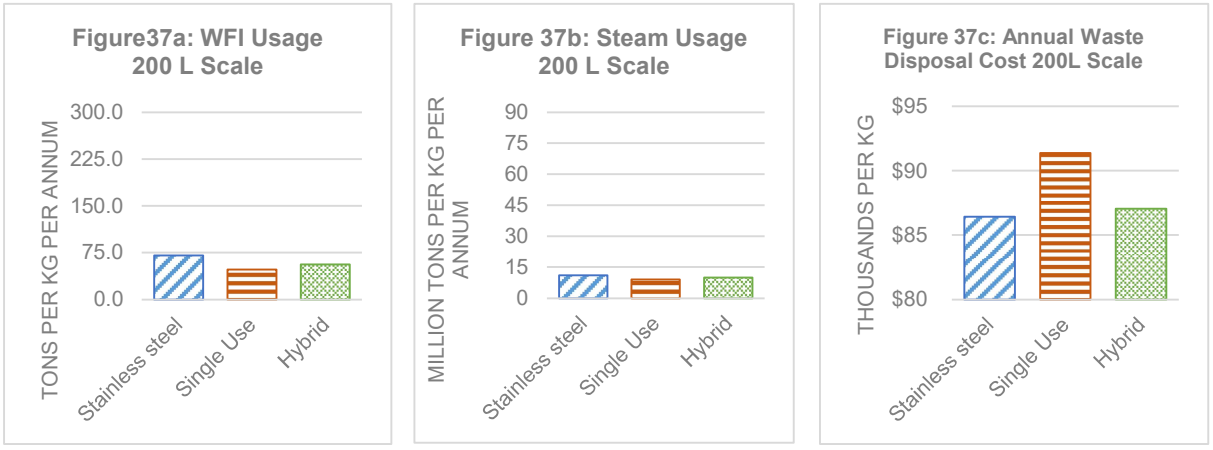

Figure 37: Annual usage of WFI and Steam per kg product, and annual cost of waste disposal per kg product, all at 200 L scale

Figure 37 shows that at 200 L scale, there is a clear difference in WFI and steam usage between stainless steel (70.7 t/kg.y WFI, 11.2 MT/kg.y steam) and single use (47.9 t/kg.y WFI, 9.1 MT/kg.y steam) technology platforms. The relative increases in these gaps (30% per kg increase for WFI, 18% per kg for steam) from the 20 L scale showed that scale-up of the process based on stainless steel technology was water resource intensive.

As shown in **Figure 37**, the waste disposal costs for stainless steel and hybrid technology were similar at $ 86 000 /kg.y and $ 87 000 /kg.y respectively. Single use technology incurred a higher waste disposal cost of $ 91 000 /kg.y. The difference in waste disposal costs from stainless steel to single use technology was reduced to $ 5000 /kg.y at 200 L scale from $ 6000 /kg.y at 20 L scale.

Capital costs at 20 L scale

The breakdown of Direct Fixed Capital (DFC, excludes working capital and start-up cost) was relatively similar across the three technology platforms at 20 L scale. **Figure 38** (above right) shows the breakdown of DFC costs for stainless steel technology at 20 L scale. Equipment comprised 21% of the total DFC cost of $ 9.4 million. Facility construction (23%), Engineering (13%), Installation (9%) and Process Piping (9%) were the next greatest costs. The category "Other" included buildings, electrical components, and yard improvement, taking up a combined 5% of DFC.

Figure 39 (below right) shows a slightly different breakdown of DFC for single use at 20 L scale. Construction costs comprised 23% of the total DFC of $ 7.1 million while equipment was only 19%. Engineering (13%) and Installation (11%) costs were next greatest. The difference in DFC distribution compared to stainless-steel was due to installation cost factors being specified for each piece of equipment rather than a single factorial for all installation costs. This resulted in minor differences observed in the break-down of DFC for the different technology platforms.

The breakdown of DFC for hybrid technology (total $ 8.5 million) shown in **Figure 40** (below left) was identical to that of stainless-steel technology at the 20 L scale.

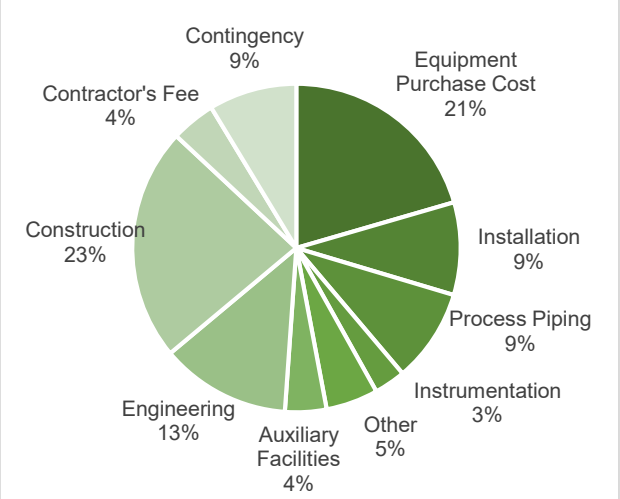

Figure 38: DFC for 20 L scale stainless steel technology

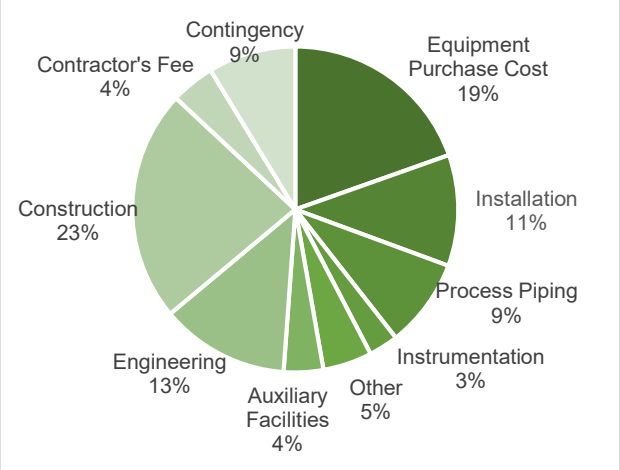

Figure 39: DFC for 20 L scale single use technology

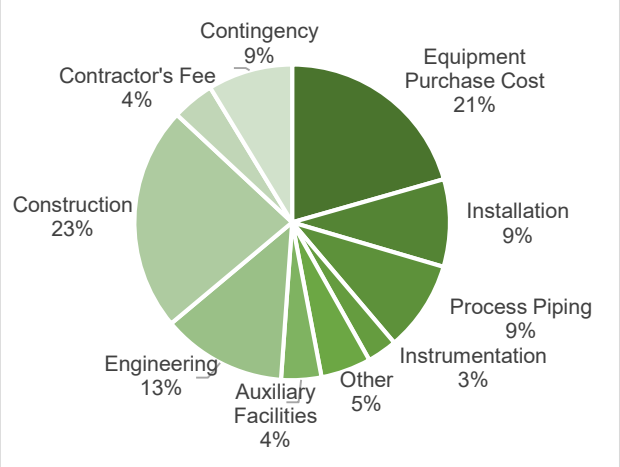

Figure 40: DFC for 20L scale hybrid technology

Capital costs at 200 L scale

At 200 L scale, the breakdowns of DFC across the three technology platforms were relatively similar, as was the case for the 20 L scale process.

DFC for the 200 L scale with stainless steel technology is shown in **Figure 41** above right. Construction costs were 23% of the total DFC of $ 18.3 million, with Equipment costs second highest at 21%. Next greatest, in descending order, were Engineering (13%), Process piping (9%), and Installation (9%) costs. An identical distribution of DFC was seen for the 200 L scale hybrid technology process (total DFC $ 18.8 million), shown in **Figure 42** below left.

The breakdown of DFC for the 200 L scale process with single use technology is shown in **Figure 43** (below right). Construction and Equipment costs were 23% and 18%, respectively, of the total DFC of $ 20.1 million. Installation costs were 13% while Engineering costs were 13%.

The same trends in DFC distribution were observed at the 200 L scale in **Figures 41, 42, and 43**, and at the 20 L scale in **Figures 38, 39, and 40**. Stainless steel and hybrid technology featured similar DFC breakdowns to each other at the same scale, whereas single use technology featured an increase in the proportions of construction and installation costs, with a reduction in the proportions of equipment and process piping costs.

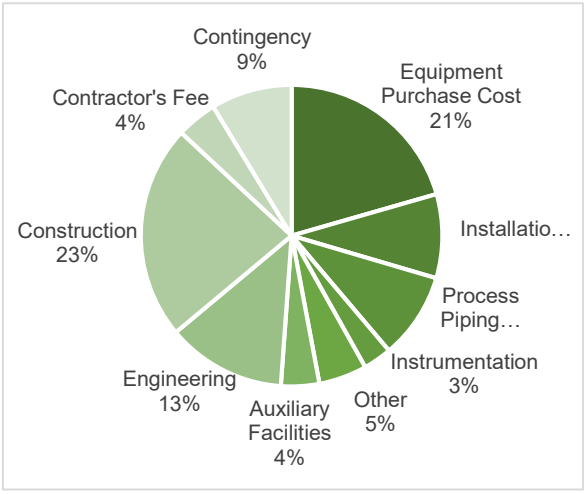

Figure 41: DFC for 200 L scale stainless steel technology

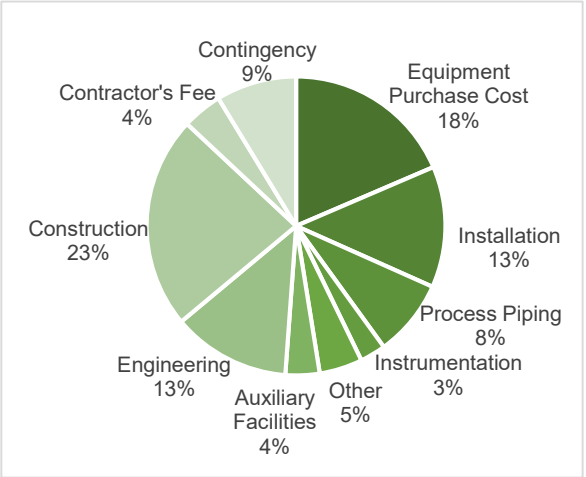

Figure 42: DFC for 200 L scale single use technology

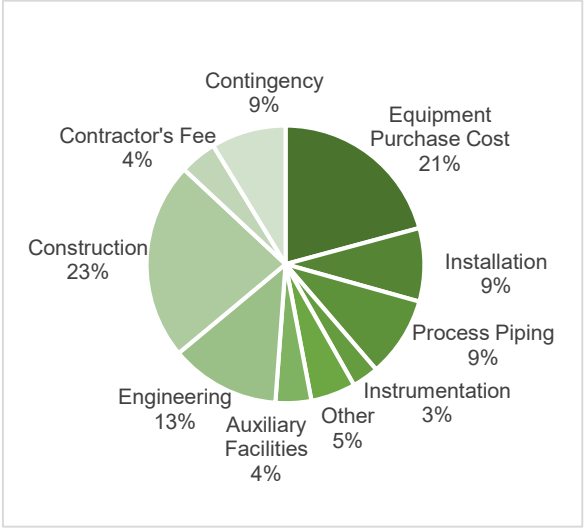

Figure 43: DFC for 200L scale hybrid technology

Operating costs at 20 L scale

Figure 44 (top right) shows the breakdown of operating costs (OPEX) for the 20 L stainless steel technology platform. Raw materials and Consumables portions of OPEX were each 16%, while Labour Dependent costs were 13% of the total OPEX of $ 1.7 million /y. More than half (54%) of the OPEX was attributed to Facility-Dependent costs, which included equipment maintenance and depreciation.

OPEX for single use technology at the 20 L scale is shown in **Figure 45** (middle right). Consumables made up 31% of the total OPEX of $ 1.7 million /y. Facility Dependent costs were second largest at 40%, while Raw materials and Labour-dependent costs were 16% and 12%, respectively.

Figure 46 (bottom right) shows the OPEX breakdown for hybrid technology at 20 L scale. Facility dependent costs were 48% of the total OPEX of $ 1.7 million /y, while consumables costs were 23%. Raw materials and Labour-dependent costs were 16% and 12%, respectively.

The trend that is observed across the three technology platforms is that stainless steel features a larger proportion of facility dependent costs, due to the larger capital cost of stainless-steel fermentation vessels as compared to single use. This was due to the estimation of facility dependent costs as a direct proportion (factorial) of equipment purchase cost, and stainless-steel equipment was more expensive at the 20 L scale.

Single use technology featured a much larger proportion attributed to consumables due to the cost of replacing single use consumables (bags, bottles etc.) for every batch.

This relationship between facility dependent and consumable costs can be elucidated by comparing **Figures 44, 45, and 46**.

Although the OPEX of the different technology platforms are relatively similar at 20 L scale, it is noted that the stainless steel was marginally less expensive than single use and hybrid technologies. Hybrid technology was marginally more expensive, suggesting that the aspects of each technology that were combined to create the hybrid platform did not provide any cost savings benefit at this scale.

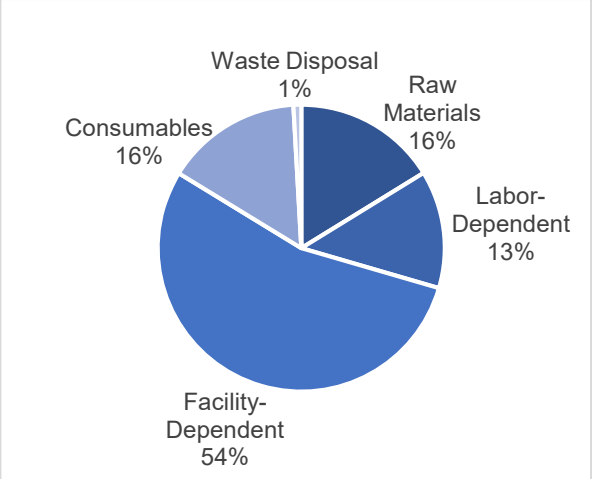

Figure 44: OPEX for 20 L Stainless Steel technology platform

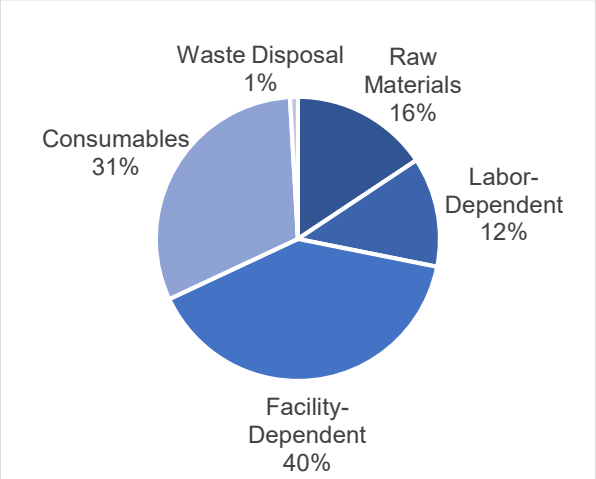

Figure 45: OPEX for 20 L Single Use technology platform

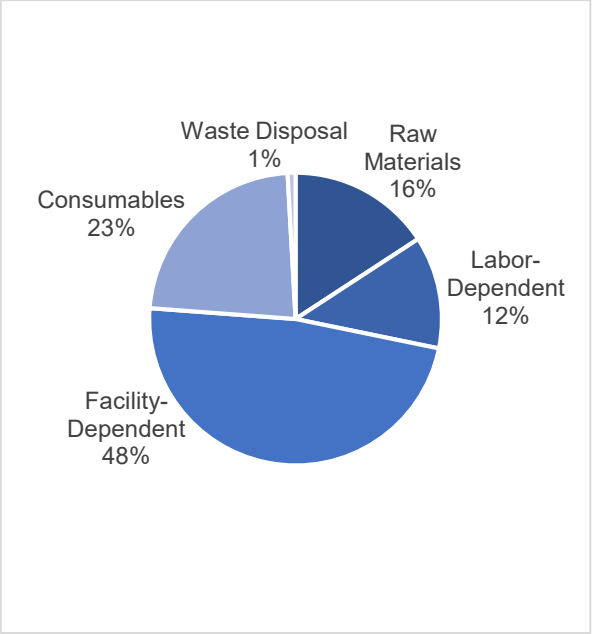

Figure 46: OPEX for 20 L Hybrid technology platform

Operating costs at 200 L scale

The breakdown of OPEX for the 200 L scale process using stainless-steel technology is shown in **Figure 47** (top right). Raw materials comprised 47% of the total OPEX of $ 6.1 million /y, while Facility dependent costs and Consumables were 29% and 17%, respectively. Labour-dependent costs and Waste disposal costs were 5% and 2%, respectively.

OPEX for single use technology at the 200 L scale is shown in **Figure 48** (middle right). Consumables were nearly a quarter (24%) of the total OPEX of $ 7.0 million /y. Raw materials were just under half (42%) of OPEX, and Facility-dependent costs were 28%.

In **Figure 49** (bottom right) the breakdown of OPEX for the Hybrid technology at 200 L scale is shown. Raw materials were 46% of the total OPEX of $ 6.2 million /y, with Facility dependent costs and consumables at 29% and 18%, respectively.

At the 200 L scale, the trend across the different technology platforms saw a proportional escalation of the variable costs for raw materials and consumables with increasing scale. Despite greater capital costs ($ 18 million - $ 20 million) compared to 20 L scale ($ 7 million - $ 10 million), the proportion of facility dependent costs at 200 L scale decreased compared to other variable costs for raw materials and consumables. The single use process at 200 L scale featured the highest operating expense at just under $ 7 million /y. This was primarily due to the increased cost of consumables.

Labour-dependent costs generally shrunk in proportion from 12% at the 20 L scale to about 5% at the 200 L scale. Labour requirements were assumed (refer to Appendix A for assumptions) to stay constant with scale. In addition, labour costs did not include Management, Validation, Regulatory, or Quality Control costs. The small proportion of Labour costs in the 200 L scale OPEXs suggests a possibility that some of the assumptions made were an oversimplification for this process.

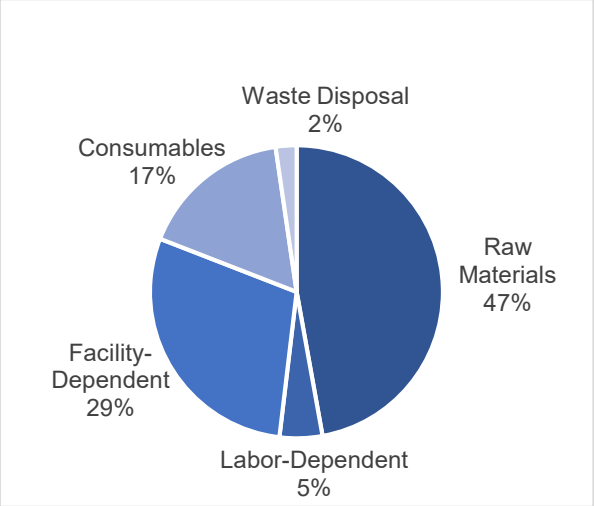

Figure 47: OPEX for 200 L Stainless Steel technology platform

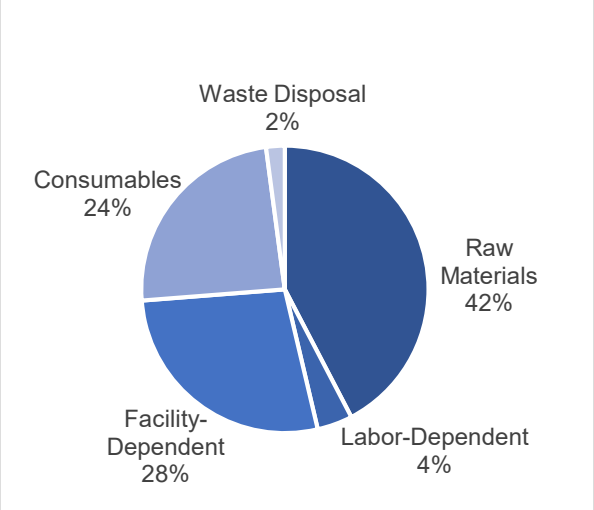

Figure 48: OPEX for 200 L Single Use technology platform

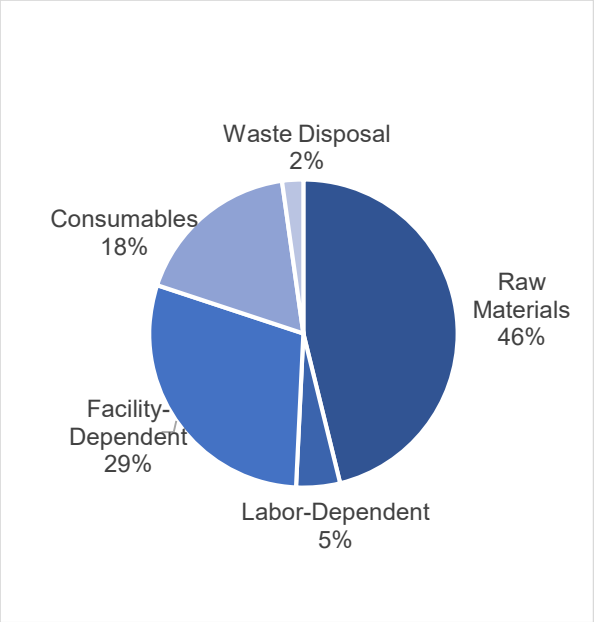

Figure 49: OPEX for 200 L Hybrid technology platform

4.3 Model Sensitivity – 200 L stainless steel technology

The 200 L scale process using stainless steel technology was chosen to proceed with as the sensitivity base case, as described in **3.6 Sensitivity Analysis**. The sensitivity base case featured a COG of $ 3.7 million /kg, and an Internal Rate of Return (IRR) of 14.9%. The hurdle rate used was 25%. The sensitivity base case parameters were 400 mg/L fermentation titer from procedure SS200-04, 67% solid-liquid separation efficiency in procedure SS200-20, TFF cartridge replacement every 10 cycles, and 0% electricity from diesel generator. The result of the sensitivity analyses produced an additional 16 model scenarios. A summary of the additional computer files submitted is shown in **Table 4-7** below. These files can also be found at DOI: **10. 25375/uct.9920081**.

Table 4-7 Sensitivity Analysis Additional Simulation models produced

Model	Fermentation scale & technology platform	Sensitivity parameter	Parameter value	File name	SuperPro Report File name
8	200 L, Stainless steel (200SS)	Fermentation titer	200 mg/L	08_200LSS_t200.spf	08_200LSS_t200_EER.xls
9			300 mg/L	09_200LSS_t300.spf	09_200LSS_t300_EER.xls
10			500 mg/L	10_200LSS_t500.spf	10_200LSS_t500_EER.xls
11			600 mg/L	11_200LSS_t600.spf	11_200LSS_t600_EER.xls
12		Solid-liquid separation efficiency	33%	12_200LSS_c33.spf	12_200LSS_c33_EER.xls
13			50%	13_200LSS_c50.spf	13_200LSS_c50_EER.xls
14			75%	14_200LSS_c75.spf	14_200LSS_c75_EER.xls
15			90%	15_200LSS_c90.spf	15_200LSS_c90_EER.xls
16		Electricity dependence on diesel	10%	16_200LSS_e10.spf	16_200LSS_e10_EER.xls
17			30%	17_200LSS_e30.spf	17_200LSS_e30_EER.xls
18			50%	18_200LSS_e50.spf	18_200LSS_e50_EER.xls
19			75%	19_200LSS_e75.spf	19_200LSS_e75_EER.xls
20		TFF cartridge replacement frequency	3	20_200LSS_tff3.spf	20_200LSS_tff3_EER.xls
21			5	21_200LSS_tff5.spf	21_200LSS_tff5_EER.xls
22			12	22_200LSS_tff12.spf	22_200LSS_tff12_EER.xls
23			15	23_200LSS_tff15.spf	23_200LSS_tff15_EER.xls

Economic performance results of each of the sensitivity scenarios described above is summarised in **Table 4-8**, in terms of COG and IRR.

Table 4-8 Sensitivity Analysis Summary

Model	Scale & technology	Sensitivity parameter	Parameter value	COG [$/kg]	IRR
8	200 L, Stainless steel (200SS)	Fermentation titer	200 mg/L	$ 8 006 000	N/A
9			300 mg/L	$ 5 400 000	N/A
10			500 mg/L	$ 2 894 000	27.1%
11			600 mg/L	$ 2 179 000	41.0%

Table 4-8 Sensitivity Analysis Summary (continued)

Model	Scale & technology	Sensitivity parameter	Parameter value	COG [$/kg]	IRR
12	200 L, Stainless steel (200SS)	Solid-liquid separation efficiency	33%	$ 7 606 000	N/A
13			50%	$ 5 021 000	0.7 %
14			75%	$ 3 348 000	20.1 %
15			90%	$ 2 790 000	28.5 %
16		Electricity dependence on diesel	10%	$ 3 759 000	14.6 %
17			30%	$ 3 771 000	14.3 %
18			50%	$ 3 784 000	14.1 %
19			75%	$ 3 809 000	13.5 %
20		TFF cartridge replacement frequency	3	$ 4 868 000	5.7 %
21			5	$ 4 228 000	11.2 %
22			12	$ 3 667 000	15.6 %
23			15	$ 3 587 000	16.2 %

Sensitivity to Fermentation Titer

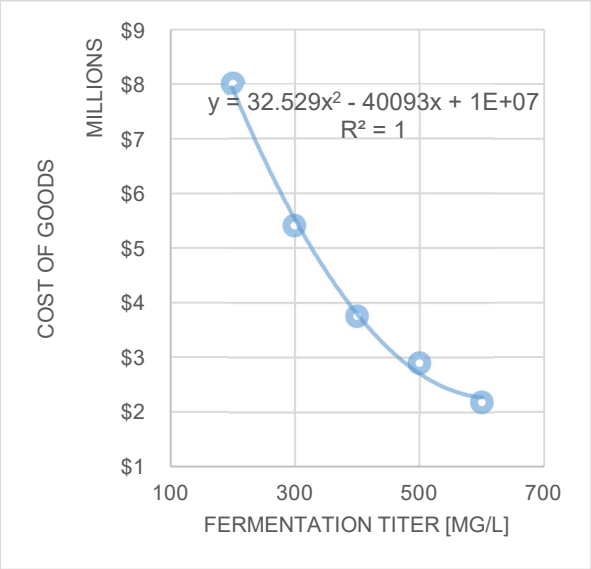

Figure 50: Sensitivity of COG to fermentation titer

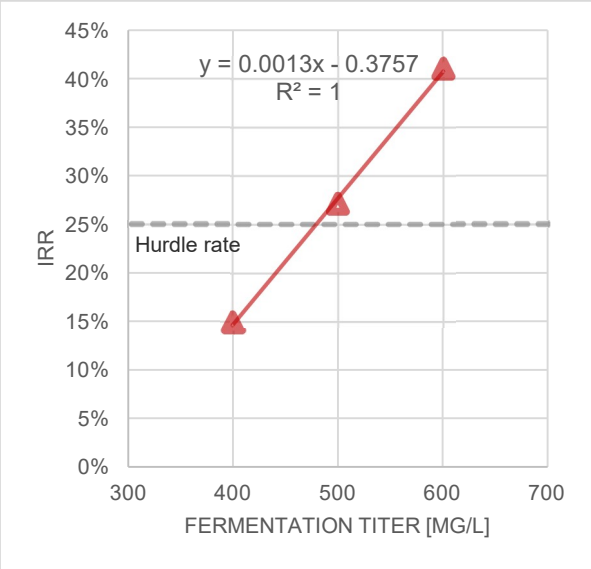

Figure 51: Sensitivity of IRR to fermentation titer

Figure 50 (top left) shows the sensitivity of Cost of Goods (COG) to fermentation titer. It can be seen that a quadratic trend-line can be fitted to the data with an R^2 value of 1. The form of the trend-line shows that the incremental increase in COG becomes smaller with incremental increases in fermentation titer, as well as exponential increases in COG as fermentation titer decreases. The lowest COG of $ 2.2 million /kg was achieved at a titer of 600 mg/L. **Figure 51** (above right) shows that IRR increases linearly with increasing fermentation titer within the range tested. The slope of this relationship shows a 13% increase in IRR for every 100 mg/L increase in titer. Fermentation titers above 480 mg/L produced scenarios where IRR was greater than the hurdle rate of 25% (dashed line in **Figure 51**), corresponding to a commercially feasible process. This showed that small improvements in titer could make the project a substantially more attractive investment. A titer of 600 mg/L resulted in the highest IRR of 41.0%, which again illustrates the process' sensitivity to increased product yields.

Sensitivity to Solid-Liquid Separation Efficiency

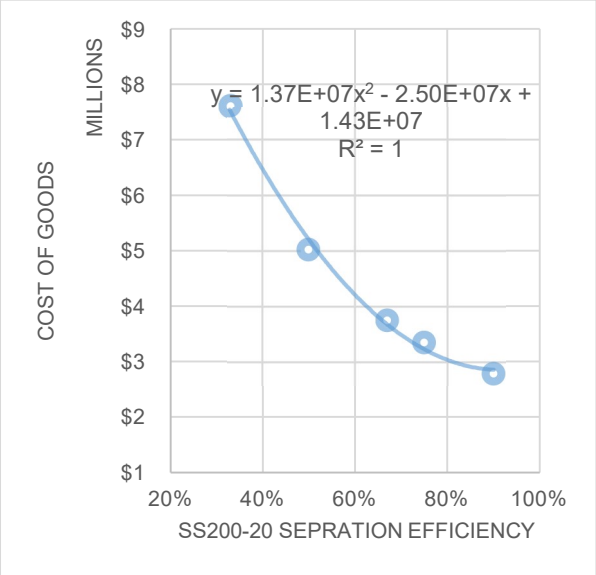

Figure 52: Sensitivity of COG to separation efficiency

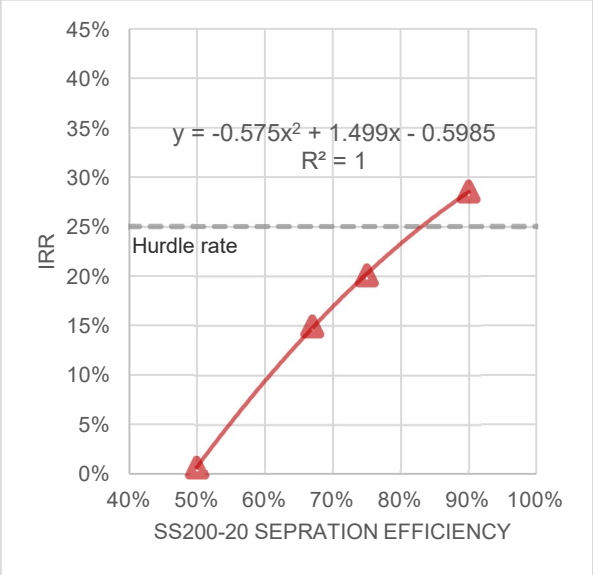

Figure 53: Sensitivity of IRR to separation efficiency

Figure 52 (above left) shows the sensitivity of COG to the solid-liquid separation efficiency of unit procedure SS200-20 in centrifuge C-301. For an increase in separation efficiency from 67% in the sensitivity base case to 75% in one of the scenarios modelled; a reduction in COG from $ 3.7 million /kg to $ 2.8 million /kg was observed. The trend-line fitted to the relationship between COG and separation efficiency was found to be quadratic (the same form as for fermentation titer) with an R^2 of 1. As shown in **Figure 52**, the quadratic relationship suggests an optimum separation efficiency, above which COG begins to increase again. Solving for the turning point ($x = -\frac{b}{2a}$) of the trend line with form $y = ax^2 + bx + c$, this point was found to be a separation efficiency of 91.5%.

In **Figure 53** (above right) the sensitivity of IRR to solid-liquid separation efficiency in SS200-20 is shown. The trend-line fitted to the data begins to fit a quadratic trend with an R^2 of 1, as opposed to the linear trend observed between IRR and fermentation titer. The highest IRR of 28.5% for this parameter was achieved at a separation efficiency of 90%. This IRR was lower than the maximum IRR achieved by increasing fermentation titer (41.0%). The threshold for IRR greater than the hurdle rate of 25% (shown by the dashed line in **Figure 53**) was found at a separation efficiency greater than 83%.

Sensitivity to TFF Cartridge Replacement Frequency

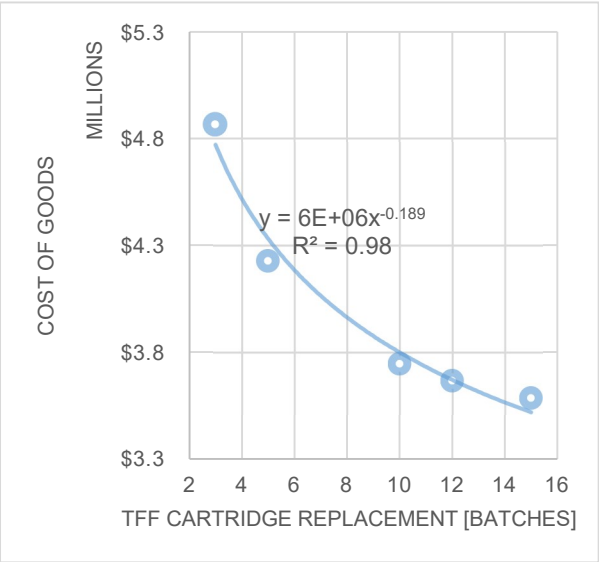

Figure 54: Sensitivity of COG to TFF cartridge replacement

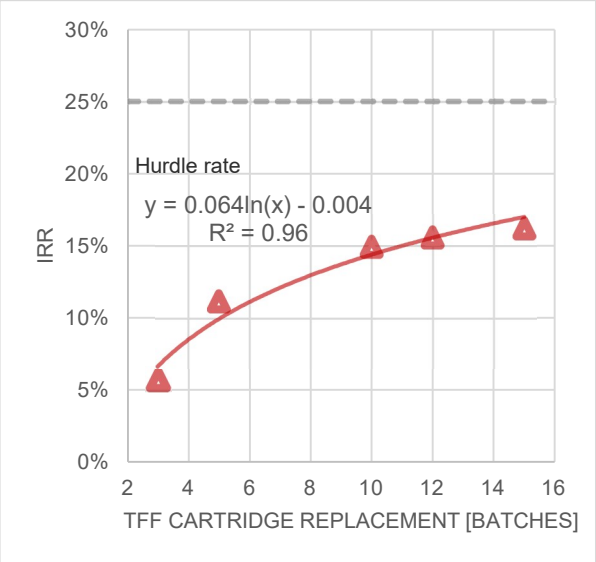

Figure 55: Sensitivity of IRR to TFF cartridge replacement

Figure 54 (above left) shows sensitivity of COG to TFF cartridge replacement frequency. The trend line fitted follows an exponential trend, with an R^2 of 0.98. The lowest COG of $ 3.6 million /kg was found when replacing TFF cartridges every 15 batches. This reduction in COG from the base case of $ 3.7 million /kg was relatively small as compared to the increase in COG for replacing TFF cartridges every 3 batches with a COG of $ 4.9 million /kg. These two results showed that COG was more sensitive to TFF cartridge replacement frequency at low replacement frequency (every 10 - 15 batches), while sensitivity decreased at high replacement frequency (every 3 - 5 batches).

The sensitivity of IRR to TFF cartridge replacement frequency is shown in **Figure 55** (above right). The trend line fitted did not follow a linear or polynomial trend but was closest to a logarithmic trend, with an R^2 of 0.96. This type of trend fitted the observed relationship between IRR and replacement frequency, similar to that between COG and replacement frequency. IRR was more sensitive at low replacement frequency and less sensitive at high replacement frequency.

Sensitivity to Percentage Electricity Generation From Diesel

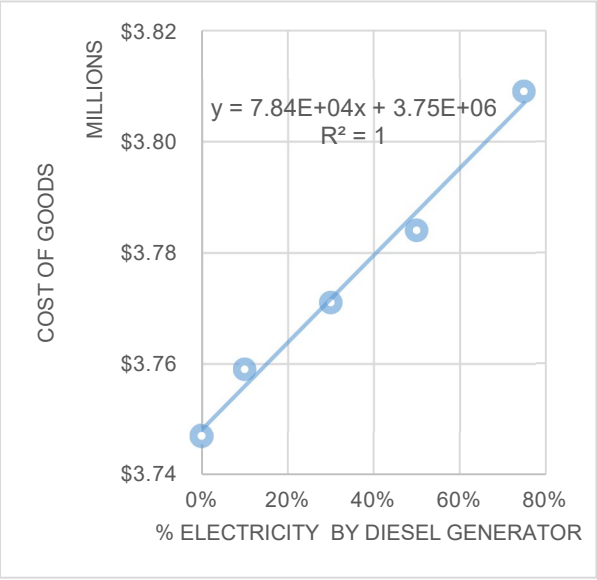

Figure 56: Sensitivity of COG to % electricity from diesel

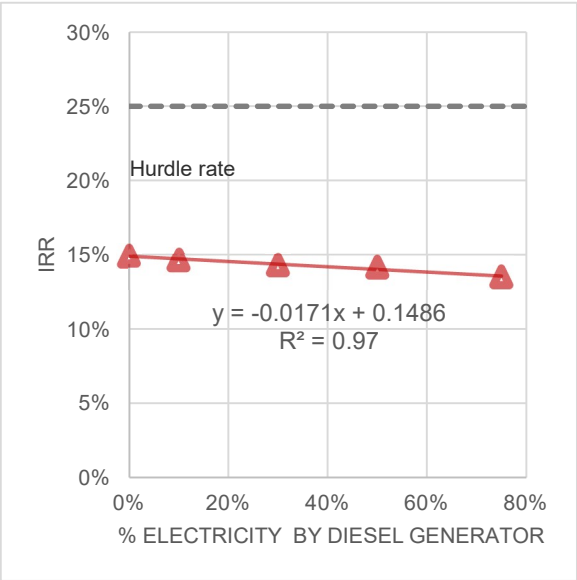

Figure 57: Sensitivity of IRR to % electricity from diesel

The sensitivity of COG to percentage electricity from diesel generator is shown in **Figure 56** (previous page bottom left). The linear trend-line fitted to the data in **Figure 56** shows that COG was not very sensitive to electricity dependence on diesel, with the slope of the trend line ($m = 7.8x10^4$) being 100 times smaller than the intercept ($c = 3.8x10^6$). It was noted that increasing electricity dependence on diesel from 0% to 75% resulted in less than a $ 0.1 million /kg increase in COG, from $ 3.7 million /kg (0% electricity from diesel) to $ 3.8 million /kg (75% electricity from diesel). The latter scenario featured a $ 250 000 increase in purchased equipment cost, with an increase in electricity cost from $ 0.10 /kWh to $ 0.35 /kWh.

Figure 57 (previous page bottom right) shows sensitivity of IRR to electricity dependence on diesel. IRR was not very sensitive to this parameter as compared to the other sensitivity parameters tested previously. An inverse linear trend was observed between IRR and electricity dependence on diesel. For each 10% increase in electricity requirements from diesel resulting in a 0.2% decrease in IRR.

Sensitivity trends

The process model at 200 L scale using stainless steel technology was not particularly sensitive to electricity dependence on diesel, with sensitivity of COG and IRR to this parameter being approximately 100 times smaller than the range of COG and IRR values respectively. An increase from 0% to 75% electricity dependence on diesel resulted in just a 2% increase in COG, from $ 3.7 million / kg to $ 3.8 million /kg. The same was found for IRR in this scenario, with a decrease of only 1.4% IRR.

Sensitivities of the 200 L stainless steel technology process model to fermentation titer and separation efficiency were more notable. Sensitivity to fermentation titer illustrated the greatest gains in both COG and IRR, suggesting that this is an area of the process to focus on for optimization. The scenario of 600 mg/L titer yielded a 40% reduction in COG from the base case $ 3.7 million /kg down to $ 2.2 million /kg. Similarly, the improvements from increasing separation efficiency were attractive as an optimization parameter. An increase from 67% to 90% separation efficiency for product recovery resulted in a 25% reduction in COG, from $ 3.7 million /kg to $ 2.8 million /kg. The relative improvements in COG between fermentation titer, separation efficiency, and TFF cartridge replacement frequency, are shown below in **Figure 58**.

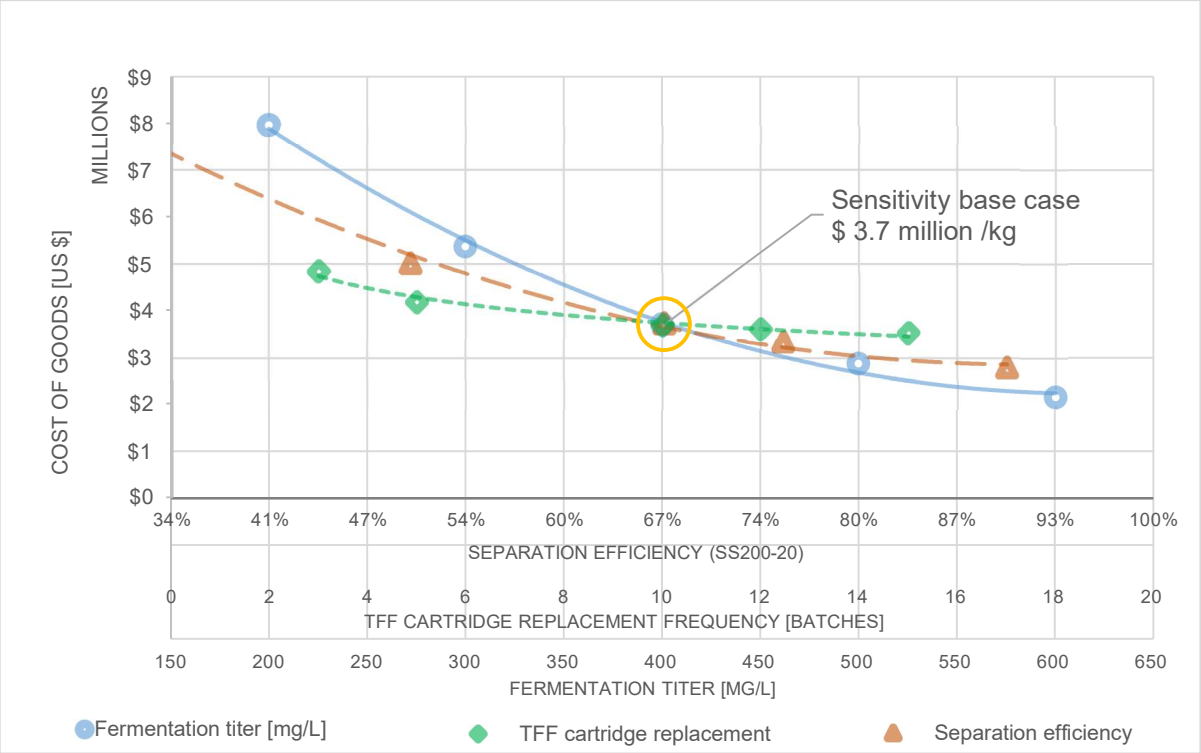

Figure 58: Comparative sensitivities of COG

In **Figure 58** (previous page) all three trends in COG are overlaid using the sensitivity base case scenario 200 L stainless steel process as a reference point (COG $ 3.7 million/kg). The comparison shows that COG sensitivity to fermentation titer was greater than the sensitivity of COG to separation efficiency or TFF cartridge replacement frequency. This can be observed by the trend-lines of the latter two parameters being more horizontal about the reference point of the sensitivity base case scenario, as compared to the solid line representing the trend in fermentation titer.

A similar comparison was generated for the sensitivity of IRR to the parameters of fermentation titer, separation efficiency, and TFF cartridge replacement frequency and is shown below in **Figure 59**.

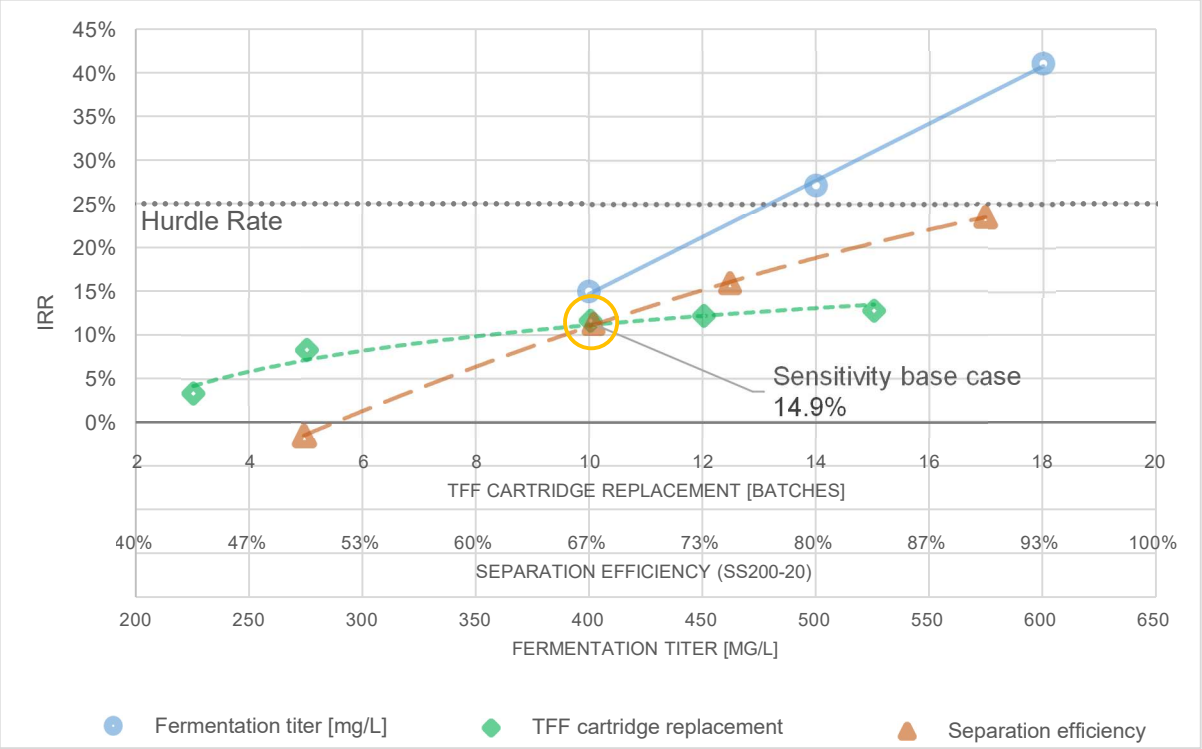

Figure 59: Comparative sensitivities of IRR

The comparitive sensitivies to IRR are illustrated in **Figure 53** by the relative slopes of each of the three trend lines about the base case scenario point, which was an IRR of 14.9 % for the 200 L stainless steel process model. IRR was most sensitive to fermentation titer, as can be seen by the slope of the solid line in **Figure 59**. IRR was also least sensitive to TFF cartridge replacement at the base case scenario reference point; however, it is noted that the trend in sensitivity to TFF cartridge replacement was non-linear, and sensitivity to this parameter was much greater at high replacement frequency (every 3 batches).

When comparing the sensitivity of the three parmaters to the hurdle rate (dotted line in **Figure 59**) it is visible that small increases in fermentation titer were sufficient to make the project viable (IRR > hurdle rate). This was found by increasing titer from 400 mg/L to 480 mg/L, a 20% relative increase. In comparison a greater improvement in separation efficiency was required, from 67 % in the sensitivity base case to 83%, a relative increase of 25%.

In terms of the trend lines fitted and relative sensitivities of the parameters, fermentation titer fitted a linear trend, separation efficiency a quadratic trend, and TFF cartridge replacement fitted a logarithmic trend. It was observed that the more linear the trend, the more sensitive the model IRR was to that parameter. Amongst the three paramters shown in **Figures 58 and 59**, the model was most sensitive to fermentation titer, followed by separation efficiency, and least sensitive to TFF cartridge replacement frequency. An exception was found at high TFF cartridge replacement frequency where COG and IRR sensitivities deviated from a linear or quadratic trends and fitted exponential trends more closely.

5 Discussion

Capital Expenses at 20 L and 200 L Scales

At 20 L scale, CAPEX for single use technology was lower than both stainless steel and hybrid technology, but at 200 L scale it was the opposite case, with stainless steel CAPEX being the lowest. The major differences in CAPEXs at the 20 L scale may be attributed to differences in equipment cost between a stainless steel fermentor ($ 403 000) and a single use fermentor ($ 118 000) at the 20 L - 50 L size range. The difference was seen again between stainless steel mixing vessels ($ 165 000) and single use mixing vessels ($ 74 000 - $ 100 000) in the 50 L - 70 L size range, which was required for the 20 L fermentor scale.

At 200 L scale CAPEX for single use technology was $ 2 million greater than for stainless steel, while hybrid technology was only $ 0.5 million greater. At this scale the major difference in CAPEX was due to the much greater cost of a 200 L single use fermentor ($ 800 000) with 200 L – 650 L single use mixing vessels ($ 150 000 - $ 300 000) compared to a 200 L stainless-steel fermentor ($ 620 000) and 200 L – 600 L stainless-steel mixing vessels ($ 171 000 - $ 199 000). The specific CAPEXs per kg of product for all three technology platforms at 200 L scale were on average 5 times less than the CAPEXs per kg of product at 20 L scale. The latter indicates a 5x economy of scale in terms of CAPEX when increasing from 20 to 200 L scale.

As process scale was increased to 200 L, single use technology lost the advantage it had at 20 L scale in terms of lower capital costs. The observed result agrees with **Table 2-6** in **Section 2.3**, which reported a decreasing technological competitiveness of single use technology at large scales. The increased cost of single use equipment at scale was described in **Section 2.3** as due to inherent technological limitations which require more expensive components to achieve equivalent performance. Although technological development of single use technology could feature improvements to mitigate this, the result in this study confirms the scalability limitation of single use technology.

Operating Expenses and Cost of Goods at 20 L Scale

At 20 L scale OPEX was relatively similar across all three technology platforms, which indicated that the cost of replacing single use consumables had little effect on OPEX at this scale. It should be noted that the qualitative benefits of single use technology such as speed to market and reduced risk of cross contamination are not reflected in the economic analysis results reported in **Chapter 4**. These benefits would make single use technology the most desirable for a process at the pre-clinical and phase I trial stage of development, given the relatively similar operating costs of single use and stainless steel at this scale. It was also noted that waste disposal costs were similar for all platforms at 20 L scale, which is a reported drawback of single use technology in **Table 2-6** in **Section 2.3**. The concern that large amounts of plastic waste would require disposal at a cost were not applicable to this process at the 20 L scale, as the cost of disposing of the additional plastic waste was not enough to impact OPEX.

At 20 L scale there was little difference in COG between the three technology options. This was a feature of the 20 L scale process, despite having 40 – 54% of OPEX attributed to facility dependent costs across the three technology platforms. Facility dependent cost contribution to OPEX was a factor of the equipment purchase costs, which were different across technology platforms at both scales. This result suggests that CAPEX had little effect on OPEX for the 20 L scale process. Equipment costs were only 19 - 21 % of Direct Fixed Capital (DFC) as shown previously in **Figures 32, 33 and 34**. This result may be better understood when considering one of the assumptions made in this simulation exercise was to use a depreciation period of 10 years. This assumption reduced the effect of CAPEX on OPEX by reducing the absolute value of facility dependent costs, and subsequently enhanced the effect of other variable costs on OPEX. The outcome was that this simulation exercise was generally more focused on variable costs than fixed costs.

Operating Expenses and Cost of Goods at 200 L Scale

At 200 L scale OPEX for single use technology was $ 1 million greater than both hybrid and stainless-steel technologies, an effect of increased consumables costs for single use technology at the 200 L scale. The trend observed in OPEXs scaling up from 20 L to 200 L when is an effect of using fixed consumables costs at both scales. A result of this decision was that the operating cost of the consumable-intensive single use technology increased proportionally as the process scale increased. Despite this result, it should be noted that a manufacturer purchasing consumables in large shipments in South Africa may be able to negotiate discounts with suppliers, which could result in a reduction in these costs. An increased uptake of single use technology in other African countries and emerging markets in the future could further reduce the price of these consumables.

Another consideration for large orders of material is increased storage and transportation costs. A simpler solution would be to select a technology platform with inherently lower capital- and consumable costs, thereby eliminating the need to buy large orders of material. The goal for a commercial process would be to minimize OPEX, which effectively excludes the choice of single use technology at the 200 L scale. The hybrid technology platform featured a relatively lower OPEX of $ 6.2 million /y compared to single use at $ 7.0 million /y, and only marginally higher than stainless steel at $ 6.0 million /y. The advantage of this technology at the 200 L scale would be the retention of some of the qualitative benefits of single use technology as mentioned previously (speed to market, validation cost), whilst also being competitive in terms of the overall COG.

At 200 L scale the best performing technology in terms of COG was stainless steel, with COG $ 650 000 /kg lower than that for single use technology. This was attributed to the greater cost of consumables for single use technology at 200 L scale, taking up a quarter of OPEX as shown previously in **Figure 42**. The observed trend in OPEX between the three technology platforms (SU>HY>SS) at the 200 L scale was similar to the trend in COG (SU>HY>SS), which suggests a direct influence of OPEX on COG when scaling up a process to 200 L. Increasing the process scale ten-fold from 20 L to 200 L had approximate effects across all the technology platforms of doubling capital costs, tripling operating costs, but halving COG. The latter effect on COG demonstrates the difference in economies of scale between 20 L and 200 L fermentation capacity.

Labour costs proportion of OPEX was reduced to about 5% for all three platforms at 200 L scale, compared to about 12 % at 20 L scale. The assumption that operational labour costs would be the same for the 200 L scale process as for the 20 L scale process was the primary reason for labour taking up such a small portion of costs as the process scale increased. In addition, the exclusion of administrative, quality (QA, QC), and regulatory labour costs also reduced the proportion of labour costs of OPEXs at 200 L scale. Including these additional labour costs could have produced a more accurate representation of the overall cost breakdown. As a result of these assumptions made for labour costs, the results in this thesis are focused more on material and consumables costs.

Further investigation into the real labour costs, as well as the costs of equipment and consumables at large process scale could identify a more accurate relationship between costs and processing scale for this particular process. Such an investigation could improve the usefulness of the simulation models produced in this thesis to accurately predict real process performance. It would also be useful to investigate the effect of reducing the depreciation period to 5 years, to determine whether CAPEX may begin to influence COG.

Internal Rate of Return and feasibility

IRR was found to be less than the hurdle rate of 25% for all six of the initial scenarios modelled, indicating that the base case process performance would not be feasible. At 20 L scale, IRR was non real, indicating an outright loss-making project at that scale. This was illustrated previously in **Table 4-3**, where break even prices at the 20 L scale were close to $ 50 /dose, almost double the recommended selling price of $ 20 – $ 30 /dose. At 200 L scale, the break-even prices were about $ 20 /dose which was within the recommended selling price range, suggesting a marketable product.

At 200 L scale IRR was highest for stainless steel technology, at 14.9 %, which formed the base case for further sensitivity analyses. The sensitivity analyses showed that optimization of some process

performance areas could make the process feasible, and a potential IRR value as high 41 % could be achieved with 600 mg/L fermentation titer. It should be noted that this performance increase may not be realistic but informs a process development decision to focus on this parameter as an area for optimization.

Increasing process scale from 20 L to 200 L made the process profitable for all three technology platforms (IRR > 0). It is postulated that increasing the process scale above 200 L would make the process inherently feasible (IRR > hurdle rate) for one or more of the technology platforms even before optimization of performance. Although sensitivity was not performed on process scale as a parameter, this should be included in any further application of this research.

Sensitivity of COG and IRR

The sensitivity of COG to fermentation titer and separation efficiency showed that increasing the profitability of the 200 L stainless steel process was possible through process optimization. Although optimization is not included in this thesis, the sensitivity of COG and IRR shown in **Figures 52 and 53** indicated that small improvements in specific areas of the process could yield valuable improvements to profitability. It should be noted that such improvements would require investment of both time and money.

The sensitivity analyses of fermentation titer and separation efficiency highlight two of the process parameters that could be improved to achieve reductions in COG and increases in IRR. For any prospective development of such a process, these parameters could be investigated for optimization. The sensitivity base case 200 L stainless steel technology process was not feasible, with an IRR of only 14.9 % which was below the hurdle rate of 25.0 %. The feasibility of the process at 200 L scale is therefore dependent on increasing at least one of the sensitivity parameters of fermentation titer or separation efficiency. As shown in **Figure 53**, the scenarios where IRR was greater than the hurdle rate were only achieved after increasing fermentation titer or separation efficiency above the threshold values where IRR = hurdle rate.

The results of the sensitivity analyses could be used to direct the process development decision making, in focusing attention on the most sensitive areas of the process. It was certainly true for the 200 L stainless steel process model's sensitivity to electricity dependence on diesel generation. While this is a real risk for manufacturers, the process model was found to not be very sensitive to this parameter. The result showed that if the relevant contingency was in place (generators, diesel storage), then this was not an area to focus on for ongoing process development. In contrast, fermentation titer and separation efficiency would need to be prioritised.

The sensitivity of COG and IRR to TFF cartridge replacement frequency also showed how operational decisions can affect profitability. Increasing the frequency of replacement from every 10 batches in the sensitivity base case, to every 3 batches resulted in a substantial increase in COG and decrease in IRR. The initial operational decisions regarding consumables would have an impact on the process feasibility, even if not as strongly as fermentation titer or separation efficiency. The magnitude of COG reduction was not the same when increasing TFF cartridge replacement from every 10 to every 15 batches. The result is valuable to consider when increasing the re-usable lifespan of consumables, as this would incur additional validation costs to show cleaning efficacy.

Environmental Impact and Sustainability

It was noted that the annual cost of waste disposal per kg of product for single use technology at 200 L scale was $ 5 000 /kg.y greater than that of stainless steel, while hybrid was only $ 600 /kg.y. This showed that the increase in consumables cost was the largest contributor to increased waste disposal costs for single use technology. In terms of mass the additional waste accounted for an additional 2.4 tons of plastic waste per year which suggests that despite the relatively small impact on costs, the physical environmental impact may be greater. Considering that the 200 L scale stainless-steel process utilised an additional 23 t/kg.y of water and 2 MT/kg.y of steam for sterilization and CIP services, it is

understood that the environmental sustainability of both processes would need to be evaluated by LCIA before a definitive answer could be given on which was more sustainable.

The effect of scaling up the process ten-fold, from 20 L to 200 L, resulted in an increase in waste disposal costs of over 800%, attributed primarily to the large increase in aqueous waste for disposal. Single use technology at 200 L scale also incurred a 6% increase in waste disposal costs compared to stainless-steel. This may be attributed to the cost of disposing of large single use reactor bags and other single use consumable items.

At industrial manufacturing scales, the large amount of plastic waste generated by single use process technology may be a serious challenge in terms of environmental impact and sustainability. Single use plastics are non-biodegradable and in many cases are not recyclable as they are classified as biohazardous waste. The result is that a process that is reliant on single use technology will produce large quantities of plastic waste that will need to be incinerated. In addition to generating this plastic waste, the industrial scale demand for single use plastics would create an economy for the extraction of fossil fuels and refining of petroleum products used to make these plastics.

In contrast stainless steel technology was water intensive, which may be more important when considered within the South African context. South Africa is a water scarce country, where the sustainability of any commercial process would be intrinsically linked to the efficient and frugal use of water. It is possible that in a South African context, a water intensive process technology like stainless steel may be less sustainable than a technology which generates large quantities of petroleum based plastic waste, such as single use technology.

South African Context

Some of the capital costs used in the simulations were estimated using built in software cost models supplied by Intelligen Inc., a software developer based in the US. For equipment costs specified using purchase costs from The Biovac Institute in South Africa, it was observed that the real cost for purchasing biopharmaceutical equipment in the South African market is more expensive than in Europe, Asia, and the US. This is due to the small relative size of the South African biopharmaceutical market, and global economic forces such as exchange rates and trade agreements. The cost of this type of equipment increases the economic appeal of single use technology at the 20 L scale, and similarly makes stainless-steel technology at the 200 L scale more appealing. The regulator of South African pharmaceutical products is also less experienced than their American counterpart with validation of single use systems, creating a further source of uncertainty over the potential speed-to-market benefit of single use technology in a South African context.

This simulation exercise indicated there was very little benefit, in terms of COG and IRR, in using single use technology in the South African context. This result is contrary to similar exercises by others for contexts in developed economies (Sinclair & Monge, 2002, 2005; Papavasileiou, Siletti & Petrides, 2008; Zheng, 2010; Flaherty & Perrone, 2012). The results of this thesis seem to indicate a *reduced benefit* when implementing single use technology in a developing economy away from main distribution and manufacturing centres, like that of South Africa. The effects on COG (identified in **Chapter 4**) from an increased cost of consumables were that single use technology featured up to 31% (at 20 L scale) of OPEX for the single use technology platform. This increased cost phenomenon is due to the African context for biopharmaceutical processing, where this region has a low market power compared to the US, Asian and European contexts in which other studies are based. Another finding was the CAPEX for single use equipment at 200 L scale being $ 2 million higher than for stainless steel. To a lesser extent this is also due to context and market power, although it may also be attributed to the decreased competitiveness of single use technology at the 200 L scale.

An example of typical costs for a 50 kg/y process to make a viral vaccine using stainless steel technology in Australia featured a consumables cost of between $ 4 200 /kg and $ 12 000 /kg (Chuan et al., 2014). The 1.6 kg/y conjugate vaccine process (200 L, stainless steel) in this exercise in a South

African context featured a consumables cost of $ 631 000 /kg, while the single use technology platform featured a consumables cost of $ 1 million /kg. Although not included in this study, these costs may be expected to decrease at larger industrial scales. A 1000 L monoclonal antibody process based on single use technology in Europe would have a typical consumable cost of about $ 60 000 /kg (Sinclair & Monge, 2005). Another example for a 2000 L mAb process featured a consumables cost of $ 39 500 /kg (Papavasileiou, Siletti & Petrides, 2008).

It should be noted that these comparisons are made between vastly different processes and technologies. Comparing monoclonal antibodies to viral vaccines to conjugate vaccines all at different process scales is not precise enough to draw meaningful conclusions; however, the example does illustrate that consumables costs are process and context specific. The increased cost of consumables observed for the GBS vaccine process in a South African context would make the same process less profitable than if it were developed in a European context.

An area where cost savings are possible due to a characteristic of the South African context is a lower average cost of labour. The simulation results showed a very small proportion of labour costs in OPEX, which was primarily due to some of the assumptions made which were discussed previously in Operating Expenses and Cost of Goods at 200 L Scale. It is also interesting to compare these costs to processes in the international contexts described above. A viral vaccine process in Australia (Chuan et al., 2014) featured a labour cost of $ 3.8 million /y, compared to the conjugate vaccine process in this study with a labour cost of $ 287 000 /y. Again, the differences between the processes are important to understanding the difference in labour costs, but context is also worth consideration.

Labour in South Africa, as for other emerging economies such as India or China, is generally cheaper than in Europe, Asia, or the US. In terms of operational labour, the salary data retrieved from the website PayScale showed that the annual cost of a process operator in South Africa was $ 10 000 /y, while the same operator in the USA would cost $ 50 000 /y (PayScale, 2019a). Similarly, a production supervisor in South Africa would cost $ 15 000 /y, and in the USA, $ 60 000 /y (PayScale, 2019b). The trend indicates that labour costs in South Africa are about five times lower than the US. This suggests setting up in a process in South Africa could provide real costs savings, especially if increased costs in other areas could be mitigated.

Process Simulation as a Decision Support Tool

The simulation exercise showed that economic performance of the different process technologies could be simulated without purchasing any equipment or consumables, nor the hiring of any personnel. The accuracy of these economic projections is; however, dependent on the availability of accurate data on the pricing of equipment, consumables, materials, and labour costs for the process being modelled. The model is only as good as the information that goes into it.

Crucial to the application of simulation modelling tools for biopharmaceutical process development is that the financial risk to a potential process developer would be considerably less than setting up a pilot scale plant. Novel biopharmaceutical processes are high risk with high project failure rates, and typically also require large upfront investment in order to develop a new product. Added to this is the opportunity cost of facility utilisation for a period of 5 - 10 years to take a new product from preclinical development to approval. A simulation exercise would provide valuable information at the pre-feasibility stage, particularly in terms of directing the technological development and direct fixed capital investment for the project, as well as providing information on how to expedite the development pathway.

The direct fixed capital cost of installation and starting up a 20 L scale pilot process in this study would be approximately $ 9.5 million, whereas the cost of a simulation exercise (a software license and one engineer’s salary) to test multiple technology options would be less than $ 100 000. The cost saving in this regard is enhanced due to the reduced labour cost of conducting this exercise in South Africa.

For any biopharmaceutical process under development the choice of which technology to use in a pilot scale process is a critical feasibility parameter. If a more expensive technology platform is chosen to build a pilot plant and also carried through for commercialization, the project would end up costing more

to the investor and could even be outright infeasible. In this project a 200 L scale process using the single use technology platform would start with an IRR of only 9% making it more challenging, even with optimization, to meet the required IRR of 25% to become feasible. Although not included here, it may not even be possible to achieve this target with the single use technology platform. This type of decision would be a fatal error during process development if realized at the stage of having built and installed a 200 L scale plant at a cost of $ 20 million.

The simulation exercise in this study provided information on which platform to start for development. The tool was able to generate information on the choice of technology, as well as the areas of the process which could achieve the greatest gains in productivity and efficiency. The one area which the simulation exercise was not able to provide information on, was the qualitative benefits of each technology platform, such as the validation benefits of single-use technology. Single use technology may be beneficial for pre-clinical development due to reduced installation, start-up time, and validation requirements. This benefit was not modelled, nor was there any indication of it in the simulation results. Basing a decision solely on the results of a simulation exercise could therefore overlook some of these considerations and should be understood when using simulation results for making process development decisions.

The information produced in a simulation exercise such as this one would definitely be of use to a process developer and could also be applied to future projects once a simulation database has been generated. The unique information related to the South African context would also be useful for mitigating some of the unique challenges faced by operating a biopharmaceutical process in this economic context. The results of this type of exercise would be able to inform the successful development of a potential process by directing technological choices, context specific decisions on areas of the process requiring optimization, and also which areas of the process in which to invest for the highest possible returns.

6 Conclusion and Recommendations

Hypothesis

Cost of goods influences a new vaccine's commercial viability in an industry where lower product price is competitive with market power. A Techno-economic evaluation of three technology options for the production of a GBS trial vaccine antigen will provide information to reduce financial risk and support more commercially viable decisions during process development.

In the case study of a trial vaccine; it is hypothesised that single use vessels will yield a lower cost of goods at 20 L and 200 L process scale, as compared to stainless steel vessels. This is hypothesised due to an expected reduction in operating costs for clean- and sterilize-in-place requirements for stainless steel technology. A hybrid of the two technology options would yield an even lower cost of goods by combining the best economic properties of both single use and stainless-steel technologies.

Conclusions

The Hypothesis is disproved. In contradiction with the hypothesis, at 20 L scale stainless steel and single use technology platforms yielded similar COGs of $ 9.7 million /kg and $ 9.8 million /kg, respectively. At 200 L scale stainless-steel technology had an advantage with a COG of $ 3.7 million /kg, compared to single use technology's COG of $ 4.3 million /kg. Hybrid technology was not the best performing at either scale, with a COG of $ 9.8 million /kg at 20 L scale and an intermediate COG of $ 3.8 million /kg at 200 L scale. The second part of the hypothesis is therefore also disproved, in that hybrid technology does combine the characteristics of single use and stainless-steel technology but does not result in the lowest COG.

The process is infeasible and loss-making at 20 L scale regardless of technology platform, while at 200 L scale the process was still infeasible but was at least profitable. Scaling the process up to 200 L and improving process performance are therefore basic requirements for commercial feasibility.

The process in this study was modelled within a South African context, which influenced the economic performance of the process technologies tested. Single use equipment and consumables were relatively expensive to purchase in South Africa, making the single use technology platform less competitive at both scales. Reduced labour costs in the South African context also increased the influence of other variable costs such as raw materials and consumables.

The environmental impacts of single use versus stainless steel technology were not investigated in this thesis; however, they are important to consider in the current global context of climate change and sustainable industries. The information required to assess and evaluate these impacts such as the quantity of plastic waste and the consumption of water and electricity was available as a product of the simulation exercise and this information must be used to quantify environmental impacts any subsequent evolutions of this type of research. The sustainability of a stainless steel or single use process technology may also be influenced by the South African context, given it is a water scarce country with a strong economic dependence on extractive industries and without particularly strong policies on reducing environmental deposition of plastic waste and its derivatives.

Process simulation modelling is applicable to biopharmaceutical process development decision making at the pre-feasibility design stage of a project and may also be extended further into feasibility assessment. This process analytical tool is able to provide information on the economic impact of process development decisions by testing multiple processing options and comparing their relative economic performance. Single use technology was associated with an increase in plastic waste, while stainless steel technology was water intensive. The environmental sustainability of different process technologies may be evaluated using simulation modelling; however, more detailed analysis is required to evaluate environmental impacts.

Recommendations

Stainless steel vessel technology is recommended for further development of a process to manufacture a novel GBS vaccine at 200 L scale or greater. Such a process could be feasible at commercial scales of 200 L with a fermentation titer of 480 mg/L or greater. Profitability could be further improved by one or more of: increasing the process scale beyond 200 L (assuming expansion into the global market), improving product recovery efficiency beyond 67%, and reducing the replacement frequency of expensive consumables such as TFF cartridges to more than 10 batches.

At 20 L scale single use technology is recommended for development of the GBS vaccine process due to inherent qualitative benefits for start-up and pre-clinical development. For increasing the process scale above 20 L it is recommended to change to stainless steel technology. This technology changeover is recommended to be integrated into the process development plan to achieve the maximum benefit from both technology platforms.

The application of process simulation modelling to biopharmaceutical process development in a South African context is strongly recommended. The unique effects of market forces and the South African economic climate require context-specific information on the performance of different process decisions. This is especially applicable to the areas of the process influenced by economic context, such as capital- and material costs. An effective simulation exercise at the pre-feasibility and feasibility stages of a novel biopharmaceutical product development project in a developing economy could save an investor from making costly decisions that would otherwise have been based on the performance of similar processes in established markets of Europe, Asia, and the US.

Future applications of this research

A future application of this research would be to expand the simulation exercise to include more detailed and updated costs for equipment, raw materials, consumables, and labour costs. Further investigation into equipment and consumables costs at 2019 prices, and adjusted pricing for large order quantities for 200 L processing scale (and above) could identify a more accurate relationship between costs and process scale. It would also be useful to investigate the effect of reducing the depreciation period to 5 years, to determine a more accurate relationship between capital expenses and cost of goods.

The scope of labour costs may also be expanded to include administration, quality assurance, quality control, and regulatory labour costs. An improvement to the sensitivity analyses would be to include process scale as a sensitivity parameter and to use Monte Carlo sensitivity analysis to provide quantitative measure of the uncertainty associated with the simulation results.

An additional analysis that could be performed in future would be to assess the environmental impact of the different technology platforms, particularly in terms of plastic waste and water footprint. These investigations could improve the potential for these simulation models to accurately predict real process performance, and to provide further information on the development of biopharmaceutical processes in a South African context.

On the use of process simulation as a decision support tool for biopharmaceutical process development in a South African context:

Process simulation is a versatile tool for process development. The tool was deployed to evaluate a novel biopharmaceutical process for which there was little existing information and produced a quantitative analysis of the commercial potential of three technological decisions. Process simulation as a decision support tool can also be used in a specific context such as the unique South African biopharmaceutical process development and manufacturing landscape, and subsequently be able to produce information that informs practical context specific process development decisions.

References

Allison, N. & Richards, J. 2014. Current status and future trends for disposable technology in the biopharmaceutical industry. *Journal of Chemical Technology and Biotechnology*. 89(9):1283–1287. DOI: 10.1002/jctb.4277.

Ampofo, W. 2016. *Vaccine Manufacturing in Africa*. Available: https://www.whhttps//www.who.int/immunization/research//forums_and_initiatives/en/ [2019, March 03].

Aranha, H. 2004. Disposable Systems. One More Manufacturing Option. *BioProcess International*. 2(9):6–16.

Aspen Technology Inc. 2017. Aspen Plus 8.8 Academic.

Bae, K., Choi, J., Jang, Y., Ahn, S. & Hur, B. 2009. Innovative vaccine production technologies: The evolution and value of vaccine production technologies. *Archives of Pharmacal Research*. 32(4):465–480. DOI: 10.1007/s12272-009-1400-1.

Baker, L. 2010. The face of South Africa's Expanded Programme on Immunisation (EPI) schedule. *SA Pharmaceutical Journal*. 77(1):18–49. Available: https://journals.co.za/docserver/fulltext/mp_sapj/77/1/mp_sapj_v77_n1_a5.pdf?expires=1570102445&id=id&accname=guest&checksum=0C5D9C0E54CD8B3C5AEA4571BB7BCAEF.

Bartoloni, A., Norelli, F., Ceccarini, C., Rappuoli, R. & Costantino, P. 1995. Immunogenicity of meningococcal B polysaccharide conjugated to tetanus toxoid or CRM197 via adipic acid dihydrazide. *Vaccine*. 13(5):463–470. DOI: 10.1016/0264-410X(94)00007-A.

Bateman, C. 2016. Vaccines: SA's immunisation programme debunked. *SAMJ: South African Medical Journal*. 106:318–319. DOI: 10.7196/samj.2016.v106i4.10765.

BD Biosciences. 2006. BD Bionutrients ™ Technical Manual - advanced Bioprocessing. 1–72.

BioPlan Associates. 2017. *Concentration of global biopharmaceutical manufacturing*. Available: http://top1000bio.com/ [2018, July 19].

Biwer, A., Griffith, S. & Cooney, C. 2005. Uncertainty analysis of penicillin V production using Monte Carlo simulation. *Biotechnology and Bioengineering*. 90(2):167–179. DOI: 10.1002/bit.20359.

Bomela, H.N., Ballott, D.E. & Cooper, P.A. 2001. Is Prophylaxis of Early-Onset Group B Streptococcal Disease Appropriate for South Africa? *South African Medical Journal*. 91(October):10–12.

Buckland, B.C. 2005. The process development challenge for a new vaccine. *Nat Med*. 11(4 Suppl):S16-9. DOI: 10.1038/nm1218.

Burns, G. & Plumb, J. 2013. GBS public awareness, advocacy, and prevention-What's working, what's not and why we need a maternal GBS vaccine. *Vaccine*. 31(S4):D58–D65. DOI: 10.1016/j.vaccine.2013.02.039.

Buurman, E.T., Timofeyeva, Y., Gu, J., Kim, J.-H., Kodali, S., Liu, Y., Mininni, T., Moghazeh, S., et al. 2019. A novel hexavalent capsular polysaccharide conjugate vaccine (GBS6) for the prevention of neonatal group B streptococcal infections by maternal immunization. *The Journal of infectious diseases*. (February). DOI: 10.1093/infdis/jiz062.

Capiau, C., Deschamps, M., Desmons, P., Laferriere, C., Poolman, J. & Prieels, J.-P. 2000. *Patent No. EP 1 163 000 B1*. European Patent Office.

Chisti, Y. 2007. Biodiesel from microalgae. *Biotechnology advances*. 25(3):294–306. DOI: 10.1016/j.biotechadv.2007.02.001.

Chu, L. & Robinson, D.K. 2001. Industrial choices for protein production by large-scale cell culture. *Current Opinion in Biotechnology*. 12(2):180–187. DOI: 10.1016/S0958-1669(00)00197-X.

Chuan, Y.P., Wibowo, N., Lua, L.H.L. & Middelberg, A.P.J. 2014. The economics of virus-like particle and capsomere vaccines. *Biochemical Engineering Journal*. 90:255–263. DOI: 10.1016/j.bej.2014.06.005.

Costantino, P., Norelli, F., Berti, F., Olivieri, R., Bazzochi, G., Maria Cicala, C. & Fontani, S. 2013. *Patent No. US 8445239 B2*. United States Patent Office.

Cox, M.M.J. 2012. Recombinant protein vaccines produced in insect cells. *Vaccine*. 30(10):1759–1766. DOI: 10.1016/j.vaccine.2012.01.016.

Cutland, C.L., Madhi, S.A., Zell, E.R., Kuwanda, L., Laque, M., Groome, M., Gorwitz, R., Thigpen, M.C., et al. 2009. Chlorhexidine maternal-vaginal and neonate body wipes in sepsis and vertical transmission of pathogenic bacteria in South Africa: a randomised, controlled trial. *The Lancet*. 374(9705):1909–1916. DOI: 10.1016/S0140-6736(09)61339-8.

Day, C.L., Tameris, M., Mansoor, N., Van Rooyen, M., De Kock, M., Geldenhuys, H., Erasmus, M., Makhethe, L., et al. 2013. Induction and regulation of T-cell immunity by the novel tuberculosis vaccine M72/AS01 in South African adults. *American Journal of Respiratory and Critical Care Medicine*. 188(4):492–502. DOI: 10.1164/rccm.201208-1385OC.

Dean, J.A. 1999. *Lange's Handbook of Chemistry*. Fiftheenth ed. McGraw Hill. DOI: 10.1080/10426919008953291.

DiMasi, J.A., Grabowski, H.G. & Hansen, R.W. 2016. Innovation in the pharmaceutical industry: New estimates of R&D costs. *Journal of Health Economics*. 47:20–33. DOI: 10.1016/j.jhealeco.2016.01.012.

Dlamini, N.R. & Maja, P. 2016. The Expanded Programme on Immunisation in South Africa: A story yet to be told. *South African Medical Journal*. 106(7):675. DOI: 10.7196/samj.2016.v106i7.10956.

Edmond, K.M., Kortsalioudaki, C., Scott, S., Schrag, S.J., Zaidi, A.K., Cousens, S. & Heath, P.T. 2012. Group B streptococcal disease in infants aged younger than 3 months: Systematic review and meta-analysis. *The Lancet*. 379(9815):547–556. DOI: 10.1016/S0140-6736(11)61651-6.

Eibl, R., Kaiser, S., Lombriser, R. & Eibl, D. 2010. Disposable bioreactors: The current state-of-the-art and recommended applications in biotechnology. *Applied Microbiology and Biotechnology*. 86(1):41–49. DOI: 10.1007/s00253-009-2422-9.

Ekambaram, A., Radcliff, W.L., Rienstra, S., Allred, L. & Stewart, D.W. 2000. *Patent No. US 6071005*. United States Patent Office.

EMD Millipore. 2013. Opticap® XL 150, 300 and 600 capsules with Millipore Express® membranes. Available: http://www.merckmillipore.com/ZA/en/product/Opticap-XL-600-Millipore-Express-SHF-Sterile-0.2m-3-4in.-TC-TC,MM_NF-KGEPS006FF3.

Eskom Holdings SOC Limited. 2019. *What is load shedding?* Available: http://loadshedding.eskom.co.za/LoadShedding/Description [2019, May 26].

Farid, S.S. 2007. Process economics of industrial monoclonal antibody manufacture. *Journal of Chromatography B: Analytical Technologies in the Biomedical and Life Sciences*. 848(1):8–18. DOI: 10.1016/j.jchromb.2006.07.037.

Farid, S.S., Washbrook, J. & Titchener-Hooker, N.J. 2007. Modelling biopharmaceutical manufacture: Design and implementation of SimBiopharma. *Computers and Chemical Engineering*. 31(9):1141–1158. DOI: 10.1016/j.compchemeng.2006.10.020.

Fisher Scientific. 2017a. *BD Select Soytone*. Available: https://www.fishersci.com/shop/products/bd-bbl-difco-media-additives-ingredients-reagents-phytone-peptone-2/p-4897968 [2017, June 12].

Fisher Scientific. 2017b. *BD Bacto Yeast Extract*. Available: https://www.fishersci.com/shop/products/bd-bacto-dehydrated-culture-media-additive-yeast-extract-3/p-4898247 [2017, June 12].

Flaherty, W. & Perrone, P. 2012. Environmental and Financial Benefits of Single-Use Technology. *ISPE Knowledge Brief*. (May 12):4.

Frasch, C.E. 2009. Preparation of bacterial polysaccharide-protein conjugates: Analytical and manufacturing challenges. *Vaccine*. 27(46):6468–6470. DOI: 10.1016/j.vaccine.2009.06.013.

Gambillara, V. 2012. The conception and production of conjugate vaccines using recombinant DNA technology. *BioPharm International*. 25(1):28–32.

Geldenhuys, H., Mearns, H., Miles, D.J.C., Tameris, M., Hokey, D., Shi, Z., Bennett, S., Andersen, P., et al. 2015. The tuberculosis vaccine H4: IC31 is safe and induces a persistent polyfunctional CD4 T cell response in South African adults: A randomized controlled trial. *Vaccine*. 33(30):3592–3599. DOI: 10.1016/j.vaccine.2015.05.036.

Godoy-Silva, R., Berdugo, C. & Chalmers, J.J. 2010. Aeration, mixing, and hydrodynamics, animal cell bioreactors. In *Encyclopedia of Industrial Biotechnology: Bioprocess, Bioseparation and Cell Technology*. M.C. Flickinger, Ed. John Wiley & Sons.

Goodwin, M., Elgan, G.P. & Larsen, J.K. 2006. *Patent No. US 7153021 B2*. United States Patent Office. DOI: 10.1016/j.(73).

Gosling, I. 2005. Process simulation and modeling for industrial bioprocessing: Tools and techniques. *Industrial Biotechnology*. 1(2):106–109. DOI: 10.1089/ind.2005.1.106.

Gottschalk, U. 2008. Disposable decisions: to achieve the right balance between disposable and reusable options, companies must consider important technical and economic factors. *BioPharm International*. 21(10):105. Available: http://link.galegroup.com/apps/doc/A189551876/AONE?u=unict&sid=AONE&xid=2f7d552c. Accessed 22 July 2018.

Hamidi, A., Kreeftenberg, H., V D Pol, L., Ghimire, S., van der Wielen, L.A.M. & Ottens, M. 2016. Process development of a new Haemophilus influenzae type b conjugate vaccine and the use of mathematical modeling to identify process optimization possibilities. *Biotechnology progress*. 4–8. DOI: 10.1002/btpr.2235.

Harrison, S.T.L. 2017. CHE5055Z The research proposal.

Haynes, W.M. 2014. *CRC Handbook of Chemistry and Physics*. 95th ed. CRC Press.

Heath, P.T. 2016. Status of vaccine research and development of vaccines for GBS. *Vaccine*. 34(26):2876–2879. DOI: 10.1016/j.vaccine.2015.12.072.

Hodge, G., Galliher, P. & Fisher, M. 2009. *Patent No. US 7629167 B2*. United States Patent Office. DOI: 10.1197/jamia.M1139.Adar.

Hotez, P.J. 2017. How the Anti-Vaxxers Are Winning. *The New York Times* (Houston). 8 February: 6–9.

Intelligen Inc. 2017. SuperPro Designer 9.5 Academic.

Jennings, H.J. & Lugowski, C. 1982. *Patent No. US 4356170*. United States Patent Office.

Josefsberg, J.O. & Buckland, B. 2012. Vaccine process technology. *Biotechnology and Bioengineering*. 109(6):1443–1460. DOI: 10.1002/bit.24493.

Kata, A. 2012. Anti-vaccine activists, Web 2.0, and the postmodern paradigm - An overview of tactics and tropes used online by the anti-vaccination movement. *Vaccine*. 30(25):3778–3789. DOI: 10.1016/j.vaccine.2011.11.112.

Khandke, L., Kim, J.-H., Liberator, P., Prasad, A.K., Ruppen, M.E., Scully, I.L., Singh, S. & Yang, C.X. 2016. *Patent No. WO 2016/178123 A1*. World Intellectual Property Organization.

Kim, S.Y., Russell, L.B., Park, J., Verani, J.R., Madhi, S.A., Cutland, C.L., Schrag, S.J. & Sinha, A. 2014. Cost-effectiveness of a potential group B streptococcal vaccine program for pregnant women in South Africa. *Vaccine*. 32(17):1954–1963. DOI: 10.1016/j.vaccine.2014.01.062.

Klugman, K.P., Madhi, S.A., Huebner, R.E., Kohberger, R., Mbelle, N. & Pierce, N. 2003. A trial of a 9-valent pneumococcal conjugate vaccine in children with and those without HIV infection. *New England Journal of Medicine*. 349(14):1341–1348.

Kobayashi, M., Schrag, S.J., Alderson, M.R., Madhi, S.A., Baker, C.J., Sobanjo-ter Meulen, A., Kaslow, D.C., Smith, P.G., et al. 2016. WHO consultation on group B Streptococcus vaccine development: Report from a meeting held on 27-28 April 2016. *Vaccine*. (April). DOI: 10.1016/j.vaccine.2016.12.029.

Kremer, M. 2002. Pharmaceuticals and the Developing World. *The Journal of Economic Perspectives*. 16(4):67–90. DOI: 10.1257/089533002320950984.

Kulkarni, N.S. 2015. Evaluating Bottlenecks and Support Functions using Simulations in Biotechnology Industry. 324–333.

Lancefield, R. 1932. A serological differentiation of human and other groups of hemolytic streptococci. *Journal of experimental medicine*. 1919(1):571–595.

Lang, Y.-D., Biegler, L.T. & Grossmann, I.E. 1988. Simultaneous optimization and heat integration with process simulators. *Computers & Chemical Engineering*. 12(4):311–327. DOI: 10.1016/0098-1354(88)85044-0.

Lee, C.H., Kuo, W.C., Beri, S., Kapre, S., Joshi, J.S., Bouveret, N., LaForce, F.M. & Frasch, C.E. 2009. Preparation and characterization of an immunogenic meningococcal group A conjugate vaccine for use in Africa. *Vaccine*. 27(5):726–732. DOI: 10.1016/j.vaccine.2008.11.065.

Lees, A., Sen, G. & Lopezacosta, A. 2006. Versatile and efficient synthesis of protein-polysaccharide conjugate vaccines using aminooxy reagents and oxime chemistry. *Vaccine*. 24(6):716–729. DOI: 10.1016/j.vaccine.2005.08.096.

Löffelholz, C., Husemann, U., Greller, G., Meusel, W., Kauling, J., Ay, P., Kraume, M., Eibl, R., et al. 2013. Bioengineering parameters for single-use bioreactors: Overview and evaluation of suitable methods. *Chemie-Ingenieur-Technik*. 85(1–2):40–56. DOI: 10.1002/cite.201200125.

Lopes, A.G. 2015. Single-use in the biopharmaceutical industry: A review of current technology impact, challenges and limitations. *Food and Bioproducts Processing*. 93(November):98–114. DOI: 10.1016/j.fbp.2013.12.002.

Lydon, P. & Raubenheimer, T. 2011. Outsourcing the vaccine supply chain and logistics system to the private sector: The Western Cape experience in South Africa. *Changes*. 2:1–54.

Madhi, S.A. 2015. From Vaccine Clinical Trials to Realising Public Health Benefit in South Africa. In *Presentation to Vaccinology Scientific Congress, National Institute of Communicable Diseases (NICD), Johannesburg*. 19–20.

Madhi, S.A., Groome, M.J., Zar, H.J., Kapongo, C.N., Mulligan, C., Nzenze, S., Moore, D.P., Zell, E.R., et al. (in press). Effectiveness of pneumococcal conjugate vaccine against presumed bacterial pneumonia hospitalisation in HIV-uninfected South African children: a case–control study. *Thorax*. 70(12):1149 LP – 1155. DOI: 10.1136/thoraxjnl-2014-206593.

Madhi, S.A., Petersen, K., Madhi, A., Wasas, A. & Klugman, K.P. 2000. Impact of human immunodeficiency virus type 1 on the disease spectrum of Streptococcus pneumoniae in South African children. *The Pediatric infectious disease journal*. 19(12):1141–1147.

Madhi, S.A., Radebe, K., Crewe-Brown, H., Frasch, C.E., Arakere, G., Mokhachane, M. & Kimura, A. 2003. High burden of invasive *Streptococcus agalactiae* disease in South African infants. *Annals of Tropical Paediatrics*. 23(1):15–23. DOI: 10.1179/000349803125002814.

Madhi, S.A., Cunliffe, N.A., Steele, D., Witte, D., Kirsten, M., Louw, C., Ngwira, B., Victor, J.C., et al. 2010. Effect of human rotavirus vaccine on severe diarrhea in African infants. *New England Journal of Medicine*. 362(4):289–298.

Makhoana, M. 2011. *Setting up vaccines human capital capacity in South Africa*. Available: https://www.who.int/phi/Session3B_Retention_local_workforce_Makhoana.pdf [2019, June 17].

Martin, J. 2010. Regulatory expectations and consensus industry recommendations for extractables testing of single-use process equipment. *BioPharm International*. 23(11 SUPPL.):6–10.

Martin, J. & Ding, W. 2009. Implementing Single-Use Technology in Biopharmaceutical Manufacturing. *Bioprocess International*. (7):46–51.

Merck Millipore. 2013. *Advancements on implementation of single use technology in vaccine manufacturing*. Available: https://www.dcvmn.org/IMG/pdf/advancements_on_implementation_of_single_use_technology_rio_oct2013.pdf [2019, October 03].

Michon, F. & Blake, M. 2001. *Patent No. US 6248570 B1*. United States Patent Office. DOI: 10.1016/j.(73).

Mickelson, M.N. 1967. Aerobic Metabolism of Streptococcus agalactiae Aerobic Metabolism of Streptococcus agalactiae. *Journal of Bacteriology*. 94(1):184–191.

Mickelson, M.N. 1972. Glucose degradation, molar growth yields, and evidence for oxidative phosphorylation in Streptococcus agalactiae. *Journal of Bacteriology*. 109(1):96–105.

Mistrette, N., Danve, E. & Moreau, M. 2010. *Patent No. US 7812006 B2*. United States Patent Office.

Monod, J. 1949. The Growth of Bacterial Cultures. *Annual Review of Microbiology*. 3(1):371–394. DOI: 10.1146/annurev.mi.03.100149.002103.

New Brunswick Scientific, Gouzheng, W., Zhang, W., Rich, M. & Gossain, V. 2009. Growing CHO Cells in a CelliGen ® BLU Benchtop , Stirred-Tank Bioreactor Using Single-Use Vessels. *Biotechnology progress*. 1–4. DOI: 10.2144/000113282.

Nienow, A.W. 2014. Stirring and stirred-tank reactors. *Chemie-Ingenieur-Technik*. 86(12):2063–2074. DOI: 10.1002/cite.201400087.

Nienow, A.W. 2015. Mass Transfer and Mixing Across the Scales in Animal Cell Culture. In *Animal Cell Culture*. M. Al-Rubeai, Ed. Springer International Publishing. 137–167. DOI: 10.1007/978-3-319-10320-4_5.

NIST Chemistry WebBook. 2019. *Isothermal Properties for Water*. Available: https://webbook.nist.gov/cgi/fluid.cgi?T=310.15&PLow=1&PHigh=1.1&PInc=0.01&Applet=on&Digits=5&ID=C7732185&Action=Load&Type=IsoTherm&TUnit=K&PUnit=bar&DUnit=kg%2Fm3&HUnit=kJ%2Fmol&WUnit=m%2Fs&VisUnit=Pa*s&STUnit=N%2Fm&RefState=DEF [2019, May 05].

Oracle. 2008. *Crystal Ball 11*. Available: https://www.oracle.com/technetwork/middleware/crystalball/cbmigration-084424.html [2019, June 09].

Pagliusi, S., Leite, L.C.C., Datla, M., Makhoana, M., Gao, Y., Suhardono, M., Jadhav, S., Harshavardhan, G.V.J.A., et al. 2013. Developing countries vaccine manufacturers network: Doing good by making high-quality vaccines affordable for all. *Vaccine*. 31(SUPPL2):176–183. DOI: 10.1016/j.vaccine.2012.11.060.

Pagliusi, S., Makhoana, M., Datla, M., Leite, L., Hendriks, J., Gholami, A., Huang, W., Gao, Y., et al. 2013. Developing Countries Vaccine Manufacturers Network (DCVMN): Engaging to step up for vaccine discovery and access. Meeting Report 2012. *Vaccine*. 31(31):311–3115. DOI: 10.1016/j.vaccine.2013.04.082.

Paoletti, L.C. 2016. Everything you want to know about GBS vaccines. In *PATH GBS Experts Meeting*.

Papavasileiou, V., Koulouris, A., Siletti, C. & Petrides, D. 2007. Optimize Manufacturing of Pharmaceutical Products with Process Simulation and Production Scheduling Tools. *Chemical Engineering Research and Design*. 85(7):1086–1097. DOI: 10.1205/cherd06240.

Papavasileiou, V., Siletti, C. & Petrides, D. 2008. Systematic Evaluation of Single-Use Systems Using Process Simulation Tools – A Case Study Involving MAb Production. *BioPharm International*. 21(June):16–29.

PayScale. 2017a. *Production Operator Salary*. Available: https://www.payscale.com/research/ZA/Job=Production_Operator/Salary [2017, June 18].

PayScale. 2017b. *Production Specialist Salary*. Available: https://www.payscale.com/research/ZA/Job=Production_Specialist/Salary [2017, June 18].

PayScale. 2017c. *Production Supervisor Salary*. Available: https://www.payscale.com/research/ZA/Job=Production_Supervisor/Salary [2017, June 18].

PayScale. 2017d. *Pharmacist Salary*. Available: https://www.payscale.com/research/ZA/Job=Pharmacist/Salary [2017, June 18].

PayScale. 2019a. *Average Production Operator Hourly Pay*. Available: https://www.payscale.com/research/US/Job=Production_Operator/Hourly_Rate [2019, August 11].

PayScale. 2019b. *Average Production Supervisor Salary*.

Perry, R.H. & Green, D.W. 2008. *Perry's Chemical Engineers' Handbook*. 8th ed. McGraw Hill. DOI: 10.1036/0071422943.

Petrides, D., Cooney, C.L., Evans, L.B., Field, R.P., Snoswell, M. & Field, B.P. 1989. Bioprocess simulation: an integrated approach to process development. *Computers & Chemical Engineering*. 13(4–5):553–561.

Petrides, D., Koulouris, A. & Siletti, C. 2003. Throughput analysis and debottlenecking of biomanufacturing facilities. What role can process simulators play? *Chimica Oggi*. (SUPPL.):22–28.

Pharmaceutical Inspection Co-operation Scheme. 2014. Guide To Good Manufacturing Practice for Medicinal Products. In *Pharmaceutical Inspection Convention*. V. 11. 1–43. DOI: 10.1186/s12889-015-1845-8.

Pörtner, R. 2015. Bioreactors for Mammalian Cells. In *Animal Cell Culture*. M. Al-Rubeai, Ed. Springer International Publishing. 89–135. DOI: 10.1007/978-3-319-10320-4_4.

Rader, R.A. & Langer, E.S. 2014. Bioprocess advances drive vaccine manufacturing in developing countries. *BioProcess International*. 12(2):10–15.

Rains, R.L. & Rathbun, L.R. 1977. *Patent No. US 4209259*. United States Patent Office.

Rana, R., Dalal, J., Chhikara, M.K. & Gill, D. 2016. *Patent No. WO2017158480A1*. World Intellectual Property Organization. Available: https://patents.google.com/patent/WO2017158480A1/en.

Ransohoff, T. 2005. The Use of Disposable and Alternative Purification Technologies for Biopharmaceuticals. In *IIR Biopharmacheutical PRoduction Conference*.

Rawlings, B. & Pora, H. 2009. Environmental impact of single-use and reusable bioprocess systems. *BioProcess International*. 7(2):18–25.

RMPRU. 2019. *About RMPRU*. Available: https://www.rmpru.com/about.html [2019, May 30].

Roy, R., Katzenellenbogen, E. & Jennings, H.J. 1984. Improved procedures for the conjugation of oligosaccharides to protein by reductive amination. *Canadian journal of biochemistry and cell biology = Revue canadienne de biochimie et biologie cellulaire*. 62(5):270–275. DOI: 10.1139/o84-037.

SAPIA - South African Petroleum Industry Association. 2019. *2017 petroleum products prices in cents per litre*. Available: http://www.sapia.org.za/Overview/Old-fuel-prices [2019, May 26].

SARB. 2019. *Exchange rate detail - Rand per US Dollar*. Available: https://wwwrs.resbank.co.za/webindicators/ExchangeRateDetail.aspx?DataItem=EXCX135D [2019, May 28].

SARS. 2015. *Tax Guide for Small Business*. Available: https://www.sars.gov.za/AllDocs/OpsDocs/Guides/LAPD-IT-G10 - Tax Guide for Small Businesses.pdf [2019, June 09].

SARS. 2019. *Corporate income tax*. Available: http://www.sars.gov.za/TaxTypes/CIT/Pages/default.aspx [2019, May 28].

Sartorius Stedim - Tap. 2018. *ambr® 15 cell culture*. Available: https://www.sartorius-stedim-tap.com/tap/cell_culture/ambr.htm [2018, November 25].

Schifferle, R.E., Jennings, H.J., Wessels, M.R., Katzenellenbogen, E., Roy, R. & Kasper, D.L. 1985. Immunochemical analysis of the types Ia and Ib group B streptococcal polysaccharides. *Journal of Immunology*. 135(6):4164–4170.

Schrag, S.J. & Verani, J.R. 2013. Intrapartum antibiotic prophylaxis for the prevention of perinatal group B streptococcal disease: Experience in the United States and implications for a potential group B streptococcal vaccine. *Vaccine*. 31(S4):D20–D26. DOI: 10.1016/j.vaccine.2012.11.056.

Shafer, D.E., Toll, B., Schuman, R.F., Nelson, B.L., Mond, J.J. & Lees, A. 2000. Activation of soluble polysaccharides with 1-cyano-4-dimethylaminopyridinium tetrafluoroborate (CDAP) for use in protein-polysaccharide conjugate vaccines and immunological reagents. II. Selective crosslinking of proteins to CDAP-activated polysaccharides. *Vaccine*. 18(13):1273–1281. DOI: https://doi.org/10.1016/S0264-410X(99)00370-9.

Shanklin, T., Roper, K., Yegneswaran, P.K. & Marten, M.R. 2001. Selection of bioprocess simulation software for industrial applications. *Biotechnology and Bioengineering*. 72(4):483–489. DOI: 10.1002/1097-0290(20010220)72:4<483::AID-BIT1010>3.0.CO;2-3.

Shukla, A.A. & Gottschalk, U. 2013. Single-use disposable technologies for biopharmaceutical manufacturing. *Trends in Biotechnology*. 31(3):147–154. DOI: 10.1016/j.tibtech.2012.10.004.

Sigma Aldrich. 2017a. *D-(+)-Glucose*. Available: https://www.sigmaaldrich.com/catalog/product/sigma/g8270 [2017, June 12].

Sigma Aldrich. 2017b. *L-Cystine*. Available: https://www.sigmaaldrich.com/catalog/product/sigma/res1520ca7 [2017, June 12].

Sigma Aldrich. 2017c. *Trizma® base*. Available: https://www.sigmaaldrich.com/catalog/product/sigma/t6066 [2017, June 12].

Sigma Aldrich. 2017d. *TRIS hydrochloride*. Available: https://www.sigmaaldrich.com/catalog/product/sigma/res3098tb7 [2017, June 12].

Sigma Aldrich. 2017e. *Sodium carbonate*. Available: https://www.sigmaaldrich.com/catalog/product/sial/s7795 [2017, June 12].

Sigma Aldrich. 2017f. *Sodium chloride*. Available: https://www.sigmaaldrich.com/catalog/product/sigma/res0926sa7 [2017, June 12].

Sigma Aldrich. 2017g. *Magnesium sulfate*. Available: https://www.sigmaaldrich.com/catalog/product/sigma/m2643 [2017, June 12].

Sigma Aldrich. 2017h. *Iron(II) sulfate heptahydrate*. Available: https://www.sigmaaldrich.com/catalog/product/sigald/12354 [2017, June 12].

Sigma Aldrich. 2017i. *Ethanol*. Available: https://www.sigmaaldrich.com/catalog/product/sigald/24105 [2017, June 12].

Sigma Aldrich. 2017j. *Hydrogen chloride*. Available: https://www.sigmaaldrich.com/catalog/product/sial/26614 [2017, June 12].

Sigma Aldrich. 2017k. *Sodium hydroxide*. Available: https://www.sigmaaldrich.com/catalog/product/sigald/30620 [2017, June 12].

Sigma Aldrich. 2017l. *CDAP*. Available: https://www.sigmaaldrich.com/catalog/product/sigma/res1458c [2017, June 12].

Sigma Aldrich. 2017m. *Acetonitrile*. Available: https://www.sigmaaldrich.com/catalog/product/sigald/494445 [2017, June 12].

Sigma Aldrich. 2017n. *Triethylamine*. Available: https://www.sigmaaldrich.com/catalog/product/sial/471283 [2017, June 12].

Sigma Aldrich. 2017o. *Adipic acid dihydrazide*. Available: https://www.sigmaaldrich.com/catalog/product/sigma/a0638 [2017, June 12].

Sigma Aldrich. 2017p. *N-(3-Dimethylaminopropyl)-N'-ethylcarbodiimide hydrochloride*. Available: https://www.sigmaaldrich.com/catalog/product/sigma/03449 [2017, June 12].

Sigma Aldrich. 2017q. *Glycine*. Available: https://www.sigmaaldrich.com/catalog/product/sigma/g5417 [2017, June 12].

Sigma Aldrich. 2017r. *Ammonium sulfate*. Available: https://www.sigmaaldrich.com/catalog/product/sigma/res1427aa7 [2017, June 12].

Sigma Aldrich. 2019a. *Calcium chloride*. Available: https://www.sigmaaldrich.com/catalog/product/sial/902179 [2019, March 13].

Sigma Aldrich. 2019b. *Acetic anhydride*. Available: https://www.sigmaaldrich.com/catalog/product/sial/320102 [2019, March 13].

Sigma Aldrich. 2019c. *MES hydrate*. Available: https://www.sigmaaldrich.com/catalog/product/aldrich/163732 [2019, March 13].

Sinclair, A. & Monge, M. 2002. Quantitative economic evaluation of single use disposables in bioprocessing Quantitative Economic Evaluation of Single Use Disposables in Bioprocessing. *BioProcess International*. 9(V06):1–11.

Sinclair, A. & Monge, M. 2005. Concept Facility Based on Single-Use Systems, Part 2. *Bioprocess International*. October(Supplement):51–55.

Singh, V. 1999. Disposable bioreactor for cell culture using wave-induced agitation. *Cytotechnology*. 30(1–3):149–158. DOI: 10.1023/A:1008025016272.

Singh, V. 2001. *Patent No. US 6190913 B1*. United States Patent Office.

Smith, J., Lipsitch, M. & Almond, J.W. 2011. Vaccine production, distribution, access, and uptake. *The Lancet*. 378(9789):428–438. DOI: 10.1016/S0140-6736(11)60478-9.

Stanford, J. 2003. R500m vaccine partnership launched. *Engineering News*. 10 October. Available: http://www.engineeringnews.co.za/printversion/%0Ar500mvaccinepartnershiplaunched20031010.

Stewart, D.W. 1999. *Patent No. US5941635*. United States Patent Office.

Swennen, E. 2012. *Patent No. EP 1951886 B1*. European Patent Office.

Tan, J., Foo, D.C.Y., Kumaresan, S. & Aziz, R.A. 2006. Debottlenecking of a batch pharmaceutical cream production. *Pharmaceutical Engineering*. 26(4):1–9. Available: http://www.geocities.ws/foodominic/PharmaEng_CreamProduction.pdf.

The Biovac Institute. 2018. Group B Streptococcus serotype III fermentation. Unpublished raw data.

Toumi, A., Jürgens, C., Jungo, C., Maier, B.A., Papavasileiou, V. & Petrides, D.P. 2010. Design and optimization of a large scale biopharmaceutical facility using process simulation and scheduling tools. *Pharmaceutical Engineering*. 30(2):1–9. Available: https://pdfs.semanticscholar.org/c158/7827817381781d104c9ac2c67d565e5008f6.pdf.

Vrang, A., Madsen, S.M., Bredmose, L., Ravn, P., Arnau, J., Johsen, M.G., Steenberg, A., Israelsen, H., et al. 2002. *Patent No. WO 01/33109 A2*. World Intellectual Property Organization.

Wessels, M.R., Benedi, V.J., Jennings, H.J., Michon, F., DiFabio, J.L., Kasper, D.L., Benedí, W.J., Jennings, H.J., et al. 1989. Isolation and characterization of type IV group B Streptococcus capsular polysaccharide. *Infection and Immunity*. 57(4):1089–1094. Available: https://iai.asm.org/content/iai/57/4/1089.full.pdf.

Wessels, M.R., Paoletti, L.C., Kasper, D.L., DiFabio, J.L., Michon, F., Holme, K. & Jennings, H.J. 1990. Immunogenicity in animals of a polysaccharide-protein conjugate vaccine against type III group B streptococcus. *Journal of Clinical Investigation*. 86(5):1428–1433. DOI: 10.1172/JCI114858.

Whitford, W.G. 2010. Single-use systems as principal components in bioproduction. *BioProcess International*. 8(11):34–42. Available: https://pdfs.semanticscholar.org/6a20/b01b75aafba836fa04dab82415577bcc964d.pdf.

WHO. 2017a. *Poliomyelitis*. Available: https://www.who.int/en/news-room/fact-sheets/detail/poliomyelitis [2017, April 17].

WHO. 2017b. *Group B Streptococcus Vaccine Development Technology Roadmap*. Geneva. Available: https://apps.who.int/iris/handle/10665/258704 [2019, June 09].

Zheng, R. 2010. The Game Changer. *BioProcess International*. 8(4):S4--S9. Available: https://pdfs.semanticscholar.org/eeb5/88650b6a32c4126acb4c57267c702c2311a4.pdf.

Zimbro, M.J. 2009. *Difco & BBL manual : Manual of microbiological culture media*. Sparks, Md: Becton, Dickinson and Company.

Appendix A Methods

A.1 Fermentation Stoichiometry: Material Balances

Aerobic glycolysis by *Streptococcus agalactiae*:

$$C_6H_{12}O_6 + a\,O_2 + b\,NH_3 \rightarrow c\,CH_{1.8}O_{0.5}N_{0.2} + d\,CO_2 + e\,H_2O + f\,CH_3CHOHCOOH + g\,CH_3COOH + h\,CH_3CHOHCOCH_3 + i\,HCOOH + j\,CPS \quad \text{Equation 3-1}$$

Table A-1 GBS aerobic glycolysis Stoichiometry

Compound	Stoichiometric coefficient	Formula	Molecular weight
Glucose	$\mathbf{1}$	$C_6H_{12}O_6$	180
Oxygen	$\boldsymbol{a}$	O_2	32
Ammonia	$\boldsymbol{b}$	NH_3	17
Biomass	$\boldsymbol{c}$	$CH_{1.8}O_{0.5}N_{0.2}$	24.6
Carbon dioxide	$\boldsymbol{d}$	CO_2	44
Water	$\boldsymbol{e}$	H_2O	18
Lactic acid	$\boldsymbol{f}$	$C_3H_6O_3$	90
Acetic acid	$\boldsymbol{g}$	$C_2H_4O_2$	60
Acetoin	$\boldsymbol{h}$	$C_4H_8O_2$	88
Formic acid	$\boldsymbol{i}$	HCOOH	46
GBS capsular polysaccharide (CPS)	$\boldsymbol{j}$	$(C_{35}H_{52}O_{31}N_2)n$	996

Carbon balance

$$C_6H_{12}O_6 = c\,CH_{1.8}O_{0.5}N_{0.2} + f\,CH_3CHOHCOOH + g\,CH_3COOH + h\,CH_3CHOHCOCH_3 + i\,HCOOH + j\,(C_{35}H_{52}O_{31}N_2)n$$

$$\mathbf{6 = c + d + 3f + 2g + 4h + i + 35j} \quad \text{Equation A-1}$$

Oxygen balance

$$C_6H_{12}O_6 + a\,O_2 \rightarrow c\,CH_{1.8}O_{0.5}N_{0.2} + d\,CO_2 + e\,H_2O + f\,CH_3CHOHCOOH + g\,CH_3COOH + h\,CH_3CHOHCOCH_3 + i\,HCOOH + j\,(C_{35}H_{52}O_{31}N_2)n$$

$$\mathbf{6 + 2a = 0.5c + 2d + e + 3f + 2g + 2h + 2i + 31j} \quad \text{Equation A-2}$$

Nitrogen balance

$$bNH_3 \rightarrow c\,CH_{1.8}O_{0.5}N_{0.2} + j\,(C_{35}H_{52}O_{31}N_2)n$$

$$\mathbf{3b = 0.2c + 2j} \quad \text{Equation A-3}$$

Hydrogen balance

$$C_6H_{12}O_6 + b\,NH_3 \rightarrow c\,CH_{1.8}O_{0.5}N_{0.2} + e\,H_2O + f\,CH_3CHOHCOOH + g\,CH_3COOH + h\,CH_3CHOHCOCH_3 + i\,HCOOH + j\,(C_{35}H_{52}O_{31}N_2)n$$

$$\mathbf{12 + 3b = 1.8c + 2e + 6f + 4g + 8h + 2i + 52j} \quad \text{Equation A-4}$$

CPS yield

$$CPS\ yield = 60\ mg\ /\ cell\ dry\ weight \text{ (Swennen, 2012)}$$

$$60\ mg\ CPS = \frac{0.06\ g}{996\ g/mol} = 6.02\ x10^{-5}\ mol$$

$$1\ g\ dry\ cell\ weight = \frac{1\ g}{24.6\ g/mol} = 0.041\ mol$$

$$Molar\ yield\ coefficient\ CPS\ per\ dry\ cell\ weight = \frac{6.02\ x\ 10^{-5}\ mol}{0.041\ mol} = \mathbf{1.47\ x10^{-3}}$$

$$\mathbf{j = 1.47\ x\ 10^{-3} \times c}$$

$$\mathbf{j = (1.47\ x10^{-3})c} \quad \text{Equation A-5}$$

Material balance Equations:

$$\mathbf{C_6H_{12}O_6 + a\,O_2 + b\,NH_3 \rightarrow c\,CH_{1.8}O_{0.5}N_{0.2} + d\,CO_2 + e\,H_2O + f\,CH_3CHOHCOOH + g\,CH_3COOH + h\,CH_3CHOHCOCH_3 + i\,HCOOH + j\,CPS} \quad \text{Equation 3-1}$$

$$\mathbf{6 = c + d + 3f + 2g + 4h + i + 35j} \quad \text{Equation A-1}$$

$$\mathbf{6 + 2a = 0.5c + 2d + e + 3f + 2g + 2h + 2i + 31j} \quad \text{Equation A-2}$$

$$\mathbf{3b = 0.2c + 2j} \quad \text{Equation A-3}$$

$$\mathbf{12 + 3b = 1.8c + 2e + 6f + 4g + 8h + 2i + 52j} \quad \text{Equation A-4}$$

$$\mathbf{j = (1.47\ x10^{-3})c} \quad \text{Equation A-5}$$

The following coefficients were used from Mickelson, (1972):

$\mathbf{f = 0.7845}$

$\mathbf{g = 0.8469}$

$\mathbf{h = 0.0896}$

$\mathbf{i = 0.1240}$

The material balance for Equation 3-1 and Equations A-1… A-4 were then solved for a, b, d, e using Microsoft Excel 2013 GRG non-linear Solver add-in by adjusting the value for c.

Equation A-5 was solved for j using the solution for c.

Solver: adjust the numerical value of variable $\boldsymbol{c}$, initial guess $\boldsymbol{c = 0.5}$, Target column $\boldsymbol{Result = 0}$

Table A-2 Material Balance Results

Balance	Equation	Mass in	Mass out	Result
Mass	Eq. 3-1	192.51	192.51	0.00
C	Eq. A-1	6.00	6.00	0.00
O	Eq. A-2	6.55	6.55	0.00
N	Eq. A-3	0.22	0.22	0.00
H	Eq. A-4	12.66	12.66	0.00

The coefficients a … j of Equation 3-1 determined in this way:

$$C_6H_{12}O_6 + 0.27\,O_2 + 0.22\,NH_3 \rightarrow 1.09\,CH_{1.8}O_{0.5}N_{0.2} + 0.35\,CO_2 + 0.80\,H_2O + 0.79\,CH_3CHOHCOOH + 0.85\,CH_3COOH + 0.09\,CH_3CHOHCOCH_3 + 0.12\,HCOOH + 0.0008\,CPS$$

Equation 3-1

$$a = 0.27 \qquad g = 0.85$$

$$b = 0.22 \qquad h = 0.09$$

$$c = 1.09 \qquad i = 0.12$$

$$d = 0.35 \qquad j = 0.0008$$

$$e = 0.80$$

$$f = 0.79$$

A.2 Fermentation Kinetics: Model parameters

$$\frac{dX}{dt} = \mu X \qquad \text{Equation 3-3}$$

$$\int_{X_o}^{X} \frac{dX}{X} = \mu \int_{t_o}^{t} dt$$

$$\mu(t - t_o) = \ln \frac{X}{X_o}$$

$$\mu(t) = \frac{\ln \frac{X}{X_o}}{t - t_o}$$

Fermentation data **set 1 of 3**: at t=T^{-1}, X=0.081; For t=1h, X=0.264:

$$\ln \frac{X_1}{X_{T-1}} = \ln \frac{0.264}{0.081} = 0.221$$

$$\mu(t = 1h) = \frac{\ln \frac{X_1}{X_{-1}}}{t_1 - t_o} = \frac{0.221}{1 - 0} = 1.1854\ h^{-1}$$

Similarly, for t(1)… t(8):

Table A-3 Fermentation data experiment 1 of 3

t [h]	X [OD590]	S [g/L]	μ [h-1]	S/μ [h.g/L]
T^{-1}	0.081	5.688	N/A	N/A
0	0.101	5.310	N/A	N/A
1.00	0.264	5.760	1.1815	4.875
2.00	1.440	7.020	1.439	4.878
3.00	3.080	5.904	1.213	4.868
4.00	6.920	3.348	1.112	3.011
5.00	11.120	3.978	0.984	4.041
5.50	12.140	4.032	0.911	4.427
6.00	13.920	3.114	0.858	3.630
6.50	15.360	2.394	0.807	2.967
7.00	16.200	0.252	0.757	0.333
7.50	17.430	2.196	0.716	3.066
8.00	17.670	2.736	0.673	4.064

(The Biovac Institute, 2018)

Kinetic parameters sample calculations:

Method 1 exponential trend line

$$\frac{dX}{dt} = \mu X \qquad \text{Equation 3-3}$$

$$\int \frac{1}{X} dX = \mu \int dt$$

$$\ln X + B = \mu t + A$$

$$\ln X = \mu t + C$$

$$X = e^{(\mu t + C)} = e^{\mu t} e^{C}$$

$$X = K e^{\mu t} \qquad \text{Equation 3-4}$$

Method 2 linear trend line

$$\mu = \mu_{max} \frac{S}{K_S + S} \qquad \text{Equation 3-2}$$

$$\mu \left(\frac{K_S + S}{S}\right) = \mu_{max} \frac{S}{K_S + S} \left(\frac{K_S + S}{S}\right)$$

$$\mu_{max} = \mu(t) \frac{K_S + S}{S}$$

$$\frac{\mu}{S} = \frac{\mu_{max}}{K_S + S}$$

$$\frac{S}{\mu} = \frac{1}{\mu_{max}} S + \frac{K_S}{\mu_{max}} \qquad \text{Equation 3-8}$$

Method 1 Exponential trend line:

$$X = K e^{\mu t} \qquad \text{Equation 3-4}$$

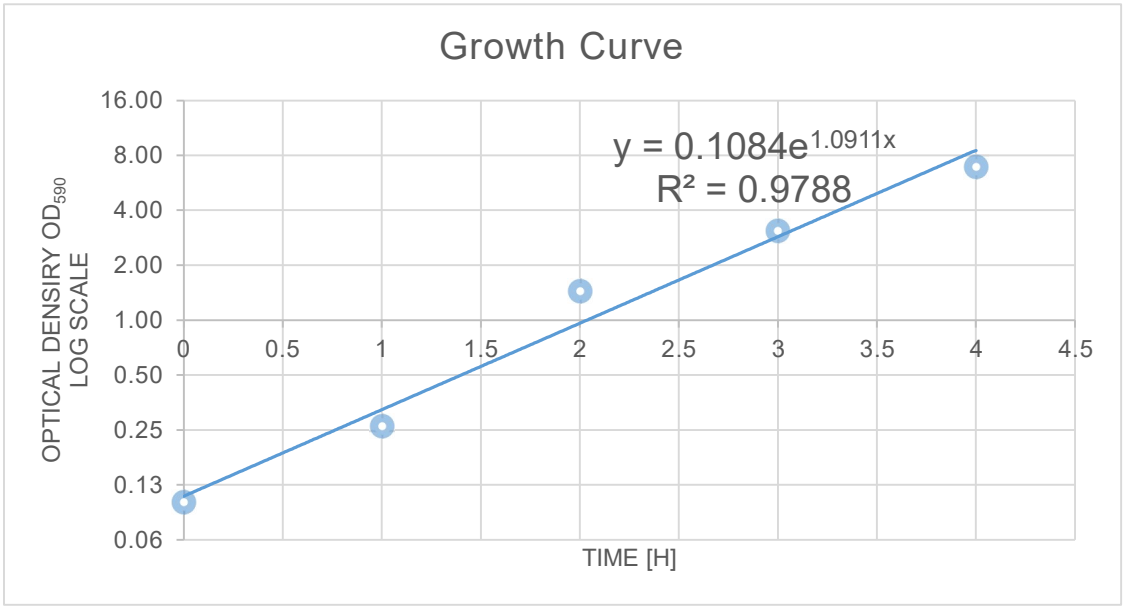

Figure 60: Growth Curve for t= 0 – 4h

$$\mu_{max} = 1.091\ h^{-1}$$

$$t_d = \frac{\ln 2}{\mu_{max}} = \frac{\ln 2}{1.091\ h^{-1}} = 0.635\ h$$

$$S\Big|_{\frac{\mu}{\mu_{max}}=0.5}$$ Equation 3-5

$$\mu = 0.5 \times \mu_{max} = 0.5(1.091) = 0.546\ h^{-1}$$

However, this point is not represented in the experimental data. An approximation is made by interpolating the value of μ vs. S:

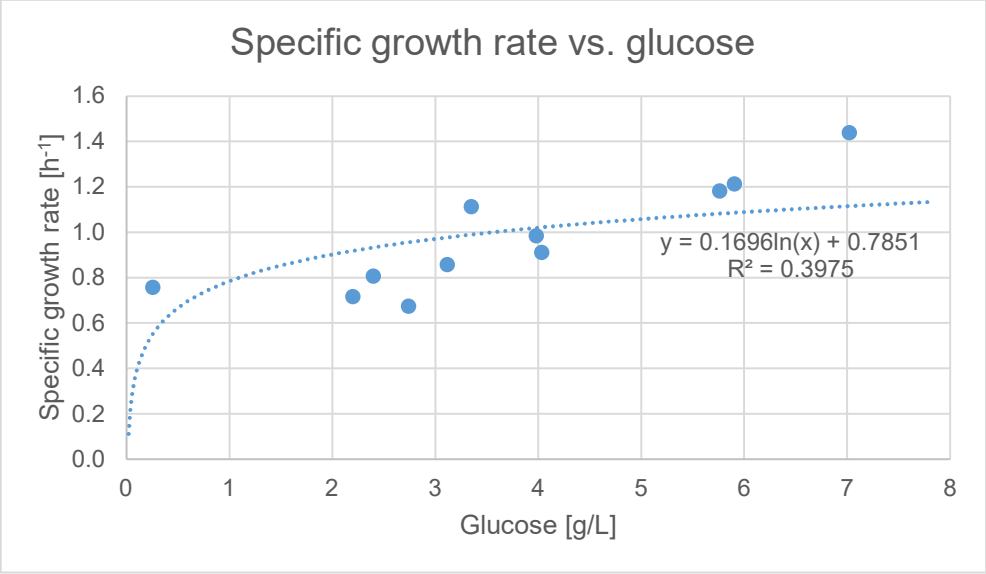

Figure 61: Growth rate for S= 0 – 7 g/L

$$\mu = \alpha \ln S + \beta$$ Equation 3-6

$$\mu = 0.1696 \ln S + 0.7851$$

$$K_s = e^{\left(\frac{0.5\mu_{max}-\beta}{\alpha}\right)}$$ Equation 3-7

$$K_s = e^{\left(\frac{0.5\mu_{max}-0.7851}{0.1696}\right)} = e^{\left(\frac{0.5(1.091)-0.7851}{0.1696}\right)}$$

$$K_s = 0.243\ g/L$$

$$\mu_{max} = 1.091\ h^{-1}$$

$$t_d = 0.635\ h$$

Fermentation experiment 1: Method 1 Exponential trend line

Method 2 Linear trend line:

$$\frac{S}{\mu} = \frac{1}{\mu_{max}} S + \frac{K_S}{\mu_{max}}$$ Equation 3-8

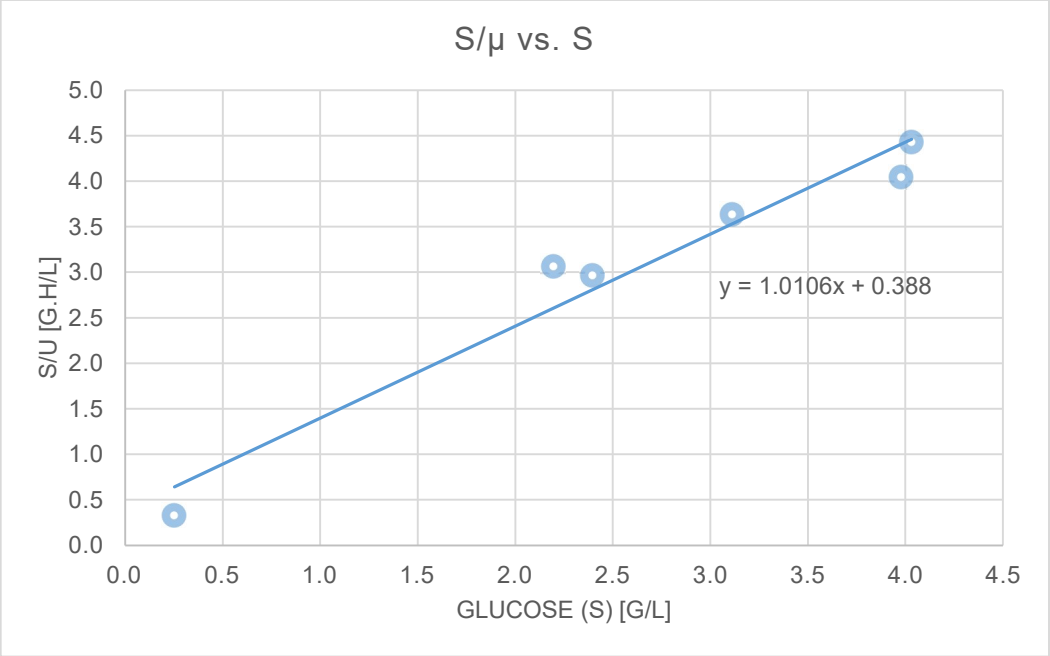

Figure 62: S/μ vs. S for exponential growth phase

$$\mu_{max} = \frac{1}{m} = \frac{1}{1.0106}$$

$$\boldsymbol{\mu_{max} = 0.9895\ h^{-1}}$$

$$K_S = \frac{c}{m} = \frac{0.3839}{1.0106}$$

$$\boldsymbol{t_d = \frac{\ln 2}{\mu_{max}} = \frac{\ln 2}{0.9895\ h^{-1}} = 0.7005\ h}$$

$\boldsymbol{K_S = 0.3839\ g/L}$
$\boldsymbol{\mu_{max} = 0.990\ h^{-1}}$
$\boldsymbol{t_d = 0.701\ h}$
Fermentation experiment 1: Method 2 Linear trend line

Table A-4 Fermentation data experiment 2 of 3

t [h]	X [OD590]	S [g/L]	μ [h-1]	S/μ [h.g/L]
0.12	0.283	15.774	0	-
0.12	0.287	17.305	0.120	144.373
0.53	0.422	23.644	0.753	31.419
0.74	0.560	25.428	0.923	27.556
0.80	0.611	25.428	0.963	26.408
0.80	0.63	27.242	1.000	27.233
1.37	1.404	30.461	1.169	26.058
1.47	1.611	30.461	1.183	25.746
1.48	1.654	30.028	1.193	25.173
1.83	2.775	26.374	1.247	21.143
2.15	3.636	22.097	1.187	18.608
2.15	3.692	19.879	1.195	16.639
2.51	5.428	14.913	1.177	12.672
2.83	8.179	7.705	1.189	6.482
3.18	11.233	0.492	1.158	0.425
3.24	11.472	0.492	1.143	0.431
3.24	11.550	3.193	1.145	2.789
3.86	12.731	2.251	0.986	2.283
3.91	13.036	2.251	0.980	2.298
3.90	13.167	0.633	0.980	0.646

(The Biovac Institute, 2018)

$$K_s = 0.000\ g/L^*$$

$$\mu_{max} = 1.203\ h^{-1}$$

$$t_d = 0.576\ h$$

Fermentation experiment 2: Method 1 Exponential trend line

* In this experiment, the calculation of K_s using this method yielded a value of 2.3 x 10^{-6}.

$$K_s = 0.097\ g/L$$

$$\mu_{max} = 1.220\ h^{-1}$$

$$t_d = 0.568\ h$$

Fermentation experiment 2: Method 2 Linear trend line

Table A-5 Fermentation data experiment 3 of 3

t [h]	X [OD590]	S [g/L]	μ [h-1]	S/μ [h.g/L]
0.72	0.711	27.594	0	-
1.04	1.087	28.748	0.408	70.530
1.40	1.780	28.809	0.655	43.956
1.45	1.927	28.809	0.687	41.913
1.45	1.976	28.935	0.705	41.046
2.07	4.168	21.434	0.854	25.091
2.13	4.379	21.434	0.853	25.115
2.13	4.442	18.789	0.860	21.845
2.75	9.405	6.073	0.939	6.467
2.80	9.964	6.073	0.943	6.441
3.84	19.592	5.826	0.864	6.746
3.89	20.091	1.225	0.859	1.426
4.16	21.481	3.778	0.819	4.611
4.51	21.301	0.915	0.754	1.214
4.57	21.296	2.305	0.744	3.098

(The Biovac Institute, 2018)

$$K_s = 0.000.\, g/L *$$

$$\mu_{max} = 1.017\, h^{-1}$$

$$t_d = 0.681\, h$$

Fermentation experiment 3: Method 1 Exponential trend line

* In this experiment, the calculation of K_s using this method yielded a value of 1.2 x 10^{-5}.

$$K_s = 0.020\, g/L$$

$$\mu_{max} = 1.102 h^{-1}$$

$$t_d = 0.629\, h$$

Fermentation experiment 3: Method 2 Linear trend line

Average values for kinetic parameters, calculated using Microsoft Excel formulae “AVERAGE” and “STDEV”:

Table A-6 Fermentation kinetic parameters summary – Method 1

Method 1	Experiment 1	Experiment 2	Experiment 3	AVERAGE	STDEV
μ max [h^{-1}]	1.091	1.203	1.017	1.104	0.076
K_s [g/L]	0.243	0.000	0.000	0.081	0.115
t_d [h]	0.635	0.576	0.681	0.631	0.043

Table A-6 Fermentation kinetic parameters summary – Method 2

Method 2	Experiment 1	Experiment 2	Experiment 3	AVERAGE	STDEV
μ max [h^{-1}]	0.990	1.220	1.102	1.104	0.094
K_s [g/L]	0.384	0.097	0.020	0.167	0.156
t_d [h]	0.700	0.568	0.629	0.633	0.054

A.3 SuperPro Simulation Model Construction: GBS III 20L Stainless Steel Technology

Table A-4 SuperPro model detailed construction

Tag	SuperPro unit procedure(s)	SuperPro unit operations(s) in sequential order	SuperPro parameters	Screen captures of SuperPro operations dialogue
SS-01f	→ Filtration → Dead End Filtration  • Equipment: Peristaltic pump P-101 • Consumables: 0.22 µm polysulfone filter 0.014m^2	Dead-End Filtration	• 100% biomass removal • 1% product loss • 4000 L/m^2.h • 60 min	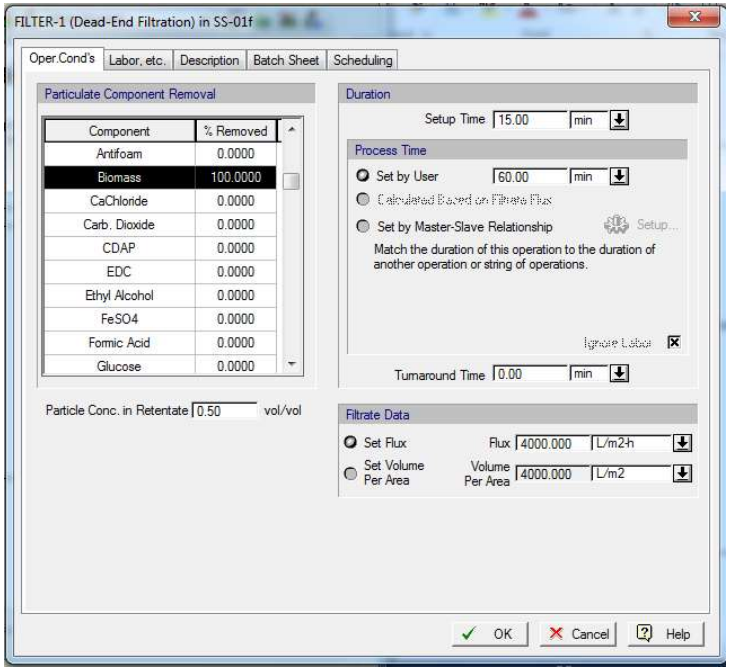

Tag	SuperPro unit procedure(s)	SuperPro unit operations(s) in sequential order	SuperPro parameters	Screen captures of SuperPro operations dialogue
SS-01	→ Inoculum preparation → in a Shake flask 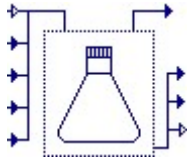 SS-01 / I-101 Inoculum • Equipment: Equipment: Shaker incubator I-101 • Consumables: 4L glass Shake Flask	Transfer-In	• Transfer in total 800 mL inoculum medium (**Table A-15**)	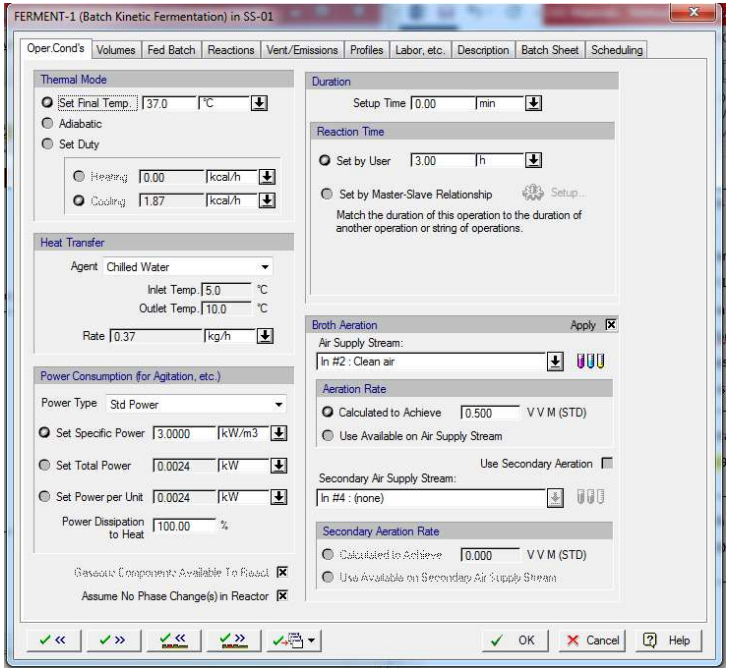
		Charge 7.	• Inoculate with total 2 mL Biomass	
		Batch heating	• Heating with electricity at 1°C/min • Final temperature 37°C	
		Batch Kinetic Fermentation	**Ferment** • 37°C for 3h, 0.5 vvm aeration with air, 3 kW/m^3 agitation. • Stoichiometry (Mickelson, 1972) • Kinetic model (Monod, 1949)	
		Transfer Out	Transfer out 300 mL to SS-03	

Tag	SuperPro unit procedure(s)	SuperPro unit operations(s) in sequential order	SuperPro parameters	Screen captures of SuperPro operations dialogue
SS-02	→ Storage/Blending → Bulk → Batch → in a Blending Tank 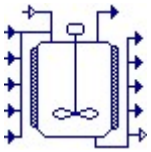 SS-02 / T-101 50L Media tank	In-Place-Cleaning	• CIP with 13L 0.1N NaOH • Rinse with 67L WFI	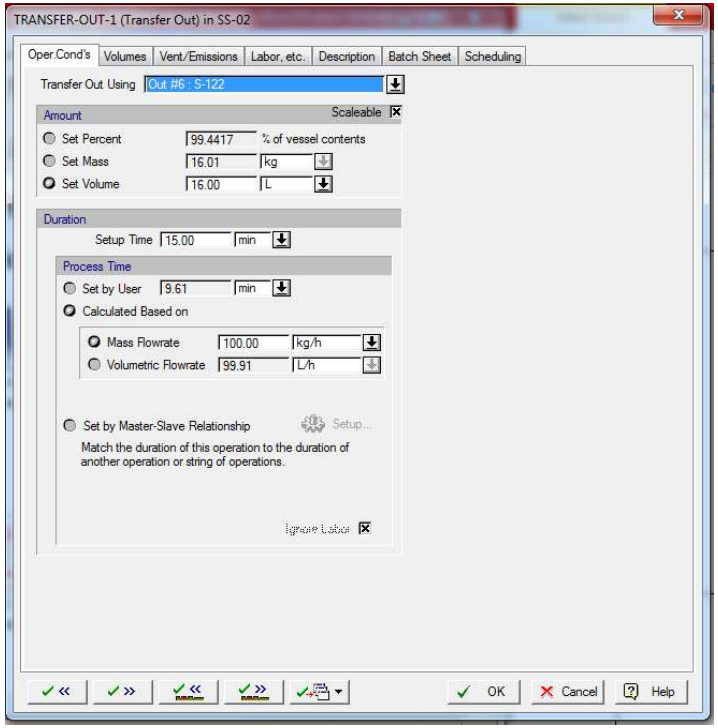
		In-Place-Steaming	Steam sterilize with saturated steam at 3 barg, 100 (kg/h)/m^3 for 30 minutes	
		Charge	Charge raw materials for 16 L of Fermentation medium (**Table A-16**) at 100 kg/h	
		Agitation	Agitate at 50 W/m^3 for 30min	
		Transfer Out	Transfer out 16L to SS-02/f 100 kg/h	
	• Equipment: 50L, jacketed, stirred, Stainless steel tank T-101	In-Place-Cleaning	• CIP with 13L 0.1N NaOH • Rinse with 67L WFI	

Tag	SuperPro unit procedure(s)	SuperPro unit operations(s) in sequential order	SuperPro parameters	Screen captures of SuperPro operations dialogue
SS-02f	→ Filtration → Dead End Filtration  SS-02f / P-101 0.22um Filtration • Equipment: Peristaltic pump P-101 • Consumables: 0.22 µm polysulfone filter, area 0.014 m^2	Dead-End Filtration	• 100% biomass removal • 1% product loss • 4000 $L/m^2.h$ • 60 min	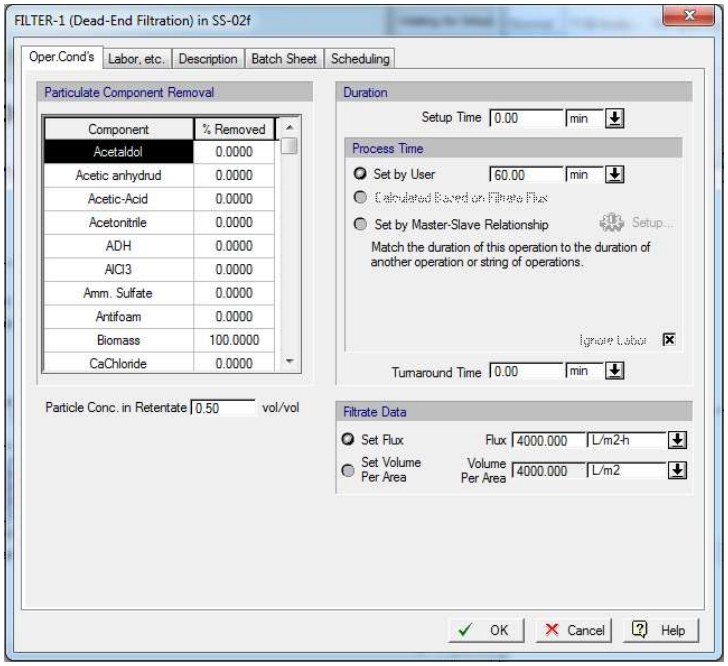

Tag	SuperPro unit procedure(s)	SuperPro unit operations(s) in sequential order	SuperPro parameters	Screen captures of SuperPro operations dialogue
SS-03	→ Batch vessel procedure → In a Seed Fermentor 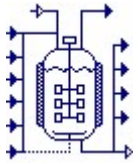 SS-03 / R-101 Fermentation • Equipment: 32 L (26L working volume) jacketed 316L stainless steel fermentor, R-101 • Consumables: 24 x 50mL single use sampling bag	In-Place-Cleaning	• CIP with 16L 0.1N NaOH • Rinse with 81L WFI	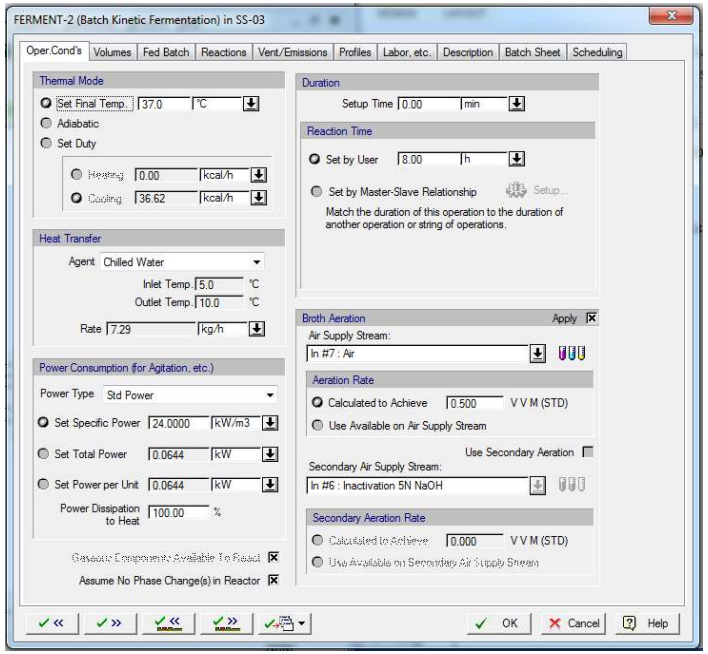
		Transfer In	Transfer in 16L from SS-02/f	
		In-Place-Steaming	Steam sterilize with saturated steam at 3 barg, 100 (kg/h)/m^3 for 30 minutes	
		Batch Heating	• Heating with saturated steam 3 barg, at 1°C/min • Final temperature 37°C	
		Transfer In	Transfer in 300 mL from SS-01	
		Batch Kinetic Fermentation	**Ferment** • 37°C for 8h, 0.5 vvm aeration with air, 2 kW/m^3 agitation. • Fed batch 5L feed medium, built in SuperPro model • Stoichiometry (Mickelson, 1972) • Kinetic model (Monod, 1949)	

		Charge	Charge 5N NaOH to a final concentration of 0.8M	
		Batch Heating	• Heating with saturated steam 3 barg, at 1°C/min • Final temperature 55°C	
		Batch Stoichiometric Reaction	**CH3COHCOOH → WFI (X=100%)** Inactivation for 16 h at 55 °C in 0.8M NaOH	
		Transfer Out	Transfer out 26L to SS-04	
		In-Place-Steaming	Steam decontamination with saturated steam at 3 barg, 100 (kg/h)/m^3 for 30 minutes	
		In-Place-Cleaning	• CIP with 16L 0.1N NaOH • Rinse with 81L WFI	

Tag	SuperPro unit procedure(s)	SuperPro unit operations(s) in sequential order	SuperPro parameters	Screen captures of SuperPro operations dialogue
SS-04	→ Storage/Blending → Bulk → Batch → in a Blending Tank 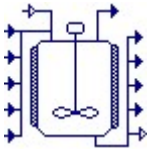 SS-04 / T-102 Neut./Precip. Equipment: 50L, jacketed, stirred, Stainless steel tank, T-102	In-Place-Cleaning	• CIP with 13L 0.1N NaOH • Rinse with 67L WFI	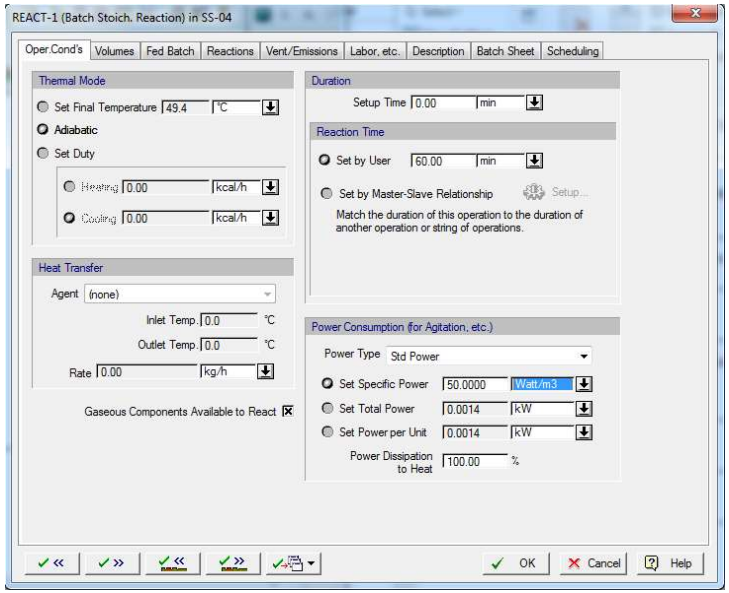
		In-Place-Steaming	Steam sterilize with saturated steam at 3 barg, 100 (kg/h)/m^3 for 30 minutes	
		Transfer In	Transfer in 26 L from SS-03	
		Charge	Charge 6N HCl, 3417 mL	
		Batch Stoichiometric Reaction	**NaOH + HCl → NaCl + H_2O (X_{NaOH}=100%)** • Adiabatic reaction for 60 min, 50 W/m3 agitation	
		Charge	Charge 2N $CaCl_2$, 2 L	
		Charge	Charge 96% Ethanol, 17 L	
		Batch Stoichiometric Reaction	**$CaCl_2$ → WFI (X=100%)** **PS-III → WFI (X=5%)** • Adiabatic reaction for 60 min, 50 W/m3 agitation	
		Transfer Out	Transfer out 48.4 L to SS-05	
		In-Place-Cleaning	• CIP with 13L 0.1N NaOH	

			• Rinse with 67L WFI	
Tag	**SuperPro unit procedure(s)**	**SuperPro unit operations(s) in sequential order**	**SuperPro parameters**	**Screen captures of SuperPro operations dialogue**
SS-05	→ Centrifugation → Disk stack 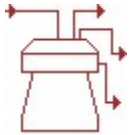 SS-05 / C-201 Centrifugation Equipment: Disk stack centrifuge C-201	In-Place-Cleaning	• CIP with 15L 0.1N NaOH • Rinse with 75L WFI	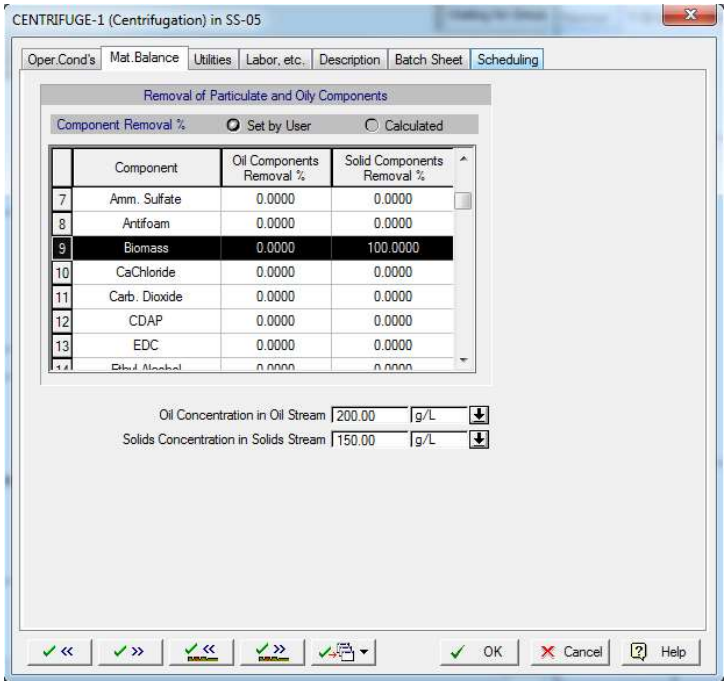
		In-Place-Steaming	Steam sterilize with saturated steam at 3 barg, 300 (kg/h)/m^3 for 30 minutes	
		Centrifugation	• 100% biomass to waste • 12% product to waste • 150 g/L solids in waste • 30 min (Σ=8200 m^2)	
		In-Place-Cleaning	• CIP with 15L 0.1N NaOH • Rinse with 75L WFI	

Tag	SuperPro unit procedure(s)	SuperPro unit operations(s) in sequential order	SuperPro parameters	Screen captures of SuperPro operations dialogue
SS-06	→ Filtration → Diafiltration 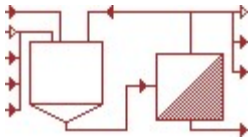 SS-06 / TF-201 TFF TRIS • Equipment: Diafiltration skid TF-201 • Consumables: 30 kDa TFF membrane	In-Place-Cleaning	CIP with 6L 0.1N NaOH	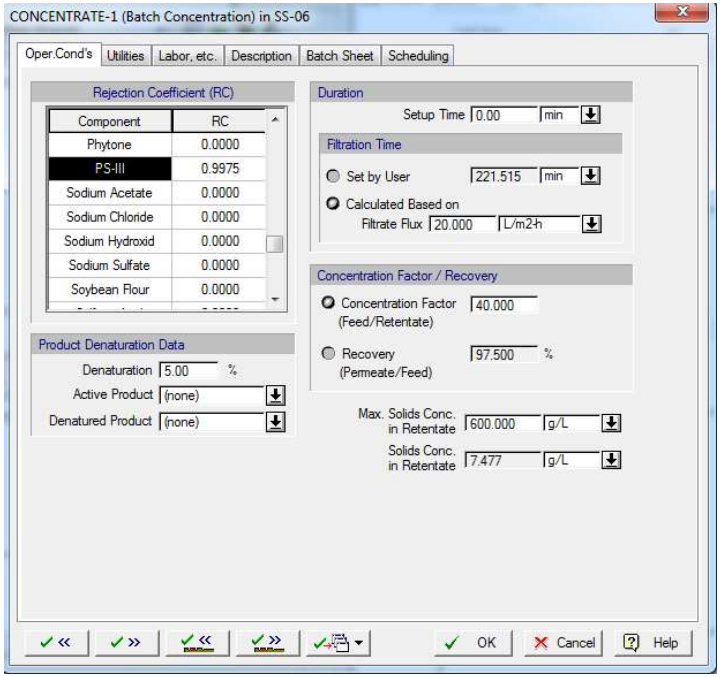
		Flush	Flush with 12L WFI, 30 min	
		Batch Concentration	• Concentrate 40 X • 20 L/m^2.h • PS-III rejection coefficient 0.9975	
		Diafiltration	• Diafilter 20 X into 8. 50 mM TRIS + 8.5 mM NaCl • 20 L/m^2.h • PS-III rejection coefficient 0.9975	
		Hold	Hold 15 min	

Tag	SuperPro unit procedure(s)	SuperPro unit operations(s) in sequential order	SuperPro parameters	Screen captures of SuperPro operations dialogue
SS-07	→ Filtration → Diafiltration 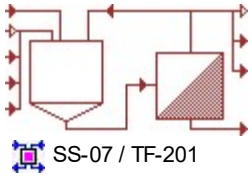 SS-07 / TF-201 TFF Na2CO3 • Equipment: Diafiltration skid TF-201 • Consumables: 30 kDa TFF membrane	Diafiltration	• Diafilter 10 X into 9. 0.3N Na_2CO_3 • 20 L/m^2.h • PS-III rejection coefficient 0.9975	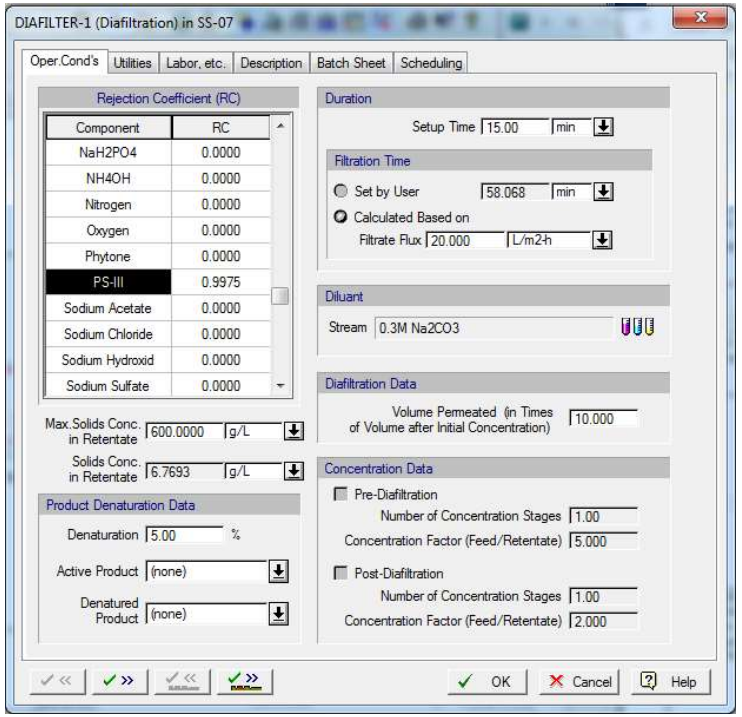
		In-Place-Cleaning	• CIP with 5L 0.1N NaOH • Rinse with 10L WFI	

Tag	SuperPro unit procedure(s)	SuperPro unit operations(s) in sequential order	SuperPro parameters	Screen captures of SuperPro operations dialogue
SS-08	→ Storage/Blending → in a Disposable → Generic container 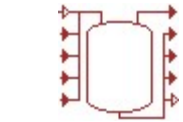 SS-08 / ST-201 TFF hold • Equipment: Magnetic stirrer ST-201 • Consumables: 5L glass bottle	Transfer In	Transfer in from SS-07 at 100 kg/h	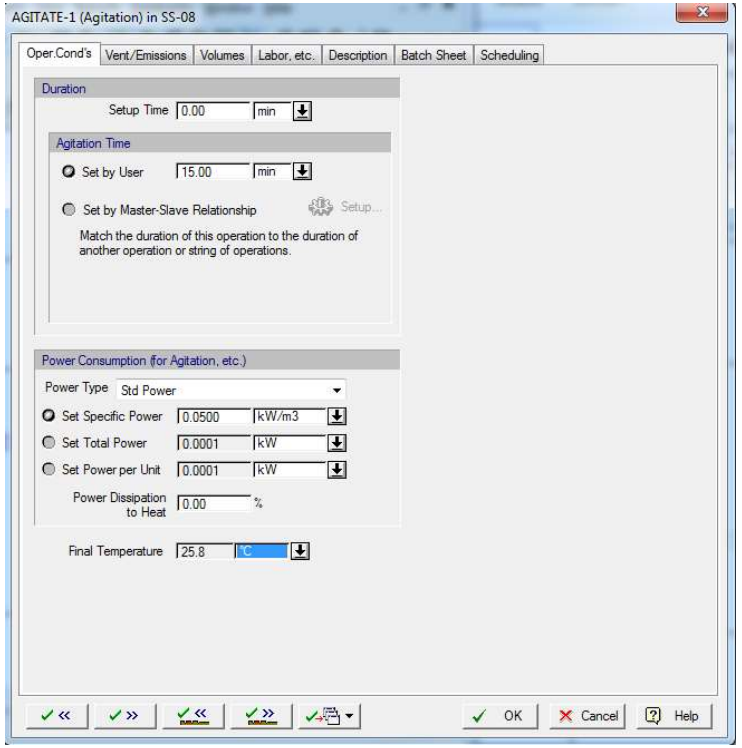
		Agitation	Agitate at 50 W/m^3 for 15 min	
		Transfer Out	Transfer out to SS-09 at 100 kg/h	

Tag	SuperPro unit procedure(s)	SuperPro unit operations(s) in sequential order	SuperPro parameters	Screen captures of SuperPro operations dialogue
SS-09	→ Filtration → Dead End Filtration 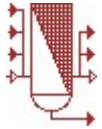 SS-09 / F-201 Protein removal • Equipment: Filter housing F-201, • Peristaltic pump P-201 • Consumables: Carbon filter pod	Dead end filtration	• 100% TT removal • 15% product loss • 250 L/m^2.h • 60 min	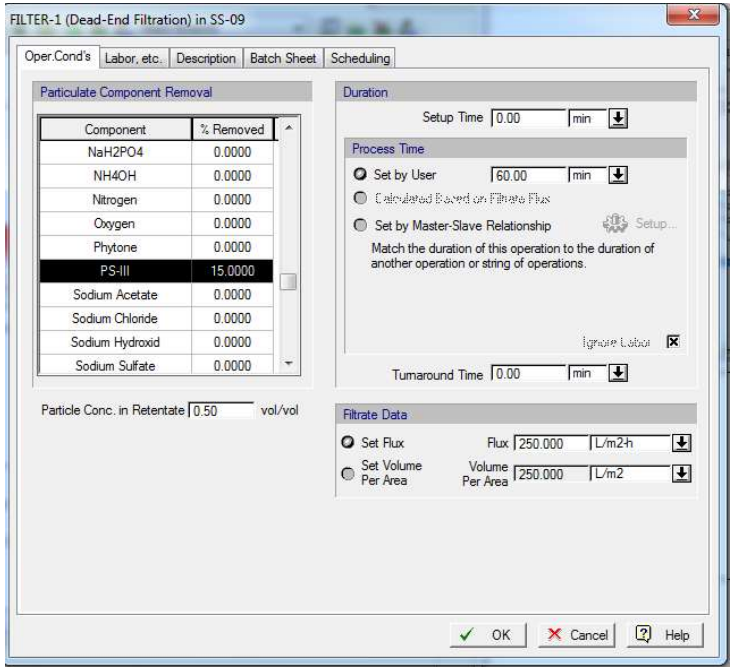

Tag	SuperPro unit procedure(s)	SuperPro unit operations(s) in sequential order	SuperPro parameters	Screen captures of SuperPro operations dialogue
SS-10	→ Storage/Blending → in a Disposable → Generic container 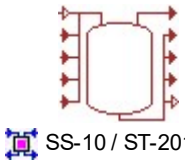 SS-10 / ST-201 Re-N-Acetylation • Equipment: Magnetic stirrer ST-201 • Consumables: 5L glass bottle	Transfer In	Transfer in from SS-09 at 100 kg/h	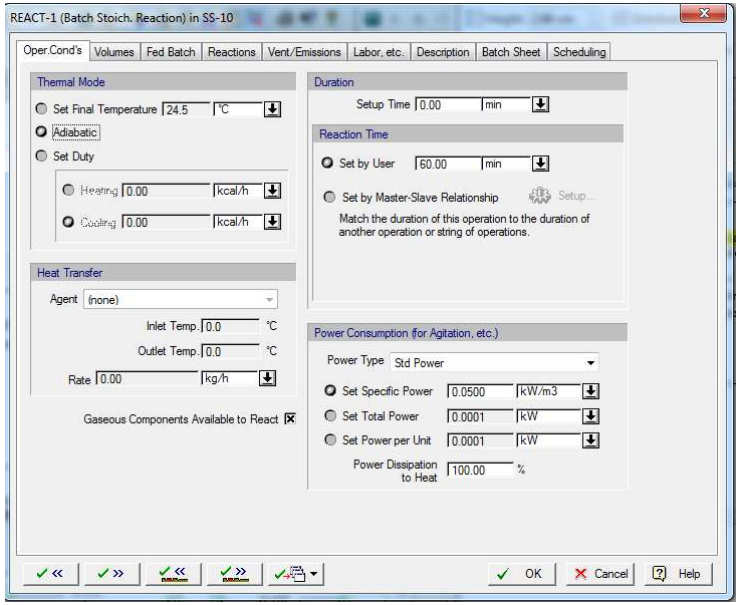
		Charge	Charge 150 mL of Ac_2O	
		Batch Stoichiometric Reaction	**$(CH_3CO)_2O$ -> WFI (X=100%)** • Adiabatic reaction for 60 min, 50 W/m3 agitation	
		Transfer Out	Transfer out to SS-11 at 100 kg/h	

Tag	SuperPro unit procedure(s)	SuperPro unit operations(s) in sequential order	SuperPro parameters	Screen captures of SuperPro operations dialogue
SS-11	→ Filtration → Dead End Filtration 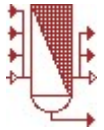 SS-11 / P-201 0.22um filtration • Equipment: Peristaltic pump P-201 • Consumables: 0.22 µm polysulfone filter, area 0.014 m^2	Dead-End Filtration	• 100% biomass removal • 1% product loss • 4000 $L/m^2.h$ • 60 min	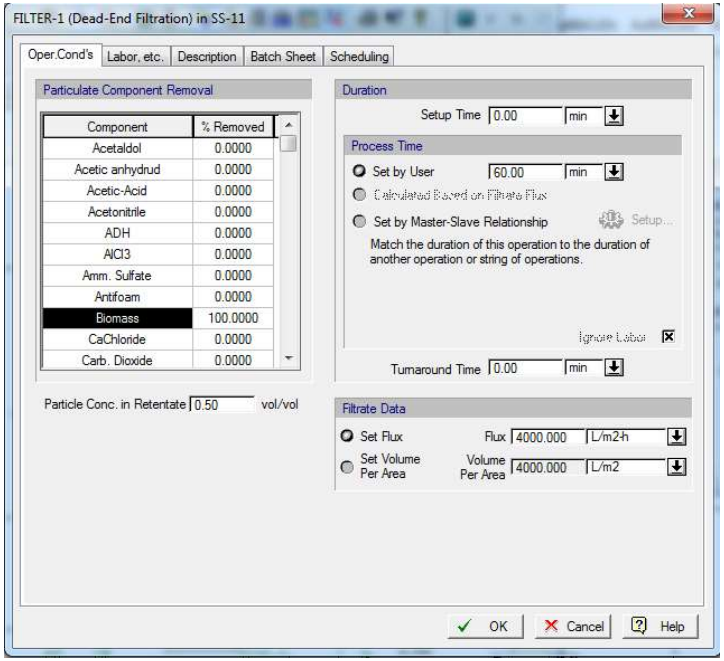

Tag	SuperPro unit procedure(s)	SuperPro unit operations(s) in sequential order	SuperPro parameters	Screen captures of SuperPro operations dialogue
SS-12	→ Storage blending → Bulk → Batch → in a Tote 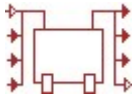 SS-12 / Cold Room 2 - 8 °C hold Consumable: 3L single use bag	Transfer In	Transfer in from SS-10 at 100 kg/h	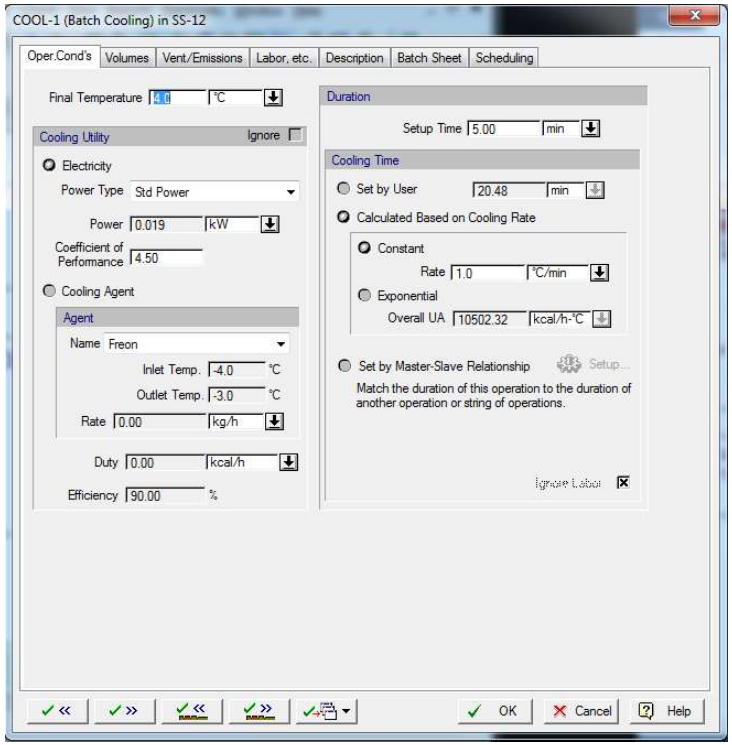
		Batch Cooling	Cooling with electricity at 1°C/min Performance coefficient 4.5 Final temperature 4°C	
		Holding	Hold for 16 hours (overnight)	
		Batch Heating	Heating at 1°C/min (no utility) Final temperature 20°C	
		Transfer Out	Transfer out to SS-13 at 100 kg/h	

Tag	SuperPro unit procedure(s)	SuperPro unit operations(s) in sequential order	SuperPro parameters	Screen captures of SuperPro operations dialogue
SS-13	→ Batch vessel procedure → in a Seed Bioreactor  SS-13 / R-301 PS activation Equipment: 2L jacketed Glass reactor R-301	In-Place-Cleaning	• CIP with 5L 0.1N NaOH • Rinse with 25L WFI	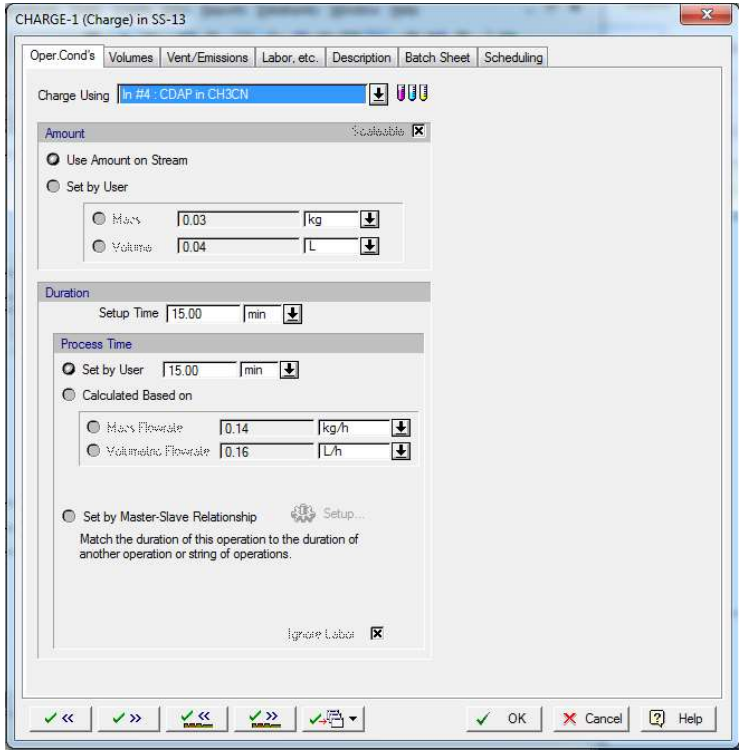
		Transfer In	Transfer in from SS-12 at 100 kg/h	
		Charge	Charge 42 mL of CDAP 100 g/L in Acetonitrile	
		Charge	Charge 84 mL of 0.2N Triethylamine (TEA)	
		Batch Stoichiometric Reaction	**PS-III → Mod-PS-III (X=90%)** **TEA → WFI (X=90%)** • React at 4 °C for 2 h, 50 W/m^3 agitation • Glycerol cooling agent	
		Transfer Out	Transfer out to SS-14 at 100 kg/h	
		In-Place-Cleaning	• CIP with 5L 0.1N NaOH • Rinse with 25L WFI	

Tag	SuperPro unit procedure(s)	SuperPro unit operations(s) in sequential order	SuperPro parameters	Screen captures of SuperPro operations dialogue
SS-14	→ Filtration → Diafiltration 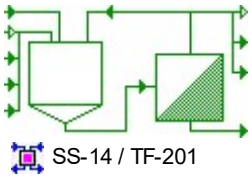 Equipment: TFF skid TF-201 Consumables: Consumables: 30 kDa TFF membrane	In-Place-Cleaning	CIP with 6L 0.1N NaOH	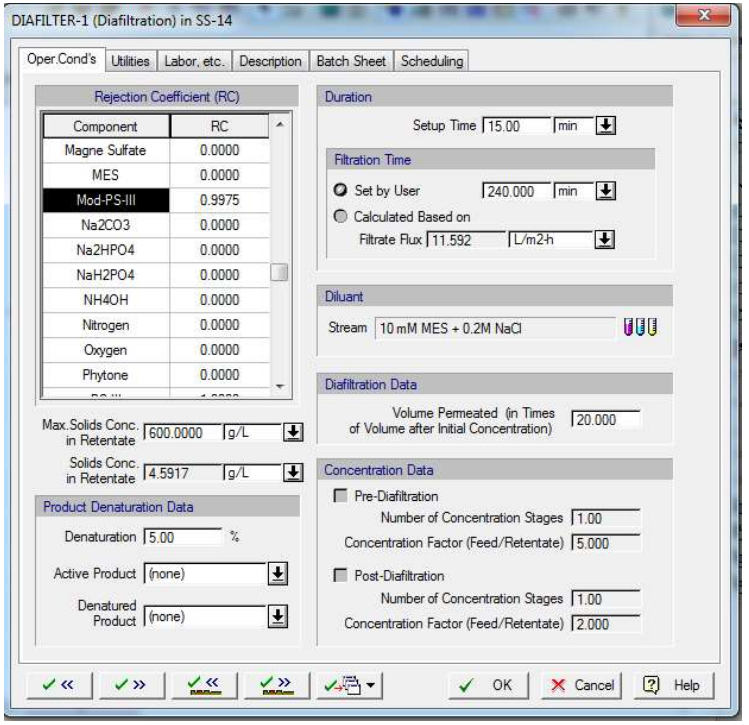
		Flush	Flush with 12L WFI, 30 min	
		Diafiltration	• Diafilter 20 X into 10. 10 mM MES + 0.2N NaCl • 20 L/m^2.h • Mod-PS-III rejection coefficient 0.9975	
		In-Place-Cleaning	• CIP with 5L 0.1N NaOH • Rinse with 10L WFI	

Tag	SuperPro unit procedure(s)	SuperPro unit operations(s) in sequential order	SuperPro parameters	Screen captures of SuperPro operations dialogue
SS-15	→ Batch vessel procedure → in a Seed Bioreactor  SS-15 / R-302 TT activation Equipment: Glass reactor R-302	In-Place-Cleaning	• CIP with 5L 0.1N NaOH • Rinse with 25L WFI	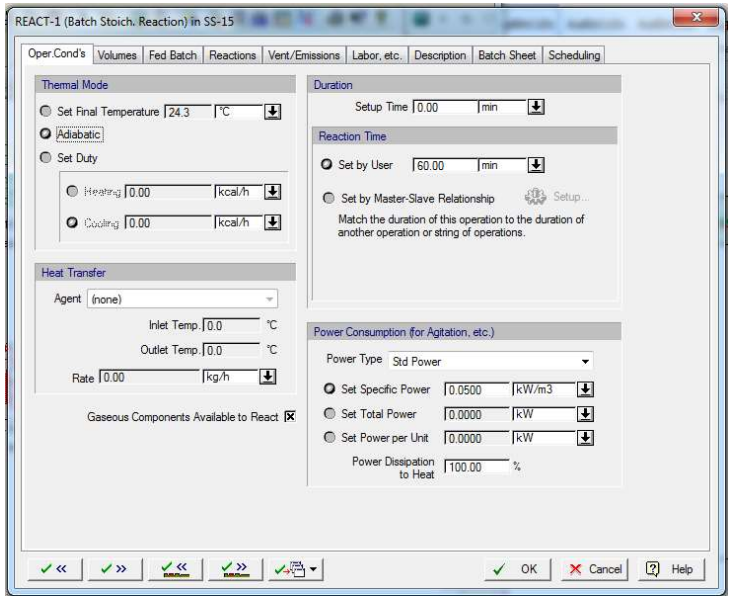
		Charge	Charge 60 mL of 50 mg/mL Carrier protein in PBS	
		Charge	Charge 26 g of ADH	
		Charge	Charge 2.6 g EDC	
		Batch Stoichiometric Reaction	**TT + ADH → TT-ADH (X_{TT}=90%)** **EDC → WFI (X=90%)** • React adiabatically for 60 min, 50 W/m^3 agitation.	
		Transfer Out	Transfer out to SS-16 at 100 kg/h	
		In-Place-Cleaning	• CIP with 5L 0.1N NaOH • Rinse with 25L WFI	

Tag	SuperPro unit procedure(s)	SuperPro unit operations(s) in sequential order	SuperPro parameters	Screen captures of SuperPro operations dialogue
SS-16	→ Filtration → Diafiltration 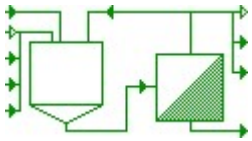 SS-16 / TF-301 TT diafilter Equipment: TFF skid TF-301 Consumables: Consumables: 30 kDa TFF membrane	In-Place-Cleaning	CIP with 6L 0.1N NaOH	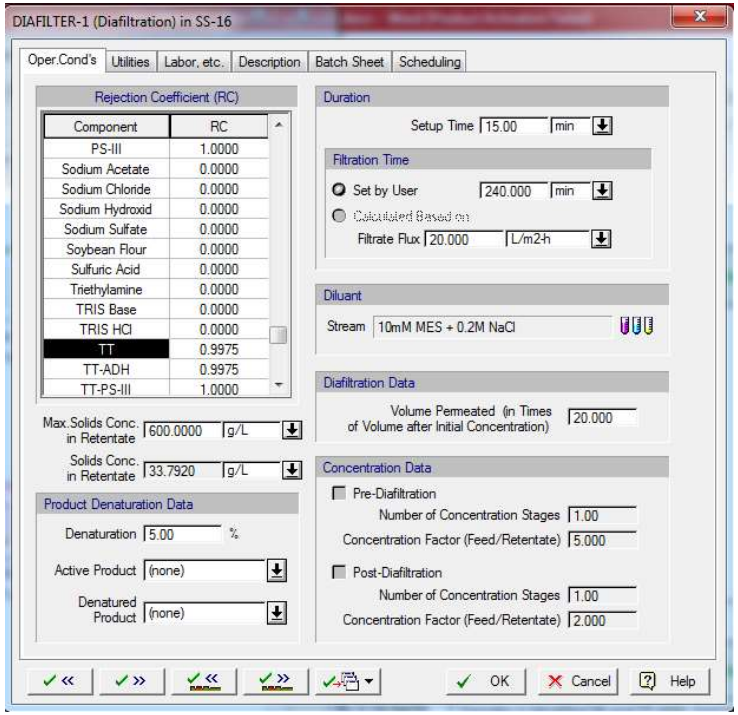
		Flush	Flush with 12L WFI, 30 min	
		Diafiltration	• Diafilter 20 X into 11. 10 mM MES + 0.2N NaCl • 20 L/m².h • TT rejection coefficient 0.9975	
		In-Place-Cleaning	• CIP with 5L 0.1N NaOH • Rinse with 10L WFI	

Tag	SuperPro unit procedure(s)	SuperPro unit operations(s) in sequential order	SuperPro parameters	Screen captures of SuperPro operations dialogue
SS-17	→ Batch vessel procedure → in a Seed Bioreactor  SS-17 / R-303 Conjugation Equipment: Glass reactor R-303	In-Place-Cleaning	• CIP with 4L 0.1N NaOH • Rinse with 22L WFI	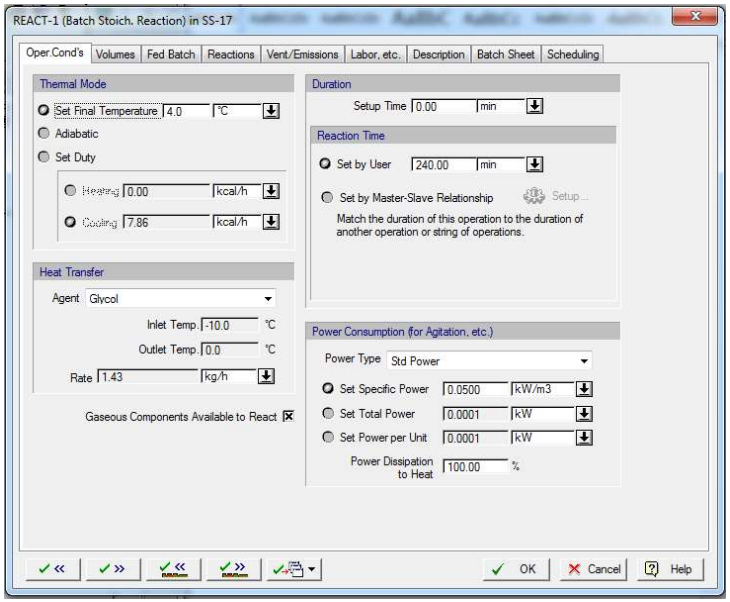
		Transfer In	Transfer in from SS-14 at 100 kg/h	
		Transfer In	Transfer in from SS-16 at 100 kg/h	
		Batch Stoichiometric Reaction	**Mod-PS-III + TT-ADH → TT-PS-III (X_{TT}=100%)** • React at 4 °C for 24 h, 50 W/m^3 agitation	
		Charge	Charge 1.14 g Glycine	
		Batch Stoichiometric Reaction	**Glycine → WFI (X=100%)** • React adiabatically for 30 min, 50 W/m^3 agitation	
		Transfer Out	Transfer out to SS-18 at 100 kg/h	
		In-Place-Cleaning	• CIP with 4L 0.1N NaOH • Rinse with 22L WFI	

Tag	SuperPro unit procedure(s)	SuperPro unit operations(s) in sequential order	SuperPro parameters	Screen captures of SuperPro operations dialogue
SS-18	→ Batch vessel procedure → in a Seed Bioreactor  SS-18 / R-304 Conj. Precipitation Equipment: Glass reactor R-304	In-Place-Cleaning	• CIP with 5L 0.1N NaOH • Rinse with 25L WFI	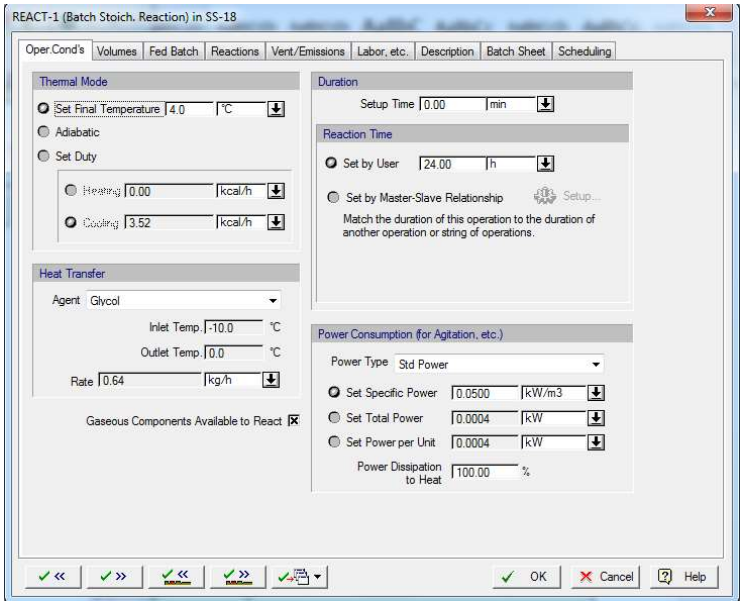
		Transfer In	Transfer in from SS-17 at 100 kg/h	
		Charge	Charge 5.88L of saturates (43wt% at 20°C) $(NH_4)_2SO_4$	
		Batch Stoichiometric Reaction	**$(NH_4)_2SO_4$ → WFI (X=95%)** **TT-PS-III → WFI (X=5%)** • React at 4 °C for 24 h with 50 W/m^3	
		Transfer Out	Transfer out to SS-19 at 100 kg/h	
		In-Place-Cleaning	• CIP with 5L 0.1N NaOH • Rinse with 25L WFI	

Tag	SuperPro unit procedure(s)	SuperPro unit operations(s) in sequential order	SuperPro parameters	Screen captures of SuperPro operations dialogue
SS-19	→ Centrifugation → Bowl 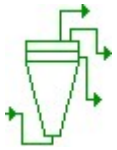 SS-19 / C-301 Centrifugation Equipment: Tubular bowl centrifuge C-301	In-Place-Cleaning	• CIP with 15L 0.1N NaOH • Rinse with 75L WFI	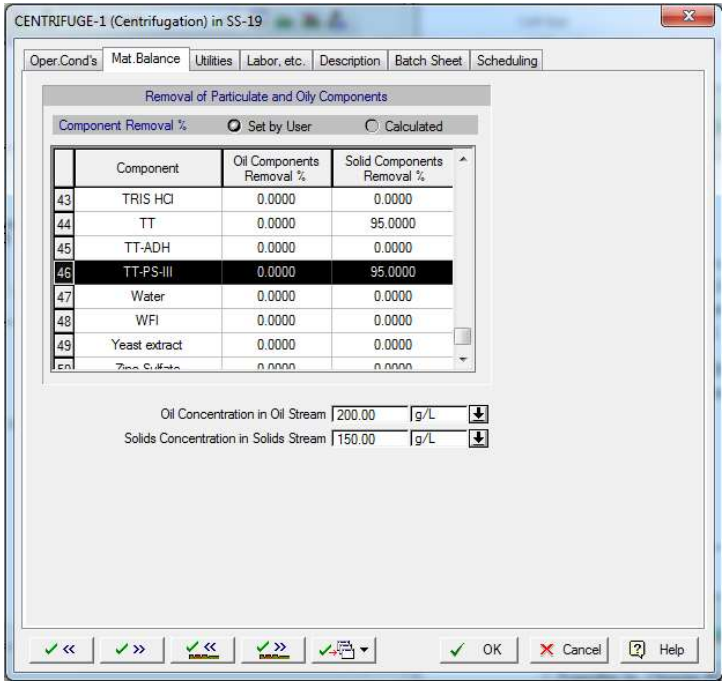
		In-Place-Steaming	Steam sterilize with saturated steam at 3 barg, 300 (kg/h)/m^3 for 30 minutes	
		Centrifugation	• 95% TT-PS-III recovery to pellet • 90% liquid to middle fraction • 10% liquid to top fraction • 30 min (Σ=440 m^2)	
		In-Place-Cleaning	• CIP with 15L 0.1N NaOH • Rinse with 75L WFI	

Tag	SuperPro unit procedure(s)	SuperPro unit operations(s) in sequential order	SuperPro parameters	Screen captures of SuperPro operations dialogue
SS-20	→ Storage/Blending → in a Disposable → Generic container 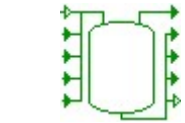 SS-20 / ST-201 Resuspension • Equipment: Magnetic stirrer ST-201 • Consumables: 5L glass bottle	Transfer In	Transfer in from SS-19 at 100 kg/h	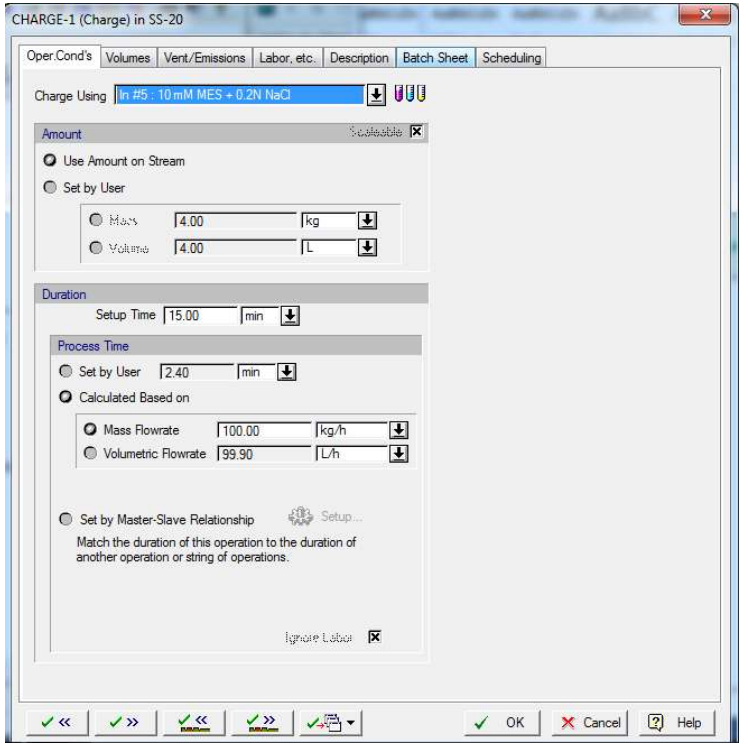
		Charge	Charge 4L of 10 mM MES + 0.2N NaCl buffer at 100 kg/h	
		Batch Stoichiometric Reaction	**TT-PS-III → WFI (X=2%)** • React adiabatically for 60 min, 50 W/m3 agitation	
		Transfer Out	Transfer out to SS-21 at 100 kg/h	

Tag	SuperPro unit procedure(s)	SuperPro unit operations(s) in sequential order	SuperPro parameters	Screen captures of SuperPro operations dialogue
SS-21	→ Filtration → Diafiltration 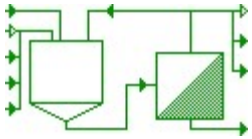 SS-21 / TF-302 TFF polish Equipment: TFF skid TF-302 Consumables: Consumables: 30 kDa TFF membrane	In-Place-Cleaning	CIP with 10L 0.1N NaOH	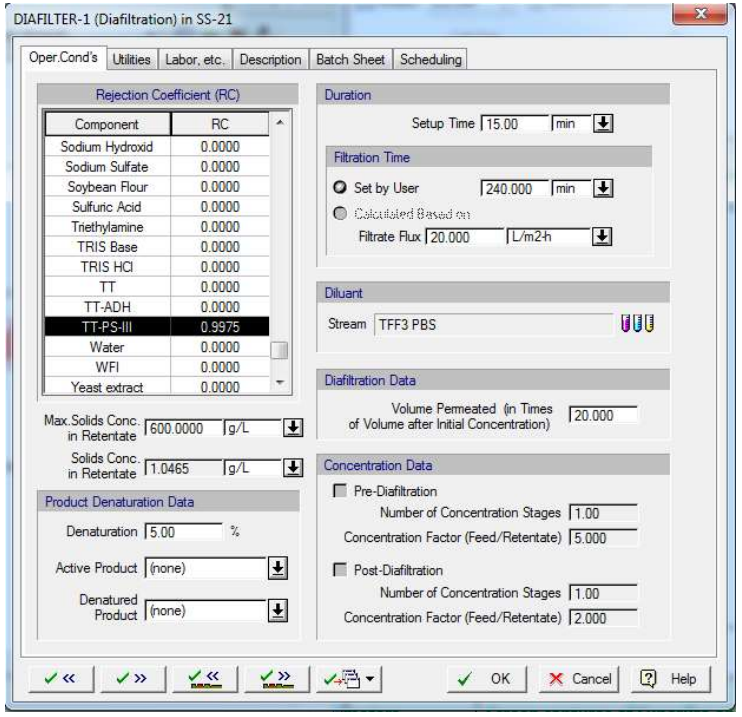
		Flush	Flush with 20L WFI, 30 min	
		Diafiltration	• Diafilter 20 X into 12. PBS • 20 L/m².h • TT-PS-III rejection coefficient 0.9975	
		In-Place-Cleaning	• CIP with 10L 0.1N NaOH • Rinse with 20L WFI	

Tag	SuperPro unit procedure(s)	SuperPro unit operations(s) in sequential order	SuperPro parameters	Screen captures of SuperPro operations dialogue
SS-22	→ Filtration → Dead End Filtration  SS-22 / P-201 Final filtration • Equipment: Peristaltic pump P-201 • Consumables: 0.22 µm polysulfone filter, area 0.014 m^2	Dead-End Filtration	• 100% biomass removal • 1% product loss • 4000 $L/m^2.h$ • 60 min	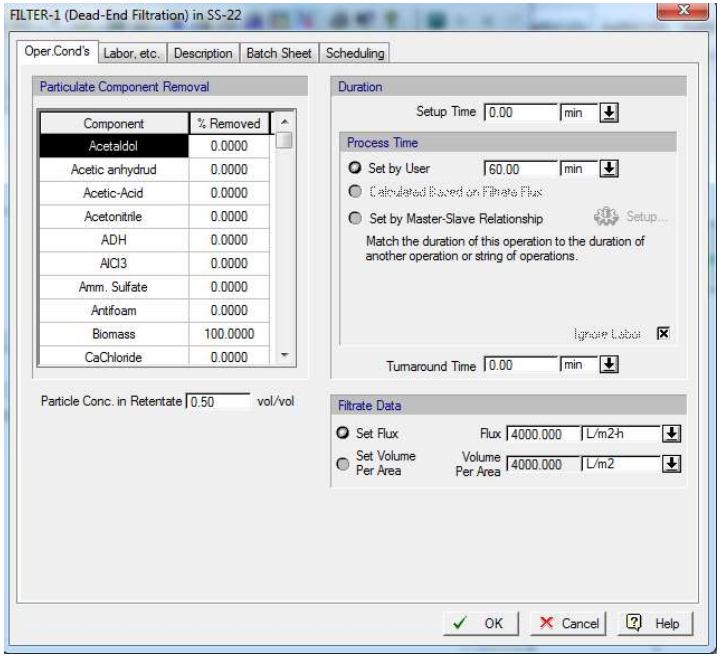

A.4 Equipment specifications

A.4.1 Fermentor geometry calculations

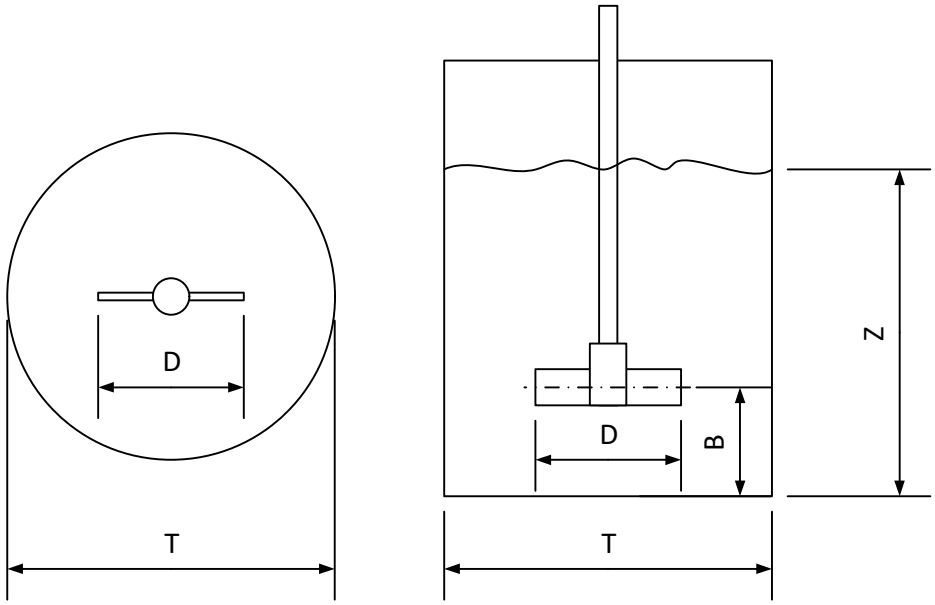

Figure 63: Stirred tank dimensions

Assumptions for geometry of a mechanically agitated stirred tank reactor (STR):

$Vessel\ diameter\ =\ T$

$Static\ liquid\ level\ =\ Z\ =\ T$

$Impeller\ diameter\ =\ D\ =\ T/3$

$Impeller\ height\ from\ bottom\ =\ B\ =\ D\ =\ T/3$

Assume a total working volume of 26 L

$$V = 0.026\ m^3$$

$$\boldsymbol{V_{cylinder} = \pi r^2 L} \qquad \text{Equation A-6}$$

$$V_{cylinder} = \pi r^2 L = \pi\left(\frac{T}{2}\right)^2 Z = \frac{1}{4}\pi T^3$$

$$T = \sqrt[3]{\frac{4V}{\pi}} = \sqrt[3]{\frac{4 \times 0.026 m^3}{\pi}}$$

$$\boldsymbol{T = 0.321\ m}$$

$$\boldsymbol{Z\ =\ T\ =\ 0.321\ m}$$

$$\boldsymbol{D\ = \frac{T}{3} = 0.107\ m}$$

$$\boldsymbol{B = D = \frac{T}{3} = 0.107 m}$$

Assume a total volume of 32 L

$Vessel\ height = H$

$$V = 0.032\ m^3$$

$$V_{cylinder} = \pi r^2 L = \pi\left(\frac{T}{2}\right)^2 H = \frac{1}{4}\pi T^2 H$$

$$\boldsymbol{T = 0.321\ m}$$

$$H = \frac{4V}{\pi T^2} = \frac{4 \times 0.032 m^3}{\pi(0.321^2) m^2}$$

$$\boldsymbol{H = 0.395 m}$$

A.4.2 Fermentor stirring power input calculation

$Assume\ the\ fluid\ is\ water\ at\ 37°C$

$T = 37 + 273.15 = 310.15\ K$

$\boldsymbol{\rho = 993.33\ kg.m^{-3}}$ (NIST Chemistry WebBook, 2019)

$\boldsymbol{\sigma = 6.9152 \times 10^{-4}\ Pa.s}$ (NIST Chemistry WebBook, 2019)

$Impeller\ rotational\ speed\ \boldsymbol{n = 600\ rpm = 10s^{-1}}$

Impeller Reynold's number:

$$\boldsymbol{N_{Re} = \frac{nD^2\rho}{\sigma}} \qquad \text{Equation A-7}$$

$$N_{Re} = \frac{nD^2\rho}{\sigma} = \frac{10s^{-1} \times (0.107m)^2 \times 993.33\ kg.m^{-3}}{6.9152 \times 10^{-4}\ kg.m^{-1}.s^{-2}.s}$$

$\boldsymbol{N_{Re} = 1.646 \times 10^5}$

Impeller Power number:

$$\boldsymbol{N_P = \frac{P}{\rho n^3 D^5}} \qquad \text{Equation A-8}$$

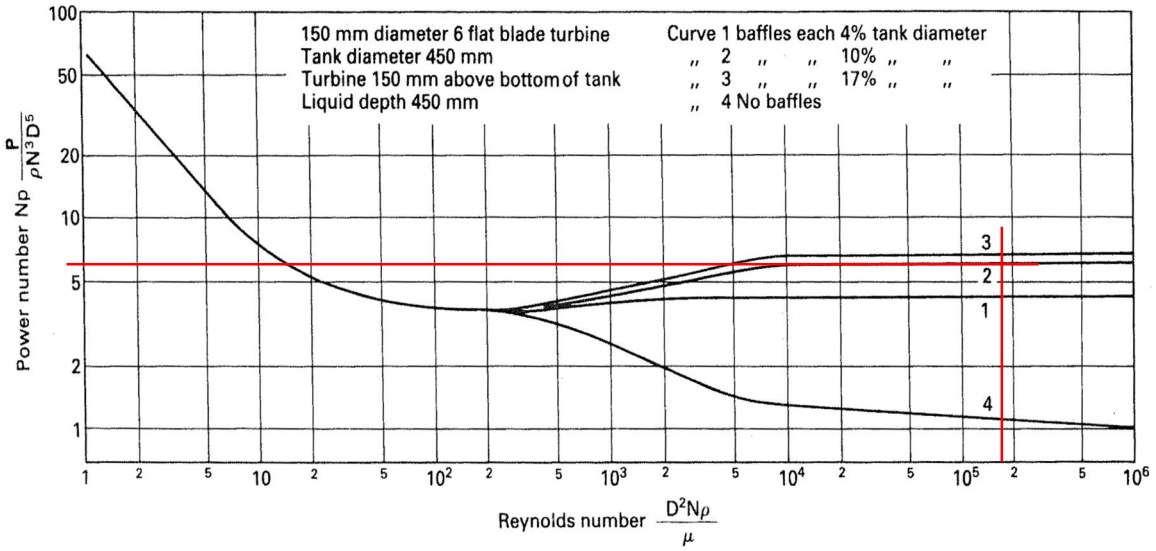

Figure 64: Impeller Reynolds' number to Power Number correlation.

$$From\ \boldsymbol{Figure\ 60, N_P \approx 7} \qquad \boldsymbol{N_P = \frac{P}{\rho n^3 D^5}} \qquad \text{Equation A-8}$$

$$P = N_P \rho n^3 D^5 = 7 \times 993.33\ kg.m^{-3} \times (10s^{-1})^3 (0.107m)^5 = 97.662 \frac{kg.m^2}{s^3} = 97.662W$$

$$Gas\ flow\ rate\ Q = 0.5\ vvm = \frac{0.5 \times V}{minute} = \frac{0.5 \times 0.026m^3}{min} \times \frac{min}{60s}$$

$\boldsymbol{Q = 2.167 \times 10^{-4} m.s^{-1}}$

Gassed Power:

$$\boldsymbol{P_g = 0.706\left(\frac{P^2 n D^3}{Q^{0.56}}\right)^{0.45}} \qquad \text{Equation A-9}$$

$$P_g = 0.706\left(\frac{P^2 n D^3}{Q^{0.56}}\right)^{0.45} = 0.706\left(\frac{(97.662W)^2 n D^3}{Q^{0.56}}\right)^{0.45}$$

$$P_g = 0.706\left(\frac{(97.662W)^2 10s^{-1}(0.107m)^3}{(2.167\times10^{-4}m.s^{-1})^{0.56}}\right)^{0.45} = \boldsymbol{50.440\ W}$$

Specific Gassed Power:

$$\boldsymbol{P_g' = \frac{P_g}{V}} \qquad \text{Equation A-9}$$

$$P_g' = \frac{P_g}{V} = \frac{50.440\ W}{0.026m^3} = \boldsymbol{1939.982\ W.m^3 \approx 2kW.m^{-3}}$$

Similarly, it was calculated that for a fermentor with a total volume of 320 L, and a maximum stirred volume of 260 L, the specific gassed power requirement would be approximately 10 kW/m³.

A.4.3 Equipment Purchase costs

Equipment Purchase cost escalation Sample calculation:

$\boldsymbol{26\ L\ Stainless\ steel\ Fermentor\ Purchase\ Cost = \$268\ 100}$

$\boldsymbol{Year\ of\ purchase = 2010}$

$\boldsymbol{Escalation\ rate = 6\%\ per\ annum}$

$$Current\ purchase\ cost = Cost \times (1 + escalation\ rate)^{current\ year - year\ of\ purchase} \qquad \text{Equation A-10}$$

$$Fermentor\ cost_{2017} = \$268\ 100 \times (1 + 0.06)^{(2017-2010)}$$

$$Fermentor\ cost_{2017} = \$403\ 123.27$$

All equipment costs rounded to the nearest $1000

$$\boldsymbol{Fermentor\ cost_{2017} = \$403\ 000}$$

Cost specifications for each piece of major equipment calculated as per the above example, are detailed in **Tables A-5… A-7** on the proceeding pages. *Costs marked with an asterisk (*) were valued using Intelligen SuperPro 9.5 Academic software built in cost models.*

Table A-5 Base case model equipment specifications

Process step	Process step Description	Equipment tag	SuperPro Equipment	Real equipment	Purchase cost [2017 US $]
SS-01	Inoculum preparation	**I-101**	Shaker incubator	Infors HT multitron	35 000
SS-01f	0.22µm Filtration	**P-101**	Peristaltic pump	Watson Marlow 620 DuN pump	8 000
SS-02f					
SS-02	Medium preparation	**T-101**	60L s/steel mixing tank	Biozeen s/steel jacketed vessel	164 000*
SS-03	Fermentation	**R-101**	32L s/steel fermentor	Pierre Guerin 32L s/steel fermentor	403 000
SS-04	Neut./Cationic precipitation	**T-102**	60L s/steel mixing tank	Biozeen s/steel jacketed vessel	164 000*
SS-05	Centrifugation	**C-201**	Disk stack bowl centrifuge	Hettich Rotosilenta 630RS	65 000
S-06	TFF into TRIS/NaCl	**TF-201**	Tangential flow filtration skid	EMD Millipore Cogent M1	76 000
S-07	TFF in Na_2CO_3				
SS-08	TFF hold	**ST-201**	Magnetic stirrer	IKA MAG MR1 magnetic stirrer	5 000
SS-10	Re-N-Acetylation				
SS-20	Resuspension				
SS-09	Protein removal	**F-201**	Filter housing	EMD Millipore Millistak filter housing	1000*
SS-11	0.22µm Filtration	**P-201**	Peristaltic pump	Watson Marlow 520 DuN pump	5 000
SS-22	Final 0.22µm Filtration				
SS-12	2 - 8 °C hold	**Cold Room**	Tote with temperature control	Cold room	5000*
SS-13	PS activation	**R-301**	Jacketed glass reactor 0 – 5 L	Radley's Reactor Ready system	14 000
SS-15	TT activation	**R-302**			
SS-17	Conjugation	**R-303**			
SS-18	Precipitation	**R-304**	Jacketed glass reactor 6 – 20 L	De Deitrich Pharma Reactor system	300 000
SS-16	TFF TT	**TF-301**	Tangential flow filtration skid	EMD Millipore Cogent M1	76 000
SS-19	Centrifugation	**C-301**	Tubular centrifuge	Riera Nadeu RINA tubular centrifuge	123 000*
SS-21	TFF final	**TF-302**	Tangential flow filtration skid	EMD Millipore Cogent M1	76 000

Table A-6 Additional Equipment specifications for 20L scale Single Use

Process step	Process step Description	Equipment tag	SuperPro Equipment	Real equipment	Purchase cost [2017 US $]
SU-02	Medium preparation	SUT-101	50L SU mixing tank	Pall Allegro 50L magnetic mixer	73 500
HY-02					
SU-04,	Neut./Cationic precipitation	SUT-102	100L SU mixing tank	Pall Allegro 100L magnetic mixer	100 000*
HY-04					
SU-03	20L Fermentation	SUR-101	50L SU fermentor	Sartorius CultiBag STR 50L	118 000*

Table A-7 Additional Equipment specifications for 200 L processing scale

Process step	Process step Description	Equipment tag	SuperPro Equipment	Real equipment	Purchase cost [2017 US $]
SS200-04	200L Fermentation	R-102	340L Stainless steel fermentor	Pierre Guerin 300L s/steel fermentor	620 000*
HY200-04					
SS200-02		T200-1	200L s/steel mixing tank	Biozeen 200L s/steel mixing tank	171 000*
SS200-0		T200-2	600L s/steel mixing tank	Biozeen 600L s/steel mixing tank	199 000*
SU200-02	Medium preparation	SUT-200-1	200L SU mixing tank	Sartorius Flexel 200L magnetic mixer	150 000*
HY200-02					
SU200-05	Neut./Cationic precipitation	SUT-200-2	650L SU mixing tank	Sartorius Flexel 650L magnetic mixer	300 000*
HY200-05					
SU200-04	200L Fermentation	SUR-102	500L SU fermentor	Xcellerex XDR MO 500L fermentor	800 000*
HY200-05	Centrifugation	C-200-1	Disk stack centrifuge	Alfa Laval BTPX 305s centrifuge	300 000*

A.5 Consumables specifications

Tables A-8… A-10 below show all consumable costs used in the simulation models. *Costs marked with an asterisk (*) are valued using Intelligen SuperPro 9.5 Academic software built in cost parameters.*

Table A-8 Base case model consumable type specifications

Process step	Process step Description	Equipment tag	SuperPro consumable	Real consumable	Cycle lifetime	Cost per unit [2017 US $]
SS-01	Inoculum preparation	**I-101**	4000 mL glass shake flask	4L glass Erlenmeyer flask	100	60
SS-01f	0.22 µm filtration	**P-101**	0.22 µm filter cartridge	Merck Opticap XL150 filter	1	630
SS-02f						
SS-11		**P-201**				
SS-22	Final 0.22 µm filtration	**P-301**				
SS-03	Fermentation	**R-101**	100 mL SU sampling bag	100 mL Sartorius Flexboy bag	1	20
SS-05	Centrifugation	**C-201**	2L centrifuge bottle	2L Nalgene centrifuge bottle	100	45
SS-06	TFF into TRIS/NaCl	**TF-201**	30 kDa TFF membrane	Merck Pellicon 30 kDa TFF membrane	15	10 000/m^2
SS-07	TFF into Na_2CO_3					
SS-14	TFF Mod-PS					
SS-16	TT diafilter	**TF-301**				
SS-21	TFF polish	**TF-302**				
SS-08	TFF hold	**ST-201**	5L Glass bottle	Schott Duran 5L Glass bottle	100	10
SS-10	Re-N-Acetylation					
SS-20	Resuspension					
SS-09	Protein removal	**F-201**	Carbon filter	EMD Millipore U-pod filter	1	210
SS-12	2-8 °C hold	**Cold Room**	3L SU storage bag	3L Sartorius Flexboy bag	1	20

Table A-9 Additional consumables specifications for 20L scale Single Use

Process step	Process step Description	Equipment tag	SuperPro consumable	Real consumable	Cycle lifetime	Cost per unit [2017 US $]
SU-01, HY-01,	Inoculum preparation	**I-101**	3000 mL SU shake flask	3L Corning Erlenmeyer single use shake flask	1	60
SU-02, HY-02	Medium preparation	**SUT-101**	50L SU mixing bag	Pall Allegro 50L mixing bag	1	900
SU-04, HY-04	Neut./Cationic precipitation	**SUT-102**	100L SU mixing bag	Pall Allegro 100L mixing bag	1	1200
SU-03	20L Fermentation	**SUR-101**	50L SU fermentation bag	Sartorius CultiBag 50L	1	3460
SU-08, HY-08	TFF hold	**ST-201**	5L SU bottle	5L Corning single use bottle	1	50*
SU-10, HY-10	Re-N-Acetylation					
SU-20, HY-20	Resuspension					

Table A-10 Additional consumables specifications for 200 L processing scale

Process step	Process step Description	Equipment tag	SuperPro consumable	Real consumable	Cycle lifetime	Cost per unit [2017 US $]
SS200-02f20	0.22 µm filtration	P-101	0.22 µm filter cartridge High capacity	Merck Opticap XL600 filter	1	1000*
SS200-02f200						
SU200-02f20						
SU200-02f200						
HY200-02f20						
HY200-02f200						
SS-200-20	Resuspension	ST-201a	5L Glass bottle	Schott Duran 5L Glass bottle	100	10
SS-08	TFF hold	ST-201	20L Glass bottle	Schott Duran 20L Glass bottle	100	40
SS-10	Re-N-Acetylation					
SS-20	Resuspension					
SU200-04, HY200-04	200L Fermentation	SUR-102	500L SU fermentation bag	Xcellerex XDR MO 500L bag	1	5530
SU200-02 HY200-02	Medium preparation	SUT-200-1	200L SU mixing bag	Sartorius Flexel 200L bag	1	2000
SU200-05, HY200-05	Neut./Cationic precipitation	SUT-200-2	650L SU mixing bag	Sartorius Flexel 650L bag	1	3000
SU200-13, HY200-13	2-8 °C hold	Cold Room	10L SU storage bag	10L Sartorius Flexboy bag	1	100

A.6 Raw material specifications

Tables A-11… A-14 below show the properties used for all raw material inputs and product outputs. These properties are located in the SuperPro materials database. For materials that were not in the SuperPro database, this data was entered from literature sources: (Dean, 1999; Perry & Green, 2008; Haynes, 2014; Aspen Technology Inc., 2017; Intelligen Inc., 2017). *Properties marked with an asterisk (*) were estimated due to no data being available.*

Table A-11 Fermentation Raw Materials

Material Name	CAS no.	Chemical Formula	Molecular weight [g/mol]	Density at 25°C [g/L]	Unit cost [US $/kg]	Cost reference
Biomass	N/A	$CH_{1.8}O_{0.5}N_{0.2}$	24.630	1050	0.00	N/A
D-(+)-Glucose	50-99-7	$C_6H_{12}O_6$	180.157	1173.7	48.49	(Sigma Aldrich, 2017a)
BD Bacto Soytone	N/A	N/A	100*	1000*	287.98	(Fisher Scientific, 2017a)
BD Bacto Yeast Extract	N/A	N/A	180*	1560*	249.28	(Fisher Scientific, 2017b)
L-Cysteine hydrochloride	52-89-1	$C_3H_8ClNO_2S$	157.612	1721	703.76	(Sigma Aldrich, 2017b)
Tris base	77-86-1	$C_4H_{11}NO_3$	121.14	1328	7.75	(Sigma Aldrich, 2017c)
Tris hydrochloride	1185-53-1	$C_4H_{11}NO_3.HCl$	157.597	2164	1588.40	(Sigma Aldrich, 2017d)
Sodium carbonate	497-19-8	Na_2CO_3	105.989	2479.8	115.98	(Sigma Aldrich, 2017e)
Sodium chloride	7647-14-5	NaCl	58.443	1935.1	133.61	(Sigma Aldrich, 2017f)
Magnesium sulfate (anhydrous)	10034-96-5	$MgSO_4$	120.366	2660	201.40	(Sigma Aldrich, 2017g)
Ferrous sulfate heptahydrate	7782-63-0	$FeSO_4.7H_2O$	278.006	2003	95.31	(Sigma Aldrich, 2017h)
Ethanol (96% vv)	64-17-5	CH_3OH	46.069	785.9	159.12	(Sigma Aldrich, 2017i)
Hydrogen Chloride	7647-01-0	HCl	36.461	797.5	223.44	(Sigma Aldrich, 2017j)
Sodium Hydroxide	1310-73-2	NaOH	39.997	1913.4	47.08	(Sigma Aldrich, 2017k)
Calcium Chloride	10043-52-4	$CaCl_2$	110.983	2400	145.16	(Sigma Aldrich, 2019a)
Air	N/A	N/A	28.97	1.2	0.0	N/A
WFI	7732-18-5	H_2O	18.015	994.7	0.40	(Intelligen Inc., 2017)

Table A-12 Additional Purification Raw Materials

Material Name	CAS no.	Chemical Formula	Molecular weight [g/mol]	Density at 25°C [g/L]	Unit cost [US $/kg]	Cost reference
Tris base	77-86-1	$C_4H_{11}NO_3$	121.14	1328	7.75	(Sigma Aldrich, 2017c)
Sodium chloride	7647-14-5	NaCl	58.443	1935.1	133.61	(Sigma Aldrich, 2017f)
Sodium carbonate	497-19-8	Na_2CO_3	105.989	2479.8	115.98	(Sigma Aldrich, 2017e)
Acetic anhydride	108-24-7	$(CH_3CO)_2O$	102.090	1082	89.38	(Sigma Aldrich, 2019b)
WFI	7732-18-5	H_2O	18.015	994.7	0.40	(Intelligen Inc., 2017)

Table A-13 Additional Conjugation Raw Materials

Material Name	CAS no.	Chemical Formula	Molecular weight [g/mol]	Density at 25°C [g/L]	Unit cost [US $/kg]	Cost reference
CDAP	59016-56-7	$C_8H_{10}BF_4N_3$	234.990	1500*	464 360.00	(Sigma Aldrich, 2017l)
Acetonitrile	75-05-08	CH_3CN	41.052	776.7	176.37	(Sigma Aldrich, 2017m)
Triethylamine (TEA)	121-44-8	$(C_2H_5)_3N$	101.191	724.5	150.74	(Sigma Aldrich, 2017n)
MES	1266615-59-1	$C_6H_{13}NO_4S$	195.240	1400	667.89	(Sigma Aldrich, 2019c)
Carrier protein	N/A	N/A	150000*	1050*	55 000.00*	N/A
Adipic acid Dihydrazide (ADH)	1071-93-8	$C_6H_{14}N_4O_2$	174.200	1230	2120.40	(Sigma Aldrich, 2017o)
EDC	25952-53-8	$C_8H_{17}N_3.HCl$	191.703	877	24 715.20	(Sigma Aldrich, 2017p)
Glycine	56-40-6	$C_2H_5NO_2$	75.067	1470.9	245.33	(Sigma Aldrich, 2017q)
Ammonium Sulfate	7783-20-2	$(NH_4)_2SO_4$	132.134	1769	102.30	(Sigma Aldrich, 2017r)
Phosphate Buffered Saline (PBS)	N/A	N/A	N/A	1003.1	0.12	(Intelligen Inc., 2017)
Potassium dihydrogen phosphate	7778-77-0	KH_2PO_4	136.077	1636	N/A	N/A
Sodium hydro phosphate	7558-79-4	Na_2HPO_4	141.950	1679	N/A	N/A
WFI	7732-18-5	H_2O	18.015	994.7	0.40	(Intelligen Inc., 2017)

Table A-14 Reaction Products and intermediates

Material Name	CAS no.	Chemical Formula	Molecular weight [g/mol]	Density at 25°C [g/L]	Value [US $/kg]	Value reference
Biomass	N/A	$CH_{1.8}O_{0.5}N_{0.2}$	24.630	1050		
Carbon dioxide	124-38-9	CO_2	44.010	2.0		
Lactic Acid	598-82-3	C_2H_5OCOOH	90.079	1220.9		
Acetic Acid	64-19-7	CH_3COOH	60.053	1042		
Acetoin	107-89-1	$C_4H_8O_2$	88.106	1100.5		N/A
Formic Acid	64-18-6	HCOOH	46.026	1213.7		
GBS 3 polysaccharide (PS-III)	N/A	$(C_{35}H_{52}O_{31}N_2)n$	996*	1050*		
Activated PS (Mod-PS-III)	N/A	N/A	996*	1050*		
Activated protein (TT-ADH)	N/A	N/A	150000*	1050*		
Conjugate API (TT-PS-III)	N/A	N/A	246000*	1050*	6 000 000 (est.)#	(Kim et al., 2014)

 # Single dose estimated as 5 µg

Tables A-15… A-18 below show the compositions of media and buffers used in the models:

Table A-15 Inoculum medium composition

Component	Conc.[g/L]
BD Bacto Soytone	20.0
D-(+)-Glucose	2.5
L-Cysteine hydrochloride	0.1
Sodium Chloride	5.0
Magnesium Sulfate (anhydrous)	0.1
Ferrous Sulfate heptahydrate	0.02
Sodium Carbonate	0.6
Tris base	0.8
Tris hydrochloride	3.0
WFI	956.1

Table A-16 Fermentation medium composition

Component	Conc.[g/L]
BD Bacto Soytone	30.0
D-(+)-Glucose	20.0
L-Cysteine hydrochloride	0.1
Sodium Chloride	5.0
Magnesium Sulfate (anhydrous)	0.1
Ferrous Sulfate heptahydrate	0.02
Sodium Carbonate	0.6
WFI	944.7

Table A-17 Fermentation feed composition

Component	Conc.[g/L]
BD Bacto Yeast Extract	30.0
D-(+)-Glucose	400.0
WFI	636.5

Table A-18 Phosphate Buffered Saline (PBS)

Component	Conc.[g/L]
Potassium chloride	0.002
Potassium dihydrogen phosphate	0.002
Sodium chloride	8.0
Sodium hydro phosphate	1.1
WFI	993.9

A.7 Utilities specifications

- Simplified CIP cycle for stainless steel vessels: 0.1N NaOH wash for 15 min at 5 L/min.m, WFI rinse for 15 min at 5 L/min.m.
- Fermentor assumed to have integrated CIP skid.
- CIP for centrifuge: 0.1N NaOH wash for 30 min at 150 L/h, WFI rinse for 30 min at 150 L/h.
- CIP for TFF skids 0.1N NaOH wash at 10 L/m^2 for 15 min, flush with WFI for 30 min at 20L/m^2
- CIP for reactors: 0.1N NaOH wash for 15 min at 5 L/min.m, WFI rinse for 15 min at 5 L/min.m.
- Upstream (fermentation) and downstream each have their own CIP skids
- Simplified SIP cycle: Sterilize for 30min at 150°C (3 barg sat. steam) at 100 kg/h/m^3 steam usage for vessels and 300 kg/h usage for centrifuge.
- Where not specified, charge / transfer rates for material are set to 100 kg/h
- Estimated utilities costs are shown in **Table A-19**:

Table A-19 Utilities used in Simulation Models

Utility	Used for	Cost
Steam (3barg saturated)	Heating vessels	12.00 $/MT
Electricity (single phase)	Heating small equipment, centrifugation	0.10 $/kWh
Hot water (40 °C, return 30°C)	Heating product after cold storage	0.05 $/MT
Chilled water (5°C, return 10 °C)	Cooling vessels, centrifuges	0.40 $/MT
Ethylene glycol (-10°C, return 0°C)	Cooling glass reactors	0.35 $/MT

A.8 Cost Assumptions and Sample calculations

- All equipment and consumables purchased new as of 2017 prices
- 7% Asset cost inflation rate
- 13.16 ZAR USD exchange rate (SARB, 2019)
- 28% Corporate Income Tax rate (SARS, 2015, 2019)
- Equipment depreciation by straight line method, 10 years, 20% scrap value
- Construction period 24 months; Start-up period 3 months; First year output 50%, Project lifetime 12 years
- API product value $ 6 million /kg based on $ 30 per 5 µg dose
- Hurdle rate 25% (High risk investment assumed)
- Direct Fixed Capital (DFC) financing 35% loan (10-year loan at 12% compound interest)
- Working capital 15% loan (6-year loan at 12% compound interest)
- Weighted Average Cost of Capital (WACC) 20%
  $WACC = Equity\ value \times cost\ of\ Equity + Loan\ value \times cost\ of\ loan$

Installation costs factors of Equipment purchase cost (EC) are shown in **Table A-20** below:

Table A-20 Installation cost factors

Unit operation/ equipment types	Equation
Filtration	$0.50 \times EC$
Shaker Incubator	$1.50 \times EC$
Stainless steel fermentor	$0.30 \times EC$
Single Use fermentor	$1.50 \times EC$
Stainless steel mixing tank	$0.30 \times EC$
Single use mixing tank	$0.10 \times EC$
Centrifuge	$0.50 \times EC$
TFF skid	$0.50 \times PC$
Generic mixing	$1.50 \times PC$
Cold room	$0.10 \times PC$
Chemical reactor	$0.50 \times PC$

$$Unlisted\ equipment\ cost\ (UC) = 0.2 \times Listed\ equipment\ cost\ (EC) \quad \text{Equation A-11}$$

$$Installation\ cost\ for\ unlisted\ equipment = 0.5 \times UC \quad \text{Equation A-12}$$

$$Total\ Purchased\ equipment\ Cost\ (PC) = EC + UC \quad \text{Equation A-13}$$

$$\boldsymbol{PC = 1.25 \times EC} \quad \text{Equation A-14}$$

$$Direct\ costs\ (DC) = PC + Installation + Piping + Instrumentation + Electrical + Buildings + Yard + Auxiliary\ facilities \quad \text{Equation A-15}$$

Table A-21 Factorial estimation for Direct Costs (DC)

Parameter	Equation
Piping	$0.45 \times PC$
Auxiliary facilities	$0.20 \times PC$
Instrumentation	$0.15 \times PC$
Electrical	$0.10 \times PC$
Buildings	$0.10 \times PC$
Yard Improvement	$0.05 \times PC$

$$Indirect\ Costs\ (IC) = Engineering + Construction \quad \text{Equation A-16}$$

Table A-22 Factorial estimation for Indirect Costs (IC)

Parameter	Equation
Engineering	$0.25 \times DC$
Construction	$0.45 \times DC$

$$Other\ costs\ (OC) = Contractors\ fee + Contingency$$ Equation A-17

Table A-23 Factorial estimation for Other Costs (OC)

Parameter	Equation
Contractors fee	$0.05 \times (DC + IC)$
Contingency	$0.10 \times (DC + IC)$

Direct Fixed Capital (DFC) = Direct Costs (DC) + Indirect Costs (IC) + Other Costs (OC)

$$DFC = DC + IC + OC$$ Equation A-18

Total Capital Cost (CAPEX) = Direct Fixed Capital (DFC) + Working Capital (WC) + Start-up cost

$$CAPEX = DFC + WC$$ Equation A-19

WC estimated as 30 days of operating cost (Labour, materials, utilities & waste treatment)

A.8.1 Sample Calculation – CAPEX for 20L Stainless Steel technology

Equipment costs as per **Table** A-5 Base case model equipment specifications **A-5**:

$EC\ (total) = \$\ 1\ 547\ 000$

$$Unlisted\ equipment\ cost\ (UC) = 0.2\ x\ Total\ equipment\ purchase\ cost\ (PC)$$ Equation A-20

$$Total\ Purchased\ equipment\ Cost\ (PC) = EC + UC$$ Equation A-21

$PC = EC + UC = \$\ 1\ 547\ 000 + 0.2PC$

$PC = \$\dfrac{1\ 547\ 000}{0.8}$

$\boldsymbol{PC = \$\ 1\ 933\ 750}$

$\boldsymbol{PC \rightarrow\ \$\ 1\ 934\ 000}$

$UC = 0.2 \times PC = 0.2 \times \$\ 1\ 934\ 000 = \$\ 386\ 750$

Installation (As per **Table A-20** with EC from **Table A-5**)

$$Installation\ for\ listed\ equipment\ (IEC) = \$\ 664\ 625$$

$$Installation\ cost\ for\ unlisted\ equipment\ (IUC) = 0.5 \times UC \quad \text{Equation A-22}$$

$$IUC = 0.5 \times \$\ 386\ 750 = \$\ 193\ 375$$

$$Installation = IEC + IUC = \$\ 664\ 625 + \$\ 193\ 375$$

$$Installation = \$\ 858\ 000$$

$$Direct\ costs\ (DC) = PC + Installation + Piping + Instrumentation + Electrical + Buildings + Yard + Auxiliary\ facilities \quad \text{Equation A-15}$$

$$DC = PC + Installation + 0.45PC + 0.15PC + 0.1PC + 0.1PC + 0.05PC + 0.2PC$$

$$DC = 2.05PC + Installation = (2.05 \times \$\ 1\ 933\ 750) + \$\ 858\ 000$$

$$\boldsymbol{DC = \$\ 4\ 822\ 188}$$

$$\boldsymbol{DC \rightarrow\ \$\ 4\ 822\ 000}$$

$$Indirect\ Costs\ (IC) = Engineering + Construction \quad \text{Equation A-16}$$

$$IC = 0.25DC + 0.45DC = 0.70DC = 0.70 \times \$\ 4\ 822\ 188$$

$$\boldsymbol{IC = \$\ 3\ 375\ 531}$$

$$\boldsymbol{IC \rightarrow\ \$\ 3\ 376\ 000}$$

$$Other\ costs\ (OC) = Contractors\ fee + Contingency \quad \text{Equation A-17}$$

$$OC = 0.05 \times (DC + IC) + 0.10 \times (DC + IC) = 0.15(DC + IC)$$

$$OC = 0.15 \times (\$\ 4\ 822\ 188 + \$\ 3\ 375\ 531)$$

$$\boldsymbol{OC = \$\ 1\ 229\ 657}$$

$$\boldsymbol{OC \rightarrow \$\ 1\ 230\ 000}$$

$$DFC = DC + IC + OC \quad \text{Equation A-18}$$

$$DFC = DC + IC + OC = \$\ 4\ 822\ 000 + \$\ 3\ 376\ 000 + \$\ 1\ 230\ 000$$

$$\boldsymbol{DFC = \$\ 9\ 428\ 000}$$

$$WC = \$\ 48\ 000, Startup\ cost = \$\ 471\ 000$$

$$CAPEX = DFC + WC \quad \text{Equation A-19}$$

$$CAPEX = \$\ 9\ 428\ 000 + \$\ 48\ 000 + \$\ 471\ 000$$

$$\boldsymbol{20L\ Stainless\ Steel\ CAPEX = \$\ 9\ 947\ 000}$$

A.9 Labour Cost Assumptions

Labour costs were estimated using the website Payscale.co.za for the year 2017. **Table A-24** below shows the estimated hourly rates for operational personnel requirements used in the models:

Table A-24 PayScale Salary data

Job title	Annual (ZAR)	Hourly (ZAR)	Annual (USD)	Hourly (USD)	Reference
Production Operator	R 122 679	R 50.11	$9 323.60	$3.81	(PayScale, 2017a)
Production Specialist	R 256 376	R 104.73	$19 484.58	$7.96	(PayScale, 2017b)
Production Supervisor	R 203 245	R 83.02	$15 446.62	$6.31	(PayScale, 2017c)
Pharmacist	R 417 287	R 170.46	$31 713.81	$12.95	(PayScale, 2017d)

The labour requirements for various process operations were estimated based on typical operations requirements for a pilot scale operation, shown in **Table A-25**:

Table A-25 Man-hours estimations for pilot-scale operations

Job title	Man-hours estimated for operation			
	Charge reagents, intermediates storage, Final filtration	**Reactions, Fermentation**	**TFF, centrifugation, CIP, SIP**	**All other (basic operations)**
Production Operator	2.0	2.0	2.0	2.0
Production Specialist	0.0	1.0	1.0	0.0
Production Supervisor	0.1	0.1	0.1	0.1
Pharmacist	1.0	0.0	0.0	0.0

- For overnight reactions and storage an assumption of 50% the above hours were applied.
- It was assumed that the operating labour requirements for the 200 L scale process were the same as the 20 L process (3-6 personnel per shift).
- Management, Quality and regulatory labour costs are not included.

A.10 Batch Recipe and Scheduling

- Plant total uptime 46 weeks / year uptime
- 6 weeks / year downtime (maintenance and validation)
- 20 L scale process scheduling:
- Batch time 110 h, 58h turnaround – Total cycle time 1 week
- 46 batches / year
- 200 L scale process scheduling:
- Batch time 142 h, 26h turnaround – Total cycle time 1 week
- 46 batches / year
- 10 % batch failure rate

A.11 Additional Operating Cost Adjustments

- Annual maintenance 10% of equipment purchase cost

$$Labour\ Cost\ \ per\ labour\ type\ =\ Cost\ per\ labour\ type \times Demand\ per\ labour\ type$$

- Start-up validation cost estimated as 5% of DFC

A.12 Model screenshots

A.12.1 20L Stainless steel technology process model screenshots

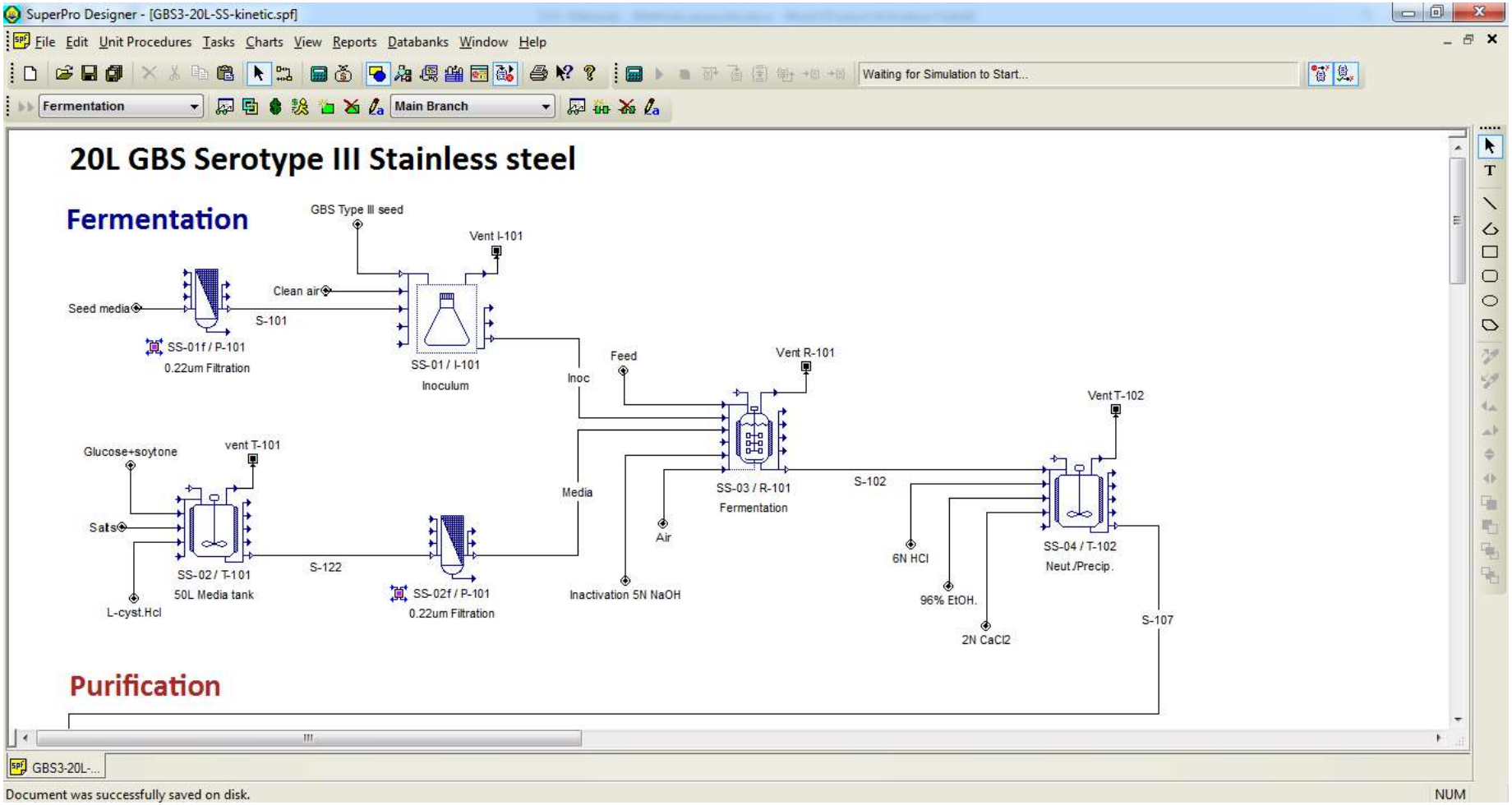

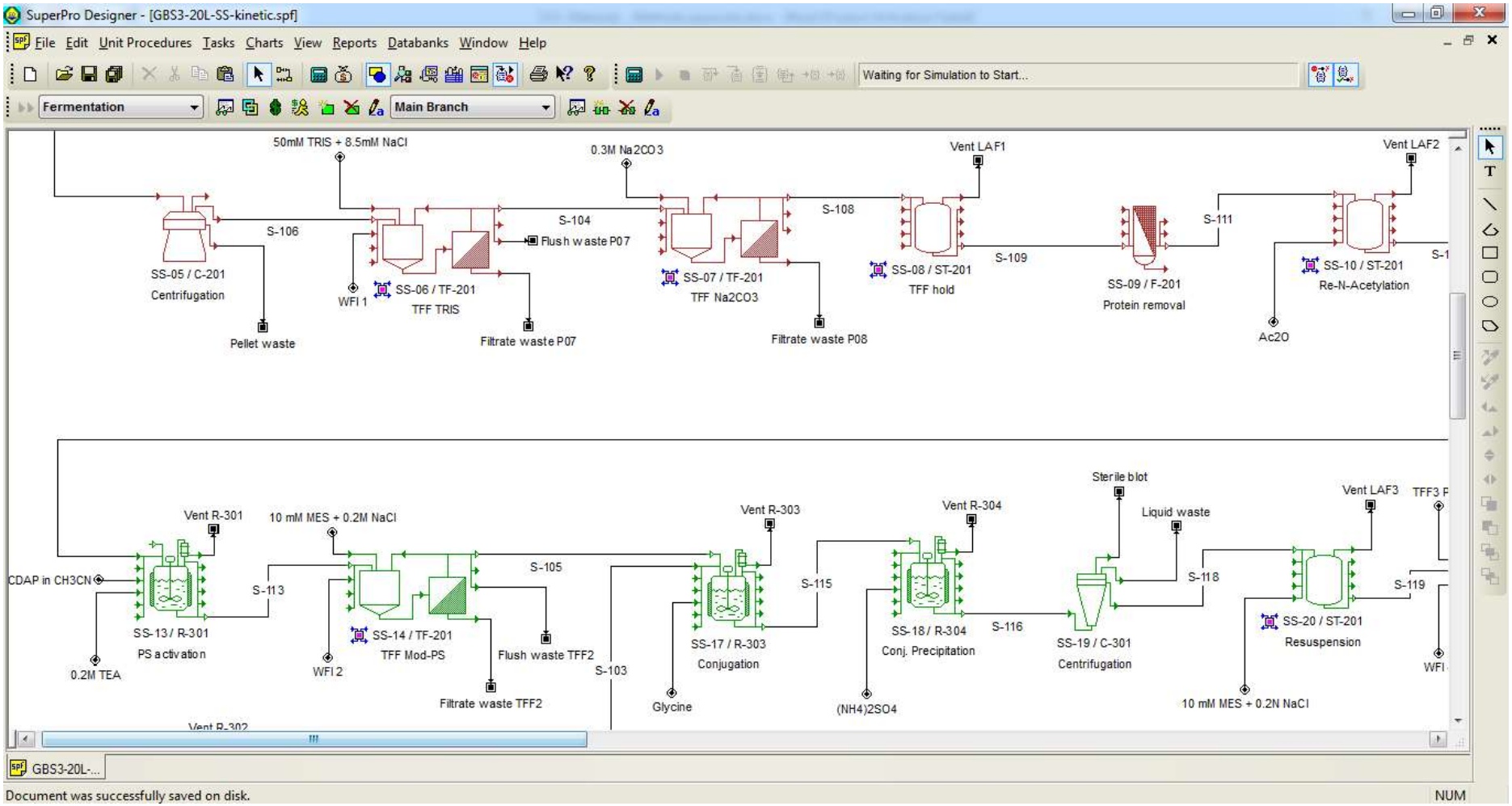
SuperPro Designer - [GBS3-20L-SS-kinetic.spf]
File Edit Unit Procedures Tasks Charts View Reports Databanks Window Help
Waiting for Simulation to Start...
Fermentation
Main Branch
50mM TRIS + 8.5mM NaCl
0.3M Na2CO3
Vent LAF1
Vent LAF2
S-106
S-104
S-108
S-109
S-111
Flush waste P07
SS-05 / C-201
Centrifugation
Pellet waste
WFI 1
SS-06 / TF-201
TFF TRIS
Filtrate waste P07
SS-07 / TF-201
TFF Na2CO3
Filtrate waste P08
SS-08 / ST-201
TFF hold
SS-09 / F-201
Protein removal
SS-10 / ST-201
Re-N-Acetylation
Ac2O
Vent R-301
10 mM MES + 0.2M NaCl
Vent R-303
Vent R-304
Sterile blot
Liquid waste
Vent LAF3
TFF3 P
CDAP in CH3CN
S-113
S-105
S-115
S-118
S-119
SS-13 / R-301
PS activation
0.2M TEA
WFI 2
SS-14 / TF-201
TFF Mod-PS
Flush waste TFF2
Filtrate waste TFF2
S-103
SS-17 / R-303
Conjugation
Glycine
SS-18 / R-304
Conj. Precipitation
(NH4)2SO4
S-116
SS-19 / C-301
Centrifugation
SS-20 / ST-201
Resuspension
10 mM MES + 0.2N NaCl
WFI
Vent R-302
GBS3-20L-...
Document was successfully saved on disk.
NUM

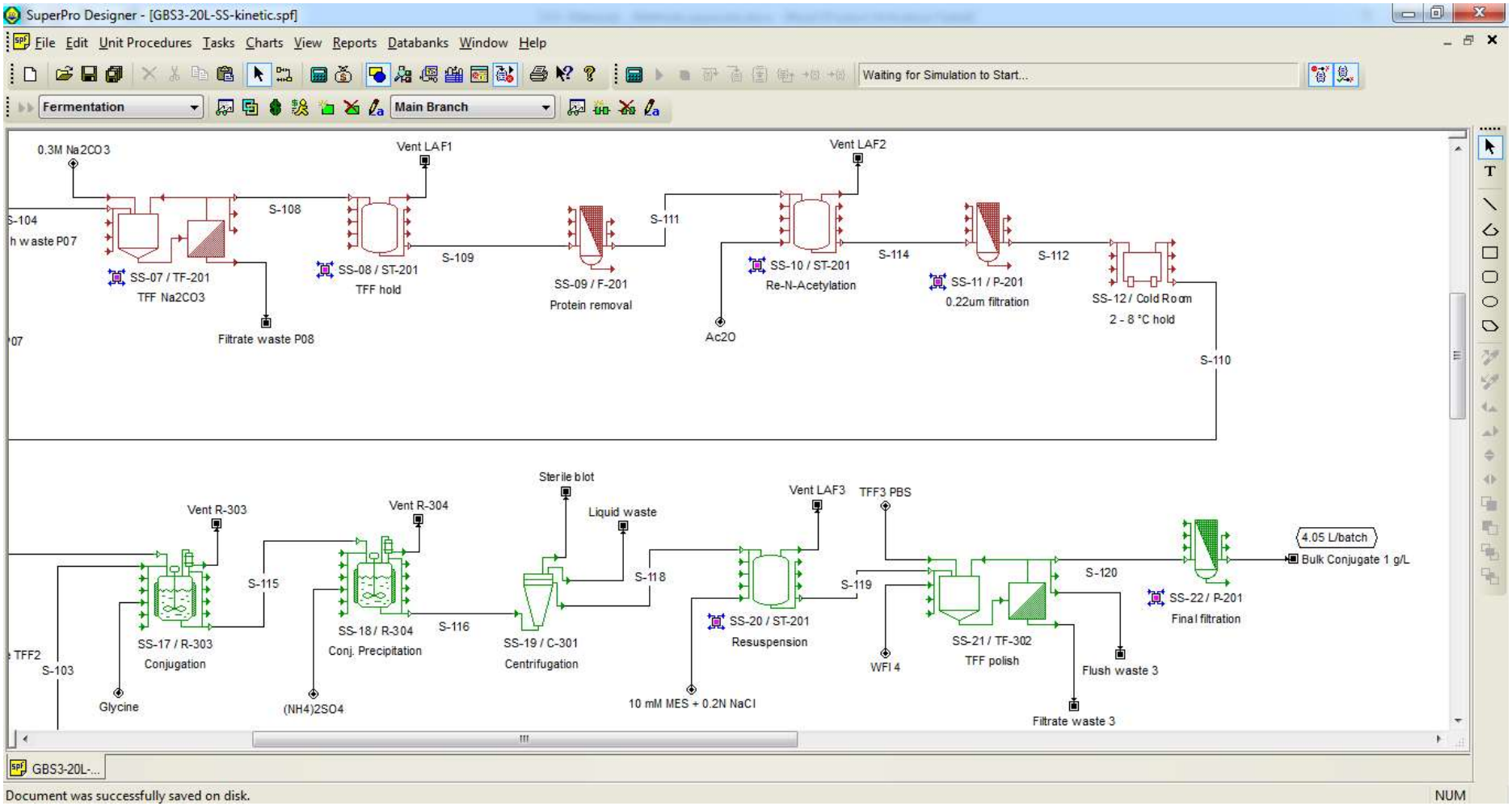
SuperPro Designer - [GBS3-20L-SS-kinetic.spf]
File Edit Unit Procedures Tasks Charts View Reports Databanks Window Help
Waiting for Simulation to Start...
Fermentation
Main Branch
0.3M Na2CO3
Vent LAF1
Vent LAF2
S-104
h waste P07
S-108
S-109
S-111
S-114
S-112
S-110
SS-07 / TF-201
TFF Na2CO3
Filtrate waste P08
SS-08 / ST-201
TFF hold
SS-09 / F-201
Protein removal
Ac2O
SS-10 / ST-201
Re-N-Acetylation
SS-11 / P-201
0.22um filtration
SS-12 / Cold Room
2 - 8 °C hold
Vent R-303
Vent R-304
Sterile blot
Liquid waste
Vent LAF3
TFF3 PBS
S-115
S-116
S-118
S-119
S-120
4.05 L/batch
Bulk Conjugate 1 g/L
SS-17 / R-303
Conjugation
SS-18 / R-304
Conj. Precipitation
SS-19 / C-301
Centrifugation
SS-20 / ST-201
Resuspension
SS-21 / TF-302
TFF polish
SS-22 / P-201
Final filtration
TFF2
S-103
Glycine
(NH4)2SO4
10 mM MES + 0.2N NaCl
WFI 4
Flush waste 3
Filtrate waste 3
GBS3-20L-...
Document was successfully saved on disk.
NUM

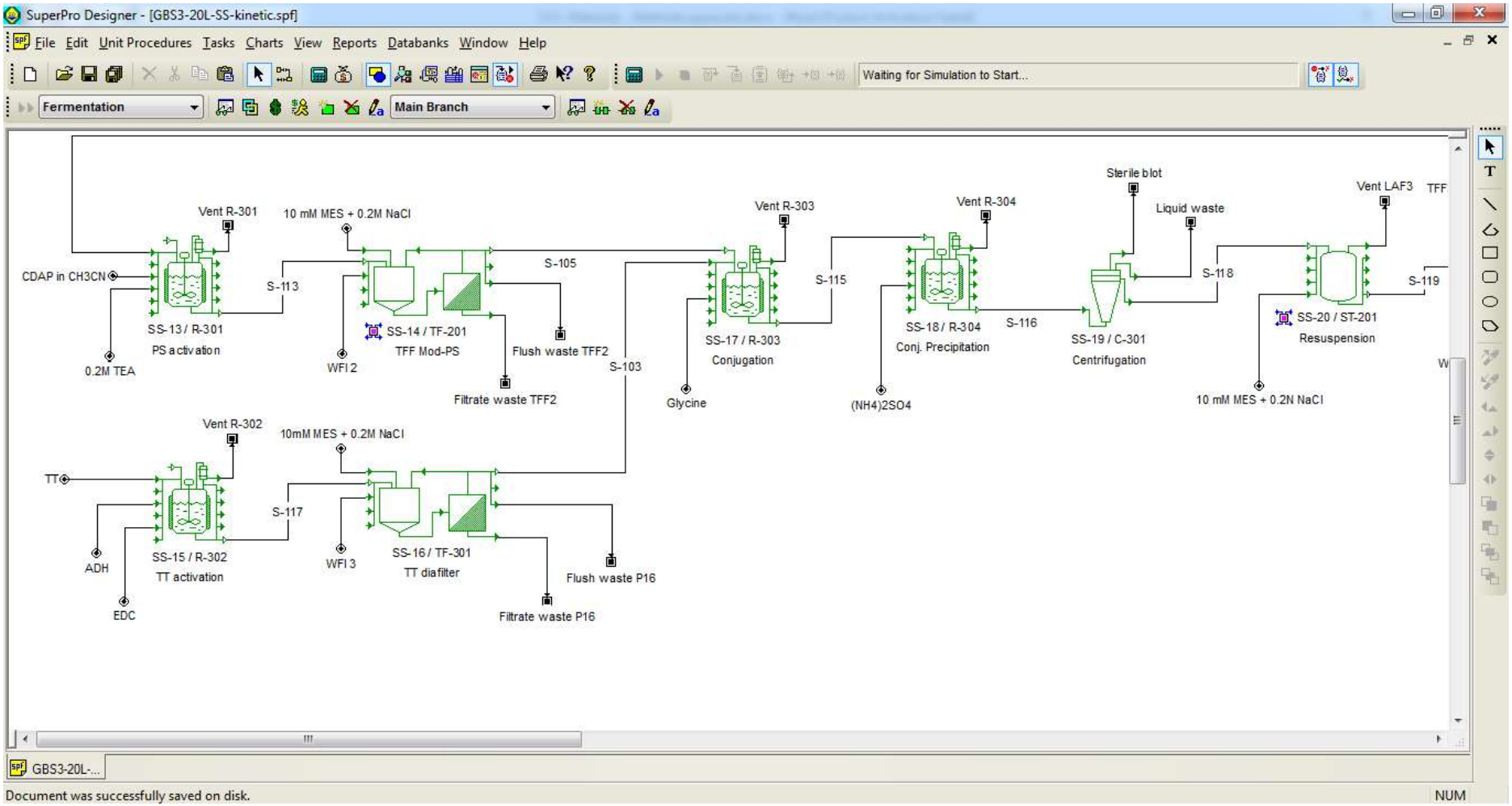
SuperPro Designer - [GBS3-20L-SS-kinetic.spf]
File Edit Unit Procedures Tasks Charts View Reports Databanks Window Help
Waiting for Simulation to Start...
Fermentation
Main Branch
Vent R-301
10 mM MES + 0.2M NaCl
Vent R-303
Vent R-304
Sterile blot
Liquid waste
Vent LAF3
TFF
CDAP in CH3CN
S-113
S-105
S-115
S-118
S-119
SS-13 / R-301
PS activation
0.2M TEA
SS-14 / TF-201
TFF Mod-PS
WFI 2
Flush waste TFF2
Filtrate waste TFF2
S-103
SS-17 / R-303
Conjugation
Glycine
SS-18 / R-304
Conj. Precipitation
(NH4)2SO4
S-116
SS-19 / C-301
Centrifugation
SS-20 / ST-201
Resuspension
10 mM MES + 0.2N NaCl
Vent R-302
10mM MES + 0.2M NaCl
TT
S-117
ADH
SS-15 / R-302
TT activation
EDC
WFI 3
SS-16 / TF-301
TT diafilter
Flush waste P16
Filtrate waste P16
GBS3-20L-...
Document was successfully saved on disk.
NUM

A.12.2 20L Single Use technology process model screenshots

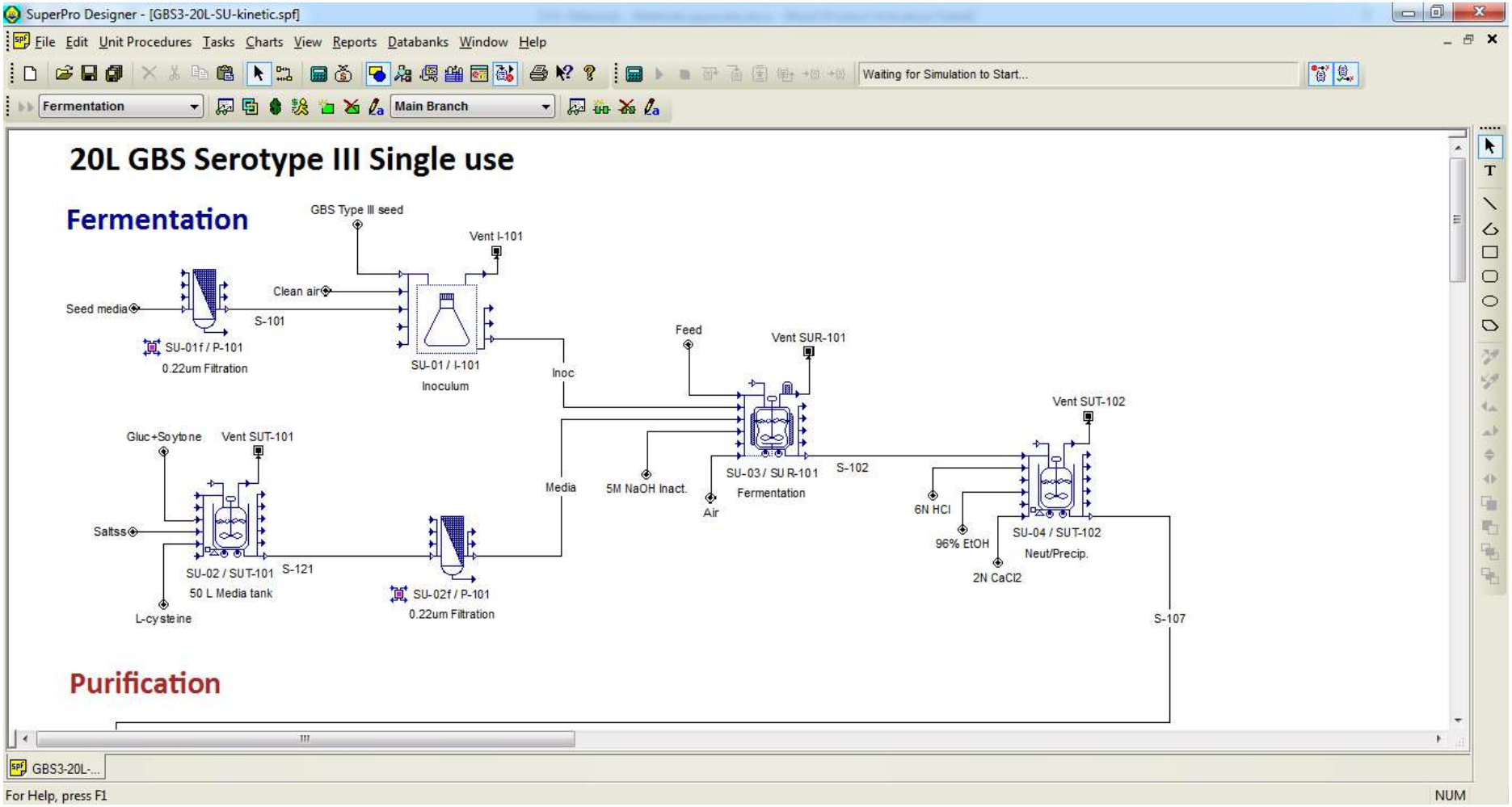

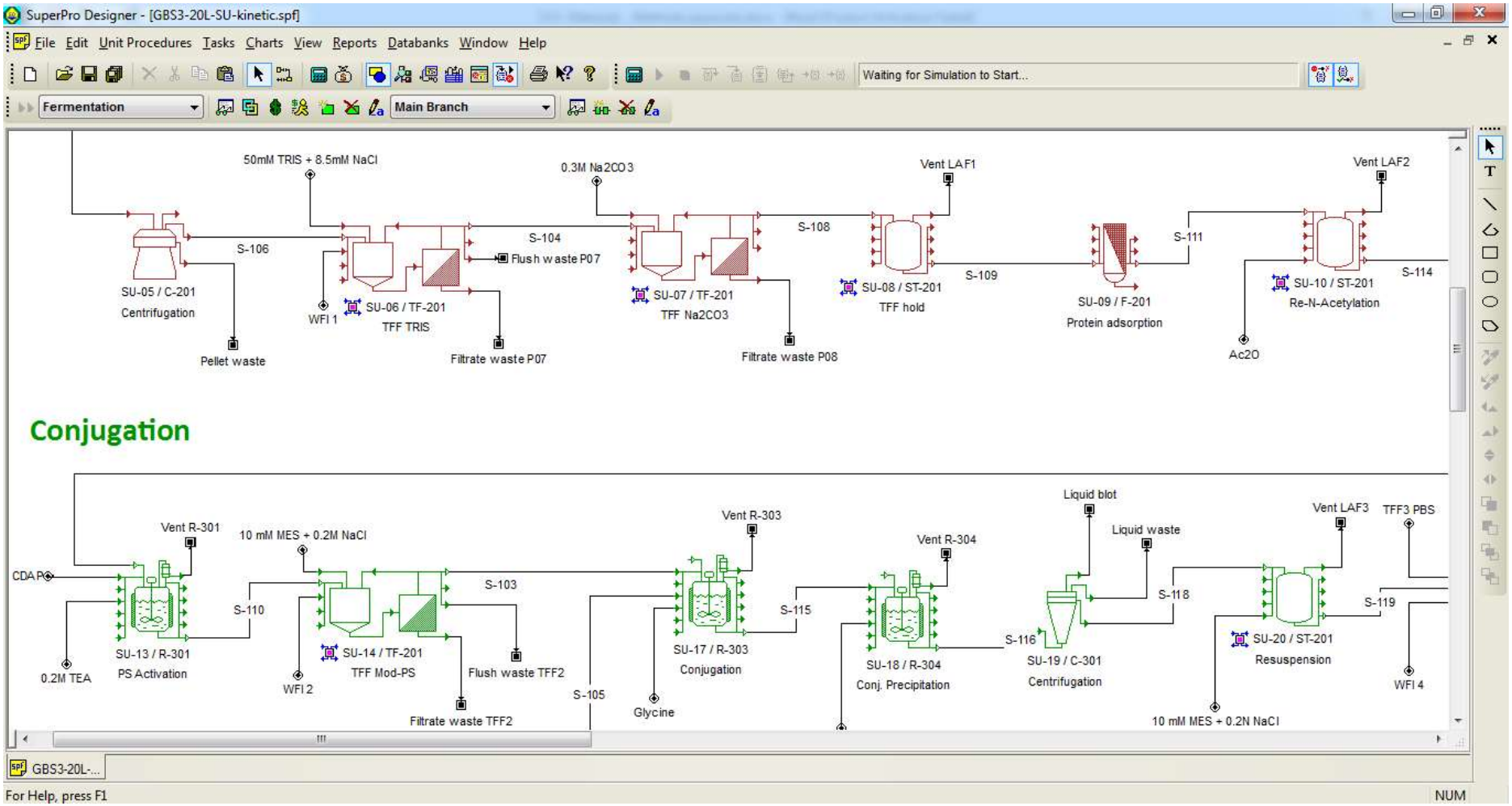
SuperPro Designer - [GBS3-20L-SU-kinetic.spf]
File Edit Unit Procedures Tasks Charts View Reports Databanks Window Help
Waiting for Simulation to Start...
Fermentation
Main Branch
50mM TRIS + 8.5mM NaCl
0.3M Na2CO3
Vent LAF1
Vent LAF2
S-106
S-104
S-108
S-109
S-111
S-114
Flush waste P07
SU-05 / C-201
Centrifugation
Pellet waste
WFI 1
SU-06 / TF-201
TFF TRIS
Filtrate waste P07
SU-07 / TF-201
TFF Na2CO3
Filtrate waste P08
SU-08 / ST-201
TFF hold
SU-09 / F-201
Protein adsorption
Ac2O
SU-10 / ST-201
Re-N-Acetylation
Conjugation
Vent R-301
10 mM MES + 0.2M NaCl
Vent R-303
Vent R-304
Liquid blot
Liquid waste
Vent LAF3
TFF3 PBS
CDAP
S-110
S-103
S-115
S-116
S-118
S-119
SU-13 / R-301
PS Activation
0.2M TEA
WFI 2
SU-14 / TF-201
TFF Mod-PS
Flush waste TFF2
Filtrate waste TFF2
S-105
Glycine
SU-17 / R-303
Conjugation
SU-18 / R-304
Conj. Precipitation
SU-19 / C-301
Centrifugation
SU-20 / ST-201
Resuspension
10 mM MES + 0.2N NaCl
WFI 4
GBS3-20L-...
For Help, press F1
NUM

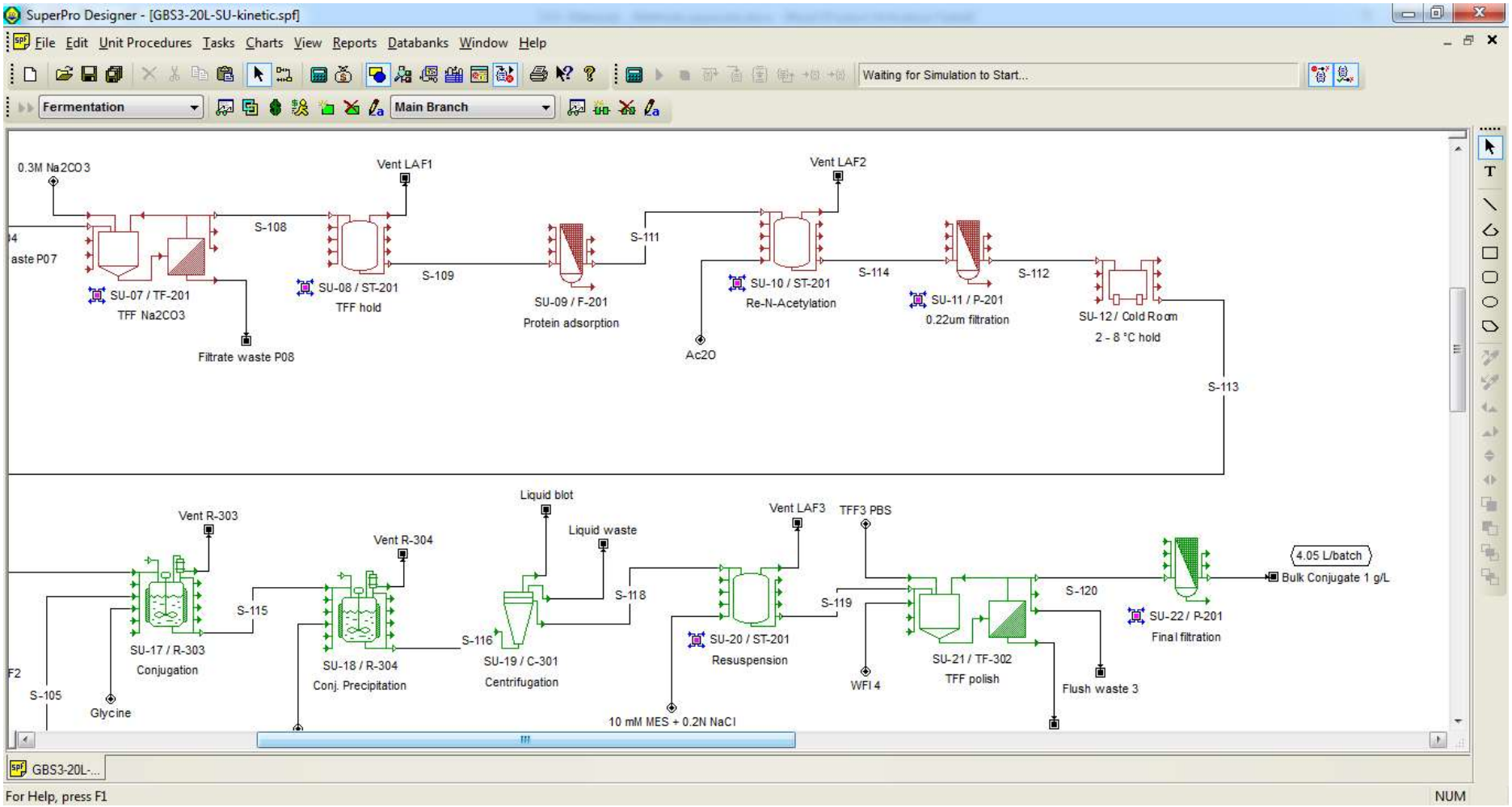
SuperPro Designer - [GBS3-20L-SU-kinetic.spf]
File Edit Unit Procedures Tasks Charts View Reports Databanks Window Help
Waiting for Simulation to Start...
Fermentation
Main Branch
0.3M Na2CO3
Vent LAF1
Vent LAF2
S-108
S-109
S-111
S-112
S-113
S-114
aste P07
SU-07 / TF-201
TFF Na2CO3
Filtrate waste P08
SU-08 / ST-201
TFF hold
SU-09 / F-201
Protein adsorption
Ac2O
SU-10 / ST-201
Re-N-Acetylation
SU-11 / P-201
0.22um filtration
SU-12 / Cold Room
2 - 8 °C hold
Liquid blot
Liquid waste
Vent LAF3
TFF3 PBS
Vent R-303
Vent R-304
S-115
S-116
S-118
S-119
S-120
4.05 L/batch
Bulk Conjugate 1 g/L
SU-17 / R-303
Conjugation
SU-18 / R-304
Conj. Precipitation
SU-19 / C-301
Centrifugation
SU-20 / ST-201
Resuspension
SU-21 / TF-302
TFF polish
SU-22 / P-201
Final filtration
F2
S-105
Glycine
WFI 4
Flush waste 3
10 mM MES + 0.2N NaCl
GBS3-20L-...
For Help, press F1
NUM

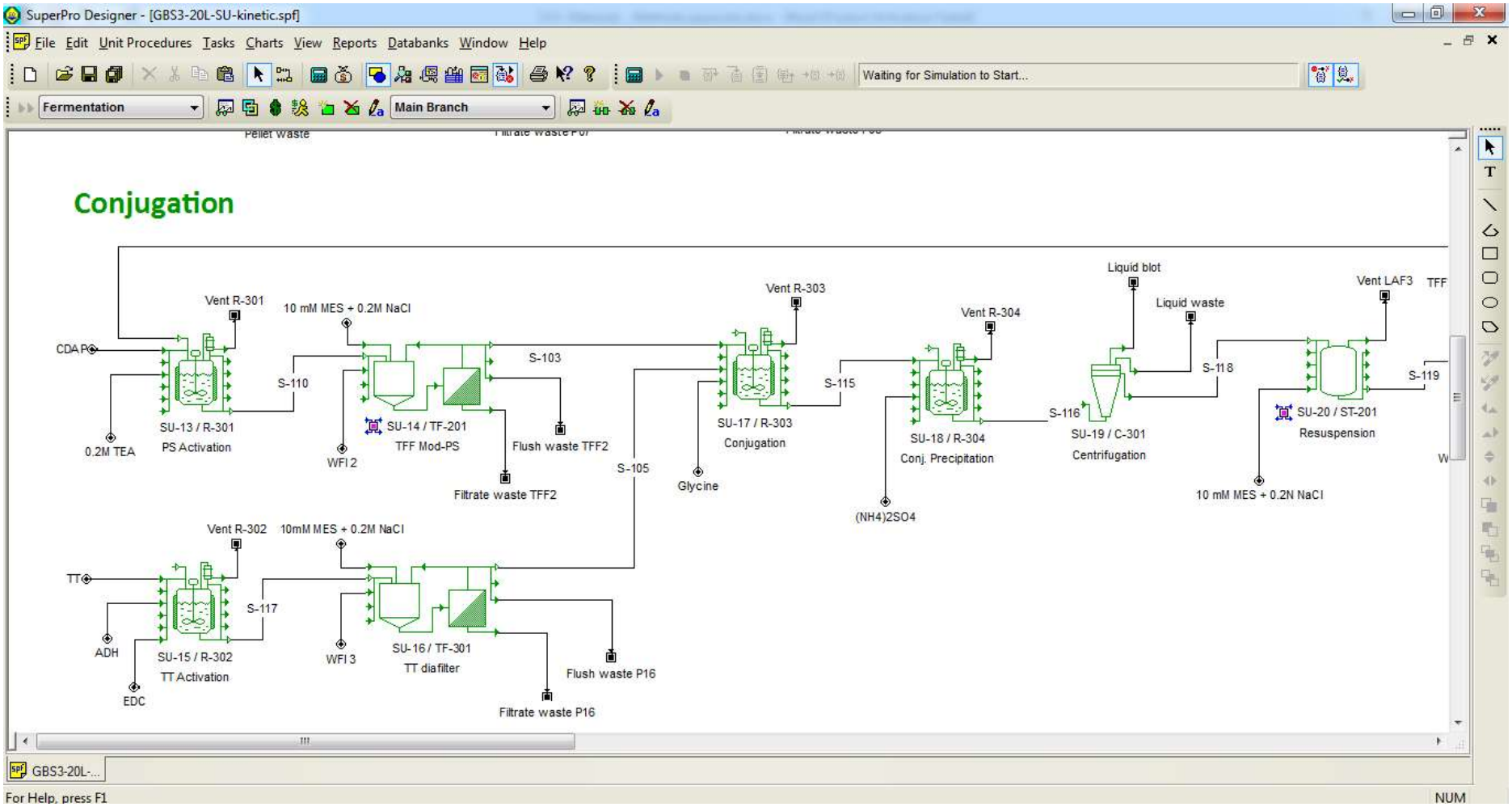
SuperPro Designer - [GBS3-20L-SU-kinetic.spf]
File Edit Unit Procedures Tasks Charts View Reports Databanks Window Help
Waiting for Simulation to Start...
Fermentation
Main Branch
Conjugation
Vent R-301
10 mM MES + 0.2M NaCl
CDAP
S-110
S-103
SU-13 / R-301
PS Activation
SU-14 / TF-201
TFF Mod-PS
0.2M TEA
WFI 2
Flush waste TFF2
Filtrate waste TFF2
Vent R-303
S-115
SU-17 / R-303
Conjugation
S-105
Glycine
Vent R-304
SU-18 / R-304
Conj. Precipitation
(NH4)2SO4
Liquid blot
Liquid waste
S-116
S-118
SU-19 / C-301
Centrifugation
Vent LAF3
TFF
S-119
SU-20 / ST-201
Resuspension
10 mM MES + 0.2N NaCl
Vent R-302
10mM MES + 0.2M NaCl
TT
S-117
ADH
SU-15 / R-302
TT Activation
EDC
WFI 3
SU-16 / TF-301
TT diafilter
Flush waste P16
Filtrate waste P16
GBS3-20L-...
For Help, press F1
NUM

A.12.3 20L Hybrid technology process model screenshots

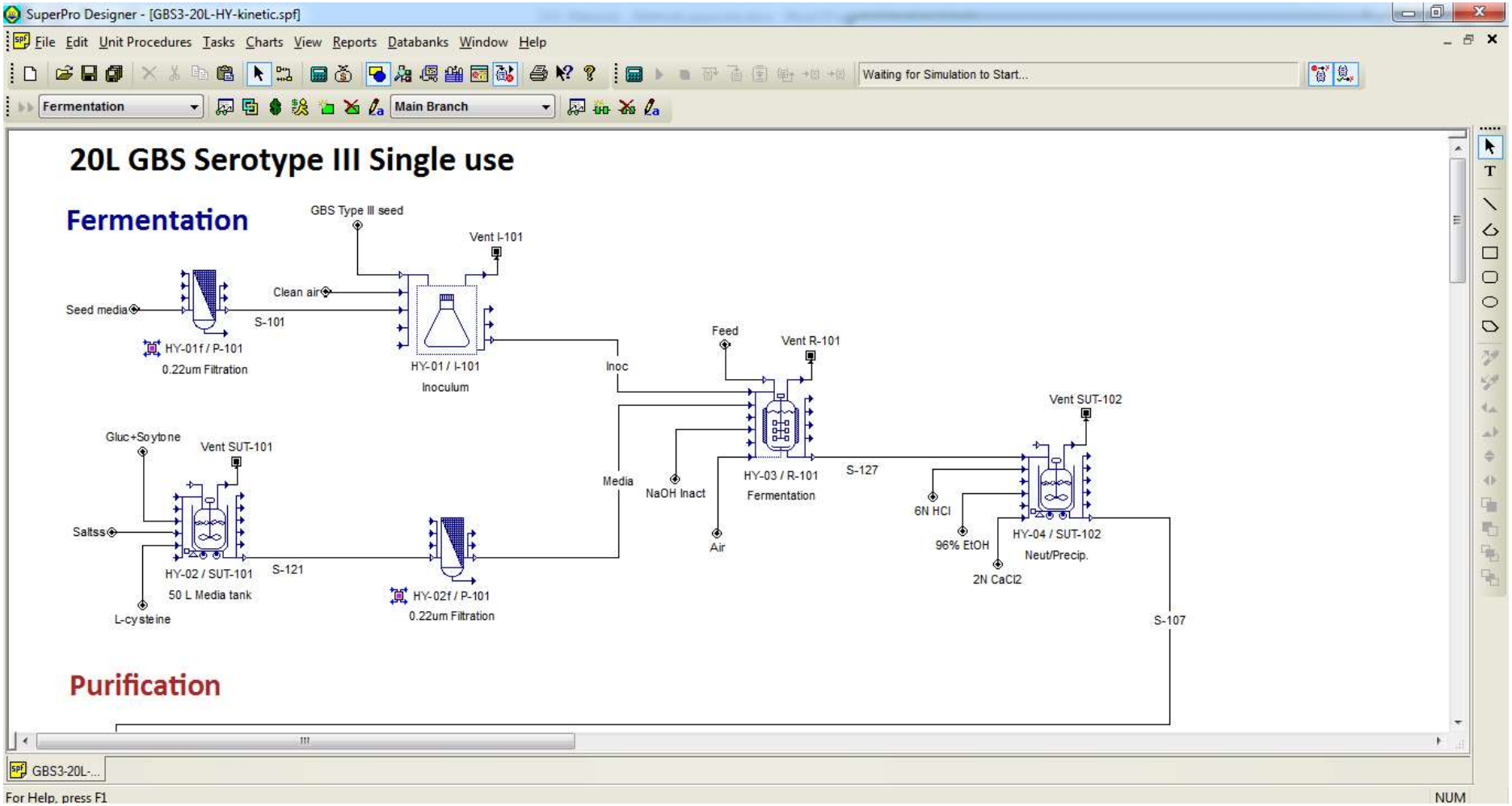

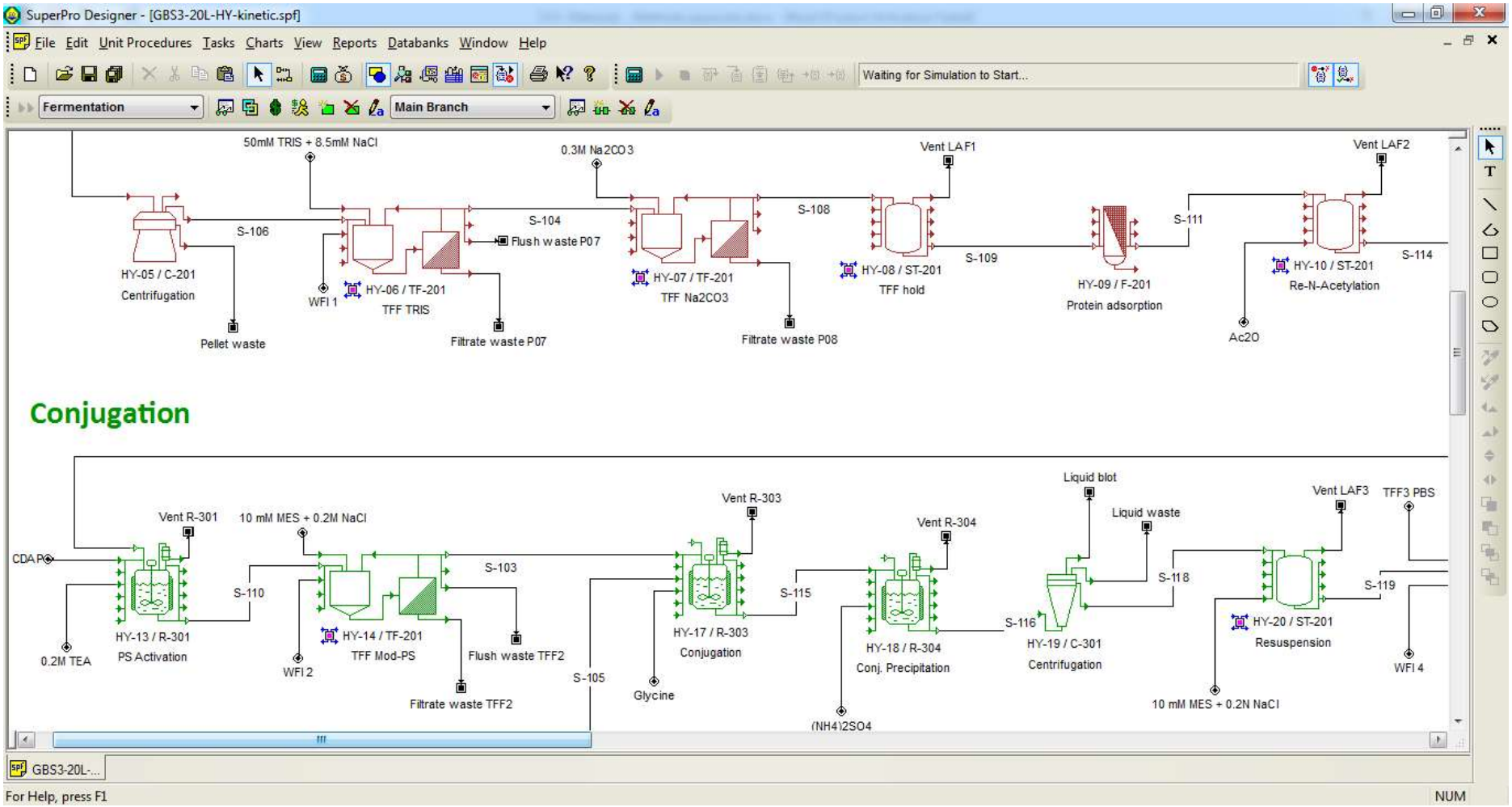
SuperPro Designer - [GBS3-20L-HY-kinetic.spf]
File Edit Unit Procedures Tasks Charts View Reports Databanks Window Help
Waiting for Simulation to Start...
Fermentation
Main Branch
50mM TRIS + 8.5mM NaCl
0.3M Na2CO3
Vent LAF1
Vent LAF2
S-106
S-104
S-108
S-109
S-111
S-114
Flush waste P07
HY-05 / C-201
Centrifugation
Pellet waste
WFI 1
HY-06 / TF-201
TFF TRIS
Filtrate waste P07
HY-07 / TF-201
TFF Na2CO3
Filtrate waste P08
HY-08 / ST-201
TFF hold
HY-09 / F-201
Protein adsorption
HY-10 / ST-201
Re-N-Acetylation
Ac2O
Conjugation
Vent R-301
10 mM MES + 0.2M NaCl
Vent R-303
Vent R-304
Liquid blot
Liquid waste
Vent LAF3
TFF3 PBS
CDAP
S-110
S-103
S-115
S-116
S-118
S-119
S-105
0.2M TEA
HY-13 / R-301
PS Activation
WFI 2
HY-14 / TF-201
TFF Mod-PS
Flush waste TFF2
Filtrate waste TFF2
HY-17 / R-303
Conjugation
Glycine
HY-18 / R-304
Conj. Precipitation
(NH4)2SO4
HY-19 / C-301
Centrifugation
HY-20 / ST-201
Resuspension
10 mM MES + 0.2N NaCl
WFI 4
GBS3-20L-...
For Help, press F1
NUM

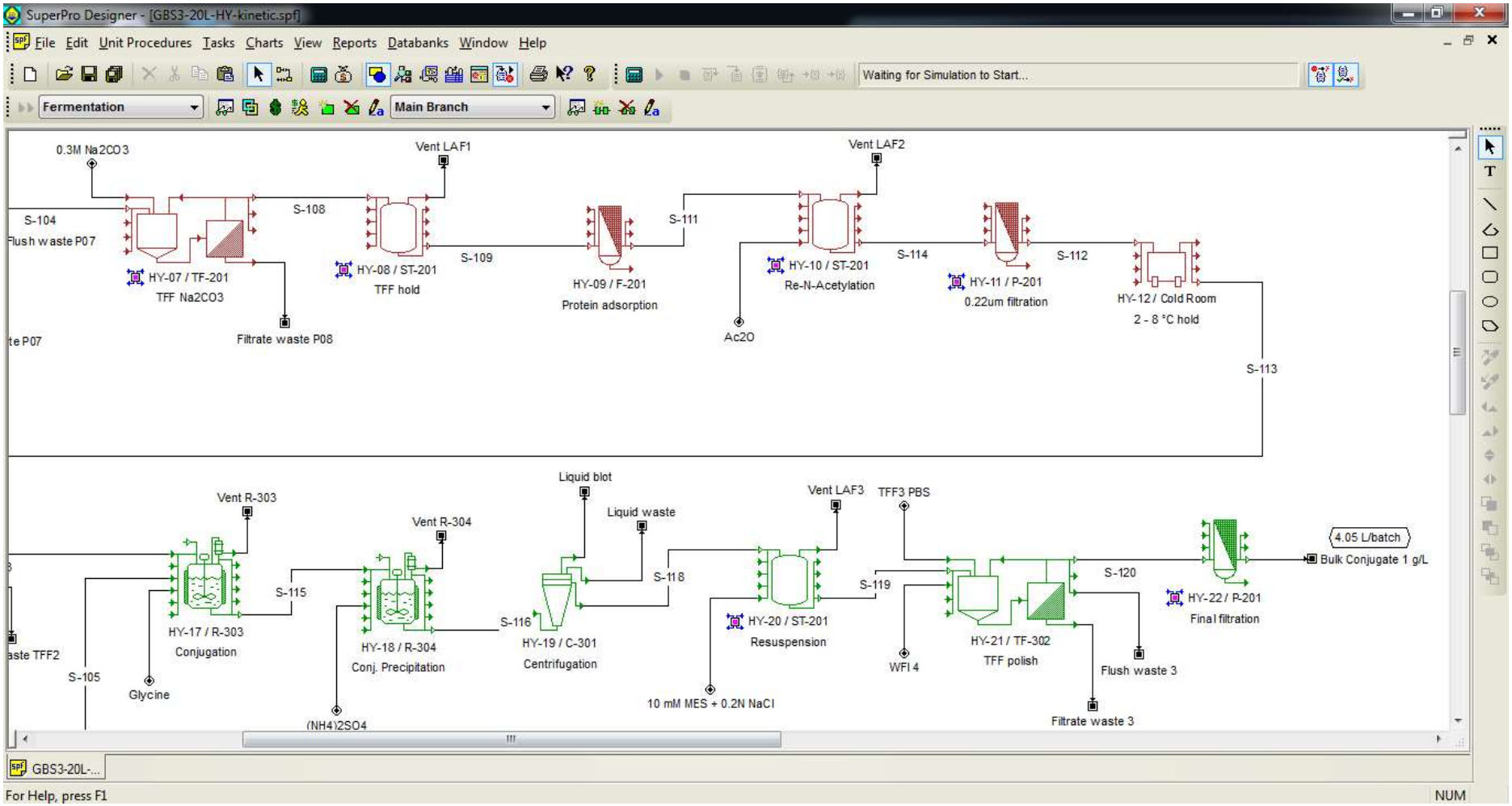
SuperPro Designer - [GBS3-20L-HY-kinetic.spf]
File Edit Unit Procedures Tasks Charts View Reports Databanks Window Help
Waiting for Simulation to Start...
Fermentation
Main Branch
0.3M Na2CO3
S-104
Flush waste P07
HY-07 / TF-201
TFF Na2CO3
Filtrate waste P08
Vent LAF1
S-108
HY-08 / ST-201
TFF hold
S-109
HY-09 / F-201
Protein adsorption
S-111
Ac2O
Vent LAF2
HY-10 / ST-201
Re-N-Acetylation
S-114
HY-11 / P-201
0.22um filtration
S-112
HY-12 / Cold Room
2 - 8 °C hold
S-113
Vent R-303
HY-17 / R-303
Conjugation
S-115
Vent R-304
HY-18 / R-304
Conj. Precipitation
(NH4)2SO4
S-105
Glycine
Liquid blot
Liquid waste
S-116
HY-19 / C-301
Centrifugation
S-118
Vent LAF3
HY-20 / ST-201
Resuspension
10 mM MES + 0.2N NaCl
TFF3 PBS
S-119
WFI 4
HY-21 / TF-302
TFF polish
S-120
Flush waste 3
Filtrate waste 3
HY-22 / P-201
Final filtration
4.05 L/batch
Bulk Conjugate 1 g/L
GBS3-20L-...
For Help, press F1
NUM

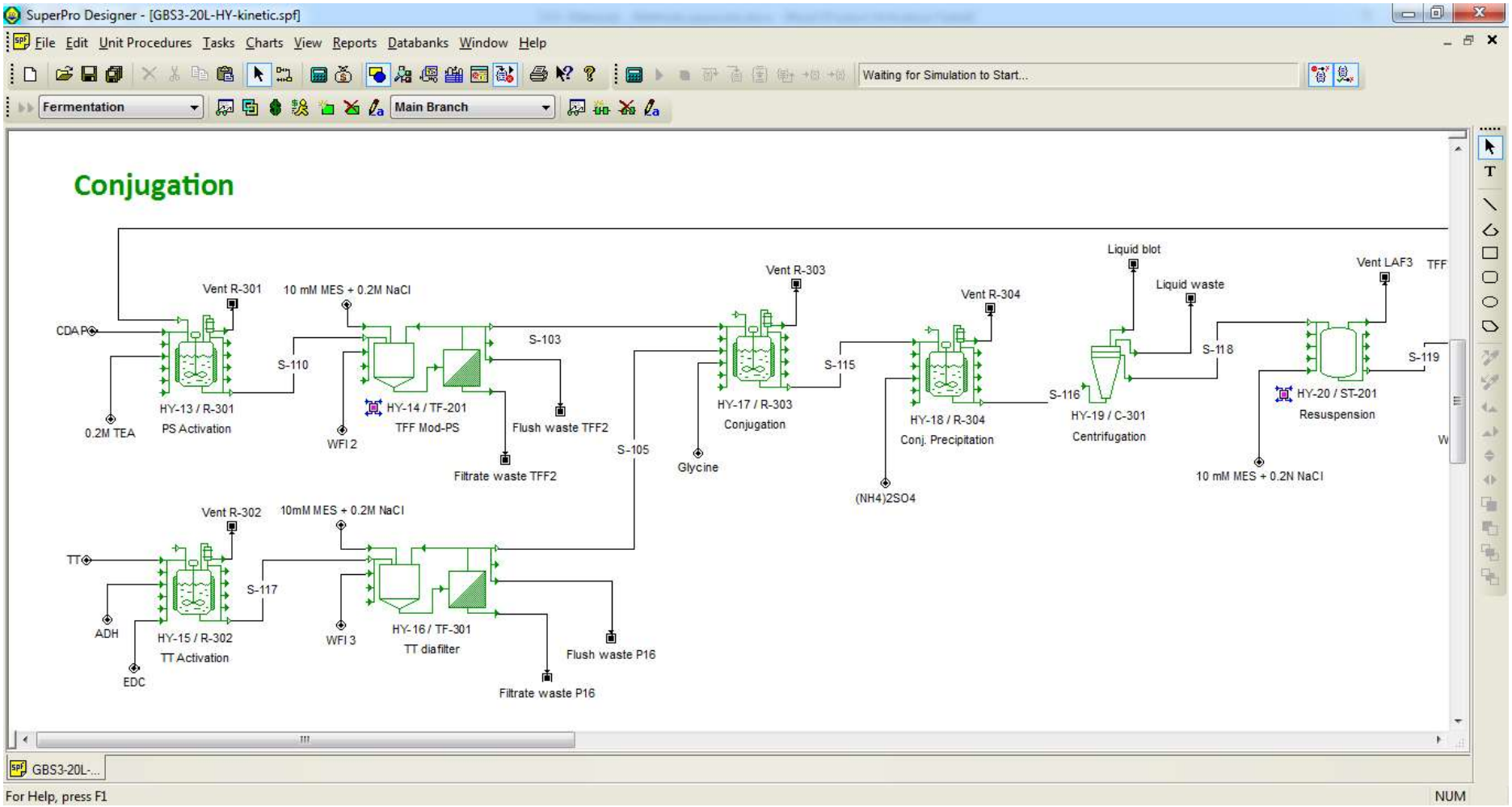
SuperPro Designer - [GBS3-20L-HY-kinetic.spf]
File Edit Unit Procedures Tasks Charts View Reports Databanks Window Help
Waiting for Simulation to Start...
Fermentation
Main Branch
Conjugation
Vent R-301
10 mM MES + 0.2M NaCl
CDAP
S-110
S-103
HY-13 / R-301
PS Activation
HY-14 / TF-201
TFF Mod-PS
0.2M TEA
WFI 2
Flush waste TFF2
Filtrate waste TFF2
Vent R-303
S-105
HY-17 / R-303
Conjugation
Glycine
S-115
Vent R-304
HY-18 / R-304
Conj. Precipitation
(NH4)2SO4
Liquid blot
Liquid waste
S-116
HY-19 / C-301
Centrifugation
S-118
Vent LAF3
TFF
S-119
HY-20 / ST-201
Resuspension
10 mM MES + 0.2N NaCl
Vent R-302
10mM MES + 0.2M NaCl
TT
S-117
ADH
HY-15 / R-302
TT Activation
EDC
WFI 3
HY-16 / TF-301
TT diafilter
Flush waste P16
Filtrate waste P16
GBS3-20L-...
For Help, press F1
NUM

A.12.4 200L Stainless steel technology process model screenshots

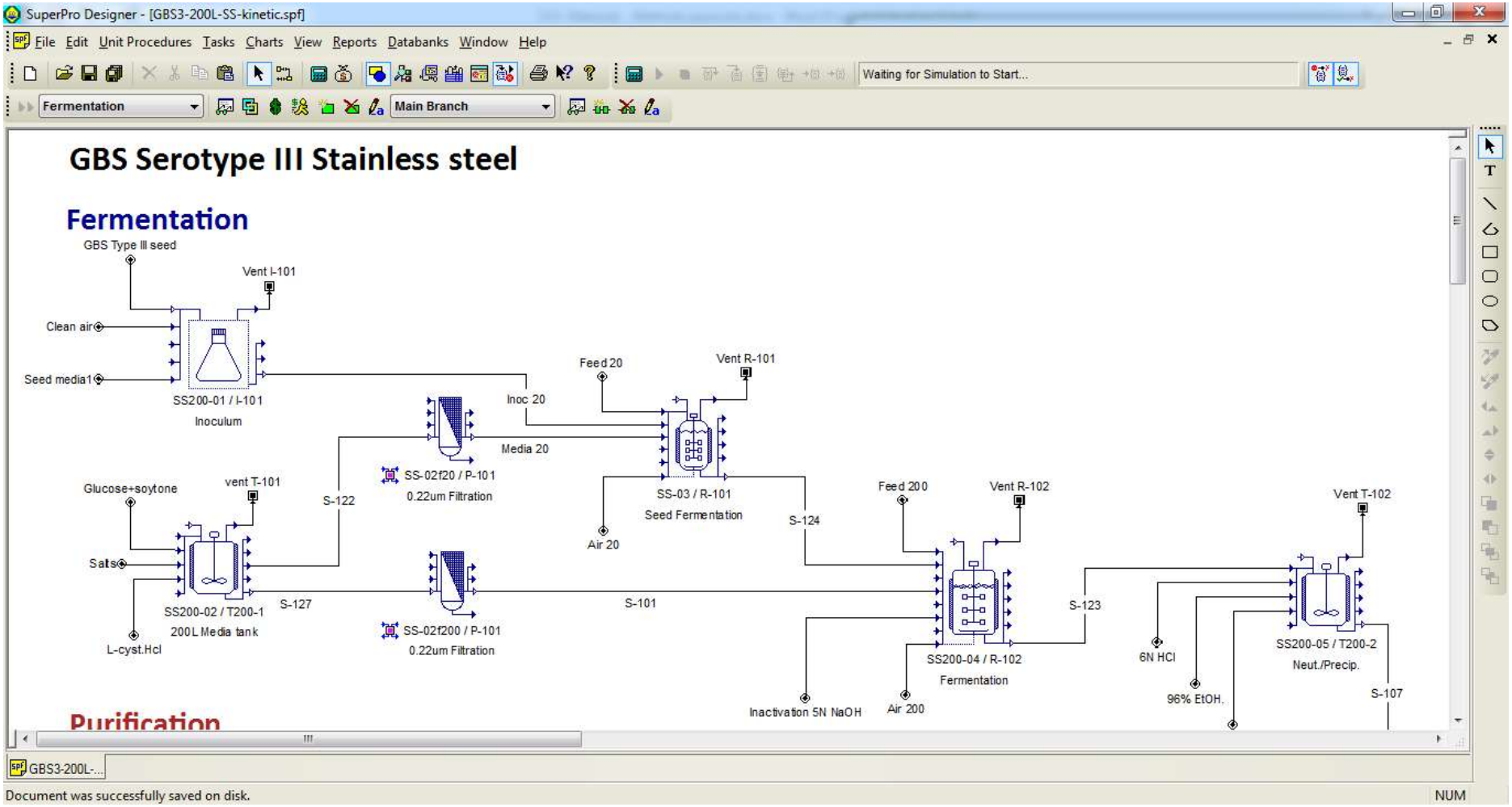

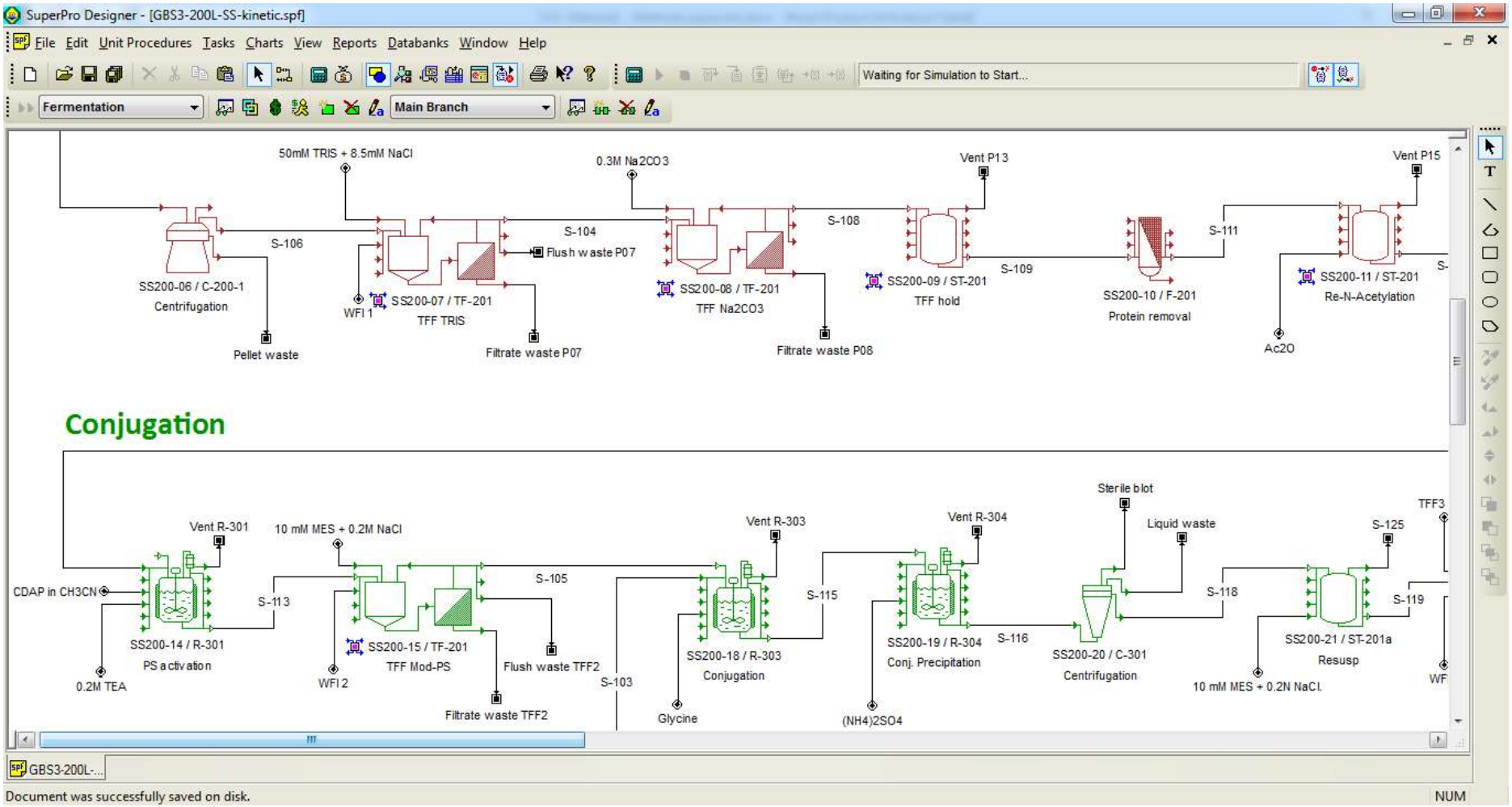
SuperPro Designer - [GBS3-200L-SS-kinetic.spf]
File Edit Unit Procedures Tasks Charts View Reports Databanks Window Help
Waiting for Simulation to Start...
Fermentation
Main Branch
50mM TRIS + 8.5mM NaCl
0.3M Na2CO3
Vent P13
Vent P15
S-106
S-104
S-108
S-109
S-111
Flush waste P07
SS200-06 / C-200-1
Centrifugation
Pellet waste
WFI 1
SS200-07 / TF-201
TFF TRIS
Filtrate waste P07
SS200-08 / TF-201
TFF Na2CO3
Filtrate waste P08
SS200-09 / ST-201
TFF hold
SS200-10 / F-201
Protein removal
SS200-11 / ST-201
Re-N-Acetylation
Ac2O
Conjugation
Vent R-301
10 mM MES + 0.2M NaCl
Vent R-303
Vent R-304
Sterile blot
Liquid waste
TFF3
S-125
CDAP in CH3CN
S-113
S-105
S-115
S-116
S-118
S-119
SS200-14 / R-301
PS activation
0.2M TEA
SS200-15 / TF-201
TFF Mod-PS
WFI 2
Flush waste TFF2
Filtrate waste TFF2
S-103
SS200-18 / R-303
Conjugation
Glycine
SS200-19 / R-304
Conj. Precipitation
(NH4)2SO4
SS200-20 / C-301
Centrifugation
SS200-21 / ST-201a
Resusp
10 mM MES + 0.2N NaCl
WF
GBS3-200L-...
Document was successfully saved on disk.
NUM

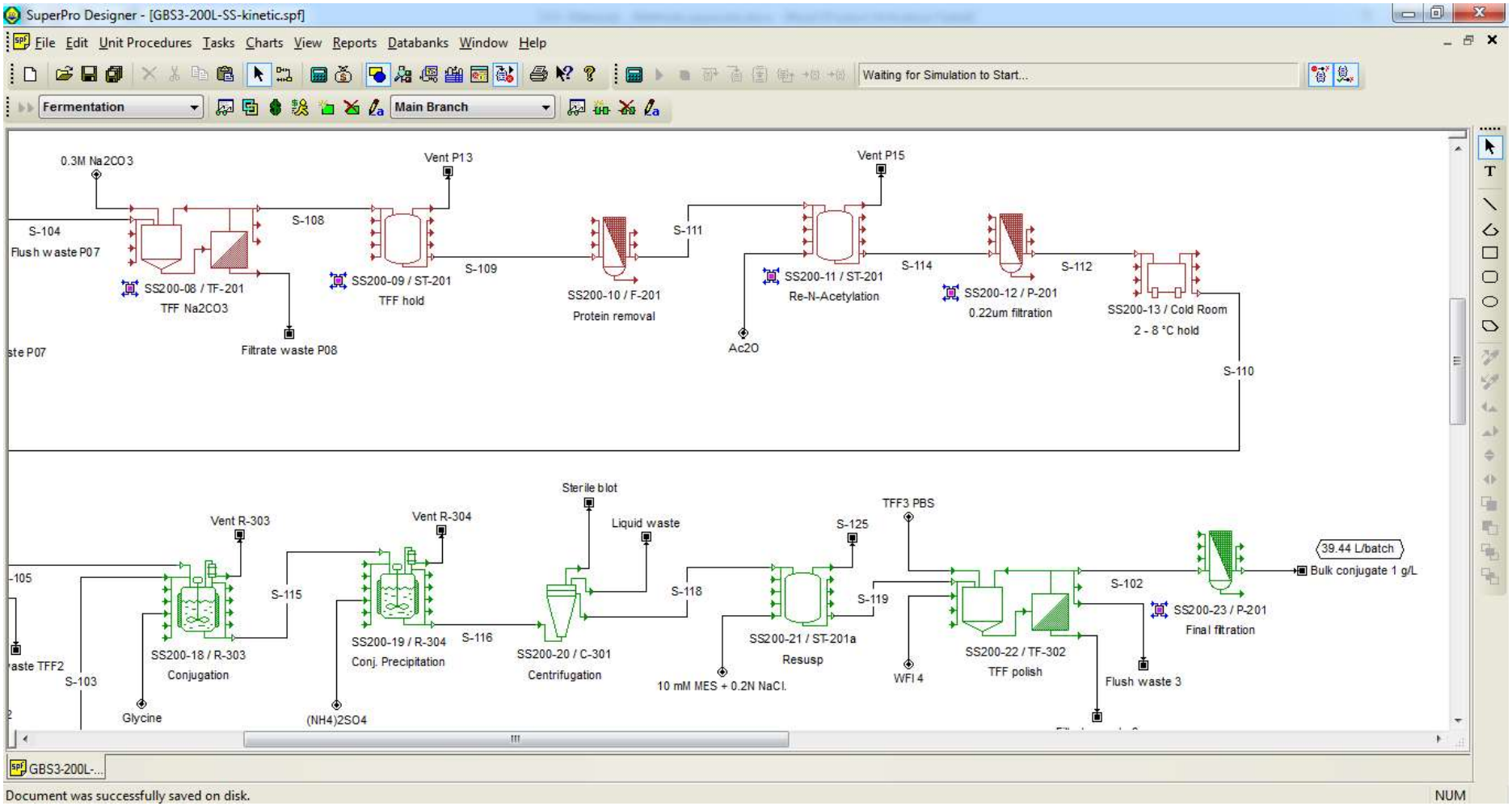
SuperPro Designer - [GBS3-200L-SS-kinetic.spf]
File Edit Unit Procedures Tasks Charts View Reports Databanks Window Help
Waiting for Simulation to Start...
Fermentation
Main Branch
0.3M Na2CO3
Vent P13
Vent P15
S-104
Flush waste P07
S-108
S-109
S-111
S-114
S-112
SS200-08 / TF-201
TFF Na2CO3
SS200-09 / ST-201
TFF hold
SS200-10 / F-201
Protein removal
SS200-11 / ST-201
Re-N-Acetylation
SS200-12 / P-201
0.22um filtration
SS200-13 / Cold Room
2 - 8 °C hold
Filtrate waste P08
Ac2O
S-110
Sterile blot
Liquid waste
TFF3 PBS
Vent R-303
Vent R-304
S-125
39.44 L/batch
Bulk conjugate 1 g/L
S-115
S-116
S-118
S-119
S-102
SS200-18 / R-303
Conjugation
SS200-19 / R-304
Conj. Precipitation
SS200-20 / C-301
Centrifugation
SS200-21 / ST-201a
Resusp
SS200-22 / TF-302
TFF polish
SS200-23 / P-201
Final filtration
S-103
Glycine
(NH4)2SO4
10 mM MES + 0.2N NaCl.
WFI 4
Flush waste 3
GBS3-200L-...
Document was successfully saved on disk.
NUM

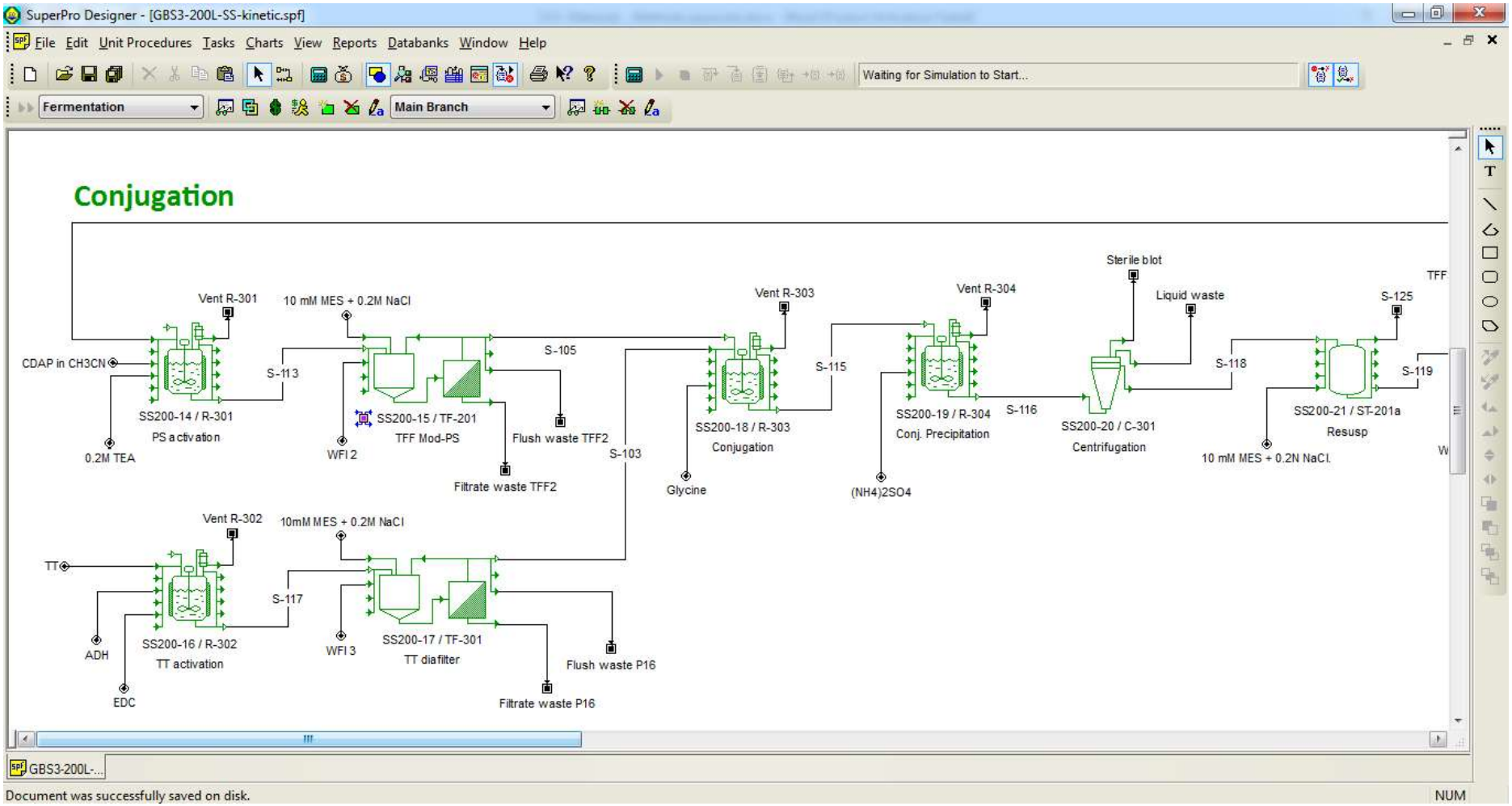
SuperPro Designer - [GBS3-200L-SS-kinetic.spf]
File Edit Unit Procedures Tasks Charts View Reports Databanks Window Help
Waiting for Simulation to Start...
Fermentation
Main Branch
Conjugation
Vent R-301
10 mM MES + 0.2M NaCl
CDAP in CH3CN
S-113
S-105
SS200-14 / R-301
PS activation
SS200-15 / TF-201
TFF Mod-PS
0.2M TEA
WFI 2
Flush waste TFF2
Filtrate waste TFF2
S-103
Vent R-303
SS200-18 / R-303
Conjugation
Glycine
S-115
Vent R-304
SS200-19 / R-304
Conj. Precipitation
(NH4)2SO4
S-116
Sterile blot
Liquid waste
SS200-20 / C-301
Centrifugation
S-118
S-125
S-119
TFF
SS200-21 / ST-201a
Resusp
10 mM MES + 0.2N NaCl
Vent R-302
10mM MES + 0.2M NaCl
TT
S-117
ADH
SS200-16 / R-302
TT activation
WFI 3
SS200-17 / TF-301
TT diafilter
Flush waste P16
EDC
Filtrate waste P16
GBS3-200L-...
Document was successfully saved on disk.
NUM

A.12.5 200L Single Use technology process model screenshots

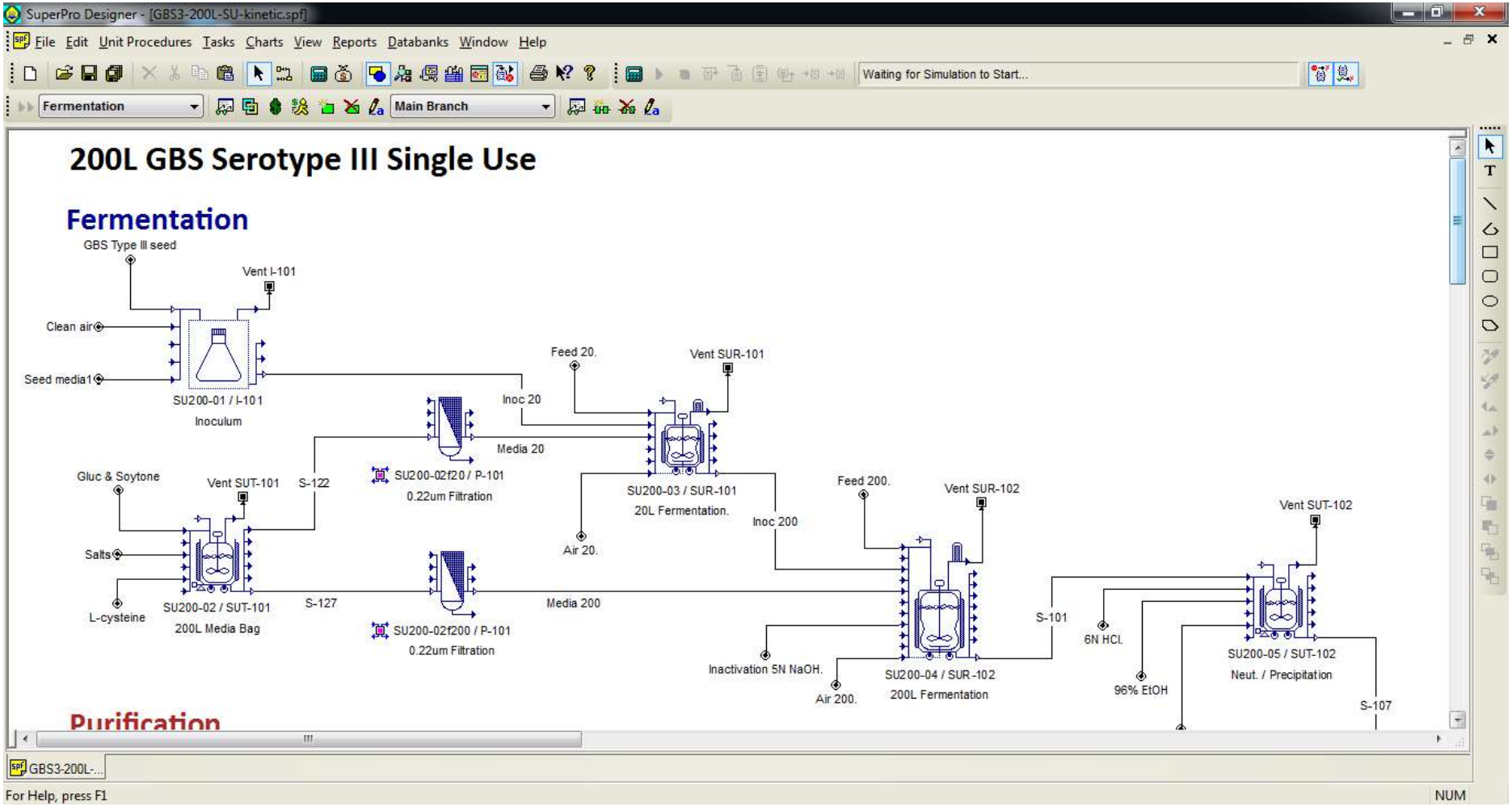

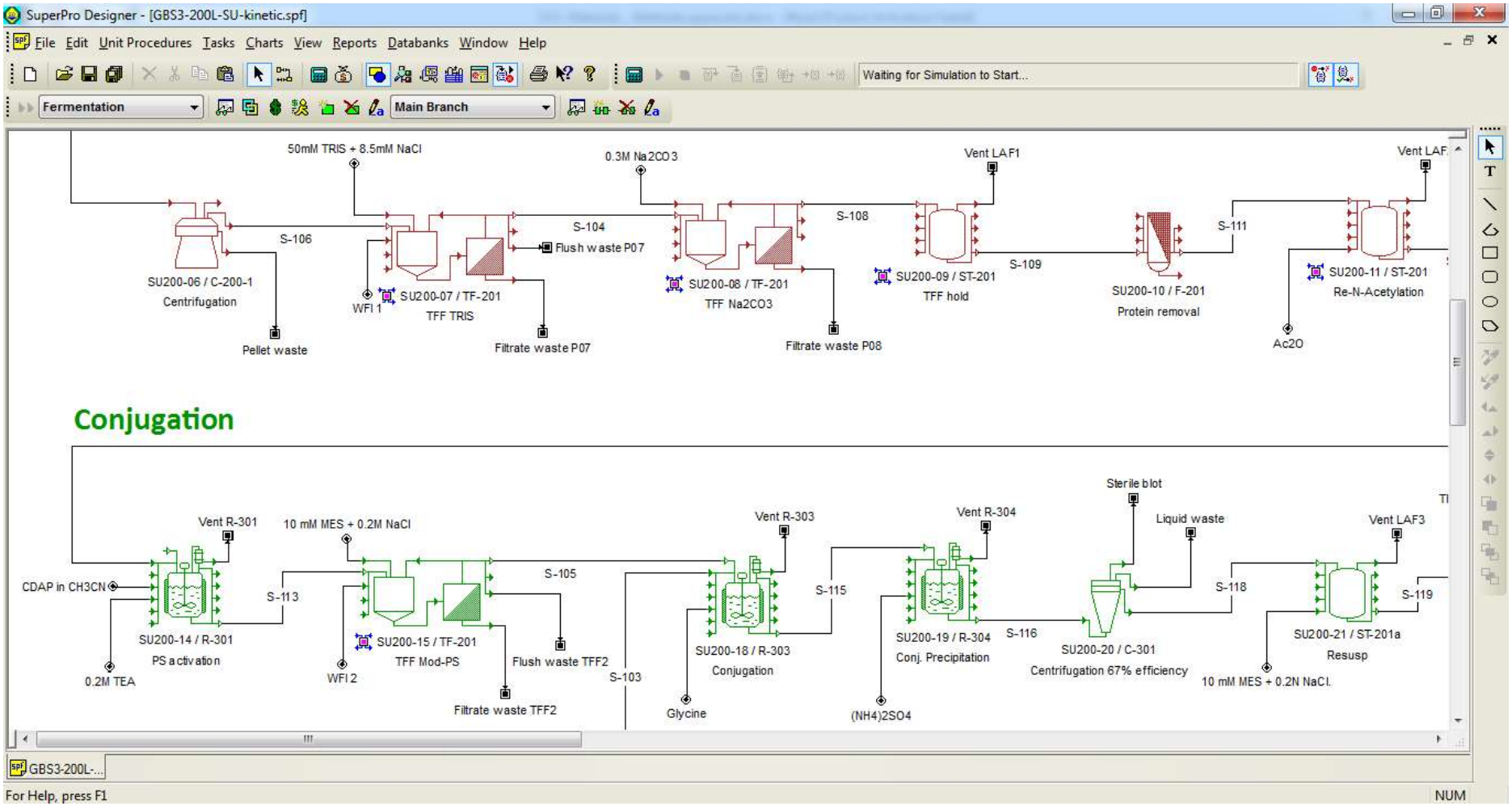
SuperPro Designer - [GBS3-200L-SU-kinetic.spf]
File Edit Unit Procedures Tasks Charts View Reports Databanks Window Help
Waiting for Simulation to Start...
Fermentation
Main Branch
50mM TRIS + 8.5mM NaCl
0.3M Na2CO3
Vent LAF1
S-106
S-104
S-108
S-109
S-111
Flush waste P07
SU200-06 / C-200-1
Centrifugation
Pellet waste
WFI 1
SU200-07 / TF-201
TFF TRIS
Filtrate waste P07
SU200-08 / TF-201
TFF Na2CO3
Filtrate waste P08
SU200-09 / ST-201
TFF hold
SU200-10 / F-201
Protein removal
SU200-11 / ST-201
Re-N-Acetylation
Ac2O
Conjugation
Vent R-301
10 mM MES + 0.2M NaCl
Vent R-303
Vent R-304
Sterile blot
Liquid waste
Vent LAF3
CDAP in CH3CN
S-113
S-105
S-115
S-116
S-118
S-119
SU200-14 / R-301
PS activation
0.2M TEA
WFI 2
SU200-15 / TF-201
TFF Mod-PS
Flush waste TFF2
Filtrate waste TFF2
S-103
SU200-18 / R-303
Conjugation
Glycine
SU200-19 / R-304
Conj. Precipitation
(NH4)2SO4
SU200-20 / C-301
Centrifugation 67% efficiency
SU200-21 / ST-201a
Resusp
10 mM MES + 0.2N NaCl
GBS3-200L-...
For Help, press F1
NUM

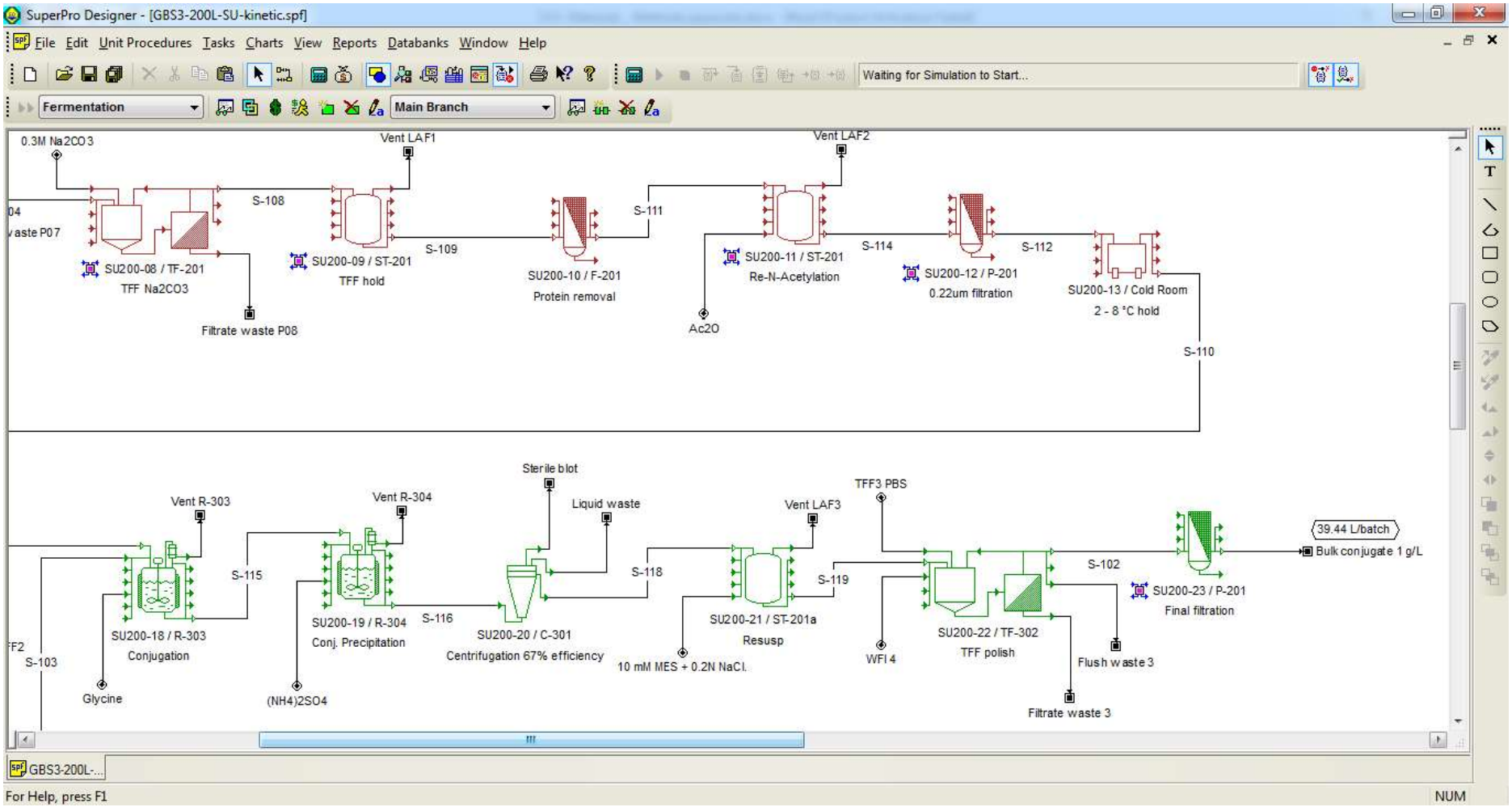
SuperPro Designer - [GBS3-200L-SU-kinetic.spf]
File Edit Unit Procedures Tasks Charts View Reports Databanks Window Help
Waiting for Simulation to Start...
Fermentation
Main Branch
0.3M Na2CO3
Vent LAF1
Vent LAF2
S-108
S-109
S-111
S-114
S-112
S-110
SU200-08 / TF-201
TFF Na2CO3
Filtrate waste P08
SU200-09 / ST-201
TFF hold
SU200-10 / F-201
Protein removal
Ac2O
SU200-11 / ST-201
Re-N-Acetylation
SU200-12 / P-201
0.22um filtration
SU200-13 / Cold Room
2 - 8 °C hold
Sterile blot
Liquid waste
TFF3 PBS
Vent R-303
Vent R-304
Vent LAF3
S-115
S-116
S-118
S-119
S-102
S-103
SU200-18 / R-303
Conjugation
Glycine
SU200-19 / R-304
Conj. Precipitation
(NH4)2SO4
SU200-20 / C-301
Centrifugation 67% efficiency
10 mM MES + 0.2N NaCl
SU200-21 / ST-201a
Resusp
WFI 4
SU200-22 / TF-302
TFF polish
Flush waste 3
Filtrate waste 3
SU200-23 / P-201
Final filtration
39.44 L/batch
Bulk conjugate 1 g/L
GBS3-200L-...
For Help, press F1
NUM

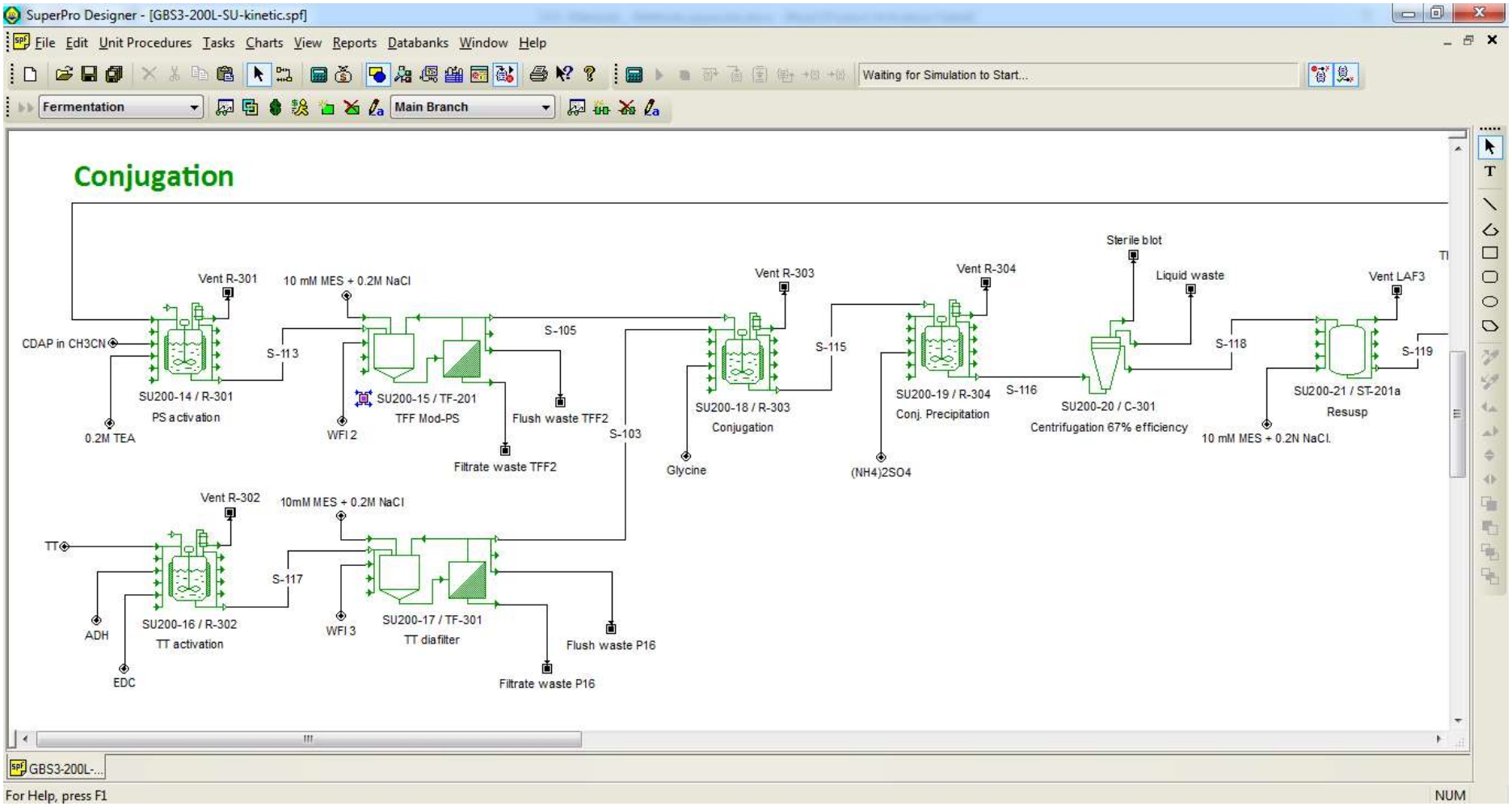
SuperPro Designer - [GBS3-200L-SU-kinetic.spf]
File Edit Unit Procedures Tasks Charts View Reports Databanks Window Help
Waiting for Simulation to Start...
Fermentation
Main Branch
Conjugation
Vent R-301
10 mM MES + 0.2M NaCl
CDAP in CH3CN
S-113
S-105
SU200-14 / R-301
PS activation
0.2M TEA
SU200-15 / TF-201
TFF Mod-PS
WFI 2
Flush waste TFF2
Filtrate waste TFF2
S-103
Vent R-303
SU200-18 / R-303
Conjugation
Glycine
S-115
Vent R-304
SU200-19 / R-304
Conj. Precipitation
(NH4)2SO4
S-116
Sterile blot
Liquid waste
SU200-20 / C-301
Centrifugation 67% efficiency
S-118
Vent LAF3
S-119
SU200-21 / ST-201a
Resusp
10 mM MES + 0.2N NaCl
Vent R-302
10mM MES + 0.2M NaCl
TT
S-117
ADH
SU200-16 / R-302
TT activation
EDC
WFI 3
SU200-17 / TF-301
TT diafilter
Flush waste P16
Filtrate waste P16
GBS3-200L-...
For Help, press F1
NUM

A.12.6 200L Hybrid technology process model screenshots

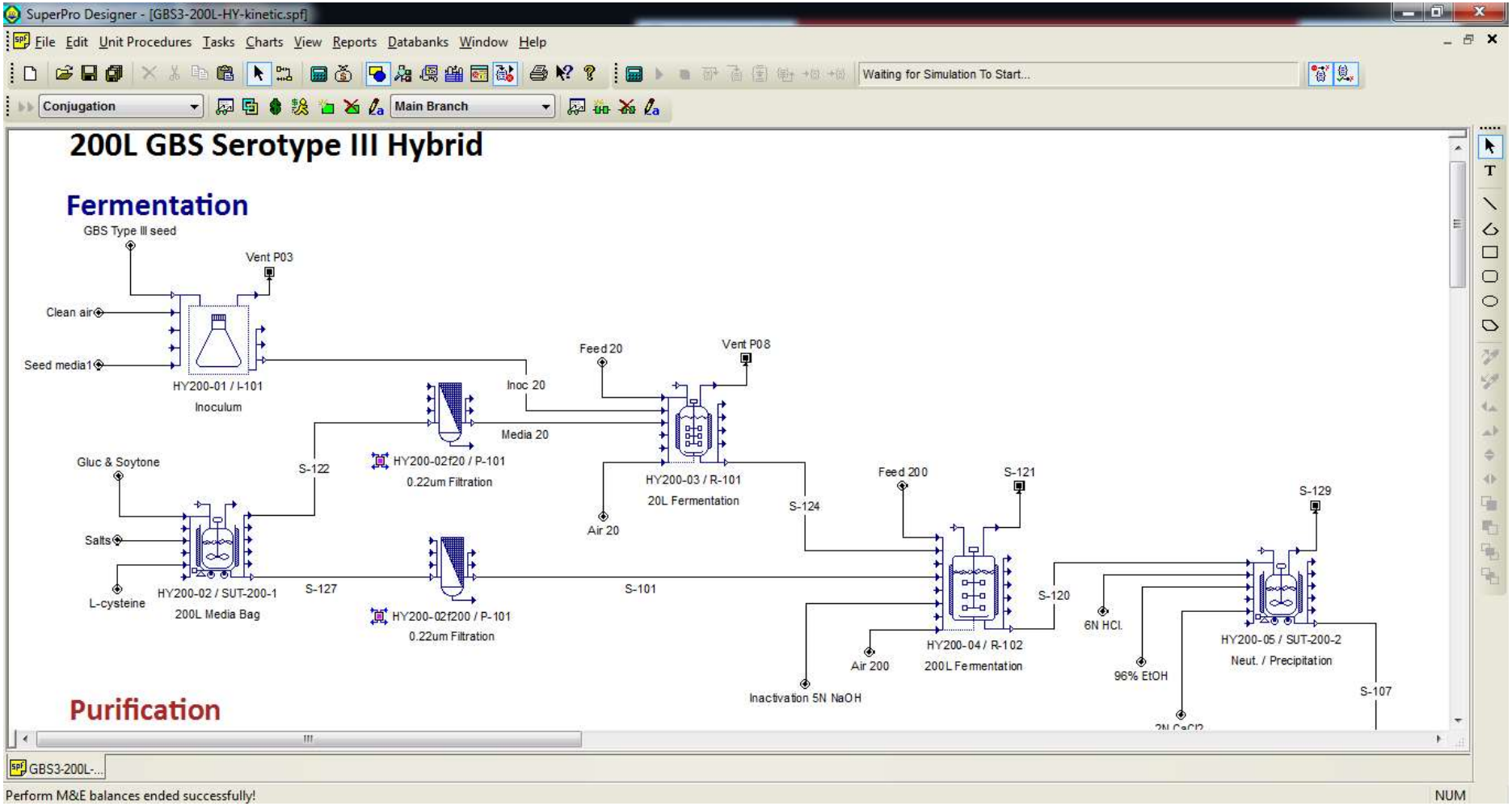

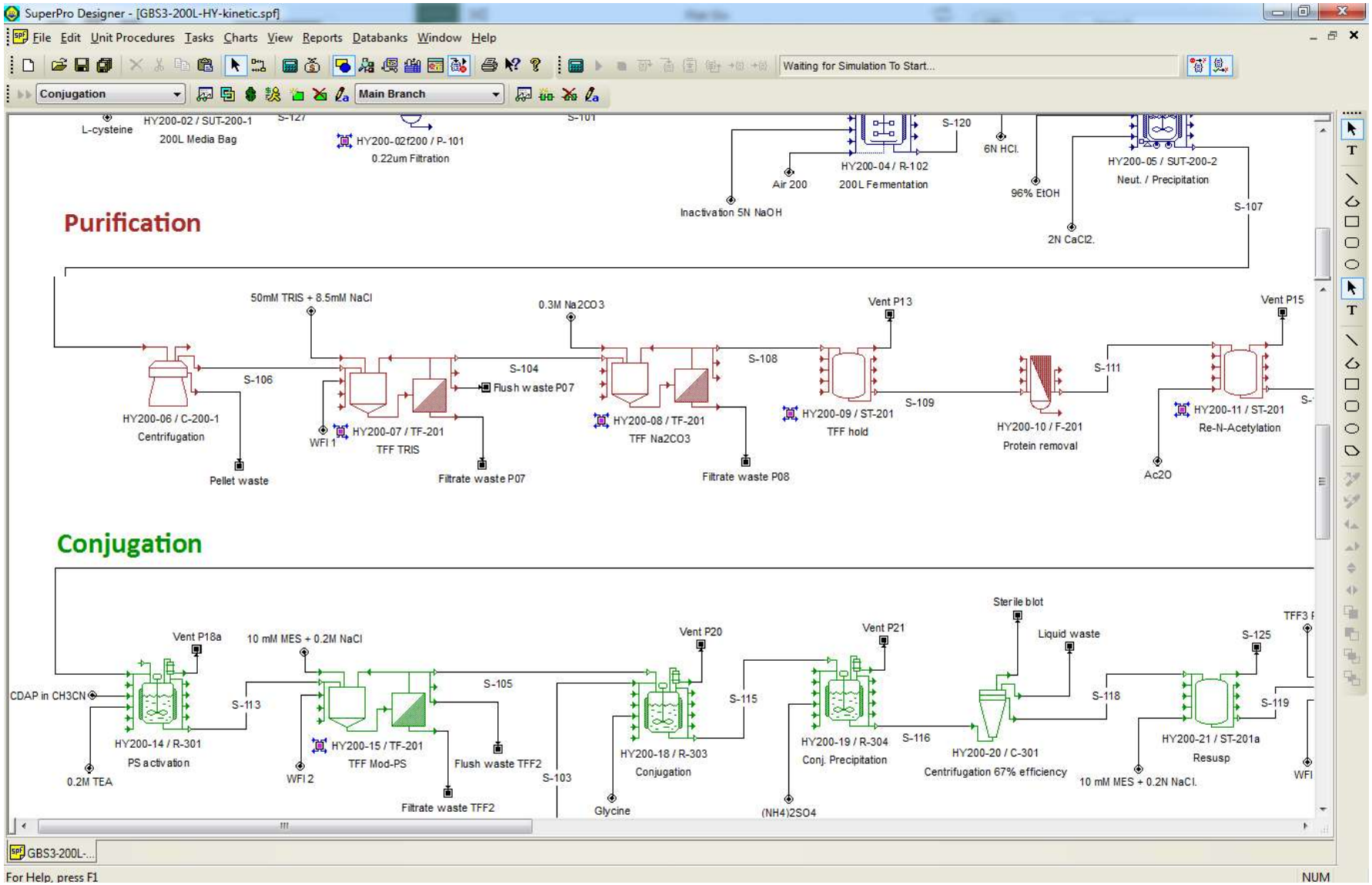
SuperPro Designer - [GBS3-200L-HY-kinetic.spf]
File Edit Unit Procedures Tasks Charts View Reports Databanks Window Help
Waiting for Simulation To Start...
Conjugation
Main Branch
Purification
L-cysteine
HY200-02 / SUT-200-1
200L Media Bag
HY200-02f200 / P-101
0.22um Filtration
Air 200
HY200-04 / R-102
200L Fermentation
S-120
6N HCl
96% EtOH
HY200-05 / SUT-200-2
Neut. / Precipitation
Inactivation 5N NaOH
2N CaCl2.
S-107
50mM TRIS + 8.5mM NaCl
0.3M Na2CO3
Vent P13
Vent P15
S-106
S-104
Flush waste P07
S-108
S-109
S-111
HY200-06 / C-200-1
Centrifugation
Pellet waste
WFI 1
HY200-07 / TF-201
TFF TRIS
Filtrate waste P07
HY200-08 / TF-201
TFF Na2CO3
Filtrate waste P08
HY200-09 / ST-201
TFF hold
HY200-10 / F-201
Protein removal
HY200-11 / ST-201
Re-N-Acetylation
Ac2O
Conjugation
Vent P18a
10 mM MES + 0.2M NaCl
Vent P20
Vent P21
Sterile blot
Liquid waste
TFF3
S-125
CDAP in CH3CN
S-113
S-105
S-115
S-116
S-118
S-119
HY200-14 / R-301
PS activation
0.2M TEA
HY200-15 / TF-201
TFF Mod-PS
WFI 2
Flush waste TFF2
Filtrate waste TFF2
S-103
HY200-18 / R-303
Conjugation
Glycine
HY200-19 / R-304
Conj. Precipitation
(NH4)2SO4
HY200-20 / C-301
Centrifugation 67% efficiency
HY200-21 / ST-201a
Resusp
10 mM MES + 0.2N NaCl.
WFI
GBS3-200L-...
For Help, press F1
NUM

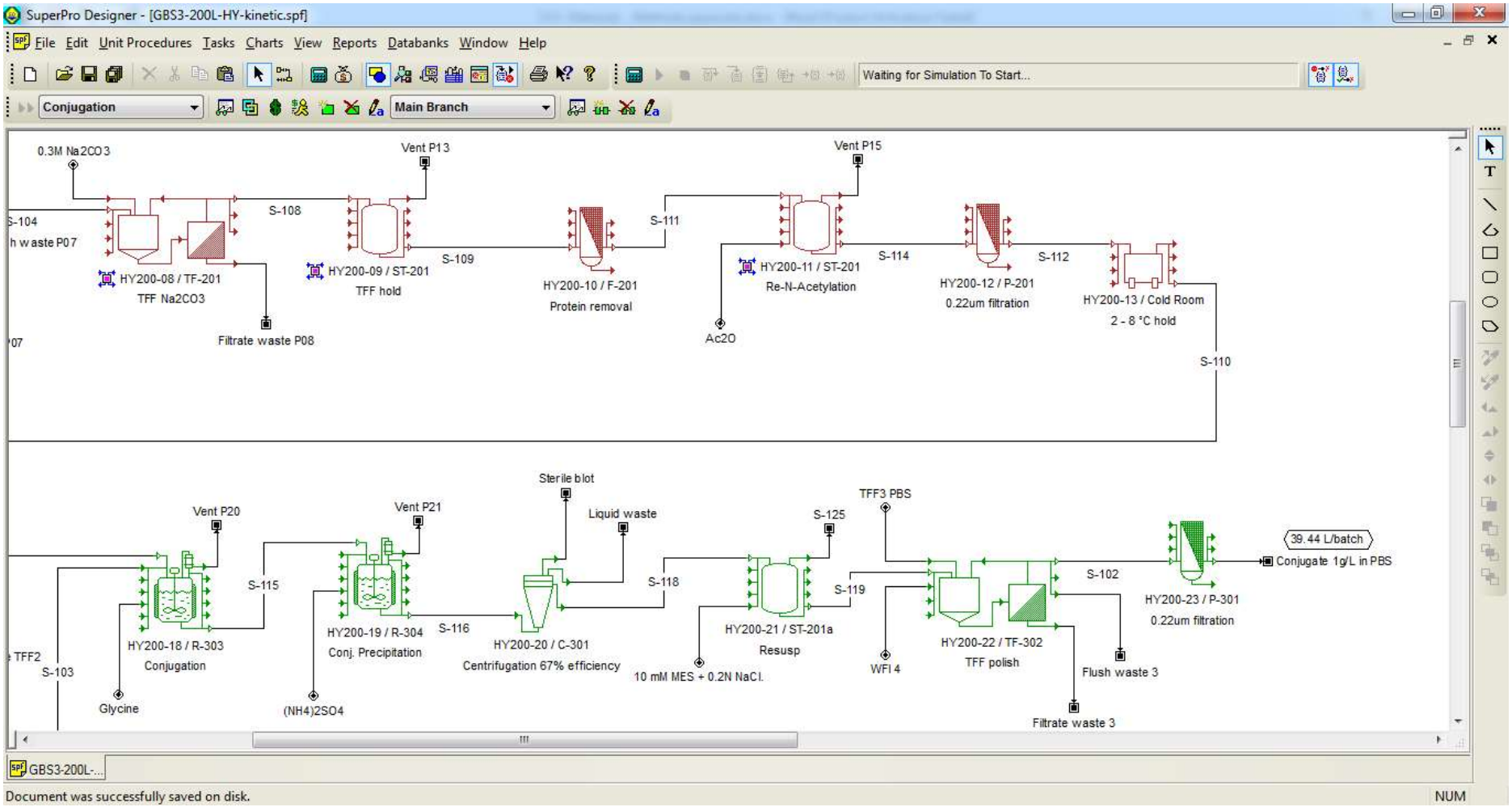
SuperPro Designer - [GBS3-200L-HY-kinetic.spf]
File Edit Unit Procedures Tasks Charts View Reports Databanks Window Help
Waiting for Simulation To Start...
Conjugation
Main Branch
0.3M Na2CO3
Vent P13
Vent P15
S-104
h waste P07
S-108
S-109
S-111
S-114
S-112
HY200-08 / TF-201
TFF Na2CO3
HY200-09 / ST-201
TFF hold
HY200-10 / F-201
Protein removal
HY200-11 / ST-201
Re-N-Acetylation
HY200-12 / P-201
0.22um filtration
HY200-13 / Cold Room
2 - 8 °C hold
Filtrate waste P08
Ac2O
S-110
Sterile blot
Vent P20
Vent P21
Liquid waste
TFF3 PBS
S-125
39.44 L/batch
Conjugate 1g/L in PBS
S-115
S-118
S-102
S-119
HY200-23 / P-301
0.22um filtration
HY200-18 / R-303
Conjugation
HY200-19 / R-304
Conj. Precipitation
S-116
HY200-20 / C-301
Centrifugation 67% efficiency
HY200-21 / ST-201a
Resusp
HY200-22 / TF-302
TFF polish
TFF2
S-103
Glycine
(NH4)2SO4
10 mM MES + 0.2N NaCl
WFI 4
Flush waste 3
Filtrate waste 3
GBS3-200L-...
Document was successfully saved on disk.
NUM

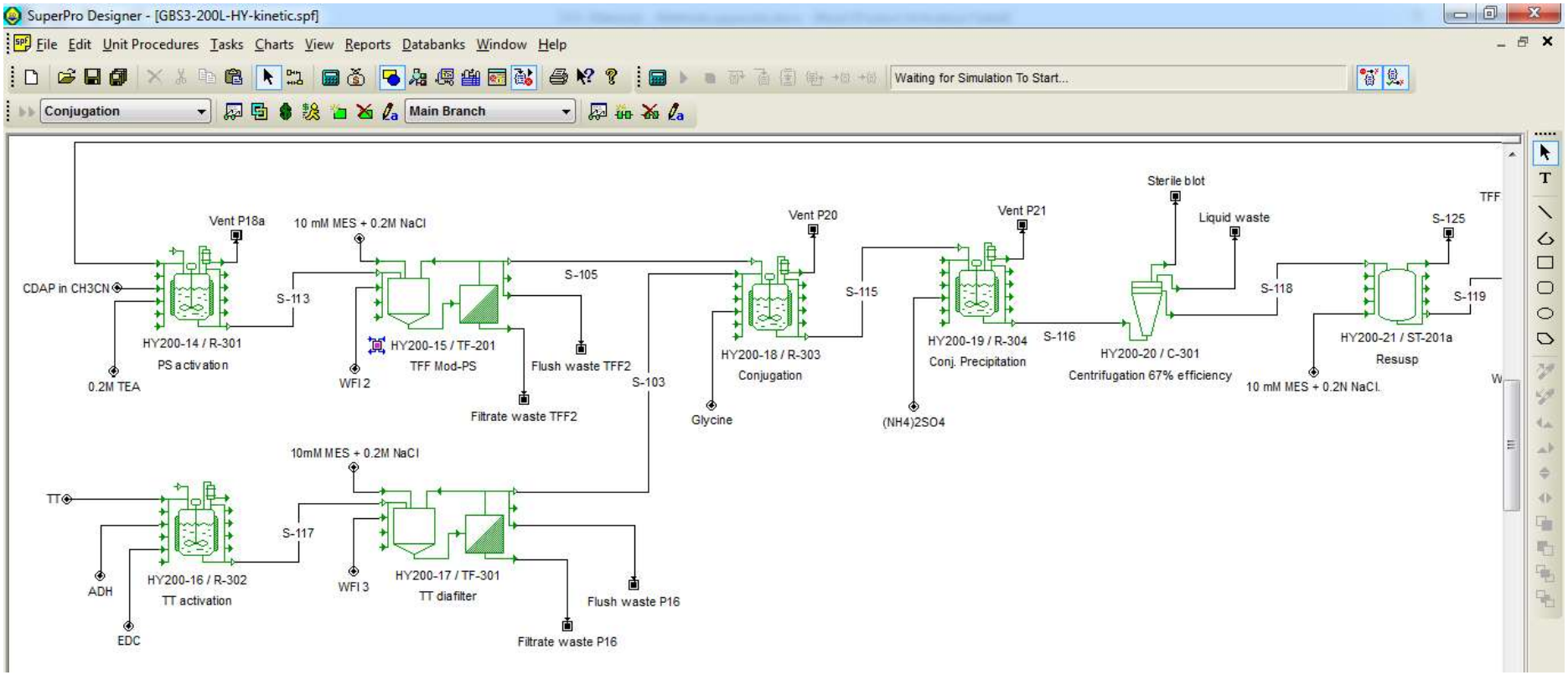
SuperPro Designer - [GBS3-200L-HY-kinetic.spf]
File Edit Unit Procedures Tasks Charts View Reports Databanks Window Help
Waiting for Simulation To Start...
Conjugation
Main Branch
Vent P18a
10 mM MES + 0.2M NaCl
Vent P20
Vent P21
Sterile blot
Liquid waste
TFF
S-125
CDAP in CH3CN
S-113
S-105
S-115
S-118
S-119
HY200-14 / R-301
PS activation
HY200-15 / TF-201
TFF Mod-PS
HY200-18 / R-303
Conjugation
HY200-19 / R-304
Conj. Precipitation
HY200-20 / C-301
Centrifugation 67% efficiency
HY200-21 / ST-201a
Resusp
0.2M TEA
WFI 2
Flush waste TFF2
Filtrate waste TFF2
S-103
Glycine
(NH4)2SO4
S-116
10 mM MES + 0.2N NaCl
10mM MES + 0.2M NaCl
TT
S-117
ADH
HY200-16 / R-302
TT activation
WFI 3
HY200-17 / TF-301
TT diafilter
Flush waste P16
EDC
Filtrate waste P16

A.13 Sensitivity Analysis Electricity price Sample Calculations

Table A-26 Monthly diesel price in cents per litre, 0.005% sulfur SA coastal 2017

Jan	Feb	Mar	Apr	May	Jun	Jul	Aug	Sep	Oct	Nov	Dec
1105.83	1126.83	1124.83	1114.03	1146.03	1123.03	1063.03	1093.03	1137.03	1179.03	1206.03	1263.33

(SAPIA - South African Petroleum Industry Association, 2019)

$$Average\ diesel\ cost\ 2017\ (Rands) = \frac{\sum_{i=Ja}^{Jan-Dec} Price_{month}}{12 \times 100 \frac{c}{R}}$$ Equation A-23

$$\sum_{i=Jan}^{Jan-Dec} Price_{month}$$
$$= (1105.83 + 1126.83 + 1124.83 + 1114.03 + 1123.03 + 1063.03 + 1093.03 + 1137.03 + 1179.03 + 1206.03 + 1263.33) = 13682.06$$

$$Average\ diesel\ cost\ 2017\ (Rands) = \frac{13\ 682.06}{12000} = R\ 11.4017\ /L$$

$$Average\ diesel\ cost\ 2017\ (\$) = \frac{Average\ diesel\ cost\ 2017\ (Rands)}{13.16 \frac{R}{\$}} = \frac{R\ 11.4017\ /L}{13.16 \frac{R}{\$}}$$

$$\boldsymbol{Average\ diesel\ cost\ 2017\ (\$) = \$\ 0.87\ /L}$$

$$Assume\ 50\ kVA\ Diesel\ generator\ efficiency\ =\ 0.5\ L/kWh$$

$$Elecrticity\ Cost\ from\ diesel = \ diesel\ cost\ 2017\ (\$) \times Diesel\ generator\ efficiency$$ Equation A-24

$$Elecrticity\ Cost\ from\ diesel = \frac{\$\ 0.87}{L} \times \frac{0.5\ L}{kWh}$$

$$\boldsymbol{Elecrticity\ Cost\ from\ diesel = \$\ 0.43\ /kWh}$$

Example: 10% electricity derived from diesel generator:

$$Composite\ electricity\ cost = \sum_{i=1}^{2} percentage_{type\ i} \times cost_{type\ i}$$ Equation A-25

$$Composite\ electricity\ cost = 10\% \times cost\ of\ diesel\ power + 90\% \times cost\ of\ coal\ power$$

$$Composite\ electricity\ cost = 0.1 \times \$\ 0.43\ /kWh + 0.9 \times \$\ 0.1\ /kWh$$

$$Composite\ electricity\ cost = \$\ 0.13/kWh, rounded\ up\ to\ \$0.15\ /kWh$$

$$\boldsymbol{Composite\ electricity\ cost, 10\%\ from\ diesel = \$0.15\ /kWh}$$